

The transducer-like proteins of
Campylobacter jejuni

Thesis submitted for the degree of
Doctor of Philosophy
at the University of Leicester

By

Randeep Sandhu, B.Sc. Hons (University of Leicester)

Department of Genetics
University of Leicester

January 2011

Abstract

The transducer-like proteins of *Campylobacter jejuni* Randeep Sandhu, BSc. (Hons)

Campylobacter jejuni is the leading cause of gastrointestinal disease in the developed world. Chemotactic motility is a pre-requisite for intestinal colonisation by *C. jejuni*. *In silico* analysis of the *C. jejuni* NCTC 11168 genome identified homologues of 10 chemotaxis receptor and two aerotaxis genes. Six of the ten putative Transducer-like proteins (Tlp 1, 2, 3, 4, 7 and 10) resemble chemoreceptors of *Escherichia coli*. The aim of this project is to characterise the *C. jejuni* Tlp1-4 chemoreceptors. The genes encoding the Tlps were inactivated using an insertional inactivation strategy. Isogenic mutants were made in *tlp1*, *tlp2* and *tlp4*; a final mutant in *tlp3* could not be obtained. A *tlp1* complement was also constructed in this work. The *tlp1* mutant showed reduced chicken colonisation ability when tested by our collaborators. Chemotactic phenotypes of the *tlp* mutants were determined in the swarm assay; the *tlp* mutants appeared defective for chemotaxis when compared with the wild-type and non-motile *flaAB* mutant. The Capillary assay and Hard-Agar Plug (HAP) assay were developed as methods to ascertain the ligand specificities of the Tlp chemoreceptors under study. Unfortunately, the Capillary assay proved to be insufficiently reproducible for effective use with *C. jejuni*. The HAP procedure was optimised using a *C. jejuni* wild-type motile variant. Positive chemoattractant responses were observed in NCTC 11168 for the first time towards a range of chemicals. Data derived from the modified HAP assay indicated that Tlp1 may be the receptor for serine. Chemotactic responses could not be detected in the *tlp2* and *tlp4* mutants in the HAP assay. The signalling domain of Tlp1 was purified using a polyhistidine tag and used to produce a polyclonal antibody. The Tlp1 primary antibody and immunofluorescence labeling has shown for the first time that the Tlps cluster at the cell poles in *C. jejuni*.

Acknowledgements

I would like to begin by thanking my supervisor Professor Julian Ketley who encouraged and supported me throughout this work. Also, thank you for giving me the opportunity to do a PhD with you. I would also like to thank Dr Colin Hewitt for being a fantastic course convenor on the BSc Immunology degree programme.

I would like to thank my student Rebecca Hall for her help with this project. Many thanks to Oliver Bridle for taking the time to teach me when I first arrived and for help with developing the Capillary assay. I would also like to thank Julie Turner for help with optimising the Hard-agar plug assay. I would like to thank Dr X. Yang for help with protein expression. I would like to acknowledge the Biotechnology and Biological Sciences Research Council (BBSRC) for funding this project. I would like to thank Dr Kornelis R Straatman for his help with microscopy and imaging.

I would like to thank my dear friends Sue, Claire and Laura. I am very grateful for our friendship. You have all kindly encouraged and supported me. I would like to say a special thanks to Miranda, lab 121 would not be the same without you! I would also like to acknowledge Ran, Adam, Abdul, Paul and everyone else who has worked alongside me in lab 121. I would also like to thank Dr Richard Haigh for supporting me with my research.

I would like to acknowledge Dr Julie Morrissey for supporting me through my corrections.

I would like to thank my closest of friends Rashmika, Ayesha, Bhavna and Gurjit. I value our friendship a great deal. A special thank you to Kam and Jin, I am blessed to have you both in my life.

Finally, I would like to say a heartfelt thank you to my dear mum and dad. Thank you for always being there to guide and encourage me. I would like to thank my sister Karen for her love and support. You are the best sister in the world! I could not have done this without you! Mum, dad and Karen thank you for *always* believing wholeheartedly that I could do this.

I would like to dedicate this thesis to my loving Grandfather Karam Singh.

Contents

Contents	1
List of Figures and Tables	7
Abbreviations	13
Chapter 1. Introduction	15
1.1. Overview	15
1.2. <i>Campylobacter</i>	16
1.2.1. History	16
1.2.2. Species	17
1.2.3. Physiology	18
1.2.4. Genomics	19
1.2.5. Transmission	22
1.2.6. Clinical presentation and epidemiology	23
1.2.6.1. Disease outbreaks in developed countries	25
1.2.6.2. Disease outbreaks in developing countries	25
1.2.6.3. Post-infection complications	26
1.3. Pathogenesis	28
1.3.1. Colonisation	28
1.3.2. <i>C. jejuni</i> virulence factors	29
1.3.2.1. Acquiring iron from the host	30
1.3.2.2. Motility as a virulence determinant	31
1.3.2.3. Adhesion to the host epithelium	34
1.3.2.4. Toxin production in <i>C. jejuni</i>	35
1.4. Chemotaxis	36
1.4.1. The chemotaxis pathway	36
1.4.2. Patterns of motility	37
1.4.3. Alternatives to the bacterial flagella	40
1.4.4. Chemotactic motility in the model organism <i>E. coli</i>	41
1.4.4.1. The structure and assembly of the flagella in <i>E. coli</i>	41
1.4.4.2. The chemosensory pathway in <i>E. coli</i>	44
1.4.4.3. The MCP receptors in <i>E. coli</i>	49
1.4.4.4. The localisation of the MCP receptor clusters in <i>E. coli</i>	52
1.4.5. Alternative chemotaxis pathways in other bacteria	53
1.4.5.1. The chemosensory system in <i>B. subtilis</i>	53
1.4.5.2. Chemotaxis in <i>Sinorhizobium meliloti</i> and <i>Rhodobacter sphaeroides</i>	56
1.5. Chemotaxis as a virulence determinant in <i>C. jejuni</i>	59
1.5.1. The flagellum in <i>C. jejuni</i>	60
1.5.2. The chemosensory pathway in <i>C. jejuni</i>	62
1.5.3. The MCP receptors in <i>C. jejuni</i>	64
1.6. Project Aims	69
Chapter 2. Materials and Methods	71
2.1. Bacterial strains and plasmids	71

2.2. Bacterial culturing, growth conditions and storage	74
2.2.1. <i>Campylobacter jejuni</i>	74
2.2.2. <i>Escherichia coli</i>	75
2.2.3. Storage and recovery of bacterial strains	76
2.3. Media, Sterilisation and Supplementation	76
2.4. Miscellaneous buffers and solutions	78
2.5. Primers	82
2.6. Amplifying DNA using the Polymerase Chain Reaction	88
2.6.1. Colony PCR	90
2.6.2. Sequencing of DNA and analysis	90
2.7. Quantification of DNA	91
2.7.1. Analysis of DNA by agarose gel electrophoresis	91
2.7.2. Quantification of DNA using a spectrophotometer	92
2.8. Isolating DNA from bacteria	93
2.8.1. Plasmid DNA preparations from <i>E. coli</i>	93
2.8.2. Large scale genomic preparations from <i>C. jejuni</i>	94
2.8.3. Small scale genomic preparations from <i>C. jejuni</i>	95
2.9. Purifying DNA	96
2.9.1. Purifying DNA fragments from PCR or other enzymatic reactions	96
2.9.2. Purifying DNA directly from agarose gels	97
2.9.3. Ethanol precipitation	98
2.10. Enzymatic alterations of DNA into bacteria	99
2.10.1. Restriction digests	99
2.10.2. Dephosphorylation of DNA	99
2.10.3. Ligations	99
2.11. Introducing DNA into bacteria	100
2.11.1. Preparation of chemically competent <i>E. coli</i>	100
2.11.2. Preparation of electro-competent <i>E. coli</i>	100
2.11.3. Introducing DNA into <i>E. coli</i> by heat shock	101
2.11.4. Introducing DNA into <i>E. coli</i> by electroporation	101
2.11.5. Preparation of electro-competent <i>C. jejuni</i>	102
2.11.6. Introducing DNA into <i>C. jejuni</i> by electroporation	102
2.11.7. Introducing DNA into <i>C. jejuni</i> by natural Transformation	103
2.12. SDS-polyacrylamide gel electrophoresis	103
2.12.1. Sample preparation	103
2.12.2. Electrophoresis of proteins and visualization	104
2.13. Immunoblotting proteins	106
2.13.1. Assembly of apparatus and running a western blot	106
2.13.2. Antibody incubation and washing	107
2.13.3. Generation of a signal and subsequent detection	108
2.14. Protein preparation, expression and purification	109
2.14.1. GST-tagged Tlp proteins	109
2.14.2. His-tagged Tlp proteins	111
2.14.2.1. His-tagged Tlp1 periplasmic domain	111
2.14.2.2. His-tagged Tlp1 cytoplasmic domain	112
2.14.3. Optimisation of protein expression	113
2.14.4. Tlp1 C-terminal signalling domain specific labelling of <i>C. jejuni</i>	114

2.15. Chemotaxis assays	116
2.15.1. Swarm plate assay	116
2.15.2. Capillary assay	117
2.15.2.1. An alternative to Adler's capillary tube assay	121
2.15.3. Hard-agar plug (HAP) assay	122
2.15.3.1. Preparation of HAPs	122
2.15.3.2. Cell preparation	123
2.15.3.3. Quantifying bacterial chemotaxis	124
2.16. Bioinformatics	126
2.17. Statistical analyses	126
Chapter 3. Creating isogenic mutants in a specific group of chemoreceptors and genetic complementation of a <i>cj1506c</i> mutation	127
3.1. Introduction	127
3.2. Creating isogenic mutants in the Tlps in <i>C. jejuni</i> NCTC 11168 using an insertional inactivation strategy	131
3.2.1. Cloning the Tlps into pUC19	131
3.2.2. Screening <i>E. coli</i> cells for recombinant plasmid constructs containing the <i>cj1506c</i> insert	133
3.2.3. Disruption of the Tlp ORFs by inverse PCR mutagenesis	140
3.2.3.1. Disrupting the <i>Cj1506c</i> ORF	140
3.2.3.2. Disrupting the <i>Cj0144</i> , <i>Cj1564</i> and <i>Cj0262c</i> ORFs	141
3.2.4. Screening putative <i>E. coli</i> transformants for recombinant plasmids	143
3.2.5. Allelic replacement of a wild-type <i>tlp</i> gene with a mutated copy	151
3.2.6. Natural transformation of the <i>C. jejuni</i> $\Delta cj1506c::cat$ mutation onto a motile variant background	158
3.3. Selecting a complementation strategy to restore the wild-type phenotype in a <i>cj1506c</i> isogenic mutant	161
3.3.1. Complementation using pRRK	163
3.3.1.1. Modifying the pRRK vector	163
3.3.1.2. Cloning the poly-linker from the pTrcHisB plasmid into pRRK	165
3.3.1.3. Cloning a functional copy of the <i>cj1506c</i> gene into pRRK-poly	167
3.4. Discussion	170
3.4.1. Introduction	170
3.4.2. Mutagenesis of <i>cj1506c</i> and creating a complement	171
3.4.3. Difficulties mutating the Tlps	172
3.4.3.1. Mutagenesis of <i>cj0144</i>	172
3.4.3.2. Mutagenesis of <i>cj0262c</i>	173
3.4.3.3. Mutagenesis of <i>cj1564</i>	174
Chapter 4. Developing chemotaxis assays to determine the chemotactic behaviour of wild-type <i>C. jejuni</i> toward different chemical stimuli	178
4.1. Introduction	178

4.2. Methods available for assessing chemotaxis in wild-type <i>C. jejuni</i>	179
4.2.1. The swarm plate assay	179
4.2.2. The Hard-agar plug (HAP) assay	180
4.2.3. Quantifying chemotactic responses in <i>C. jejuni</i> using a capillary tube assay	183
4.3. Results: assessing the chemotactic behaviour of wild-type <i>C. jejuni</i>	185
4.3.1. The migration of wild-type <i>C. jejuni</i> in semi-solid complex media	185
4.3.2. Quantifying chemotaxis responses using Adler's capillary tubes assay	190
4.3.2.1. A simplified version of the capillary assay designed specifically for use with microaerobic bacteria	193
4.3.3. The HAP procedure	196
4.3.3.1. Modifying the HAP procedure	196
4.3.3.2. Reattempting the HAP assay using Hugdahl <i>et al</i> 's (1988) original methodology	199
4.4. Discussion	206
4.4.1. Motility in wild-type <i>C. jejuni</i>	206
4.4.2. Possible explanations for failure of the capillary assay	208
4.4.3. The HAP procedure	212
Chapter 5. Phenotypic studies on Transducer-like protein (Tlp) 1 and the significance of Tlp2 and Tlp4 in <i>Campylobacter jejuni</i> chemotaxis	215
5.1. Introduction	215
5.1.1. Tlp receptors in other bacteria	215
5.1.2. Chemotaxis assays optimised with the <i>C. jejuni</i> wild-type motile-variant	216
5.1.3. Previous research on the Tlps in <i>C. jejuni</i> NCTC 11168	217
5.2. Results	218
5.2.1. Assessment of the <i>tlp</i> mutants in the swarm assay	218
5.2.2. Determining the ligand-specificity of the <i>tlp</i> mutants in the HAP assay	223
5.3. Discussion	233
5.3.1. The requirement of the Tlps in colonisation of the host	233
5.3.2. Phenotypes of the <i>tlp</i> mutants in the swarm plate assay	234
5.3.3. Determining the specificity of the Tlp receptors	235
5.3.4. Testing the <i>tlp1</i> isogenic mutant ($\Delta cj1506c::cat$) and complementing mutant <i>in vitro</i> and <i>in vivo</i> models of colonisation	239
5.3.5. Alternative chemotaxis assays	241
Chapter 6. Cloning, expressing and purifying different domain structures from the Tlps	242
6.1. Introduction	242

6.1.1. Protein domains of interest in the Group A transducer-like proteins (Tlps)	242
6.2. Do the Tlps localise to the poles of the cell in <i>C. jejuni</i> similar to other bacteria and archaea?	243
6.3. Protein purification strategies	245
6.4. Results	248
6.4.1. The proposed structure and function of the Group A Tlps	248
6.4.2. Bioinformatic analysis of the secondary structures of the Tlps	249
6.4.3. The cloning of the domains of Tlp1 and Tlp2 to 4 into a suitable expression vector containing a peptide or protein tag	254
6.4.3.1. Cloning the carboxyl-terminal signalling domain of Tlp1 and Tlp2 to 4 into pGEX-4T-1	254
6.4.3.2. Screening <i>E. coli</i> cells for potential plasmid constructs containing the correct <i>tlp1</i> HCD insert	255
6.4.4. Cloning the periplasmic domain of Tlp1 into the pLEIC-05 plasmid containing a His-tag	259
6.4.5. Purifying the N-terminal ligand-binding domain in Tlp1	261
6.4.5.1. Optimising the extraction protocol for the His-tagged Tlp1 periplasmic (Tlp1_Peri) protein	261
6.4.6. Purifying the C-terminal signalling domain in Tlp1	266
6.4.6.1. Expression and purification of the C-terminal signalling domain in Tlp1 and Tlp2 to 4 using a GST-tag	266
6.4.6.2. Detecting the GST-tag in the purified cytoplasmic proteins of Tlp1 and Tlp2 to 4 using an anti-GST antibody	269
6.4.6.3. Optimising the yield of Tlp1_HCD recombinant protein	271
6.4.6.4. Cleavage of the GST-tag	273
6.4.6.5. Further attempts to clone the Tlp1 HCD	274
6.4.6.6. Testing the Tlp1_HCD polyclonal antibody	276
6.5. Discussion	280
6.5.1. Summary of key findings	280
6.5.2. Problems purifying GST-tagged Tlp proteins	281
6.5.3. Future work using the polyclonal antibodies generated to the Tlps_HCD	282
6.5.4. Expressing the Tlp1 Periplasmic domain of Tlp1	283
Chapter 7. General discussion	285
7.1. Summary of main findings and conclusions	285
7.2. Chemoreceptors in other bacteria	288
7.3. A proposed model for chemoreceptor based chemotaxis signal transduction and pathogenesis in <i>C. jejuni</i>	289
7.4. Future work and implications of research	291

Addenda consisting of one data CD

Software required: Microsoft Word (2003 onwards) and Adobe Acrobat Reader (version 9).

Appendices

CD-ROM

1. A pdf file of Hartley-Tassell *et al.*, 2010. The paper is titled “Identification and characterization of the aspartate chemosensory receptor of *Campylobacter jejuni*.”
2. Construct map of the $\Delta cj1564::aphA-3$ mutant
3. Swarm assay data and statistics for the *tlp* mutants
4. Protein expression vectors

Bibliography.....294

List of Figures and Tables

Figures

- 1.1. The number of *Campylobacter* cases reported to the health protection agency (HPA) for England and Wales from 1989 to 2008 (page 24).
- 1.2. Flagella rotation in *E. coli* (page 39).
- 1.3. Flagellum rotation in *C. jejuni* (page 39).
- 1.4. A schematic drawing of assembly of the flagellum in enteric bacteria (page 43).
- 1.5. The signal transduction pathway in *E. coli* (page 48).
- 1.6. The structure of an MCP receptor (page 51).
- 1.7. Domain organisation of the 10 chemoreceptor orthologues and two aerotaxis genes identified in *C. jejuni* NCTC 11168 (page 68).
- 2.1. An outline of the capillary assay (page 120).
- 3.1. Genomic organisation of the Tlps in *C. jejuni* NCTC 11168 (page 130).
- 3.2. Summary of the steps undertaken to clone the *cjI506c* gene (including DNA flanking sequence) into pUC19 and PCR amplification of *cj0144* (page 136).
 - 3.2.1. PCR amplification of *cjI506c* (page 136).
 - 3.2.2. PCR amplification of *cj0144* (page 136).
 - 3.2.3. Planning the mutagenesis of Cj0262c (page 137)
 - 3.2.4. Colony PCR screen of recombinant plasmid constructs using gene specific primers (page 137).
 - 3.2.5. *PvuI* digest to identify *cjI506c* recombinant plasmid constructs (page 138).
- 3.3. Initial construct map of pRS01 (page 139).
- 3.4. Summary of the steps undertaken to disrupt the *cjI506c* gene in *C. jejuni* (page 142).
 - 3.4.1. Inverse PCR amplification of *cjI506c* (page 142).

- 3.4.2. PCR amplification of the *cat* cassette from pAV35 (page 142).
- 3.5. Colony PCR screen on putative pRS02 transformants of *E. coli* (page 145).
 - 3.5.1. Final construct map of pRS02 (page 146).
 - 3.5.2. Colony PCR screen on putative final construct transformants for Cj0144 (Tlp2), Cj1564 (Tlp3) and Cj0262c (Tlp4) (page 147).
 - 3.5.3. Final construct map of *cj0144* (pRS04) (page 148).
 - 3.5.4. Final construct map of *cj1564* (pRS06) (page 149).
 - 3.5.5. Final construct map of *cj0262c* (pRS08) (page 150).
- 3.6. PCR screen on two putative *C. jejuni* $\Delta cj1506c::cat$ mutants (page 154).
 - 3.6.1. PCR screen on a putative *C. jejuni* $\Delta cj0144$ mutant containing the *ermC'* gene (page 155).
 - 3.6.2. Colony PCR screen of *C. jejuni* cells transformed with pRS03 containing the $\Delta cj1564::ermC'$ insert (page 156).
 - 3.6.3. PCR screen on a putative *C. jejuni* $\Delta cj0262c$ mutant containing a *chloramphenicol acetyl transferase (cat)* cassette (page 157)
 - 3.6.4. Colony PCR screen of *C. jejuni* $\Delta cj1506c::cat$ mutants transformed onto a motile variant background (page 159).
- 3.7. Summary of steps undertaken to mutate *cj1506c* (page 160).
- 3.8. Plasmid map of pRRK-poly (page 164).
- 3.9. Summary of the steps undertaken to clone the poly-linker from the pTrcHisB plasmid into pRRK (page 166).
 - 3.9.1. PCR amplification of the poly-linker from the pTrcHisB plasmid (page 166).
 - 3.9.2. *Pst*I digest of pRRK-poly recombinant plasmid constructs (page 166).
- 3.10. Summary of the steps involved in cloning a functional copy of *cj1506c* into pRRK-poly (page 168).
 - 3.10.1. *Bgl*II and *Kpn*I digests of pRRK-poly and *cj1506c* (page 168).
 - 3.10.2. Colony PCR screen of *E. coli* cells transformed with pRRK-poly containing the *cj1506c* insert (page 168).

- 3.11. Plasmid map showing the construct used to complement the $\Delta cj1506c::cat$ mutation in *C. jejuni* (pRS12) (page 169).
- 4.1. Illustration of how positive and negative chemotaxis responses in *C. jejuni* are assessed according to the hard agar plug (HAP) procedure (page 182).
- 4.2. The phenotypes of the wild-type motile variant, *flaAB* mutant and chemotaxis mutants in the swarm plate assay (page 188).
- 4.3. Swarm diameters of *C. jejuni* (11168) wild-type motile variant (MV) and *flaAB* mutant (81116) cells (page 189).
- 4.4. Accumulation of wild-type motile variant cells into 1 μ l capillary tubes containing either 0.1 M fucose or PBS (buffer only control) (page 192).
- 4.5. An alternative to Adler's capillary tube chemotaxis assay (page 194).
- 4.6. Accumulation of wild-type *C. jejuni* into a 1 ml tuberculin syringe containing MHB (Mueller-Hinton Broth) or PBS (page 195).
- 4.7. Assessing chemotaxis using mem- α medium plus agar (page 198).
- 4.8. Positive chemotaxis towards different chemical stimuli (pages 202-203).
- 4.9. Radius of the zone of accumulation around a HAP containing various concentrations of serine (page 205).
- 5.1. Swarming phenotypes of the *tlp* mutants relative to the wild-type *C. jejuni* MV (page 221).
- 5.2. Comparing the differences in swarm diameters between the *tlp1* and *tlp4* mutants and the wild-type *C. jejuni* MV (motile variant) and non-motile *flaAB* control (page 222).
- 5.3. Chemotactic responses in the *tlp1* mutant towards a range of putative chemoattractants (page 227-228).
- 5.4. Determining chemotactic responses in the wild-type MV strain and the *tlp1* mutant using the Hard-agar plug (HAP) assay (page 229).
- 5.5. Chemotactic responses in the *tlp1* mutant towards a range of putative *C. jejuni* chemoattractants (page 230).
- 5.6. Chemotactic responses in the *tlp2* mutant towards a range of putative *C. jejuni* chemoattractants (page 231).

- 5.7. Determining chemotactic responses in the *tlp4* mutant towards a range of putative *C. jejuni* chemoattractants (page 232).
- 6.1. Figure showing the arrangement of domains in Tlp1-4 (page 245).
- 6.2. Histograms showing the putative transmembrane helices in Tlps 1 to 4 (pages 251-252).
- 6.3. A summary of the steps involved in cloning the carboxyl-terminal HCD of Tlp1 into the expression vector pGEX-4T-1 (page 257).
- 6.3(a). PCR amplification of the cytoplasmic domains of Tlp1 and Tlp2 (page 257).
- 6.3(b). Colony PCR screen of putative pRS09 constructs in *E. coli* DH5 α E (page 257).
- 6.3 (c). Colony PCR screen of putative pRS09 constructs in *E. coli* BL21 (page 257).
- 6.4(a). Figure showing the gene encoding the HCD of Tlp1 cloned into pRS09 (page 258).
- 6.4 (b). Figure showing the gene encoding the HCD of Tlp2 to 4 cloned pRS10 (page 258).
- 6.5 (a). PCR amplification of the N-terminal periplasmic ligand-binding domain (PLD) of Tlp1 (page 260).
- 6.5 (b). Figure showing the gene encoding the PLD of Tlp1 cloned into the expression vector pLEIC-05 to produce pRS11 (page 260).
- 6.6. Optimising the extraction protocol for the His-tagged Tlp1 periplasmic (Tlp1_Peri) protein (page 264).
- 6.6 (a). The effects of using varying concentrations of IPTG and then incubating cells at 18°C on the solubility of the His-tagged Tlp1 periplasmic protein (Tlp1_Peri) (page 264).
- 6.6 (b). The effects of using varying concentrations of IPTG and then incubating cells at 18°C & 26°C on the solubility of the His-tagged Tlp1 periplasmic protein (Tlp1_Peri) (page 264).
- 6.6 (c). The effects of using varying concentrations of IPTG and then incubating cells at 26°C & 30°C on the solubility of the His-tagged Tlp1 periplasmic protein (Tlp1_Peri) (page 265).

- 6.6 (d). The effects of using varying concentrations of IPTG and then incubating cells at 30°C on the solubility of the His-tagged Tlp1 periplasmic protein (Tlp1_Per1) (page 265).
- 6.7. The expression and purification of GST-tagged fusion proteins (page 268).
- 6.7 (a). Coomassie stained SDS-PAGE gel showing the expression of GST-tagged Tlp1 and Tlp2 to 4 HCD (page 268).
- 6.7 (b). Coomassie blue stained SDS-PAGE gel showing the purification of the GST-tagged Tlp1 HCD protein (page 268).
- 6.8. Western blot analysis of solubilised Tlp1 and Tlp2 to 4 HCD proteins (prepared from *E. coli* BL21 cells) using an anti-GST antibody (page 270).
- 6.9. Western blot analysis of the purified Tlp1_HCD protein post-treatment with 6M guanidine hydrochloride (HCl) (page 272).
- 6.10. Figure showing the gene encoding the HCD of Tlp1 cloned into the pTrcHisB plasmid (page 275).
- 6.11. Controls used for the staining of *Campylobacter jejuni* cells for the Tlp1 localisation immunofluorescence light microscopy studies (page 278).
- 6.12. Determining the Intracellular positioning of the Tlp1 chemoreceptors in *Campylobacter jejuni* (NCTC 11168) by indirect immunofluorescence light microscopy (page 279).
- 7.1. Proposed model for chemoreceptor based chemotaxis signal transduction in *Campylobacter jejuni* (page 290).

Tables

- 1.1. A comparison of the chemotaxis proteins present in *E. coli* with those in *C. jejuni* (page 64).
- 1.2. Chemoreceptors in different strains of *C. jejuni* (page 67).
- 2.1. Bacterial strains used/produced in this study (page 71).
- 2.2. Vectors used or created in this study (page 72).
- 2.3. Plasmid constructs created in this study (page 73).
- 2.4. Media used in this study (page 77).

- 2.5. Antibiotics used in this study (page 78).
- 2.6. Primers used in this study for PCR amplification (page 83).
- 2.7. Components in a typical PCR reaction mix (page 89).
- 2.8. Standard PCR thermal cycling program (page 89).
- 2.9. Standard sequencing thermal cycling programme (page 91).
- 2.10. Composition of the resolving and stacking gels used for SDS-PAGE (page 105).
- 2.11. The assembly of equipment required for electro-transfer of proteins from an SDS-PAGE gel to a PVDF membrane (page 107).
- 2.12. Putative chemoattractants/chemorepellents screened in the Capillary and HAP assays (page 125).
- 3.1. A list of all *tlp* genes cloned, mutated and complemented in this study (page 135).
- 4.1. This table shows the responses in wild-type *C. jejuni* motile variant cells to a range of chemicals (page 204).
- 6.1. The advantages and disadvantages for using different protein or peptide based fusion tags (page 247).
- 6.2. A summary of the proposed location of the transmembrane domains within the secondary domain structures of the Group A Tlps (page 253).
- 6.3. Table showing the PCR reactions performed to amplify target domains in the Tlps (page 256).
- 6.4. Different domains in the Tlps expressed and purified (page 263).

List of Abbreviations

Abbreviation	Definition
A	Adenine
Amp	Ampicillin
ATP	Adenosine triphosphate
bp	Base pairs
BSA	Bovine Serum Albumin
C	Centrigrade
C	Cytosine
°C	Degrees celsius
cat	Chloramphenicol acetyl-transferase
CCW	Counter-clockwise
CDT	Cytolethal distending toxin
cfu	Colony forming unit
Cl	Chloride
Cm	Chloramphenicol
CTAB	Hexadecyltrimethyl ammonium bromide
CO₂	Carbon dioxide
CW	Clockwise
Δ	Delta
DNA	Deoxyribonucleic acid
dNTP	Deoxyribonucleotide triphosphate
DTT	Dithiothreitol
dH₂O	Distilled water
EB	Elution buffer
Ery	Erythromycin
EtBr	Ethidium bromide
x g	Centrifugal force (gravity)
G	Gram(s)
G	Guanine
GBS	Guillain-Barré syndrome
GST	Glutathione-S-transferase
HAP	Hard-agar plug
HCD	Highly conserved signalling domain
IPTG	Isopropyl-β-D-thiogalactopyranoside
His	Histidine
Km	Kanamycin
kV	Kilo volts
kb	Kilobase pairs
kDa	Kilo daltons
L	Litres
LA	Luria-Bertani Agar
μ	Micro (10 ⁻⁶)
m	Milli (10 ⁻³)
m	Mitre

M	Mole(s)
MCP	Methyl-accepting chemotaxis protein (s)
mcs	Multiple cloning site
MEMα	Minimal Essential Medium Alpha
MFS	Miller-Fisher syndrome
MHA	Mueller-Hinton agar
MHB	Mueller-Hinton broth
mHAP	Modified hard-agar plug
MV	Motile-variant
n	Number of samples
n	Nano (10^{-9})
N₂	Nitrogen
NaCl	Sodium chloride
NaOH	Sodium hydroxide
NCTC	National Collection of Type Cultures
Ω	Ohm(s)
O₂	Oxygen
OD₆₀₀	Optical density at 600 nm
ORF	Open Reading Frame
%	Percent
P	Phosphate group
PAGE	Polyacrylamide gel electrophoresis
PAS	<i>Drosophila</i> period (PER), vertebrate aryl hydrocarbon receptor nuclear translocator (ARNT), <i>Drosophila</i> single-minded (SIM).
PBP	Periplasmic binding protein
PBS	Phosphate buffered saline
PLD	Periplasmic ligand-binding domain
Peri	Periplasmic
RNA	Ribonucleic acid
rpm	Revolutions per minute
SAP	Shrimp alkaline phosphatase
S.D.	Standard deviation
SEM	Standard error of the mean
SDS	Sodium dodecyl sulphate
spp.	Species
T	Thymine
TCP	Toxin coregulated-pilus
TEMED	N,N,N',N' tetramethylethylenediamine
Tlp	Transducer-like protein
UV	Ultra-violet
v/v	Volume/volume
w/v	Weight/volume
X-Gal	5' bromo-4' chloro-3' indolyl β -D-galactopyranoside

Chapter 1. Introduction

1.1. Overview

This introductory chapter will begin by exploring the history and the emergence of *Campylobacter jejuni* and *Campylobacter coli* as the leading cause of bacterial gastroenteritis in the developed world. The physiology, genomics, epidemiology and transmission of *C. jejuni* to humans will be reviewed in this chapter so that we can further our understanding of how this bacterium causes disease in humans.

Colonisation of the host intestine is a necessary prerequisite for pathogenesis of *C. jejuni*. Chemotactic motility has been shown to be necessary for both colonisation of the intestine and disease progression (Takata *et al.*, 1992, Yao *et al.*, 1997; Hendrixson and DiRita, 2004). Once the bacterium has colonised the intestinal mucosa it then up-regulates a number of virulence determinants which enables it to adhere to and invade the intestinal epithelium. The damage to and subsequent inflammation of the epithelium manifests as diarrhoea in humans. Chemotactic motility involves members of a two component signal transduction pathway, which helps the bacterium to navigate towards more favourable conditions. Environmental signals are detected by methyl-accepting chemotaxis proteins (MCPs) which are found at the cell surface. This signal is transduced from the cell surface to the flagellar motor to alter the direction of flagellar rotation. Characterising the MCPs in *C. jejuni* NCTC 11168 and determining the signals that these receptors respond to will be the primary focus of this dissertation and will be discussed in more detail towards the end of the introduction where the aims of this project can be found.

1.2. Campylobacter

1.2.1. History

Although it has long been suspected that the campylobacters were first observed over a century ago by Theodor Escherich in 1886, it was not until 1913 that the first report of a *Campylobacter* infection was made. A vibrio-like organism was isolated from aborted ovine fetuses (McFadyean and Stockman, 1913). These infections were reported to be by *Vibrio fetus*, but are now known to be by *Campylobacter fetus*. *C. fetus* is commonly associated with septic abortion and reproductive tract infections in cattle and sheep (Skirrow, 1994 & Allos, 2001). The campylobacters were originally placed in the genus *Vibrio*. It was not until 1963 that the new genus-*Campylobacter* was formed (Sebald & Veron, 1963).

In 1957 a study carried out by Elizabeth King established for the first time, a link between *Campylobacter* and humans suffering from acute gastroenteritis. Developments in filtration techniques in the early 1970s meant that *Campylobacter* could be isolated directly from a human stool sample (Dekeyser *et al.*, 1972; Butzler *et al.*, 1973). Further progress followed in diagnostic microbiology laboratories when Skirrow, in 1977, developed a specific media which had been supplemented with vancomycin, trimethoprim and polymyxin B that selected for campylobacters over other gastrointestinal bacteria. It was the development and wide-spread use of this selective media that brought to attention by the end of the 1980s that *C. jejuni* was the most frequent bacterial causes of diarrhoea world-wide (Allos, 2001).

1.2.2. Species

The genus *Campylobacter* is comprised of 16 species, 12 of which cause disease in humans (Lastovica and Skirrow, 2000). These species have been placed in three groups based on similarity of their 16S ribosomal RNA gene sequences. The first of these groups includes *C. hyointestinalis*, *C. lanienae*, *C. mucosalis* and *C. fetus*. All of these species are commonly found in the intestines of large animals and shared features include resistance to nalidixic acid and an inability to hydrolyse indoxyl acetate (On, 2005). The next group includes species which are mainly resident in the oral cavity in humans; this includes *C. consisus*, *C. hominus*, *C. gracilis*, *C. sputorum*, *C. curvus*, *C. showae* and *C. rectus*. These species are anaerobic and grow better in the presence of atmospheric hydrogen. The third and final group, which are often referred to as the thermophilic campylobacters, includes *C. jejuni*, *C. coli*, *C. lari*, *C. upsaliensis* and *C. helveticus*; these are known or suspected enteropathogens. *C. coli* and *C. jejuni* are the most significant human pathogens in the *Campylobacter* genus. *C. jejuni* is responsible for 80-90% of all reported cases of acute gastroenteritis in the developed world (Ketley, 1997). The thermophilic campylobacters' optimum temperature for growth is 42°C, which may reflect an adaptation to the avian gut where this group of bacteria are most commonly found (On, 2005). Although *C. jejuni* is an important human pathogen our understanding of the virulence mechanisms this bacterium uses to cause disease is limited. However, the release of the complete genome sequence of *C. jejuni* NCTC 11168 (Parkhill *et al.*, 2000) and the development of strategies for random and site directed mutagenesis have enabled the better understanding of this bacterium.

1.2.3. Physiology

C. jejuni belongs to the delta-epsilon group of proteobacteria (On, 2005). *C. jejuni* is a spirally curved, slender, Gram-negative rod shaped bacterium. It is approximately 1.5-6.0 µm long and 0.2-0.5 µm wide (Ketley, 1997 & Park, 2002). *C. jejuni* is highly motile by means of a polar flagellum, which is positioned at either one end or both ends of the cell (van Vliet and Ketley, 2001). *C. jejuni* is microaerophilic which means that it requires a low oxygen environment of between 3-15% O₂ (and 3-10% CO₂, 85% N₂) for optimal growth. The campylobacters are naturally transformable organisms (Ketley, 1997). It is suspected that *C. jejuni* undergoes a morphological change from being spirally curved to a coccoid form upon exposure to environmental stresses such as a shortage of nutrients or exposure to atmospheric oxygen concentrations (Rollins and Colwell, 1986). When *C. jejuni* is in its coccoid form it may enter a viable non-culturable (VNC) state, where it is dormant but is non-culturable by standard laboratory methods. This VNC state may help *C. jejuni* survive under unfavourable conditions which do not support its growth, for example upon transmission between hosts. However, the very existence of this coccoid form has been questioned and is still awaiting experimental confirmation (van Vliet and Ketley, 2002).

The campylobacters are surprisingly sensitive to environmental stresses when it is outside of the host. They appear to lack adaptive response mechanisms that are commonly found in other pathogenic bacteria. It is apparent from the genome sequence that *C. jejuni* NCTC 11168 lacks the global regulator RpoS that is commonly found in other Gram negative bacteria (Parkhill *et al.*, 2000). The RpoS global regulator is responsible for protecting the bacterial cell when it enters into the stationary phase or when it is exposed to environmental stresses. The campylobacters

are unable to replicate at temperatures below 30°C. Cold shock proteins have been reported in other bacteria which enable them to resist cold temperatures and continue growing (Hazeleger *et al.*, 1998). However no known cold shock proteins have been found in *C. jejuni* (Parkhill *et al.*, 2000). Although *C. jejuni* appears to lack these adaptive response mechanisms it is still metabolically active at low temperatures, even down to temperatures as low as 4°C. Campylobacters show a gradual reduction in growth at low pH and growth is inhibited below pH 4.9 (Park, 2002). Subjecting the campylobacters to a pH lower than pH 4.9 can be harmful (Blaser *et al.*, 1980). In general, campylobacters are fastidious organisms and are usually grown in complex growth media. They are unable to ferment carbohydrates, so amino acids are usually added to the growth media as a carbon source.

1.2.4. Genomics

C. jejuni NCTC 11168 has a chromosome of 1,641,481 base pairs (bp) (Parkhill *et al.*, 2000). This is relatively small in comparison with other enteropathogens such as *E. coli* whose genome is approximately 4.5 Mb, a size almost three times bigger than that of *C. jejuni* (van Vliet and Ketley, 2001). It is estimated that the *C. jejuni* NCTC 11168 genome encodes for 1,654 proteins and 54 stable RNA species. *C. jejuni* NCTC 11168 has a low GC content (30.6 %) which makes it highly AT rich (Parkhill *et al.*, 2000). These AT rich sequences can present some difficulties when trying to clone into *E. coli* (van Vliet and Ketley, 2001). These AT rich sequences can also be misinterpreted in *E. coli* as promoter sequences (Ketley, 1997). A significant proportion of the *C. jejuni* genome encodes for proteins (94.3%) (Parkhill *et al.*, 2000).

One interesting finding from the genome sequence of *C. jejuni* NCTC 11168 was the absence of homologues of classical virulence mechanisms. Examples of such virulence mechanisms include type III protein secretion apparatus and the presence of pathogenicity islands, both of which are present in *Helicobacter pylori*, which is closely related to *C. jejuni* (Bereswill and Kist, 2003). Other findings from the genome sequence included the absence of any inserted sequence (IS) elements, transposons, retrons or prophages (Parkhill *et al.*, 2000). The discovery of hypervariable sequences in the NCTC 11168 genome sequence by Parkhill *et al.* (2000) came as an unexpected finding. These hypervariable sequences are essentially short homopolymeric runs of nucleotides and have been found amongst genes involved in the biosynthesis of LOS, extracellular polysaccharide (EP) or genes involved in flagella modification (Parkhill *et al.*, 2000). Variation in the tract length of these homopolymeric sequences may be produced by mechanisms such as slipped-strand mispairing during DNA replication (Linton *et al.*, 2000). These mechanisms could subsequently alter the transcription and translation of the genes involved in the biosynthesis of bacterial surface structures giving rise to phase variation (Linton *et al.*, 2000).

Other unusual findings from the genome sequence of *C. jejuni* NCTC 11168 included the presence of only four DNA repeat sequences in the whole genome (Parkhill *et al.*, 2000). The genome of *C. jejuni* is not very well organised as most genes do not appear to be grouped into operons or clusters which often means that functionally unrelated genes are co-transcribed (Parkhill *et al.*, 2000). There are certain exceptions to this lack of organisation and these include the two ribosomal protein operons and the genes involved in the biosynthesis of lipooligosaccharide (LOS), EP and flagellar modification, which are all arranged in clusters (Parkhill *et*

al., 2000). As *C. jejuni* is unable to ferment carbohydrates for energy, very few genes capable of degrading carbohydrates were found (Parkhill *et al.*, 2000).

Since the release of the genome sequence of *C. jejuni* NCTC 11168 other *Campylobacter* genomes have been sequenced. These include *C. lari* strain RM2100, *C. upsaliensis* strain RM3195 and *C. coli* strain RM2228 (Fouts *et al.*, 2005). *C. jejuni* strains that have been sequenced since NCTC 11168 include the strains: RM1221, 81-176 and 81116 (Fouts *et al.*, 2005; Hofreuter *et al.*, 2006; Pearson *et al.*, 2007). *C. jejuni* RM1221 differs from the NCTC 11168 strain in that it contains four large integrated elements (Fouts *et al.*, 2005). *C. jejuni* 81-176 is a highly pathogenic and invasive strain and is known to contain two plasmids: pVir and pTet (Bacon *et al.*, 2000; Hofreuter *et al.*, 2006). It is predicted that between 19 and 53% of *C. jejuni* strains are able to maintain plasmids however none of the strains NCTC 11168, RM1221 nor 81116 contain plasmids. The presence of plasmids in *Campylobacter* spp. is not believed to contribute to pathogenicity. The pVir plasmid of *C. jejuni* 81-176 contains 54 open reading frames (ORFs) of which four ORFs are comparable to components of type IV secretion systems (Bacon *et al.*, 2000; Hu and Kopecko, 2005). Site specific mutagenesis of each of the four putative type IV secretion genes resulted in a reduction in invasion of intestinal epithelial cells (INT407) by *C. jejuni*. One of the mutants made in *C. jejuni* 81-176 (a *virB11* homologue) showed reduced virulence in the ferret diarrhoeal disease model compared to the wild-type strain 81-176 (Bacon *et al.*, 2000; 2002; Hu and Kopecko., 2005). It is notable that *C. jejuni* NCTC 11168 is unable to cause disease in the ferret diarrhoeal model of disease (Bacon *et al.*, 2000).

1.2.5. Transmission

Campylobacter spp. are found in the gastrointestinal tract of wild and domesticated animals including poultry, sheep, cattle, dogs and cats (Park, 2002). Although a commensal organism in the intestinal tracts of these animals, *C. jejuni* does have the potential to cause symptoms of disease. It is notable that for human infection the most common reservoir for *C. jejuni* is poultry, examples of which include: chickens, turkeys, ducks and geese (Miller and Mandrell, 2005). In poultry, *C. jejuni* principally colonises the lower gastrointestinal tract which includes the caeca, large intestine and cloaca (Beery *et al.*, 1988). Furthermore, histological examination of the caecum from an 8-day old chicken inoculated with *C. jejuni* has revealed that *C. jejuni* penetrates deep into the mucus covered crypts of the large intestine (Beery *et al.*, 1988). *Campylobacter* is associated with disease in humans and it has been proven that as few as 500 organisms are enough to cause disease (Blaser *et al.*, 1980; Black *et al.*, 1988). The consumption and handling of under cooked poultry is one of the most common sources of *Campylobacter* infection for humans (Allos, 2001). The consumption of unpasteurised milk and untreated water are also considered significant sources of *Campylobacter* infection for humans (van Vliet and Ketley, 2001). The prevalence of *C. jejuni* in poultry is remarkably high and as many as 10^{10} cfu of *C. jejuni* have been reported per gram of caecal contents (Shreeve *et al.*, 2000). Research has shown that when a bird contaminated with *Campylobacter* is placed in a flock of birds that are otherwise *Campylobacter*-free, three days later the entire flock is colonised (Shanker *et al.*, 1990). Possible explanations for such rapid dissemination of *Campylobacter* amongst the flock of birds may be due to the communal food and water supply becoming faecally contaminated (Shanker *et al.*, 1990). Another possible

explanation could be that the chickens were ingesting contaminated faeces directly (coprophagy) (Miller and Mandrell, 2005).

1.2.6. Clinical presentation and epidemiology

Recent Figures for 2008, reported to the Health Protection Agency (HPA) revealed that the number of cases of *Campylobacter* for England and Wales were as many as 49, 880 (Figure 1.1). As this is the number of laboratory confirmed cases it is thought that the actual number of cases in the population could be 10 times greater (Adak *et al.*, 2002). The numbers of *Campylobacter* infections reported to the Health Protection Agency (from 1992-2004) were significantly higher than the number of cases resulting from other enteric pathogens such as *Salmonella* and *Shigella*, which are often considered by the media to be more newsworthy (www.hpa.org.uk/cdr/archives/archive05/enteric05.htm).

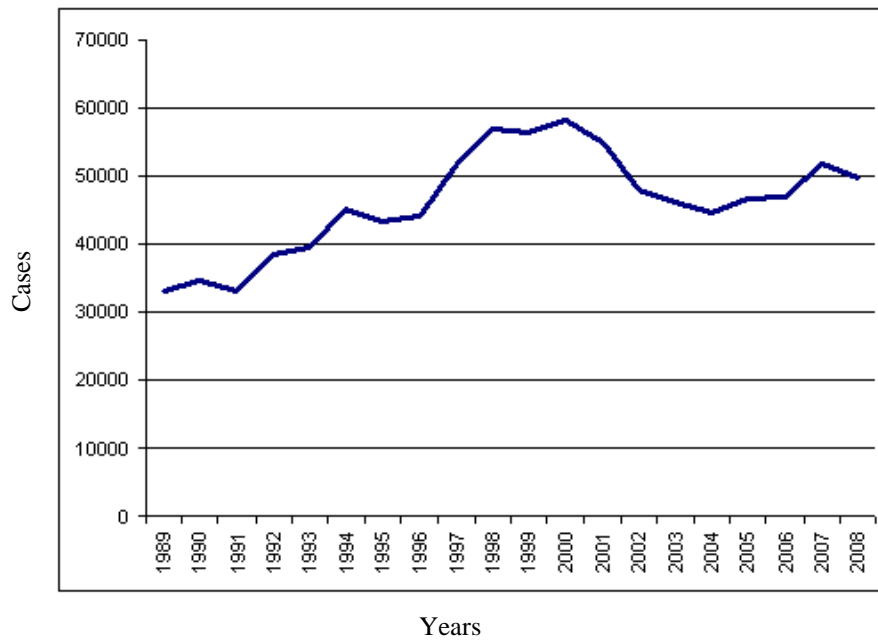


Figure 1.1. The number of *Campylobacter* cases reported to the health protection agency (HPA) for England and Wales from 1989 to 2008. In 2008 49, 880 cases were reported to the HPA. The peak of *Campylobacter* infections occurred in 1998 (58, 089 cases; taken from www.hpa.org.uk/infections/topics_az/campy/data_ew.htm)

1.2.6.1. Disease outbreaks in developed countries

Persons infected with *C. jejuni* in the industrialised nations usually present with acute gastroenteritis. Following an initial incubation period of 24-72 hours, severe inflammatory diarrhoea will ensue and the presence of red blood cells and leukocytes in the stools is commonly observed in most cases (Allos, 2001). Infected individuals can have up to 8-10 bowel movements per day at the summit of infection (Young and Mansfield, 2005). Infection is usually accompanied by a range of symptoms which includes high fever, acute abdominal pain, nausea and general malaise (Madigan *et al.*, 2003). *C. jejuni* infection is self limiting as it is common for the infection to clear up within a week without any complications. Patients with acquired immune deficiency syndrome (AIDS), the elderly and pregnant women represent those groups of people that are at greater risk, as campylobacteriosis can be chronic and more invasive in immunocompromised individuals (Allos, 2001). The highest incidence of *C. jejuni* infections in industrialized nations is seen in young adults (Wooldridge and Ketley, 1997). The incidence of *Campylobacter* infections appears to demonstrate a seasonal pattern where the number of cases of *Campylobacter* peak at the beginning of the year and once again in the summer; this fluctuation may be a reflection of holiday periods when there is increased consumption of poultry products.

1.2.6.2. Disease outbreaks in developing countries

C. jejuni infection in the developing world could result in one of three possible outcomes: severe inflammatory illness, mild watery diarrhoea or an asymptomatic carrier state (Young and Mansfield, 2005). Severe inflammatory diarrhoea tends to occur more commonly in young infants below the age of two versus young adults

which is seen in the developed world (Allos, 2001). Any kind of diarrhoeal sickness in young infants can be dangerous. *C. jejuni* is responsible for a high proportion of mortality and morbidity in infants suffering with acute gastroenteritis (Young and Mansfield, 2005). Asymptomatic carriage and shedding of *C. jejuni* is common in young adults living in the developing world (Pazzaglia *et al.*, 1991). Nevertheless, it is extremely rare for healthy individuals in the developed world to be infected with *C. jejuni* without exhibiting any overt symptoms. Also there is no seasonal pattern link with the incidence of *C. jejuni* infections in the developing world. Some of the differences in the symptoms presented in individuals from the developing versus the developed world could be due to strain variation. However there must be other contributing factors because isolates of *C. jejuni* strains which cause watery diarrhoea in infants living in developing countries have also been found in visitors who were suffering with acute inflammatory diarrhoea (Skirrow and Blaser, 1992). One plausible explanation for the milder symptoms seen in individuals from the developing world may be due to them having had previous exposure to *Campylobacter* strains. Those persons living in the developing world have developed partial immunity to *C. jejuni* as well as other microbes that may be found in the environment, thus a milder response to *C. jejuni* is commonly observed (Calva *et al.*, 1988 and Taylor, 1988). In contrast, in the developed world, individuals are less likely to have had any previous exposure to *C. jejuni* or other *Campylobacter* strains and an acute inflammatory response is typical.

1.2.6.3. Post-infection complications

C. jejuni infection has been associated with a range of diseases, examples of which include: proctitis, septicaemia, meningitis and haemolytic uremic syndrome (Young

and Mansfield, 2005). Long term complications associated with *C. jejuni* infection include autoimmune disorders such as Guillain-Barré syndrome (GBS) and Miller Fisher syndrome (MFS). GBS and MFS are both diseases that target the peripheral nervous system and lead to acute flaccid paralysis (Nachamkin *et al.*, 1998). The symptoms associated with MFS include ophthalmoplegia as well as a loss of limb reflexes (areflexia) and general muscle weakness (ataxia) (Fischer, 1956). Persons affected with GBS progressively lose motor and sensory control of the lower extremities to begin with which can later spread to the upper extremities (Nachamkin *et al.*, 1998). Loss of tendon reflexes like in MFS also occurs, weakness of the respiratory muscles can occur (one third of patients) in GBS patients which can mean that they will need mechanical ventilation (Nachamkin *et al.*, 1998). The disease is self limiting, but symptoms can persist for 2 to 3 weeks and recovery can take place over a period of weeks or even months (Nachamkin *et al.*, 1998). Although the majority of people with GBS go on to fully recover a small proportion of individuals never make a full recovery and are left with long term neurological damage (Nachamkin *et al.*, 1998). Although the chances of developing GBS after *C. jejuni* infection is extremely low (<1 case of GBS per 1000 *C. jejuni* infections), one third of all cases of GBS have proceeded after a *C. jejuni* infection (Allos, 2001). Molecular mimicry between the host peripheral nerve glycolipids and the surface polysaccharide structures found in the *C. jejuni* cell wall is considered to be responsible for *C. jejuni* induced GBS (Allos, 2001; van Vliet and Ketley, 2001).

1.3. Pathogenesis

1.3.1. Colonisation

Upon entry into the host via either contaminated food or water, *C. jejuni* is presented with a number of different innate immune defence mechanisms which enable humans to protect themselves against bacterial pathogens. The presence of gastric acid in the stomach helps protect the host from invading bacteria. A study carried out by Black *et al.* (1988) showed that patients who were defective in gastric acid production were at greater risk of infection by *Campylobacter*. Once *C. jejuni* has successfully made its way through the inhospitable conditions found in the stomach, the continual motion of peristalsis in the small intestine makes it difficult for the campylobacters to remain in one place. The campylobacters colonise the distal end of the small intestine as well as the colon. For successful colonisation the campylobacters need to be able to penetrate the thick mucus layer found covering the intestinal epithelial cells. The mucus layer is not only a physical barrier but it is also a chemical barrier that is composed of anti-microbial compounds as well as antibodies such as immunoglobulin A.

Research carried out by Lee *et al.* (1986) showed that *C. jejuni* colonises mucus along its outer surface. *C. jejuni* has a preference for colonising the caecal crypts within the intestine (Lee *et al.*, 1986). Gnotobiotic and germ free mice were used as a model of mucus colonisation by *C. jejuni* in this study and using a range of microscopic techniques the researchers were able to show that the campylobacters were highly motile in preparations of gut tissue (Lee *et al.*, 1986). The campylobacters were seen to track quite rapidly along the mucosal surface (Lee *et al.*, 1986). Lee *et al.* (1986) concluded that the ability to colonise the mucosal surface is a key virulence determinant in *C. jejuni* pathogenesis. The researchers of this study

failed to find any evidence for adhesion of *C. jejuni* to epithelial cells found in the gut mucosa (Lee *et al.*, 1986). However since this study, the campylobacters have been shown to adhere to intestinal epithelial cells through (1) outer membrane proteins (OMPs), (2) outer membrane associated structures such as lipopolysaccharide (LPS) and the flagella itself has been implicated as a secondary adhesin (McSweeney and Walker, 1986; Pei *et al.*, 1998; Konkel *et al.*, 1999; Ziprin *et al.*, 1999; Jin *et al.*, 2001). For successful disease progression a bacterial pathogen needs to be able to colonise the mucosal surface, adhere to and go onto invade the underlying intestinal epithelial cells. Invasion of the intestinal epithelium results in cell death and tissue inflammation in the gut and subsequent diarrhoea due to the ensuing damage to the absorptive epithelium (Everest *et al.*, 1992). *C. jejuni* has developed virulence strategies which enable it to escape host immune defence mechanisms which will now be discussed in the next section (1.3.2).

1.3.2. *C. jejuni* virulence factors

Enteric campylobacters are thought to up-regulate a number of putative virulence mechanisms that enable them to successfully colonise the host intestine and overcome host immune defence mechanisms. Motility is conferred by the flagellum in *Campylobacter* spp. and this has been one of the most intensively studied virulence mechanisms in *Campylobacter* so far (Ketley, 1997). Flagellum based motility has been shown to be an important virulence determinant for many other pathogenic bacteria including *Vibrio* spp., *Helicobacter* spp., and *Proteus* spp. (Josenhans and Suerbaum, 2002). Other virulence mechanisms of importance in pathogenesis include: iron acquisition, adhesion and invasion, the production of toxins, motility and chemotaxis. Each of these virulence determinants will be discussed excepting the

role of chemotaxis in *C. jejuni* pathogenesis, which will be discussed in more detail later (see section 1.5.4).

1.3.2.1. Acquiring iron from the host

Iron is an essential nutrient for not just microorganisms but any living organism. Iron is a cofactor in a number of enzymes that are involved in important cellular processes such as DNA synthesis. Although iron is essential in most biological processes, too much iron can also be detrimental to the host. An excess of iron coupled with oxygen leads to the production of harmful reactive oxygen species through Haber-Weiss-Fenton chemistry (Wooldridge and van Vliet, 2005). Therefore balancing the levels of iron within the host is essential, and in humans this is tightly regulated (Palyada *et al.*, 2004). As iron is needed by all the cells and tissue in the human body, iron is circulated around the body in blood complexed to the iron binding protein-transferrin. In the host intestine, which is the principal site for colonisation by *C. jejuni*, lactoferrin binds iron in mucosal secretions. A number of iron acquisition systems are found in *C. jejuni* that are up-regulated under low iron conditions (Miller, 2009). One of these iron acquisition systems, the haemin/haemoglobin uptake system is encoded by *chuABCD* (Ridley *et al.*, 2006). Various bacteria are known to secrete low molecular weight iron binding proteins known as siderophores (siderophores have a very high affinity for iron) in to their surroundings. These siderophores scavenge iron from host iron-binding proteins. However, no siderophore biosynthesis genes have been found within the genome of *C. jejuni* NCTC 11168 (Parkhill *et al.*, 2000). Nevertheless, it has been shown that *C. jejuni* can use exogenous siderophores produced by other bacteria by a process known as ‘siderophore piracy’ (Schubert *et al.*, 1999).

1.3.2.2. Motility as a virulence determinant

Motility in *C. jejuni* is principally conferred by the flagella, which can be found at the cell poles at either one or both ends of the cell (van Vliet and Ketley, 2001). *C. jejuni* is well suited for the viscous mucus found in the intestine, as it is spirally curved in shape and is highly motile in this environment (Lee *et al.*, 1986; Szymanski *et al.*, 1995). *C. jejuni* is able to avoid being moved along the intestine by the motion of peristalsis and is able to escape from the intestinal lumen and penetrate the mucus barrier so that it can get to the underlying intestinal epithelial cells (van Vliet and Ketley, 2001).

Factors such as the pH and viscosity of the growth medium have been shown to have a significant effect on *C. jejuni* motility (Szymanski *et al.*, 1995). The results from this study also showed that *C. jejuni* showed a significant increase in binding to and invasion of differentiated Caco-2 cells when carboxymethylcellulose was added to the growth medium in order to mimic the natural viscosity of the gut (Symanski *et al.*, 1995). It was originally perceived that *Campylobacter* spp. were only able to invade cultured cells when coinfecting with other enteropathogens such as *Shigella* or *Salmonella*, it has since been shown that the *C. jejuni* can invade HEp-2 cells (human tracheal epithelial cell line) alone (Hu and Kopecko, 2005). The interesting finding was that invasion of Hep-2 cells was enhanced in the presence of mucin (de Melo and Pechere, 1988).

The importance of flagella in *C. jejuni* pathogenesis was demonstrated when part of the FlaA flagellin of *C. coli* was fused with the maltose binding protein (MBP) of *E. coli* to form an effective subunit vaccine against *C. jejuni* (Lee *et al.*, 1999). The amino and carboxyl terminal of the flagellin protein in *C. jejuni* appears to contain a high degree of sequence homology with other bacterial flagellins (Nuijten *et al.*,

1990a), such as those found in *Salmonella* Typhimurium and *Bacillus subtilis* (Ketley, 1997). The flagellum in *C. jejuni* is highly immunogenic, thus it is a likely target for the host immune response. As well as being glycosylated, DNA rearrangements within the flagellin locus and slipped-strand mispairing mechanisms in glycosylation genes, highlight some of the different ways *C. jejuni* maintains antigenic variation of its flagellum (Nuijten *et al.*, 2000; Karlyshev *et al.*, 2002).

Research has shown that the flagellin genes in *C. jejuni* are subject to phase and antigenic variation (Caldwell *et al.*, 1985; Harris *et al.*, 1987). This means that *C. jejuni* is able to switch the flagellin genes on and off depending on whether or not the flagellum is needed. The production of the flagellum imposes a massive energy toll on the cell. A vast amount of cellular energy is required to not only produce the flagellum but to propel the flagella as well, hence its expression needs to be tightly regulated. The study carried out by Caldwell *et al.* (1985) showed that flagella biosynthesis was switched off in laboratory media but switched on *in vivo* once inside a rabbit intestine. In addition, this study carried out by Caldwell *et al.* (1985) demonstrated that flagella based motility is an important virulence determinant in the host intestine and in the pathogenesis of *C. jejuni* infection (Caldwell *et al.*, 1985).

Flagellum based motility has been shown to be necessary for adherence to and invasion of intestinal epithelial cells (Wassenaar *et al.*, 1991; Grant *et al.*, 1993; Yao *et al.*, 1994). Mutants made in the *flaA* flagellin gene leads to an aflagellate and non-motile phenotype. These *flaA* mutants lose their ability to adhere to and invade human embryonic intestinal (INT407) cells (Wassenaar *et al.*, 1991; Yao *et al.*, 1994). Adherence to INT407 cells by aflagellate mutants (*flaA*⁻) can be restored in part by centrifugation of these mutant cells onto host cells (Wassenaar *et al.*, 1991). However it is notable that invasion ability could not be restored in these

nonflagellated mutants indicating that the flagellum must play an additional role in invasion (Hu and Kopecko, 2005). A *pflA* mutant created in *C. jejuni* 81-176 has an intact full-length, but paralysed, flagellum. The paralysed flagella mutant was able to adhere to but was unable to invade, INT407 cells (Yao *et al.*, 1994). These studies demonstrate that motility is not only required to reach and adhere to the epithelial cells, but is also required for subsequent invasion *in vitro* (Wassenaar *et al.*, 1991; Yao *et al.*, 1994). Aflagellate (*flaA*⁻) and *pflaA* mutants have also been tested in the intestinal tracts of suckling mice as well as in three day old chicks and in both studies the authors concluded that a fully motile and intact flagellum is required for colonisation (Morooka *et al.*, 1985; Nachamkin *et al.*, 1993).

Flagellum based motility has been shown to be an important virulence determinant for many other pathogenic bacteria including *Vibrio* spp., *Helicobacter* spp., and *Proteus* spp. (Josenhans and Suerbaum, 2002). *H. pylori*, like *C. jejuni*, is spiral shaped and motility in *H. pylori* is conferred by five sheathed flagella, which are also found at the cell pole (Ottemann and Miller, 1997; Anderman *et al.*, 2002). *H. pylori* is the causative agent of chronic gastritis, gastric ulcers as well as gastric cancer (Ottemann and Miller, 1997). Flagella based motility has been shown to be important for gastric colonisation (Eaton *et al.*, 1996). Mutants created in flagellar components or the flagella genes (*flaA* and *flaB*) affected the ability of this bacterium to colonise the gastric mucosa in the gnotobiotic piglet model of disease (Eaton *et al.*, 1996).

Vibrio cholerae is the causative agent of cholera in humans (Boin *et al.*, 2004). *V. cholerae* is also a gastrointestinal pathogen like *C. jejuni* and motility in this bacterium is conferred by a single polar flagellum. Cholera is a waterborne disease and is commonly transmitted to humans through contaminated food or water. This

bacterium also colonises the small intestine like *C. jejuni*, but causes disease by producing the potent cholera toxin (CT) which is responsible for the damage caused to the host intestine. The damage caused to the host intestine usually manifests itself as severe watery diarrhoea. No gene encoding CT has been found in *C. jejuni* NCTC 11168 (Parkhill *et al.*, 2000). Flagellum based motility has been implicated in pathogenesis of cholera infection and non-motile strains of *V. cholerae* were shown to be attenuated in an infant mouse model for colonisation (Correa *et al.*, 2000). The most interesting finding was that the chemotaxis genes in *V. cholerae* have been found to be the key regulators of CT production (Merrell *et al.*, 2002).

1.3.2.3. Adhesion to the host epithelium

Once *C. jejuni* has successfully breached the mucus barrier, it then needs to be able to adhere to the underlying intestinal epithelium. Bacterial pathogens commonly adhere to their host target structures by producing fimbrial structures (van Vliet and Ketley, 2001). However, no fimbrial candidate gene has been identified in the *C. jejuni* NCTC 11168 genome sequence. A number of adhesins have been implicated in the attachment of *C. jejuni* to host cells. Fibronectin is a component of the extracellular matrix and CadF is a fibronectin binding protein that has been shown to initiate the binding of *C. jejuni* with fibronectin (Konkel *et al.*, 1999). Another *Campylobacter* protein, PEB1, encoded by the *peb1A* locus, has been shown to play a key role in not only adherence and invasion of epithelial cells in culture, but also in intestinal colonisation in a mouse model (Pei *et al.*, 1998). The lipoprotein JlpA has also been shown to be involved in adhesion and is found on the *Campylobacter* cell surface (Jin *et al.*, 2001). Surface polysaccharide moieties have also been implicated in mediating attachment to host cells. Lipo-oligosaccharide (LOS) is a major chemical component

of the outer membrane in most Gram-negative bacteria (Fauchere *et al.*, 1986; McSweeney and Walker, 1986). These outer membrane structures have been shown to be sialylated which can make them appear similar to gangliosides found on host nerve cells. Antibodies produced by the host as part of the immune response to these outer membrane components can lead to nerve damage and this damage has been implicated as being responsible for the paralysis observed in GBS.

1.3.2.4. Toxin production in *C. jejuni*

Once *C. jejuni* has successfully adhered to the host intestinal epithelium, it is speculated that it is the release of toxins that predominantly enables *C. jejuni* to invade and translocate across the epithelium. The damage to the epithelium initiates an inflammatory response and the release of various inflammatory mediators (Wooldridge and Ketley, 1997). This results in net fluid loss, which is usually observed as inflammatory diarrhoea. So far, six different toxins have been reported to be produced by *Campylobacter* species including one related to the cholera toxin. However their role or even their very existence in *C. jejuni* remains controversial (Wassenaar, 1997).

One cytotoxin has been confirmed and has been identified from the genome sequence of *C. jejuni* NCTC 11168, this is the cytolethal distending toxin (CDT) (Parkhill *et al.*, 2000). The *C. jejuni* NCTC 11168 genome sequence contains the following three genes: *cdtA*, *cdtB* and *cdtC*, which encode the CDT (Parkhill *et al.*, 2000). CDT has been shown to be capable of arresting HeLa and Caco-2 cells in the G2 phase of the cell cycle and trigger their entry into cell death, possible nuclease activity has also been reported (Whitehouse *et al.*, 1998; Pickett and Lee, 2005). More specifically, CDT inhibits the formation of the cyclin/cdk (cyclin dependent

kinase) complex; cdc2/cyclin B, that permits cells to exit out of the G2 phase of the cell cycle and enter mitosis. Furthermore, insertional mutants generated of the *cdtB* toxin in *C. jejuni* demonstrated impaired invasiveness into blood, liver and spleen tissue in adult severe combined immunodeficient (SCID) mice (Purdy *et al.*, 2000). It is notable that the *cdtB* toxin mutation had no effect on colonisation.

1.4. Chemotaxis

1.4.1. The chemotaxis pathway

Bacterial chemotaxis is the basis of movement in bacteria either towards more favourable areas, which contain high concentrations of nutrients or away from areas containing toxins. Chemotaxis in bacteria involves a signal transduction pathway. In general all bacterial signal transduction pathways are composed of three basic core components (Bren and Eisenbach, 2000; Lux and Shi, 2004). Firstly, there are a set of bacterial chemoreceptors found on the cell surface that are responsible for sensing the extracellular milieu. Bacterial chemoreceptors are membrane spanning proteins that can be methylated at specific glutamate and glutamine residues on their receptor arm (Lux and Shi, 2004). Thus, they are more commonly referred to as methyl-accepting chemotaxis proteins (MCPs). Next, the signal needs to be relayed from the cell surface to the flagellar motor, altering the direction of flagellar rotation. This signal transfer is achieved through a phospho-relay system and involves members of a two-component regulatory family: the histidine kinase CheA and the response regulator (RR) CheY. CheY is responsible for transducing the signal from the receptor complex to the flagellar motor. Finally, all bacteria need an adaptation mechanism that enables them to return the receptor back to pre-stimulus status; this is achieved through changes in the methylation status of the MCP receptors.

1.4.2. Patterns of motility

E. coli is estimated to have between 5-8 flagella which are randomly distributed over its cell surface (Wadhams and Armitage, 2004). Bacteria have an uncoordinated three dimensional pattern of walk and tend not to swim in straight lines, but in curves (Armitage, 1999). Bacteria are too small to detect changes in levels of chemoeffectors along their length therefore they operate by temporally sensing the gradient and comparing it to a previous gradient (Armitage, 1999). Upon sensing a positive stimulus in the environment such as the presence of an attractant, bacteria are able to bias their random swimming pattern so that they can move towards a more favourable environment (Armitage, 1999; Stock and Re, 1999). The default setting for flagella rotation in *E. coli* is counterclockwise (CCW). When the flagella are rotating in a CCW direction the flagella coalesce to form a bundle, which is usually positioned at the cell poles, and the bacteria swim off smoothly. However, this smooth swimming pattern of motility is routinely disrupted, usually every few seconds, and flagella rotation is switched to clockwise (CW) rotation (Armitage, 1999). When the flagella are rotating in CW rotation the flagellar bundle formed from when the cells were swimming smoothly is forced apart and the cell tumbles. Thus two modes for motility exist in *E. coli*: CW rotation of the flagella where the bacteria tumble on the spot, and CCW rotation of the flagella which enables the bacteria to swim smoothly. In the absence of a chemical gradient or in the presence of a repellent, bacterial movement is random and flagella rotation is biased towards a CW direction (Madigan *et al.*, 2003; Wadhams and Armitage, 2004) (Figure 1.2).

If a bacterium has a single polar flagellum which is unidirectional i.e. only rotates in one direction, then the cell needs to have some way of changing direction (for example in *Rhodobacter sphaeroides*, the flagellum only rotates in one direction,

this is usually CW). This is overcome by the bacterium incorporating routine stops during flagellum rotation, during these stops the bacterium reorientates itself presumably due to brownian motion and once flagellum rotation has resumed the bacterium moves off in a new direction (Berry and Armitage. 1999; Madigan *et al.*, 2003). *C. jejuni* has a polar flagellum, which is positioned at either end of the cell (van Vliet and Ketley, 2001). *C. jejuni* is likely to change the direction it is moving in by switching the direction of motor rotation between CW and CCW. This means that the cell can either be pushed forwards or dragged backwards, depending on which direction of motor rotation (see Figure 1.3) (Madigan *et al.*, 2003).

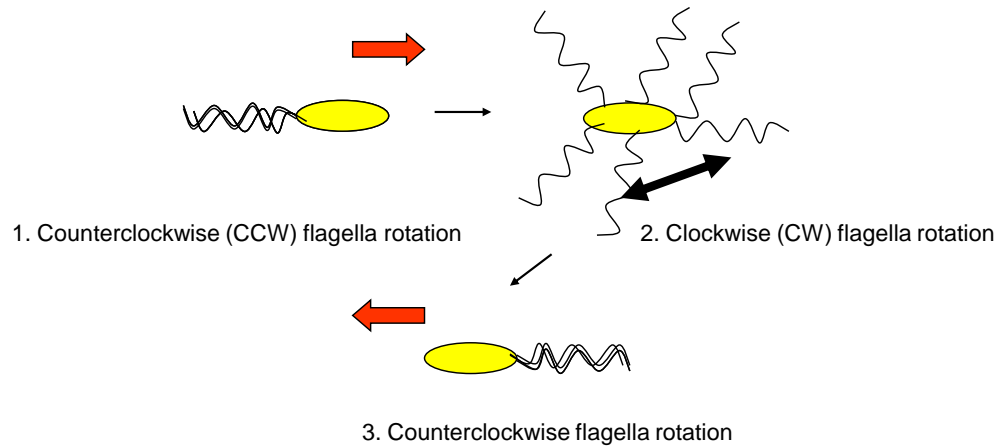


Figure 1.2. Flagella rotation in *E. coli*. When the flagella bundle together and rotate in a CCW rotation the bacterium swims smoothly in one direction¹. Conversely, when flagella rotation switches to CW the flagella pull apart and the bacterium subsequently tumbles on the spot. After the bacterium has tumbled it is usually facing in a new direction and swims off in this direction³ (adapted from Madigan *et al.*, 2003).

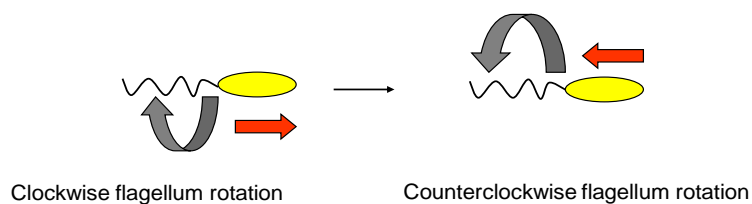


Figure 1.3. Flagellum rotation in *C. jejuni*. *C. jejuni* has a polar flagellum at either one or both ends of the poles. *C. jejuni* is able to change the direction in which it is moving in by changing the direction of flagellum rotation. CW rotation propels the cell forwards whereas CCW rotation drags the cell backwards (adapted from Madigan *et al.*, 2003).

1.4.3. Alternatives to the bacterial flagella

Although most bacteria are motile and swim freely through the operation of either singular or multiple flagella, this is not the only means by which bacteria are motile. Examples of other mechanisms of motility without flagella are well illustrated by the soil bacterium *Myxococcus xanthus* (Armitage, 1999; Wadhams and Armitage, 2004). This bacterium uses gliding or twitching employing a type-IV pili to move across surfaces. These pili protrude from the cell poles and are used to form an attachment to the surface over which the bacterium is gliding, these pili then retract which subsequently propel the bacterium forwards (Mattick, 2002). Free swimming, flagellated bacteria can move at speeds of $15\text{-}100\ \mu\text{m s}^{-1}$, whereas gliding bacteria move slowly (approximately $1\ \mu\text{m min}^{-1}$) (Wadhams and Armitage, 2004). *M. xanthus* exhibit two modes of motility: ‘adventurous’ and ‘social’ (Armitage, 1999). *M. xanthus* form vegetative swarms when in a nutrient rich environment and release a secretion consisting of proteases, lipases and nucleases into their immediate surroundings, which causes the lysis of other bacteria. When nutrients become scarce the cells clump together to form tight aggregates which transform into fruiting bodies with spores. An ‘adventurous’ pattern of motility enables individual cells to break free from the tightly formed aggregates and ‘social’ motility is when a group of cells move off together (McBride, 2001).

1.4.4. Chemotactic motility in the model organism *E. coli*

1.4.4.1. The structure and assembly of the flagella in *E. coli*

The flagella are helically shaped and are fairly rigid structures that are predominantly composed of the polymer flagellin. Each individual flagellum moves by a rotary motion, which is powered by the flagellum motor. This is different to what occurs in eukaryotes where the flagella flex versus rotating (Macnab, 2003). The flagellum in *E. coli* is built from the tip inwards and assembly involves the coordinated expression of approximately 50 different genes. At the base of the flagellum is a motor, which is built from a rotor and stator (Berg, 2003). The cytoplasmic component of the rotor is composed of approximately 32 FliG proteins. The rotor is also built from the proteins FliM and FliN, which all together (FliG, FliM and FliN) form the motor/switch complex to which the response regulator CheY interacts to alter the direction of flagellum rotation. The stator of the motor is made up of the two motor proteins MotA and MotB; approximately 8 independent motor proteins are required (Manson *et al.*, 1998). These two Mot proteins together form a proton channel that is anchored to the cell wall by MotB. It is the inward flow of protons through this channel which generates the torque for flagellum rotation. The motor complex found at the base of the flagellum has been described as a modified type III secretion system (Macnab, 2003).

The basal body is made up of three rings: the MS ring which is located just outside of the cytoplasmic membrane and is embedded in the inner cell membrane; the P ring which is found in the peptidoglycan layer of the cell envelope and finally the L ring which is embedded in the outer membrane. A rod traverses the periplasmic space and passes through the three rings (MS, P and L rings). The rod is made of the following proteins: FlgB, FlgC, FlgF and FlgG (Macnab, 2003). The protein FlgJ is

bifunctional because it is used to cap the end of the rod and digest away some of the peptidoglycan layer through muramidase activity. The flagellar filament is joined to the flagellar basal body via a hollow and flexible hook, which functions as a universal joint and is made of the hook protein FlgE (Macnab, 2003). An outline of the structure of the flagellum can be seen in Figure 1.4.

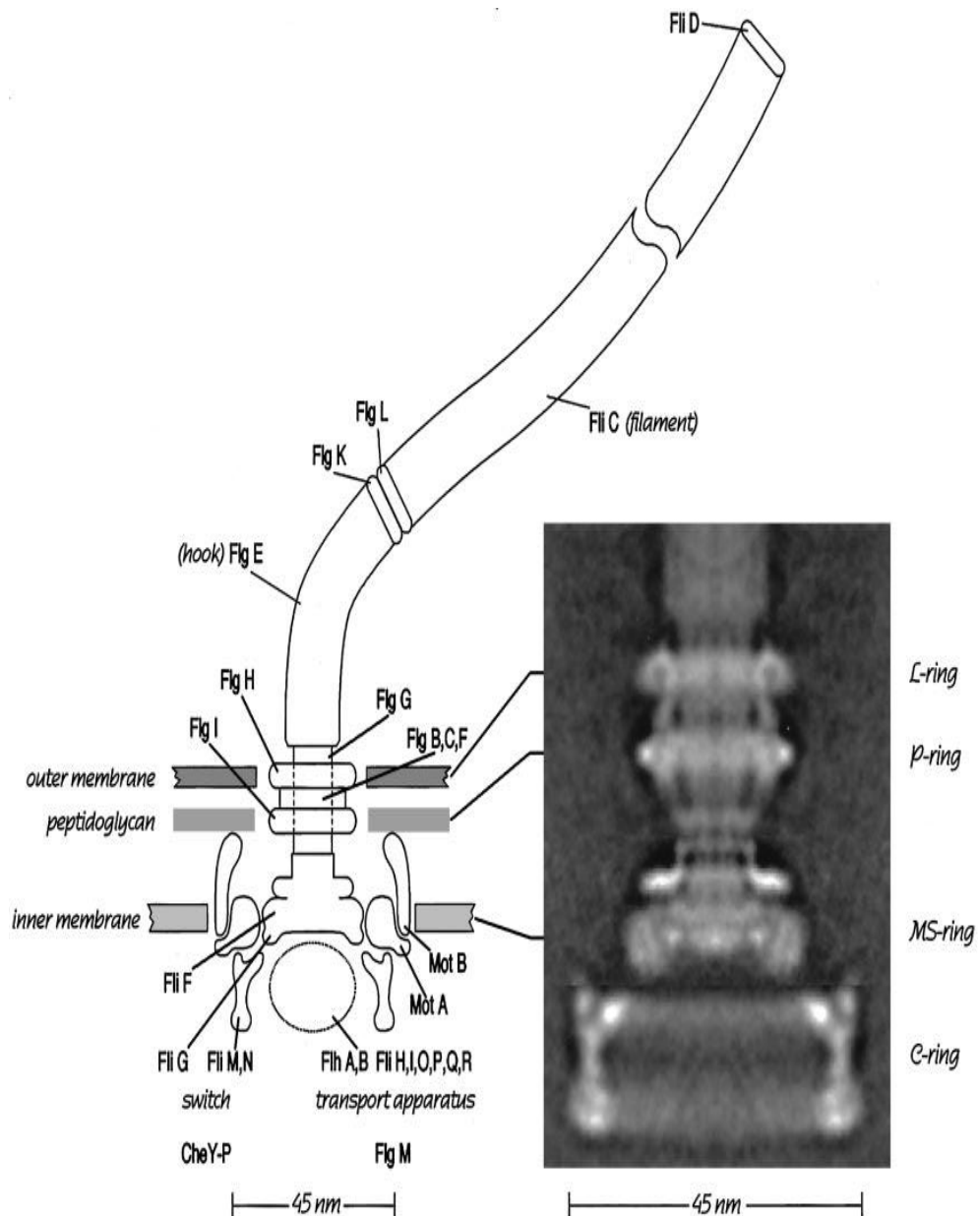


Figure 1.4. A Schematic drawing of assembly of the flagellum in enteric bacteria (this Figure has been taken from Berg, 2003). An Electron micrograph image is shown to the right of the schematic diagram which has been reconstructed from various reconstructions of hook basal bodies. For information regarding the protein components of the flagellum motor please refer to the text (see section 1.4.4.1).

1.4.4.2. The chemosensory pathway in *E. coli*

The chemotaxis systems in the enteric bacteria *E. coli* and *Salmonella enterica* serovar Typhimurium have been extensively characterised and are therefore considered the model organisms for bacterial chemotaxis signal transduction pathways (Wadhams and Armitage, 2004). In order to try and better understand bacterial chemotaxis the chemotaxis signal transduction pathway in the model organism *E. coli* will be discussed first and will be referenced later when reviewing the chemosensory components present in *C. jejuni* (see section 1.5.2). Environmental stimuli are detected by a set of MCP receptors located at the cell surface. *E. coli* has four MCP receptors with each of them differing in their ligand binding specificity (section 1.4.4.3) (Grebe and Stock, 1998). Chemotactic responses in *E. coli* towards individual ligands have been effectively quantified using the capillary tube method, which was originally developed by Adler in 1973. Essentially, this method involves the preparation of a chamber or “well” in which the bacteria are contained. In Adler’s method, a chamber was formed by laying a u-shaped capillary tube between a microscope slide and a cover slip. A capillary tube filled with a test chemical is immersed in the bacterial suspension. Following incubation for an appropriate period, the contents of the capillary tube are serially diluted and then transferred onto nutrient agar plates to determine the number of bacteria that have accumulated into the capillary tube. The numbers of bacteria which have migrated into a capillary tube containing buffer only are compared with those numbers of bacteria that have entered the capillary tube containing the test chemical. If the test chemical is an attractant then chemotactic and motile bacteria can detect the chemotactic gradient and bias their movement into the capillary tube. Therefore significantly higher numbers of bacteria would be expected to accumulate in the capillary tube containing an

attractant than a non-attractant compound. If the test compound is a chemorepellent then the compound can be placed into the chamber filled with the bacteria and determine whether the bacteria accumulate into a capillary tube containing buffer only to establish whether the bacteria are attempting to flee into the buffer only tube.

Chemotaxis in not only *E. coli* but all bacteria analysed to date involves members of a two component regulator family. The first member of the two component regulator family is the histidine kinase CheA. Although primarily functioning as a dimer, CheA exists as a 71 kDa monomer composed of five domains (known as P1-P5, starting from the N terminus to the C terminus) (Wadhams and Armitage, 2004). Autophosphorylation of CheA increases with (1) decreasing levels of attractant or (2) increasing levels of repellent. CheA autophosphorylates *in trans*, by transferring the gamma-phosphoryl group of ATP, which is found bound to the histidine (his) kinase catalytic core of one monomer, to the his48 phosphotransfer (HPt) domain of the cognate monomer (Wadhams and Armitage, 2004; and Re, 1999). CheA forms a quaternary complex with the cytoplasmic signalling domain of an MCP and the 18 kDa scaffold protein CheW *in vivo* (Armitage, 1999). CheW is composed of two SRC-Homology 3 (SH3) domains, but shows no catalytic activity (Armitage, 1999). The presence of CheW is essential for signal transduction as it forms the necessary link between the signalling domains of an MCP with CheA.

CheA interacts with CheY, which is another member of the two component regulatory family, at a conserved Asp57 (Aspartate) residue. CheY is a 14 kDa response regulator, which is composed of a single phosphorylatable response regulator domain and an active site that is able to catalyze phosphorylation, both of these features are conserved amongst CheYs. Phosphorylation of CheY at the Asp57 residue initiates a conformational change in CheY, which causes the release of CheY

from the Y-binding domain of CheA (Stock and Re, 1999). This conformational change in CheY ultimately reduces its affinity for CheA and concomitantly increases its affinity for the flagellar motor protein FliM (Welch *et al.*, 1993). CheY binding to FliM results in an alteration in flagellar rotation to CW, causing the cell to tumble (Wadhams and Armitage, 2004). Rapid termination of the initial signal input is essential in the bacterium as it needs to retain acute responsiveness to minute changes in chemoeffectors in the environment. Signal termination in *E. coli* is achieved through the activity of the phosphatase CheZ. The half-life of phosphorylated (CheY-P) is ~20 seconds however CheZ can dephosphorylate CheY in ~200 milliseconds (Wadhams and Armitage, 2004). It is noteworthy that the presence of CheZ was thought to be restricted to the β - and γ -subgroups of proteobacteria, however this may not be the case as orthologues of CheZ have been found in other phyla (Szurmant and Ordal, 2004).

Adaptation enables a cell to return back to a pre-stimulus status. Bacteria have to have the ability to rapidly terminate the initial signal and re-set their receptors back to a basal state, so that they are able to continuously detect minute changes in levels of chemoeffectors. Adaptation of an MCP in *E. coli* is achieved through the methylation activity of the methyltransferase CheB and methyltransferase CheR. CheR functions by continuously adding methyl groups onto the cytoplasmic portion of the MCP, whereas CheB removes these methyl groups and releases them as methanol into the cytoplasm. In addition to this, CheB also actively competes with CheY for the P2 binding domain on CheA and is phosphorylated by CheA on a conserved Asp56 residue (Wadhams and Armitage, 2004). Methylation specifically occurs on conserved glutamate and glutamine residues within the signalling domain of an MCP (Lux and Shi, 2004). The glutamine residues undergo deamidation to glutamate by

CheB, CheR then methylates glutamate as part of an S-adenosyl-methionine-dependent reaction (Lux and Shi, 2004). Figure 1.5 shows a summary of the signalling transduction pathway in *E. coli*.

E. coli also exhibits chemotaxis to substrates that are transported not through the MCP receptors but via the phosphoenolpyruvate (PEP)-dependent carbohydrate phosphotransferase system (PTS) (Alexandre and Zhulin, 2001). Transport of sugars occurs once the sugar has been phosphorylated by a membrane bound Enzyme II (EII) transport protein. EII then accepts phosphate from the PEP-dependent histidine kinase enzyme I (EI). The signal is then relayed to CheA via EI; which interacts directly with CheA to activate it by autophosphorylation. The signal is then transduced to the flagellar motor. It has been shown that PTS taxis occurs through a MCP receptor dependent manner in the bacterium *B. subtilis* (Alexandre and Zhulin, 2001).

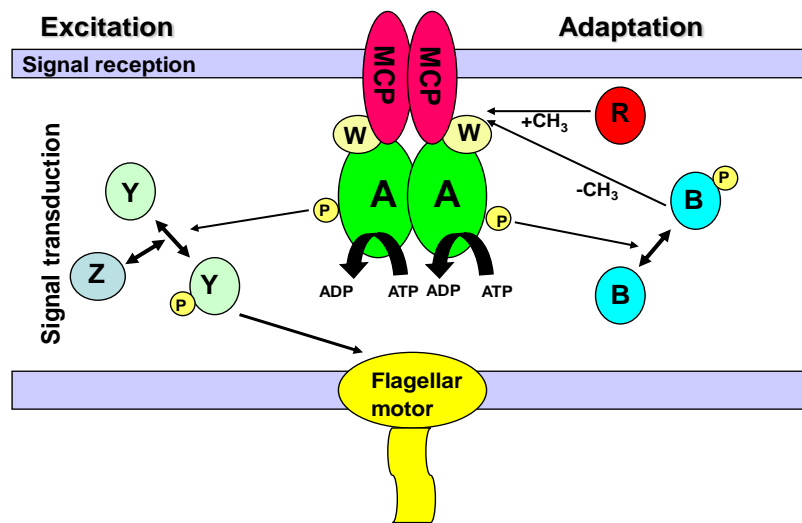


Figure 1.5. The signal transduction pathway in *E. coli*. In the absence of an attractant or in the presence of a repellent, CheA autophosphorylates and subsequently phosphorylates CheY, which then interacts with the flagellar motor to alter flagellar rotation to CW rotation (tumbles). CheY is then rapidly dephosphorylated by CheZ and the MCP receptors are de-sensitised to the initial signal by CheB, which demethylates the MCP receptors. Conversely, in the presence of an attractant, CheA autophosphorylation is inhibited and CheY is no longer able to interact with the flagellar motor complex, thus favouring CCW flagellar rotation (smooth runs). CheR is as a methyltransferase and thus methylates the MCP receptors. The MCP receptors eventually reach a point of saturation, through the continuous addition of methyl groups by CheR, at which point CheA autophosphorylation is no longer inhibited and CheB and CheY phosphorylation levels are restored back to pre-stimulus levels (Figure adapted from Lux and Shi (2004)).

1.4.4.3. The MCP receptors in *E. coli*

The MCP receptors are able to sense extra-cellular levels of chemo-attractants/repellents in the μM -nM range (Lux and Shi, 2004). Bacterial chemoreceptors are fundamentally composed of three core components. A periplasmic ligand-binding domain linked to a transmembrane domain(s), both of which are connected to the cytoplasmic MCP signalling domain (Figure 1.6) (Lux and Shi, 2004). *E. coli* has a total of five MCP receptors each of which has its own unique ligand binding specificity. Tar and Tsr are major receptors in *E. coli* and bind to the ligands aspartate and serine, respectively. It is estimated that there are several thousand copies of Tar and Tsr present on a single cell *versus* only a few hundred copies of the minor receptors Tap and Trg. The Tap receptor specifically binds to dipeptides, whereas the Trg receptor is specific for ribose and galactose (Sourjik, 2004).

Structural analysis of Tar, Tsr, Tap and Trg has shown that they are all composed of predominantly α -helical coiled-coil structures (Wadhams and Armitage, 2004). More specifically, the extra-cellular ligand binding domain is formed of four helix bundles. Two of these helix bundles further extend into the cytoplasmic domain to form the transmembrane segment of the receptor (Stock and Re, 1999). The cytoplasmic domains of all four MCPs form stable homodimers, which are further organized into trimers of dimers at the cell poles (Kim *et al.*, 1999). The MCPs link together with one another through the formation of disulphide bonds (Milligan and Koshland, 1988). The biological significance of clustering at the cell poles will be discussed in section 3.7.2. The MCPs contain a highly conserved signalling domain that appears to be conserved amongst bacteria and archaea, namely the HAMP ('histidine kinases, adenylyl cyclases, methyl-binding proteins and phosphatases')

domain (Lux and Shi, 2004). There appears to be a link between the membrane and the cytoplasm (Figure 1.5). Finally the signalling domain appears to serve two main functions. Firstly, the signalling domain contains at least 4 glutamate residues, which serve as a docking domain for CheR and CheB. Secondly, the signalling domain also has specific binding sites for CheA and CheW (Figure 1.6).

Aer is the fifth chemoreceptor in *E. coli* and is involved in aerotactic responses, which means that it senses changes in oxygen levels. It has a different structure compared to the other four *E. coli* MCPs in that the cytoplasmic signalling domain is comprised of an N-terminal Flavin Adenine Dinucleotide (FAD)-binding PAS domain (named after the three proteins it was first discovered in: Period circadian protein, Ah receptor nuclear translocator protein and the Single-minded protein (Wadhams and Armitage, 2004; Stock and Re, 1999). Aer also contains a hydrophobic sequence, which is thought to direct it to the membrane (Stock and Re, 1999). As the PAS domain in the Aer receptor is able to bind to FAD, it is therefore able to sense any changes in the redox state of elements in the electron transport system (Stock and Re, 1999).

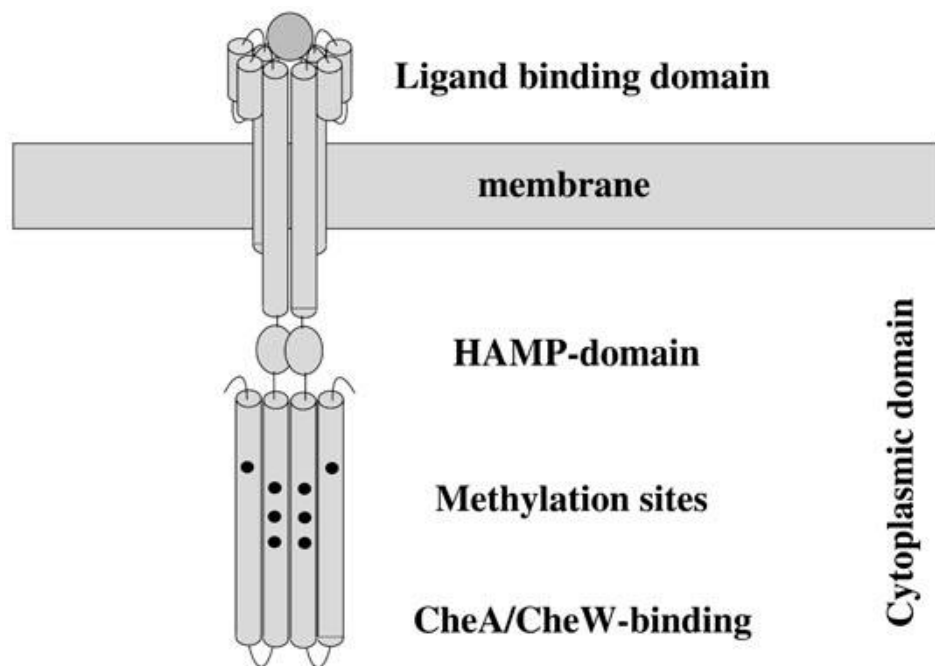


Figure 1.6. The structure of an MCP receptor. An MCP has an extra-cellular ligand binding domain at the cell surface and a transmembrane domain, which is connected to the cytoplasmic domain *via* a HAMP domain. The cytoplasmic domain of the MCP has docking domains for CheW/CheA and methylation sites for the methylesterase and methyltransferase CheB and CheR, respectively (figure taken from Lux and Shi, 2004).

1.4.4.4. The localisation of the MCP receptor clusters in *E. coli*

Interestingly, research has shown that the MCPs localise at the poles in *E. coli* (Maddock *et al.*, 1993). The clustering of MCPs has been shown to be reliant on the presence of CheA and CheW (Lux and Shi, 2004). The clustering of MCPs at the cell poles and along the length of the cells has not just been observed in *E. coli*, but MCP localisation appears to have been conserved through evolution in a diverse range of bacteria including *B. subtilis*, *R. sphaeroides* and *Caulobacter crescentus* and in *Archaea* (Gestwicki *et al.*, 2000; Armitage, 1999). The clustering of the MCP receptors at the cell poles helps to localize all the MCP receptors with differing ligand specificities at one point. Another function of clustering may be to increase the sensitivity of the MCPs to minute changes in chemoeffectors (Lux and Shi, 2004). This argument is supported by the observation that the MCPs in *E. coli* are able to sense chemoeffectors in the nm range (Sourjik, 2004). It is noteworthy that a large increase in attractant concentration has been shown to disrupt the polar localization of MCPs in both *E. coli* and *B. subtilis* (Lamanna *et al.*, 2005).

1.4.5. Alternative chemotaxis pathways in other bacteria

Although the chemotaxis systems in the enteric bacteria *E. coli* and *S. enterica* have been extensively studied and have been accepted as the model organisms for bacterial chemotaxis, they are not representative of chemotaxis systems in all bacteria. In fact bacterial species outside of the enterobacterial paradigm have chemotaxis systems that are often more complex and have chemosensory components that are absent in the enteropathogens. For example *R. sphaeroides* has multiple chemotaxis pathways which are adapted to different environments (Armitage and Schmitt, 1997; Szurmant and Ordal, 2004). Also many species have more putative MCP receptors than *E. coli*, for example *Pseudomonas aeruginosa* has 26 putative MCP receptors and unlike *E. coli* not all of these receptors are constitutively expressed (Guvener *et al.*, 2006).

Furthermore some species have MCP receptors that are missing transmembrane domains and have in fact been shown to be cytoplasmic (Wadhams *et al.*, 2002). By reviewing the chemotaxis pathway components present in *E. coli* and other bacteria will enable us to underline important differences between those chemosensory components found in other bacteria and those found in *C. jejuni* (Marchant *et al.*, 2002). When reviewing the chemotaxis pathway in *C. jejuni* it will become apparent that it too contains chemosensory components not present in *E. coli* (Marchant *et al.*, 2002; Korolik and Ketley, 2008).

1.4.5.1. The chemosensory system in *B. subtilis*

B. subtilis is a Gram-positive soil bacterium. The chemotaxis system in *B. subtilis* has also been studied in depth and offers an alternative chemotaxis mechanism to study that diverges away from the *E. coli* paradigm. *B. subtilis* encodes chemotaxis components that do not have counterparts in *E. coli*, this includes the proteins: CheC,

CheD, CheV and CheX (Szurmant and Ordal, 2004). One variation from the *E. coli* paradigm is that there is also no CheZ homologue in *B. subtilis*. In *E. coli* the flagellar switch is composed of FliM, FliN and FliG whereas in *B. subtilis* homologues of FliM and FliG exist but in place of FliN *B. subtilis* has FliY. It has been shown that dephosphorylation of CheY occurs at the flagellar switch by FliY which has been shown to have phosphatase activity (Szurmant *et al.*, 2003).

Another interesting variation from the *E. coli* paradigm exists in the phosphorylation pathway in *B. subtilis*. The phosphorylation pathway i.e. the flow of phosphate in *E. coli* is inverted in *B. subtilis*. For instance the binding of an attractant to the MCP receptor leads to increased CheA autophosphorylation and therefore also increased CheY-P versus a decrease in CheA and CheY phosphorylation, which is the case in *E. coli*. Also the default setting for flagellar rotation in *B. subtilis* is CW as opposed to CCW in *E. coli* and therefore in *B. subtilis* binding of CheY-P to the flagellar motor favours a smooth swimming phenotype over tumbling, which is observed in *E. coli*. Further variation from the chemotaxis system in *E. coli* will become more apparent when attempting to compare the chemotaxis system of *E. coli* with that of *C. jejuni* (Table 1.1).

The mechanism for adaptation in *B. subtilis* deviates significantly from the mechanism that exists in *E. coli*. Although the methyltransferase CheR and methylesterase CheB are both present in *B. subtilis*, the process of methylation also involves additional chemotaxis proteins: CheC, CheD and CheV. Methylation of the receptors is more tightly regulated in *B. subtilis* and methylation and demethylation of certain glutamate residues on the MCP receptors can result in different outcomes (Zimmer *et al.*, 2000). CheD has been shown to deamidate the MCP receptor arms on selected glutamine residues (Kristich and Ordal, 2002). Methanol is released upon the

addition and removal of an attractant both during methylation and demethylation of specific glutamate residues, which is not the case in *E. coli* as methanol is only released during demethylation. CheV is a fusion protein that is composed of two domains; at its N-terminus there is a CheW domain that is fused to a response regulator domain at the C terminus (Rosario *et al.*, 1994; Karatan *et al.*, 2001). CheV is thought to help couple the receptor to CheA as well play a role in adaptation (Saulmon *et al.*, 2004). A CheV homologue has also been discovered in the genome of *C. jejuni* NCTC 11168 and may play a similar role in the adaptation pathway in *C. jejuni* (Parkhill *et al.*, 2000). CheC in addition to its role in the adaptation pathway may also be involved in the dephosphorylation of CheY-P, as it has been shown to share some sequence homology at its N-terminal domain with the switch proteins FliM and FliY (Kirby *et al.*, 2001; Saulmon *et al.*, 2004; Szurmant *et al.*, 2003). CheX is also likely to aid in signal termination in *B. subtilis* as it too shares some sequence homology with the switch proteins (Park *et al.*, 2004). The role of CheX in chemotaxis as a phosphatase has already been demonstrated in the bacterium *Borrelia burgdorferi* (Motaleb *et al.*, 2005).

The *B. subtilis* genome encodes for 10 putative chemotaxis receptors (Kunst *et al.*, 1997). There are three MCP receptors: McpA, McpB and McpC (Hanlon and Ordal, 1994; Muller *et al.*, 1997); three transducer-like proteins TlpA, TlpB and TlpC (Hanlon and Ordal, 1994); the aerotaxis receptor HemAT (Hou *et al.*, 2000) and finally three further proteins of unknown function (Kunst *et al.*, 1997). It is known that McpB is the sole receptor for asparagine through a receptor methylation-independent or dependent mechanism, which occurs through changes in levels of attractant (Hanlon and Ordal, 1994; Zimmer *et al.*, 2002). It is also known that McpC is the receptor for azetidine-2-carboxylate and proline (Muller *et al.*, 1997).

1.4.5.2. Chemotaxis in *Sinorhizobium meliloti* and *Rhodobacter sphaeroides*

S. meliloti and *R. sphaeroides* belong to the alpha subgroup of *Proteobacteria*. These bacteria offer an alternative chemotaxis pathway to study compared to the chemotaxis system found in the enterics. The chemotaxis pathways that exist in these two members of the alpha subgroup of *Proteobacteria* are more complex than those found in the enterics (Armitage and Schmitt, 1997). Multiple chemotaxis systems, additional copies of chemotaxis genes as well as chemotaxis components with no homologues in *E. coli* are a few examples that illustrate the level of complexity and degree of variation that exist within members of the alpha subgroup of *Proteobacteria* (Wadhams and Armitage, 2004; Szurmant and Ordal, 2004).

S. meliloti is a Gram-negative soil bacterium and is most commonly found in plant root nodules where it is in symbiosis with leguminous plants. This makes *S. meliloti* capable of nitrogen fixation and it is subsequently able to convert atmospheric nitrogen into ammonium (Schmitt, 2002). *S. meliloti* has several flagella, but unlike *E. coli*, the flagella in *S. meliloti* are rigid *versus* being flexible and form right handed helical filaments. The flagellar filaments are composed of not one single flagellin subunit-as is the case in *E. coli*, but is composed of four flagellin subunits (Schmitt, 2002). The pattern of swimming in *S. meliloti* also differs significantly from that seen in *E. coli*, because in *S. meliloti* the flagellar motor is unidirectional, only rotating in one direction-this is most commonly in the CW direction (Armitage and Schmitt, 1997; Schmitt, 2002). This therefore raises the question of how does this bacterium change direction? What is peculiar about *S. meliloti* as well as other members of the alpha subgroup of *Proteobacteria* (for example *R. sphaeroides*) is that it is able to vary the speed of rotation of each of its individual flagellar motors, contrary to flagellar rotation in the enterics where flagellar rotation occurs at constant speed. This was

demonstrated when *S. meliloti* showed a gradual increase in swimming speed upon increasing amounts of the attractant proline a phenomenon known as chemokinesis (Sourjik and Schmitt, 1998). The chemotaxis (*che*) operon in *S. meliloti* contains the chemotaxis genes which encode CheA, CheW, CheR, CheB as well as two response regulators, which have been named CheY1 and CheY2 (Greck *et al.*, 1995). As *S. meliloti* lacks a homologue of the CheZ phosphatase, which is present in many enteric bacteria the question then arises-how does this bacterium rapidly dephosphorylate CheY-P? It has been shown that CheY2 alone interacts with the flagellar motor to influence flagellar rotation (Sourjik and Schmitt, 1996). CheY1 on the other hand behaves as a 'phosphate sink' by accepting phosphate from CheA and subsequently sequestering the majority of the phosphate from CheY2. Interestingly, it has been shown that any excess phosphorylated CheY2 that has not yet bound to the flagellar motor is able to retro-phosphorylate CheA (Sourjik and Schmitt, 1998). The phosphate is then subsequently shuttled to CheY1. This mechanism of retro-phosphorylation ensures rapid dephosphorylation of CheY2 and means that the bacterium retains its sensitivity to new stimuli (Sourjik and Schmitt, 1998).

S. meliloti appears to demonstrate positive chemotactic responses to a wide range of substrates which includes sugars and amino acids as well as to exudates from roots of legume plants (Meier *et al.*, 2007). *S. meliloti* has 9 putative chemoreceptors, eight of which encode for MCP receptors (McpS to McpZ) and one gene which encodes a transducer-like protein (Tlp) IcpA (Galibert *et al.*, 2001). The IcpA receptor and McpY both appear to lack transmembrane domains and are therefore based in the cytoplasm and are most likely responsible for sensing internal stimuli (Meier *et al.*, 2007). These receptors appear to detect changes linked to the metabolic

state of the cell. Furthermore it appears as if the genes *mcpU* and *mcpX* are expressed at a higher level than the other *mcp* genes (Meier *et al.*, 2007).

R. sphaeroides is a purple, non-sulphur bacterium which is able to grow aerobically as a heterotroph or anaerobically as a photoheterotroph (Armitage and Schmitt, 1997). The genome of this photosynthetic bacterium contains three operons which encode for *che* components that all appear to be necessary for both chemotaxis and phototaxis (Porter *et al.*, 2002). Two of these complete operons have been shown to be necessary for chemotaxis in an *in vitro* study (Porter *et al.*, 2002). In summary, these operons encode for: 13 chemoreceptors, four CheW, four CheA, six CheY, two CheB and three CheR homologues (Martin *et al.*, 2001). *R. sphaeroides* has a single flagellum. The flagellum is unidirectional and the bacterium switches direction by incorporating routine stops and varying the speed of the flagellum rotor (Armitage and Schmitt, 1997). During these periodic stops, the flagellum relaxes to form a short-wavelength, large amplitude coil which ultimately enables the cell to reorientate itself (Armitage and Schmitt, 1997).

R. sphaeroides has nine putative chemoreceptors (with transmembrane domains) and four cytoplasmic receptors (Wadhams *et al.*, 2000; Wadhams *et al.*, 2002; Wadhams *et al.*, 2003). The Tlps found in the cytoplasm are similar to the cytoplasmic Tlp receptors found in *S. meliloti*, which are responsible for sensing changes in levels of metabolite intermediates (Ward *et al.*, 1995; Armitage and Schmitt., 1997). TlpA in *R. sphaeroides* appears to regulate chemotaxis to all compounds under aerobic conditions as deletion of this gene resulted in impaired chemotaxis to these compounds. Whereas TlpB seems to be expressed under anaerobic conditions and deletions of this gene does not appear to have any significant effect on chemotaxis under aerobic or anaerobic conditions (Ward *et al.*,

1995; Armitage and Schmitt., 1997). The MCPs have all been shown to cluster at the cell poles and the Tlps have been found also to cluster together in the cytoplasm (Wadhams *et al.*, 2004).

1.5. Chemotaxis as a virulence determinant in *C. jejuni*

Chemotaxis and motility are intimately linked and have both been shown to be an important virulence determinant in *C. jejuni* pathogenesis *in vivo* in mice (Takata *et al.*, 1992), ferrets (Yao *et al.*, 1997) and in chickens (Golden and Acheson, 2002; Hendrixson and DiRita, 2004). The importance of chemotaxis in *C. jejuni* colonisation was first demonstrated when undefined non-chemotactic mutants with intact flagella failed to colonise the intestinal tract of suckling mice (Takata *et al.*, 1992). It has already been shown experimentally that *C. jejuni* is highly motile in a viscous environment such as the mucus found in the intestine (Szymanski *et al.*, 1995). Furthermore, chemotaxis towards mucin has been observed previously (Lee *et al.*, 1986). Human volunteers that were fed equal numbers of non-motile and motile bacteria only the motile bacteria could be recovered from stool samples (Black *et al.*, 1988). This was further supported in chickens as even when chickens were fed non-motile bacteria, only motile bacteria could be recovered (Jagannathan and Penn, 2005).

The chemotactic behaviour of *C. jejuni* was first characterised by Hugdahl *et al.* in 1988. The Hard Agar Plug (HAP) assay enabled the determination of the chemotactic response of *C. jejuni* to various chemicals. *C. jejuni* showed a positive chemotactic response to the amino acids L-aspartate, L -cysteine, L -glutamate and L -serine. More significantly, *C. jejuni* was attracted to L -fucose and L-serine which

are components of bile and mucin. *C. jejuni* displayed a negative chemotactic response to most other constituents of bile, which included cholic acid and deoxycholic acid.

Mutations have already been created in the *che* genes *cheY* response regulator and *cheA* histidine kinase, the results of which will be discussed here. The *cheY* gene has been implicated in *C. jejuni* pathogenesis as a *cheY* mutant has been shown to be defective in colonisation of the intestine in chickens (Hendrixson and DiRita, 2004). A *cheY* mutant has also been found to have an altered pattern of walk when compared to the wild type (Marchant *et al.*, 1998). However *cheY* mutants have also been found to be hyperinvasive and showed a threefold increase in adherence and invasion compared to the wild-type strain (Golden and Acheson, 2002; Yao *et al.*, 1997). CheA mutants in *C. jejuni* have also been shown to be unable to colonise mice and were shown to lose invasiveness when trying to invade intestinal epithelial cells (Hendrixson and DiRita, 2004; Chang and Miller, 2006). Tlp10 (Cj0019) is one of the putative chemoreceptors in *C. jejuni* and it is the only receptor so far to be shown to be required for chicken intestinal colonisation (Parkhill *et al.*, 2000; Hendrixson and DiRita, 2004).

1.5.1. The flagellum in *C. jejuni*

The flagellum of *C. jejuni* is unsheathed and its filament is principally composed of subunits of the structural protein flagellin (Madigan *et al.*, 2003). Flagellin has been shown to be encoded by the flagellin genes *flaA* and *flaB* (Nuijten *et al.*, 1990a). The flagellin genes are both approximately 1.7 kbp in size and share 95% sequence homology (Nuijten *et al.*, 1990a). The two flagellin genes are positioned adjacent to one another on the *C. jejuni* chromosome (Nuijten *et al.*, 1990b). The flagellin genes

flaA and *flaB* are independently transcribed from their own individual promoters and their expression is regulated by the σ^{28} and σ^{54} promoters, respectively (Wassenaar *et al.*, 1994). There are potentially three regulators of flagellar expression in *C. jejuni*: *rpoN*, *flgR* and *fliA*. These encode the alternative sigma factor σ^{54} , FlgR which is the σ^{54} associated transcriptional activator and the sigma factor σ^{28} respectively (Jagannathan *et al.*, 2001). The master regulator of flagellar gene expression present in the enteric *bacteria*, *flhDC*, is not present in *C. jejuni* (Jagannathan and Penn, 2005). It is worth mentioning that although most of the components required for flagellar assembly and regulation do exist in *C. jejuni* there are some differences worth mentioning (Jagannathan and Penn, 2005). Firstly, the *flgJ* gene which encodes the cap protein which has hydrolase activity is missing. There also appears to be two copies of the hook protein *flgE* and the second copy (*flgE2*) appears to be required for flagellar expression and motility in *C. coli* (Kinsella *et al.*, 1997).

A number of mutational studies have been undertaken to establish the roles of *flaA* and *flaB* in *C. jejuni*. Mutants generated in the *flaA* gene in *C. jejuni* (*flaA*⁻ *flaB*⁺) produce a short truncated flagellum and are non-motile (Nachamkin *et al.*, 1993; Wassenaar *et al.*, 1994; Nuijten *et al.*, 2000). In contrast, a *C. jejuni* *flaA*⁺ *flaB*⁻ mutant maintained an intact flagellum but had reduced motility compared to the wild-type (Wassenaar *et al.*, 1994). The *flaA* gene is also expressed at a higher level than the *flaB* gene and the flagellum is principally composed of the FlaA protein (Wassenaar *et al.*, 1994; van Vliet and Ketley, 2001).

C. jejuni contains two specific protein glycosylation systems: N-linked and O-linked (Karlyshev *et al.*, 2005). Although it has long been recognized that the flagellum is post-translationally modified, it is now known that the flagellin (particularly FlaA) is O-link glycosylated (Symanski *et al.*, 2003). Interestingly, the

flagellin in *C. jejuni* is not modified with sialic acid but with a number of monosaccharides, which are similar to the sugar pseudaminic acid (Szymanski *et al.*, 2003). There are approximately 50 genes that have been grouped to the putative flagellar glycosylation locus in *C. jejuni* NCTC 11168 (Szymanski *et al.*, 2003).

1.5.2. The chemosensory pathway in *C. jejuni*

The genome sequence of *C. jejuni* strain NCTC 11168 unveiled the presence of orthologues of chemotaxis regulatory genes (Parkhill *et al.*, 2000). Unlike in *E. coli*, the *che* genes in *C. jejuni* are not found clustered together but are found in three separate regions of the genome (Marchant *et al.*, 2002). What is even more intriguing is that the *che* genes are found amongst other genes that have no role in chemotaxis. Although *C. jejuni* contains the same common backbone i.e. the presence of CheA, CheY and CheW, there are some obvious differences which reveal a novel chemotaxis system in *C. jejuni* (Table 1.1).

CheA, CheY and CheV each contain a response regulator (RR) domain. CheY has all the conserved features characteristic of a response regulator domain, which suggests that it interacts with the flagellar motor, once it has been phosphorylated by CheA (Marchant *et al.*, 2002). CheA mutants have been tested in *C. jejuni* and have been shown to be defective in chemotaxis (whilst retaining motility) when tested on semi-solid agar (Hendrixson *et al.*, 2001; Bridle *et al.*, 2007). The presence of a RR domain in CheA is somewhat more unclear. The presence of extra RR domains has been observed in other organisms besides *C. jejuni*, such as *R. sphaeroides* (Armitage, 1999) and it has been suggested that these RR domains may act as a 'phosphate sink' helping to rapidly dephosphorylate CheY (Marchant *et al.*, 2002). In *B. subtilis*, CheV has been shown to be phosphorylated by CheA *in vitro* (Kirby *et al.*,

2000). CheV is a fusion protein comprised of the amino-terminal CheW domain and RR domain at the carboxyl terminal (Marchant *et al.*, 2002). The CheV protein in *B. subtilis* shows 23% identity with the *Campylobacter* CheV (Rosario *et al.*, 1994). *H. pylori* has three CheV proteins; one of which shares 41% identity with CheV in *C. jejuni* NCTC 11168 (Tomb *et al.*, 1997). However it has been shown that not all three of the CheVs in *H. pylori* are essential for chemotaxis; only CheV1 was shown to be necessary for chemotaxis (Pittman *et al.*, 2001). Furthermore this study also showed that none of the CheV paralogues were able to compensate for a *H. pylori cheW* null mutant (Pitman *et al.*, 2001).

Until recently it was thought that due to the presence of all of the extra RR domains in chemotaxis proteins in *C. jejuni* that the most plausible mechanism for rapid signal termination would be through a phosphate sink pathway; similar to the one seen in *S. meliloti* (section 1.4.5.2). However, it seems that the phosphatase CheZ may not just be restricted to the β and γ subgroups of the proteobacteria and may be present in the ϵ -proteobacteria too (Terry *et al.*, 2006). It was in *H. pylori*, a close relative of *C. jejuni*, that a distant homologue of CheZ was discovered, HP0170 (Terry *et al.*, 2006). Sequence analysis revealed that HP0170 shared 7 highly conserved residues with the CheZ phosphatase found in *E. coli*. HP0170 was only discovered upon the appearance of spontaneous *cheW* revertants on soft agar (Terry *et al.*, 2006). This study also detailed other bacteria that may also contain homologues of the CheZ phosphatase; *C. jejuni* was one of a number of bacteria to be mentioned. The protein *Cj0700* has been tested and been shown to be involved in chemotaxis in *C. jejuni* but furthermore has shown capable of interacting with CheA, CheY and CheV; all of which contain the extra RR domains (O. Bridle and J. Ketley, unpublished data). It is still plausible that the extra RR domains present in CheA,

CheY and CheV may still play a role in CheY dephosphorylation. With the absence of a RR domain in CheB and the presence of an RR domain in CheV, it could be speculated that CheV may directly inhibit CheB methylesterase activity (Marchant *et al.*, 2002). CheV has been implicated in the adaptation pathway in *B. subtilis* (Rosario *et al.*, 1994).

<i>E. coli</i>	<i>C. jejuni</i> 11168
CheA	CheA*additional RR domain
CheY	CheY
CheW	CheW
CheB	CheB*missing RR domain
CheR	CheR
CheZ	Cj0700
-	CheV*contains RR domain

Table 1.1. A comparison of the chemotaxis proteins present in *E. coli* with those in *C. jejuni*. Differences in chemotaxis components present/absent in the two organisms are indicated (*).

1.5.3. The MCP receptors in *C. jejuni*

In silico analysis of the *C. jejuni* NCTC 11168 genome sequence identified the presence of orthologues of 10 chemotaxis genes and two aerotaxis genes (Parkhill *et al.*, 2000; Marchant *et al.*, 2002). The MCPs are also commonly referred to as Tlps (transducer-like proteins) and were identified through the presence of a signalling domain that could be readily methylated. In 2002, Marchant *et al.* attempted to put into groups all of the MCPs based on overall structural similarities (Figure 1.7). Thus,

the MCPs were finally classified into four groups (A-C) and the two aerotaxis genes were grouped separately from the MCPs to form the fourth group (Figure 1.7).

The Group A receptors (Tlps: 1, 2, 3, 4 and 10) (see Table 1.2) are characteristic of a 'classic' MCP receptor in that they have a periplasmic-ligand binding domain, transmembrane domain(s) and a signalling domain that can be methylated (Figure 1.6). This suggests that the Group A receptors are responsible for sensing changes in the extracellular environment. The presence of differing periplasmic domains in all Group A receptors further suggests that they must each sense a different range of signals external to the cell. The Tlps in Group A are typically similar to the MCPs found in *E. coli* (Wadhams and Armitage, 2004). However, unlike the MCPs in *E. coli* little is known about the signal that these MCPs respond to. One unique feature of the *C. jejuni* genome is the lack of repetitive DNA sequences. There are only four repetitive DNA sequences in the entire *C. jejuni* genome. It is therefore noteworthy that the carboxyl-terminal signalling domains of Tlps 2, 3 and 4 are identical copies of repeat 1 (Parkhill *et al.*, 2000).

Unlike the other Group A Tlps, the Tlp7 (Cj0951c) receptor in *C. jejuni* NCTC 11168 is composed of only a C-terminal signalling domain. The absence of transmembrane domains and a periplasmic ligand-binding domain in Tlp7 in *C. jejuni* indicates that it is unlikely to be involved in sensing external signals similarly to the other Group A Tlp receptors. It is proposed that Tlp7 in at least *C. jejuni* NCTC 11168 could be a pseudogene. Although Tlp7 could still be a MCP if there was continual read through upstream of the open reading frame (*orf*) of *cj0951c* into *cj0952c* (Parkhill *et al.*, 2000; Korolik and Ketley, 2008). The Cj0952c receptor contains transmembrane domains and does resemble MCPs found in other bacteria.

The adjoining of the *orfs* of *cj0951c* and *cj0952c* would make Tlp7 a functional Tlp in some strains of *C. jejuni* (Korolik and Ketley, 2008). The likelihood of the Group A receptors (Tlp1, 2, 3, 4, 7 and 10) being present in all strains of *C. jejuni* is variable; this is shown in Table 1.2. To date, the Tlp10 (Cj0019) and Tlp4 (Cj0262) receptors are the only chemoreceptors in *C. jejuni* found to be required for chicken intestinal colonisation (Hendrixson and DiRita, 2004).

Energy taxis in *E. coli* is regulated solely by the Aer protein (see section 3.7.1; Bibikov *et al.*, 1997). There is evidence to support that *aer2* (*cetB*) and *tlp9* (*cetA*) may also regulate a similar energy taxis response in *C. jejuni* (Hendrixson *et al.*, 2001; Vegge *et al.*, 2009). CetA (for *C**ampylobacter* *e**nergy* *t**axis*) contains a transmembrane domain and a highly conserved domain. There are two Aer proteins in *C. jejuni*, namely Aer1 (Cj1191) and Aer2 (Cj1189/CetB). A random transposon mutagenesis screen undertaken by Golden *et al.* (2002) was able to demonstrate that mutants defective in the *aer1* gene had no effect on motility or energy taxis (Hendrixson *et al.*, 2001). Cj1189 (Aer2/CetB) contains a PAS (an acronym of the genes found to contain the repeat sequences) domain which is predicted to bind to the cofactor flavin adenine dinucleotide (FAD) similarly to the Aer protein in *E. coli* (Bibikov *et al.*, 1997). It is proposed that CetB uses FAD as a redox sensor to monitor electron transport and then via direct interaction with CetA transduces this signal into the chemotaxis pathway to subsequently alter flagellar rotation. An energy taxis mechanism such as the one described here would be beneficial to the campylobacters as it would enable them to move towards energy generating environments (Hendrixson *et al.*, 2001; Korolik and Ketley, 2008).

The Tlps 5, 6 and 8 form Group C. These receptors are different to the other MCPs in *C. jejuni* in that they only contain a cytoplasmic domain. Interestingly, these

are very similar to the Group C receptors found in *Halobacterium salinarum* (Zhang *et al.*, 1996). They are likely to sense signals internal to the cell.

Chemoreceptor/Gene	11168	81116	RM1221	81176
Tlp1 (<i>cj1506</i>)	+	+	+	+
Tlp2 (<i>cj0144</i>)	+	+	+	+
Tlp3 (<i>cj1506</i>)	+	+	+	-
Tlp4 (<i>cj0262</i>)	+	+	-	+
Tlp7 (<i>cj0951/0952</i>)	+	+	-	+
Tlp10 (<i>cj0019</i>)	+	+	+	+

Table 1.2. Chemoreceptors in different strains of *C. jejuni*. This table shows the presence (+) or absence (-) of the Group A chemoreceptors in different *C. jejuni* strains (Figure adapted from Korolik and Ketley, 2008).

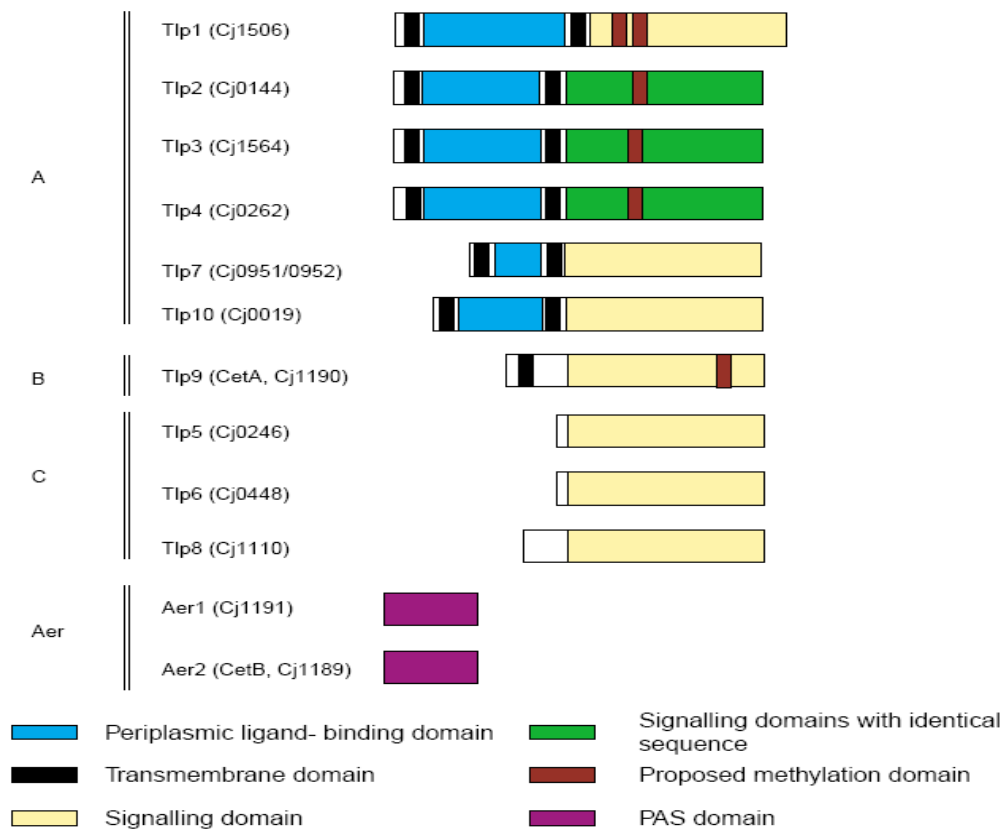


Figure 1.7. Domain organisation of the 10 chemoreceptor orthologues and two aerotaxis genes identified in *C. jejuni* NCTC 11168. The *tlp* and aerotaxis genes have been placed into groups based on overall structural similarities (refer to section 1.5.3 for more information regarding these receptors; Figure taken from Marchant *et al.*, 2002).

1.6. Project Aims

The intestinal tract is the natural habitat for the campylobacters, the overall objective of this dissertation is to further our understanding of the sensory system *C. jejuni* uses to detect and respond to external influences present within this harsh environment.

Although research has been done on the cytoplasmic components of the chemotaxis system in *C. jejuni* (Hendrixson and DiRita, 2001; Bridle, MPhil thesis), little progress has been made on elucidating the roles of the chemoreceptors in *C. jejuni* chemotaxis. Six of the ten putative Transducer-like proteins (Tlp, 1, 2, 3, 4, 7 and 10; Parkhill *et al.*, 2000; Marchant *et al.*, 2002) identified in the *C. jejuni* NCTC 11168 genome display a classical MCP domain organisation within their secondary structures similar to the arrangement found in the MCPs of *E. coli*. Those Tlps which contained a periplasmic ligand-binding domain (PLD), and contained proposed methylation sites (indicating that they are capable of adaptation to external stimuli) are going to be investigated in this study (Tlp 1-4, excluding Tlp7 and Tlp10, which were missing these proposed methylation sites). Furthermore, Tlp7 is proposed to be a pseudogene, at least in *C. jejuni* NCTC 11168.

Previous research has shown that Tlp4 (Cj0262c) and Tlp10 (Cj0019c) are necessary for successful colonisation of the chick gastrointestinal tract (Hendrixson and DiRita, 2004). In order to determine what role Tlps 1-4 fulfil in *C. jejuni* chemotaxis, a set of isogenic mutants are to be created in this project. The mutagenesis strategy will require deleting a significant proportion of the open reading frame of the target gene and then subsequently replacing it with a selectable marker. The selectable marker will identify the Tlp mutant further on in this work, once the insertionally inactivated copy of the gene has recombined back into the *C. jejuni* chromosome.

Chemotaxis assays are an essential part of this present study, particularly if the phenotype/ligand-binding specificity of the *tlp* mutants are to be determined. The only chemotaxis assay that had been firmly established in the laboratory previous to this study was the swarm assay (Marchant, PhD thesis; Bridle, MPhil thesis). In order to verify any mutant phenotypes revealed upon testing the mutants in chemotaxis assays, the wild-type phenotype will need to be restored. As *C. jejuni* NCTC 11168 is unable to maintain plasmids, the wild-type copy of the gene to be complemented is to be reintroduced into ribosomal RNA clusters present on the *C. jejuni* chromosome carrying the mutation (Karlyshev and Wren, 2005).

The hard agar plug (HAP) assay (Hugdahl *et al.*, 1988) will be used to determine the specific receptor-ligand binding specificity of the Tlps. The HAP assay will need to be first optimised using wild-type *C. jejuni* cells, before it can be used to test the *tlp* mutants. Chemotactic responses will be determined using putative *C. jejuni* chemoattractants (Hugdahl *et al.*, 1988). An attempt will also be made to develop a quantitative, chemotaxis assay using wild-type *C. jejuni*.

It is also unknown at this stage, where in the cell the Tlps are located. Thus, one further objective of this study will be to determine the proximity of the Tlps in the *C. jejuni* cell. It is already known that for all bacteria tested to date, all MCP receptors appear in clusters at the poles of the cell (section 1.4.4.4; Armitage, 1999). This aim will be specifically addressed by creating GST-tagged fusions with conserved domain structures in Tlps1 to 4. The purified proteins will be used to generate a polyclonal antibody, which will be used to localise the Tlps in *C. jejuni*. An attempt will also be made to express and purify the PLD of Tlp1 (His-tagged). The PLD will be used to determine the specific ligand-binding specificity of the Tlps using a NMR spectroscopy based technique.

2. Materials and Methods

2.1. Bacterial strains and plasmids

Details of the bacterial strains, vectors and plasmids used or constructed in this study are provided in Tables 2.1, 2.2 and 2.3.

Table 2.1. Bacterial strains used/produced in this study.

Strain Name	Genotype/features	Source/Reference
<i>C. jejuni</i> NCTC 11168	Wild-type clinical isolate	National Collection of Type Cultures, Colindale, London, U.K, (Parkhill <i>et al.</i> , 2000).
<i>C. jejuni</i> NCTC 11168 Motile Variant	Motile Variant isolated from the wild-type strain <i>C. jejuni</i> NCTC 11168	Bridle, MPhil thesis.
<i>C. jejuni</i> 81116 FlaAB	<i>FlaAB::aphA-3</i> (Km ^R)	M. Wösten and Wassenaar <i>et al.</i> , 1991).
<i>C. jejuni</i> RS01Tlp1Mut	<i>C. jejuni</i> NCTC 11168 $\Delta cj1506c::cat$ (Cm ^R)	This study.
<i>C. jejuni</i> OB6CYM	$\Delta cheY::cat$ (Cm ^R)	Bridle, MPhil thesis.
<i>C. jejuni</i> OB3CAM	$\Delta cheA::cat$ (Cm ^R)	Bridle, MPhil thesis.
<i>C. jejuni</i> RS02Tlp2Mut	<i>C. jejuni</i> NCTC 11168 $\Delta cj0144::ermC'$ (Ery ^R)	This study.
<i>C. jejuni</i> RS03Tlp3Mut	<i>C. jejuni</i> NCTC 11168 $\Delta cj1564::ermC'$ (Ery ^R)	This study.
<i>C. jejuni</i> RS04Tlp4Mut	<i>C. jejuni</i> NCTC 11168 $\Delta cj0262::cat$ (Cm ^R)	This study.
<i>C. jejuni</i> 11168- $O\Delta tlp1::cat\Omega IG(16S rRNA-23S RNA)::tlp1-aphA3$	<i>C. jejuni</i> NCTC 11168 $\Delta cj1506::cat$ (Cm ^R) with the addition of the wild-type copy of the <i>cj1506</i> gene (Km ^R)	This study and Hartley-Tassell <i>et al.</i> , 2010 (Appendix 1).
<i>E. coli</i> DH5 α E	F Φ 80 <i>lacZ</i> Δ M15 $\Delta(lacZYA-argF)$ U169 <i>deoR recA1 endA1 hsdR17</i> (r _K ⁻ , m _K ⁺) <i>gal⁻ phoA supE44 λ^- thi⁻1 gyrA96 relA1</i>	Invitrogen (Paisley, UK).
<i>E. coli</i> DS941	AB11157 <i>recF143 lacI^f lacZ</i> Δ M15	Pham <i>et al.</i> , 2002.
<i>E. coli</i> BL21	<i>F⁻, ompT, hsdS</i> (r _B ⁻ , m _B ⁻), <i>gal, dcm</i>	New England Biolabs (NEB, Hitchin, UK).

<i>E. coli</i> Rosetta	Lactose permease (<i>lacY</i>) mutant, deficient in <i>lon</i> and <i>ompT</i> proteases; contains plasmid encoding <i>argU</i> , <i>argW</i> , <i>glyT</i> , <i>IleX</i> , <i>leuW</i> , <i>metT</i> , <i>proL</i> , <i>thrT</i> , <i>thrU</i> , and <i>tyrU</i>	Novagen
------------------------	---	---------

Table 2.2. Vectors used or created in this study.

Plasmids	Features	Antibiotic resistance marker	Source/Reference
pUC18 and pUC19	High copy number cloning vectors used for cloning; contains a multiple cloning site (mcs).	Amp ^R	NEB
pAV35	pBluescript vector containing a promoter, chloramphenicol acetyl transferase (<i>cat</i>) cassette which confers Cm ^R .	Amp ^R , Cm ^R	van Vliet <i>et al.</i> , 1998
pTrcHisB	Expression vector containing a polyhistidine tag.	Amp ^R	Invitrogen (Paisley, UK).
pRR	pRR complementation vector.	Amp ^R	Karlyshev <i>et al.</i> , 2005
pRRK	pRR vector containing cloned <i>aphA-3</i> gene.	Amp ^R , Km ^R	Ridley <i>et al.</i> , 2006
pRRKpoly	pRR vector containing cloned poly-linker from the pTrcHisB plasmid.	Amp ^R , Km ^R	This study
pRRE	pRR vector containing the cloned <i>ermC'</i> gene.	Amp ^R , Ery ^R	O. Bridle
pGEX-4T-1	Protein expression vector containing the sequence encoding a glutathione S-transferase (GST) moiety (26kDa).	Amp ^R	GE Healthcare (Chalfont St.Giles, UK)
pLEICS-05	Protein expression vector containing a poly-histidine tag.	Amp ^R	Dr X. Yang (Protein Expression Laboratory, University of Leicester).
pRDH215	pUC18 vector containing the <i>aphA-3</i> gene (Km ^R)	Amp ^R , Km ^R	Dr R. D. Haigh

	with cloned terminator sequence from the <i>Campylobacter flaA</i> gene.		
--	--	--	--

Table 2.3. Plasmid constructs created in this study.

Plasmid	Features	Size of insert	Antibiotic resistance marker	Reference
pRS01	The <i>cj1506c</i> gene from <i>C. jejuni</i> NCTC 11168 cloned in pUC19 between the <i>EcoRI</i> and <i>KpnI</i> sites.	2875 bp	Amp ^R	This study
pRS02	The <i>cj1506c</i> gene with 940 bp of the ORF deleted and inserted into a <i>NotI</i> site created by the insertion of a Cm ^R cassette.	2752 bp	Amp ^R , Cm ^R	This study
pRS03	The <i>cj0144</i> gene from <i>C. jejuni</i> NCTC 11168 cloned in pUC19 between the <i>EcoRI</i> and <i>KpnI</i> sites.	3234 bp	Amp ^R	This study
pRS04	The <i>cj0144</i> gene with 926 bp of the ORF deleted and inserted into a <i>NotI</i> site created by the insertion of a Ery ^R cassette.	3354 bp	Amp ^R , Ery ^R	This study
pRS05	The <i>cj1564</i> gene from <i>C. jejuni</i> NCTC 11168 cloned in pUC18 between the <i>EcoRI</i> and <i>BamHI</i> sites.	3009 bp	Amp ^R	This study
pRS06	The <i>cj1564</i> gene with 923 bp of the ORF deleted and inserted into a <i>NotI</i> site created by the insertion of the <i>ermC'</i> gene.	3126 bp	Amp ^R , Ery ^R	This study
pRS07	The <i>cj0262c</i> gene from <i>C. jejuni</i> NCTC 11168 cloned in pUC19 between the <i>EcoRI</i> and <i>BamHI</i> sites.	1740 bp	Amp ^R	This study. R. Hall under the supervision of R. Sandhu.
pRS08	The <i>cj0262c</i> gene with 695 bp of the ORF deleted and inserted into a <i>NotI</i> site	2085 bp	Amp ^R , Cm ^R	This study

	created by the insertion of a Cm ^R cassette.			
pRS09	The pGEX-4T-1 expression vector containing the C' terminal, highly conserved signalling domain (HCSD) of <i>cj1506c</i> (<i>tlp 1</i>) translationally fused to a GST-tag.	996 bp (amino acids 358-688).	Amp ^R	GE Healthcare (Chalfont St.Giles, UK), this study
pRS10	The pGEX-4T-1 expression vector containing the HCSD of <i>cj0144</i> (<i>tlp 2</i>) translationally fused to a GST-tag (the HCSD present in <i>cj0144</i> is identical in sequence to the HCSD found in <i>cj1564</i> (<i>tlp 3</i>) and <i>cj0262</i> (<i>tlp 4</i>)).	1067 bp (amino acids 311-659).	Amp ^R	GE Healthcare (Chalfont St.Giles, UK), this study
pRS11	The pLEICS-05 expression vector containing the <i>cj1506c</i> (<i>tlp 1</i>) N-terminal, periplasmic signalling domain (PSD) translationally fused to a poly-histidine tag.	891 bp (amino acids 30-326).	Amp ^R	Dr X. Yang (Protein Expression Laboratory, University of Leicester) and this study.
pRS12	pRRK-poly complementation vector containing the <i>cj1506c</i> (<i>tlp 1</i>) gene cloned in between the <i>KpnI</i> and <i>BglII</i> restriction sites.	2517 bp	Amp ^R	Karlyshev <i>et al</i> , 2005, K. Ridley <i>et al</i> , 2006 and this study.

2.2. Bacterial culturing, growth conditions and storage

2.2.1. *Campylobacter jejuni*

All *C. jejuni* strains were routinely grown at 37°C in a Variable Atmospheric Incubator (VAIN) (Don Whitley Scientific Limited, Shipley, UK) which maintains an atmosphere of 85% nitrogen, 10% carbon-dioxide and 5% oxygen. Sealed gas jars containing a gas pack (2.5 litres) which provided a microaerobic environment were also used when required (CampyGen gas packs; Oxoid). *C. jejuni* strains were grown

predominantly on Mueller-Hinton agar (MHA; Table 2.4) which had been supplemented with trimethoprim and vancomycin (Table 2.5). Blood agar was used with poor growing mutant strains. Blood agar was prepared by adding 5% (w/v) defibrinated horse blood (Oxoid) to MHA. Specific antibiotics were added to the media when trying to select for *C. jejuni* mutant strains constructed by insertion of an antibiotic resistance cassette (Table 2.5).

2.2.2. *Escherichia coli*

E. coli strains were grown aerobically at 37°C in Luria-Bertani broth (LB; Roth, 1970) with shaking, at 200-250 rpm in a G10 Gyrotory shaker (New Brunswick Scientific Co., USA) or on either Luria-Bertani agar (LA) plates or M9 minimal media plates (see Table 2.4). *E. coli* strains plated out on LA plates were grown overnight (12-16 hours) whereas *E. coli* strains grown on M9 minimal media plates required a minimum of 48 hours before there was any visual evidence of growth. Following bacterial transformations by heat shock or electroporation (section 2.10.2), *E. coli* strains were recovered in SOC medium (Table 2.4). For the purpose of blue/white screening of bacterial colonies which contained the plasmid pUC19 or other derivatives of this plasmid, LA or M9 minimal media agar plates were supplemented with the lactose analogue-IPTG (Isopropyl- β -D-thiogalactopyranoside (0.2 mM) and the chromogenic substrate X-Gal (5-bromo-4-chloro-3-indolyl- β -D-galactopyranoside) (40 μ g/ml). LA plates were supplemented with antibiotics (Table 2.5) when selecting for *E. coli* strains containing recombinant plasmids (Table 2.3).

2.2.3. Storage and recovery of bacterial strains

Bacterial strains were stored long-term as glycerol stocks at -80°C (Sambrook and Russell, 2001). To prepare the glycerol stocks, *E. coli* and *C. jejuni* strains were grown on media plates until there was confluent growth after which all cells were harvested off plates using either Mueller-Hinton broth (MHB) or Luria-Bertani (LB) broth (Table 2.4) for *C. jejuni* and *E. coli* cells, respectively. The resulting cell suspensions were transferred to cryo-tubes and mixed with an equal volume of sterile, 25% (v/v) glycerol. *C. jejuni* and *E. coli* strains were recovered from frozen stocks by bringing them straight out onto dry ice. Bacterial cells were scraped off the surface of the frozen culture using a sterile cotton swab and transferred onto media plates. The bacterial cells were spread over the surface of the media using the cotton swab to ensure even distribution over the plate. *E. coli* strains were incubated overnight (O/N) at 37°C on LA (Table 2.4) plates after which they were routinely transferred in to LB and grown with shaking (supplemented with the appropriate antibiotics; Table 2.5). *C. jejuni* strains were grown on MHA plates and incubated in the VAIN cabinet for 2-3 days before being transferred onto fresh MHA plates and incubated for a further 48 hours. A confluent lawn of *C. jejuni* cells was usually visible after 5 days of incubation.

2.3. Media, Sterilisation and Supplementation

Any media used in this study is listed below in Table 2.4. Media was sterilised at 121°C, 15 lb/inch for 15 minutes by autoclave, unless otherwise stated. The media was cooled to 55°C before any antibiotics or other reagents could be added to the media. Once cooled, agar was poured into Petri dishes (Sterilin). Antibiotics, IPTG,

X-gal and solutions that could not be sterilised by autoclaving were sterilised by filtration. Filtration was carried out using a vacuum pump (Fischer scientific) and passing the required solution through a 0.22 µm filtered membrane using stericups (Millipore) or by using an acrodisc (PALL Life Sciences, Portsmouth UK) fitted to a 10 ml syringe (Beckton, Dickenson and Company, UK).

Table 2.4. Media used in this study.

Media	Components
Luria-Bertani (LB) medium	LB medium was prepared by mixing 1% (10 g/l) bacto-tryptone ¹ , 0.5% (5g/l) bacto-yeast extract ¹ and 1% (10 g/l) NaCl ² in 900 ml dH ₂ O. The medium was then adjusted to pH 7.0 with 10 M NaOH before the volume was adjusted to the final volume of 1 litre. Solid LB agar was prepared by addition of 15 g/l Bioagar ³ . The medium was sterilised by autoclaving.
Mueller-Hinton(MH) medium	MH broth (MHB; 30% (w/v) beef dehydrated infusion, 0.15% (w/v) starch and 1.75% (w/v) casein hydrolysate) was prepared by mixing 21 g of MHB powder in 1 litre of dH ₂ O. When preparing MH agar (MHA), 38 g of MHA powder ¹ which had been supplemented with 1.7% Bioagar ³ (17 g/l) was mixed in 1 litre of dH ₂ O.
Minimal Essential Medium alpha (MEMα)	MEM-α was prepared by mixing 10.1 g of MEM-α powder (Invitrogen), 2.2 g Na ₂ CO ₃ (sodium bicarbonate) and 3.0 g (0.3%) of Bioagar ³ in 1 litre of dH ₂ O. The medium was sterilised by autoclaving.
Half-strength MEM-α	MEM-α was prepared by mixing 5.05 g of MEM-α powder (Invitrogen), 2.2 g Na ₂ CO ₃ (sodium bicarbonate) and 3.0 g (0.3%) of Bioagar ³ in 1 litre of dH ₂ O. The medium was sterilised by autoclaving.
Quarter-strength MEM-α	MEM-α was prepared by mixing 2.52 g of MEM-α powder (Invitrogen), 2.2 g Na ₂ CO ₃ (sodium bicarbonate) and 3.0 g (0.3%) of Bioagar ³ in 1 litre of dH ₂ O. The medium was sterilised by autoclaving.
Phosphate Buffered Saline (PBS) medium	PBS-agar medium was prepared by dissolving 0.1, 0.8 or 4% (w/v) Bioagar ³ per 100 ml of PBS. PBS solution was prepared by dissolving 1 tablet of PBS (ICN Biomedicals) in 100 ml of dH ₂ O. The medium was sterilised by autoclaving.
SOC medium	2% bacto-tryptone ¹ , 5% bacto-yeast extract ¹ , 10 mM NaCl ² , 2.5 mM KCl ² , 10 mM MgCl ₂ ² and 10 mM MgSO ₄ ² was added to 180 ml of dH ₂ O) and sterilised by autoclaving. 20 mM of filter-sterilised glucose ² was added after autoclaving to give a final volume of 200 ml. The broth was stored as 1 ml aliquots and stored at -20°C for

	long-term storage.
M9 Minimal medium	300 ml of sterile tap water was used to make M9 minimal medium; tap water provides essential trace elements. 1.5% (w/v) Bioagar ³ was added to the tap water. The medium was sterilised by autoclaving. The following sterile supplements were added post-autoclaving the medium: 80 ml of 5×M9 salts ⁴ , 40% filter-sterilised glucose ² , 1M CaCl ₂ ⁵ , 1M MgSO ₄ ² , 4% (w/v) sterile yeast extract ¹ , 0.01% (w/v) Thiamine ⁴ , 0.01% (w/v) Proline ⁴ supplements and finally dH ₂ O was added to give a final volume of 400 ml.

Oxoid¹ (Basingstoke, UK), Fisher Scientific² (Loughborough, UK), Bioagar³ (Biogene Ltd, UK), Sigma-Aldrich⁴ (Dorset, UK), Fisons Scientific⁵ Equipment, (Loughborough, UK).

Table 2.5. Antibiotics used in this study. Antibiotics were routinely added to media plates and liquid cultures for the purpose of growing and selecting mutant strains.

Antibiotic	Stock Concentration	Final Concentration
Ampicillin	100 mg/ml	100 µg/ml
Chloramphenicol	20 mg/ml	20 µg/ml
Kanamycin	50 mg/ml	50 µg/ml
Erythromycin	5 mg/ml	5 µg/ml
Trimethoprim	5 mg/ml	5 µg/ml
Vancomycin	10 mg/ml	10 µg/ml

2.4. Miscellaneous buffers and solutions

Chloroform:Iso-amyl alcohol (24:1): this solution was prepared by mixing 240 ml of chloroform (Fisher Scientific) with 10 ml of iso-amyl alcohol (Fisher Scientific); which was carefully overlaid over the chloroform. This solution was used when performing chromosomal DNA extractions.

CTAB/NaCl solution: 0.7 M NaCl (Fisher Scientific) was added along with 10% (w/v) hexadecyltrimethyl ammonium bromide (CTAB; Sigma-Aldrich) to dH₂O,

whilst being heated and stirred. The volume was adjusted to the required final volume by the addition of dH₂O. This solution was not autoclaved.

EDTA (0.5 M): 0.5 M Disodium diaminoethane tetra acetate (EDTA; Fisher Scientific) was dissolved in approximately 300 ml of dH₂O. NaOH pellets were added to adjust the solution to pH 8.0, which is the point at which the disodium salt of EDTA dissolves. The volume was adjusted to the final volume of 400 ml using dH₂O before sterilising.

Loading buffer: 1.25 ml 40 x buffer TAE, 2.50 ml glycerol, 0.6 g orange G mixed in 6.25 ml dH₂O to give a final volume of 10 ml.

1 x Phosphate buffered saline (PBS): 1 tablet of PBS (ICN Biomedicals) was dissolved in 100 ml of dH₂O. The buffer was sterilised by autoclaving.

Sodium dodecyl sulphate (SDS; 2.2% or 10% w/v): SDS (Fisher Scientific) solution was prepared by dissolving SDS in dH₂O. The solution was heated with continual stirring until all of the powder had dissolved. This solution was not autoclaved.

3 M Sodium acetate: 40.8 g of sodium acetate (Fisher Scientific) was dissolved in 90 ml of dH₂O. The pH of the solution was adjusted to pH 5.2 using glacial acetic acid. The volume was adjusted to the correct final volume of 100 ml before sterilisation.

40 x Tris-acetate-EDTA (TAE) buffer: 0.04 M tris (hydroxymethyl) aminomethane (Fisher Scientific) and 1 mM EDTA (Fisher Scientific) dissolved in dH₂O. The pH of the buffer was adjusted to pH 7.8 with glacial acetic acid (Fisher Scientific) and the final volume was then amended with dH₂O before autoclaving the buffer.

4% Paraformaldehyde (Sigma-Aldrich): 4 g of paraformaldehyde was dissolved in 90 ml of PBS. To dissolve the solid 5M NaOH was used and the solution was mildly heated. The volume was adjusted to the correct final volume of 100 ml and then stored at 4°C.

Tris-EDTA (TE) buffer: 10 mM Tris-Cl (pH 8.0) and 1 mM EDTA dissolved in dH₂O. The final volume was amended with dH₂O prior to sterilisation.

1 M Tris-HCl buffers: 121.14 g Tris base (Fisher Scientific) was dissolved in 800 ml of dH₂O. Concentrated hydrochloric acid was added to the buffer to give the following required pH values of: pH 6.8 (~100 ml of HCl added to the buffer) and pH 8.8 (~5 ml of HCl added to the buffer). The buffers were left to equilibrate overnight whilst being continuously stirred. The volume was adjusted to the final volume of 1 litre with dH₂O. The solution was sterilised by autoclaving.

Binding buffer for purification of polyhistidine-tagged proteins: 20 mM sodium phosphate buffer, 20 mM imidazole and 500 mM NaCl dissolved in dH₂O.

Elution buffer for purification of polyhistidine-tagged proteins: 20 mM sodium phosphate buffer (Sigma-Aldrich), 500 mM NaCl and 500 mM imidazole (Sigma-Aldrich) was dissolved in dH₂O.

Elution buffer for purification of Glutathione-S-Transferase-tagged proteins: 40 mM reduced L-glutathione (Sigma-Aldrich), 50 mM Tris-HCl and 0.2 M NaCl dissolved in dH₂O. The pH of the solution was adjusted to pH 9.

Protein solubilisation buffer: 50 mM Hepes –NaOH, 6 M guanidine hydrochloride (Melford Laboratories, Ipswich) and 25 mM dithiothreitol (DTT) was dissolved in dH₂O. The pH of the solution was adjusted to pH 7.5.

Molecular weight markers: Molecular weight markers of known molecular size and concentration were loaded in one lane of each gel prepared in this study. The markers used in this study were ΦX174 and λ DNA which had been restricted with *Hae*III and *Hind*III, respectively (Gibco-BRL). The markers were prepared by mixing: 50 µl of λ*Hind*III at 200 ng/µl, 20 µl ΦX *Hae*III at 200 ng/µl, 3 µl of NaCl, 60 µl of loading buffer and 67 µl of dH₂O. The marker sizes for λ*Hind*III (bp) were 23130, 9146, 6557, 4361, 2322, 2027, 564, 125 and for ΦX *Hae*III (bp) were 1353, 1078, 872, 683, 310, 281, 271, 234, 174, 118, 72. 1 kb and 100 bp DNA ladders (NEB) were also used, the marker sizes for the 1 kb ladder were (bp) 10000, 8000, 6000, 5000, 4000, 3000, 2000, 1500, 1000, 500 and for the 100 bp DNA ladder the marker sizes were (bp) 1517, 1200, 1000, 900, 800, 700, 600, 500, 400, 300, 200 and 100. HyperLadder I (Bioline Ltd, UK) was also used in this study for which the marker sizes were (bp)

10,000, 8000, 6000, 5000, 4000, 3000, 2500, 2000, 1500, 1000, 800, 600, 400 and 200.

2.5. Primers

All primers were custom made by Invitrogen (Paisley, UK). A list of all of the primers used in this study is listed in Table 2.6. Primers were designed using Clone Manager (version 8; Scientific and Educational Software, 2005). All *C. jejuni* sequence information was obtained from CampyDB (<http://campy.bham.ac.uk/Program>). Primer sets had restriction sites added to the 5' end to ensure that genes could be cloned into the cloning vector; pUC19/pUC18 (Table 2.2). Inverse PCR primers were also designed for the inverse PCR mutagenesis strategy employed in this study and were positioned midway within the gene to be mutated (facing outwards). The inverse PCR primers had restriction sites added onto the 5' end of each primer (*NotI*) that were compatible with the restriction sites added to the primers used to amplify each of the selectable markers used in this study.

Table 2.6. Primers used in this study for PCR amplification. The purpose of each primer in this study has been indicated.			
Primer Name	Purpose of primer	Primer sequence 5' to 3' with the restriction site (shown in bold).	Restricti-on Site
Cj1506F	Cloning.	GGGGTACCGAACTTATCGGACAA ACAGGTAG	KpnI
Cj1506R	Cloning.	GGAATTCCCCTCACCCACTTTGTC	EcoRI
Cj0144F	Cloning.	GGGGTACCAATGCCCATGTTCGT GGTGTTC	KpnI
Cj0144R	Cloning.	GGAATTCGCCACCATAGAACCTA AAGCTGAACC	EcoRI
Cj1564F	Cloning.	GGAATTCAGGAACTTGGGCGTAT TATGGG	EcoRI
Cj1564R	Cloning.	CGGGATCCACTTACGCACCTAAG GCCATTG	BamHI
Cj0262F	Cloning.	GGAATTCTCGTGAGGATTGACAT CTTC	EcoRI
Cj0262R	Cloning.	CGGGATCCGTTCAATAAGCTGTG GGTTTC	BamHI
Cj1506invF	Inverse PCR Mutagenesi s.	ATAAGAAT GCGGCCGCCTTGCTG ATGGCTCTAATGC	NotI
Cj1506invR	Inverse PCR Mutagenesi s.	ATAAGAAT GCGGCCGCGTCATG CCTATGACACCTAC	NotI
Cj0144invF	Inverse PCR Mutagenesi s.	ATAAGAAT GCGGCCGCCTGCAG CAGCTTTAGAAGAG	NotI
Cj0144invR	Inverse PCR Mutagenesi s.	ATAAGAAT GCGGCCGCGCCGCA AGAATATCTACAGC	NotI
Cj1564invF	Inverse PCR Mutagenesi s.	ATAAGAAT GCGGCCGCCTGCAG CAGCTTTAGAAGAG	NotI
Cj1564invR	Inverse PCR Mutagenesi s.	ATAAGAAT GCGGCCGCGGTATA TCGACACCCAGTACC	NotI

Cj0262invF	Inverse PCR Mutagenesis.	ATAAGAATGCGGGCCGCCACCAA GGCGTAGATTATGC	NotI
Cj0262invR	Inverse PCR Mutagenesis.	ATAAGAATGCGGGCCGCTTCCAAC CCATAGCGTAAGC	NotI
M13F	Screening transformants in <i>E. coli</i> .	GTTGTAAAACGACGGCCAGTG	N/A
M13R	Screening transformants in <i>E. coli</i> .	GGAAACAGCTATGACCATGATTAC	N/A
CatinvF	Screening transformants in <i>E. coli</i> and <i>C. jejuni</i> .	GGAATGTCCGCAAAGCCTAATCC	N/A
CatinvR	Screening transformants containing the <i>cat</i> cassette in <i>E. coli</i> and <i>C. jejuni</i> .	GCGGTCCTGAACTCTTCATGTC	N/A
ErmCIF	Screening transformants containing the <i>ermC</i> ' gene in <i>E. coli</i> and <i>C. jejuni</i> .	CATGCAGGAATTGACGATTTAAAC	N/A
ErmCIR	Screening transformants containing the <i>ermC</i> ' gene cassette in <i>E. coli</i> and <i>C. jejuni</i> .	GAACATGATAATATCTTTGAAATCGGC	N/A

pAV35F	Amplifying the <i>cat</i> cassette out of pAV35.	ATAAGAATGCGGCCGCGCGCGG TGTTTCCTTTCC	NotI
pAV35R	Amplifying the <i>cat</i> cassette out of pAV35.	ATAAGAATGCGGCCGCGCAGCTGC GCCCTTTAGTTCC	NotI
pRREF	Amplifying the <i>ermC'</i> gene out of pRRE.	ATAAGAATGCGGCCGCGCGTTAA ACCGTGTGCTCTAC	NotI
pRRER	Amplifying the <i>ermC'</i> gene out of pRRE.	ATAAGAATGCGGCCGCAACTAGT GGATCTGCGATTC	NotI
pTrcHisBF	Amplifying the poly-linker out of the pTrcHisB vector.	GCTCTAGATACGACGATGACGAT AAGG	XbaI
pTrcHisBR	Amplifying the poly-linker out of the pTrcHisB vector.	GCTCTAGACTGCGTTCTGATTTA ATCTG	XbaI
Cj1506FSeq	Sequencing <i>C. jejuni</i> transformants (positioned 956 bp before the start of the <i>cj1506</i> coding sequence).	ACGGCTCCTACTTGTTTAGGG	N/A
Cj1506RSeq	Sequencing <i>C. jejuni</i> transformants (positioned 356 bp into the ORF of <i>cj1506c</i>).	TATTCTGGCGGATCAATAAG	N/A

Cj0144FMut Ver	Sequencing <i>C. jejuni</i> transformants (positioned 325 bp from the Cj0144 ATG start site).	ATGCTTGAGGTGCTATACTG	N/A
Cj0144RMut Ver	Sequencing <i>C. jejuni</i> transformants (positioned 51 bp from the end of Cj0145).	AGCCACCATAGAACCTAAAG	N/A
Tlp1PeriF	Amplifying the <i>Tlp1</i> periplasmic domain (amino acids 30-326).	AGGAGATATACATATGATCACAA AACAAGTAAGTCAAA	N/A
Tlp1PeriR	Amplifying the <i>Tlp1</i> periplasmic domain (amino acids 30-326).	GAAGTACAGGTTCTCTTTTTTTAA GGGTTTAAATACTG	N/A
Tlp1CtermF	Amplifying the <i>Tlp1</i> cytoplasmic signalling domain (amino acids 358-688).	CGGGATCCTTGCCTGTGATTCTT AGTTC	BamHI
Tlp1CtermR	Amplifying the <i>Tlp1</i> cytoplasmic signalling domain (amino acids 358-688).	GGAATTCAGCAGCAATTTGATTG ACTTC	EcoRI

Tlp2CtermF	Amplifying the <i>Tlp2</i> cytoplasmic signalling domain (amino acids 311-659).	CGGGATCCAAAAAATACCTCTCC CCACTTG	<i>Bam</i>HI
Tlp2CtermR	Amplifying the <i>Tlp2</i> cytoplasmic signalling domain (amino acids 311-659).	GGAATTCAAACCTCTTCTTCTTAA CATCTTC	<i>Eco</i>RI
Tlp1CompF	Complementation of <i>cj1506c</i> .	GGGGTACCAAGGACGCTCTAAA GAATC	<i>Kpn</i>I
Tlp1CompR	Complementation of <i>cj1506c</i> .	GAAGATCTAACTATAGGCTGAGG ACAAG	<i>Bgl</i>II

2.6. Amplifying DNA using the Polymerase Chain Reaction

The Polymerase Chain Reaction (PCR) (Sambrook and Russell, 2001) was used to amplify specific regions of DNA that were to be used in cloning experiments and to verify constructs and *tlp* mutants. All reaction components and recommended thermal cycling conditions were carried out per manufacturer's recommendation (Triple Master PCR system, Eppendorf AG, Hamburg, Germany). Briefly, extension times and primer annealing temperatures were calculated according to the following parameters; 1 minute per Kb PCR product and for primer annealing temperatures between 5-10°C lower than the melting temperature of the primer-without the restriction site attached. PCR reactions were contained in 0.2 ml thin-walled PCR tubes (ABgene) and run in an Eppendorf Mastercycler (Eppendorf AG). Optimisation of PCR conditions was carried out when: PCR reactions failed, there was poor amplification of the required PCR product or there was primer mis-priming occurring elsewhere in the *C. jejuni* NCTC 11168 genome. Optimisation of PCR conditions involved adjusting the primer annealing temperature, using reduced concentrations of magnesium ions per PCR reaction and finally extending or reducing the primer extension time. For the purpose of PCR optimisation reactions or when screening large numbers of recombinant plasmids for inserts a standard *taq* polymerase was considered suitable (ABgene, UK). A higher fidelity *taq* polymerase (Triple Master Enzyme Mix) was used when cloning DNA or when carrying out inverse PCR mutagenesis. The components that make up a standard PCR reaction mix are listed in Table 2.7 and an example of a standard thermal cycle program is shown in Table 2.8.

Table 2.7. Components in a typical PCR reaction mix.

Components	PCR reaction (20µl)
Forward Primer	4 pM
Reverse Primer	4 pM
Template DNA	for genomic DNA: 10-50 ng for 0.1-3 kb targets 50-100 ng for 3-10 kb targets For plasmid DNA: 0.1-1 ng for 0.1-3 kb targets
10× High Fidelity Buffer with 25mM Mg ²⁺	2 µl
10 mM of each Deoxynucleotide triphosphates (dNTPs): dATP, dTTP, dCTP, dGTP) (Amersham Biosciences, UK).	0.4 µl
Triple master polymerase mix or standard <i>taq</i> polymerase.	0.2 µl (1 unit)
Molecular Biology Grade Water	Up to 20 µl

Table 2.8. Standard PCR thermal cycling programme.

Cycle	Step	Temperature	Time	Description
1×	1	94 °C	2 minutes	Initial template denaturation
29×	2	94 °C	20 seconds	Template denaturation
	3	50 -70 °C	15 seconds	Primer annealing (the primer annealing temperature is 5-10°C lower than the melting temperature of the primer set-without the restriction site)
	4	72 °C	20 seconds-8 minutes	Primer extension time
1×	5	72 °C	5 minutes	Final extension (the extension time is calculated as approximately 1 kb PCR product size per minute)

2.6.1. Colony PCR

Colony PCR enabled amplification of DNA directly from bacterial colonies. This technique proved to be useful when screening large numbers of bacterial recombinants. A bacterial colony, approximately 1mm wide was picked off a plate using a sterile toothpick and then suspended in 25 µl of dH₂O in 0.2 ml PCR tubes. The cell suspensions were then heated in a thermocycler for 5 minutes at 96°C in order to lyse the bacterial cells. The cell suspensions were centrifuged for two minutes at $11,300 \times g$ to remove cell debris. Two µl of the clarified supernatant was used as template DNA in PCR reactions.

2.6.2. Sequencing of DNA and analysis

A standard sequencing thermal cycling programme can be seen in Table 2.9. All sequencing reactions were carried out using the Big Dye v3.1 Terminator Cycle Sequencing kit (Applied Biosystems). The appropriate amounts of template DNA required in sequencing reactions depended on the template type. For double-stranded plasmid (up to 20 kb), 200-300 ng of template DNA was required. The amount of DNA required when using PCR reactions depended on the size of the PCR product (PCR products of (bp): 100-200, 200-500, 500-1000, 1000-2000, >2000 required the following amount of template DNA (ng): 1-3, 3-10, 5-20, 10-40 and 40-100, respectively). Each sequencing reaction contained the appropriate amount of template DNA, 8 µl of diluted BigDye Terminator v3.1 (diluted 1 in 8 using dH₂O and sequencing buffer; provided by the Protein and Nucleic Acid Chemistry Laboratory (PNACL) based at the University of Leicester), 4 pM of sequencing primer and molecular grade water to give a final reaction volume of 20 µl. Sequencing reactions were purified by adding 0.2% (v/v) SDS solution and then boiling at 98°C for 5

minutes in a thermo cycler. The sequencing reactions were passed through DyeEx 2.0 Spin columns (Qiagen) and were used according to the manufacturer's instructions. The columns were used to remove any excess dye terminators which had not been used up in the sequencing reaction. The completed reactions were submitted to PNACL for sequence analysis. Sequencing reactions were processed using an ABI 377 DNA sequencer (Applied Biosystems). All sequencing files received from PNACL were viewed as a chromatogram using the program Chromas (V1.45) (Griffith University, Queensland, Australia). The DNA sequence was compared with a known DNA sequence using either Clone Manager (version 8; Scientific & Education Software) or Blast Two Sequences (<http://www.ncbi.nlm.nih.gov/blast/bl2seq/bl2.html>).

Table 2.9. Standard sequencing thermal cycling programme.

Step	Temperature	Time
1.	96°C	10 seconds
2.	96°C	10 seconds
3.	<i>Temperature 5-10°C lower than the melting temperature of the primer.</i>	10 seconds
4.	60°C	4 minutes
5.	Repeat steps 2 ->4 29 times	-
6.	60°C	5 minutes
7.	END	END

2.7. Quantification of DNA

2.7.1. Analysis of DNA by agarose gel electrophoresis

DNA molecules were routinely analysed and separated according to their molecular size by agarose gel electrophoresis (Sambrook and Russell, 2001). The agarose gel was prepared by dissolving SeaKem LE Agarose (Cambrex, USA) in 1 x TAE buffer

to a final concentration of 0.8-1.5% (w/v). The percentage of agarose to be used depended on the size range of fragments to be separated. In general, low agarose concentrations allow better resolution of large DNA molecules whereas high agarose concentrations allow for better separation of smaller DNA molecules. Once the agarose had been cooled to 55°C, ethidium bromide was added to the molten agarose to a final concentration of 0.5 µg/ml (Fischer Scientific). The gel was poured into a gel casting tray into which a comb was inserted at one end (the depth of the gel casting tray was of 0.5-0.75 cm). Once the gel had solidified the comb was removed and the gel was placed in an electrophoresis tank which was then filled with 1 x TAE buffer. DNA samples were prepared prior to loading by mixing 2 µl of loading buffer with 10 µl DNA sample. The samples were loaded into the wells, which had been created through the removal of the comb. The first well in the gel always contained a molecular weight marker that was run alongside the DNA samples. The molecular weight marker was used to determine the molecular size and concentration of the DNA sample. The gel was run at a constant voltage of between 5-10 V/cm. The orange dye present in the samples could be seen directly and this was allowed to run through approximately 75% of the gel before the power was switched off. DNA was viewed by placing the gel on an ultraviolet (UV) transilluminator (Syngene Gene Genius Bioimaging System) and exposed to 260 nm UV light and photographed (Genesnap software).

2.7.2. Quantification of DNA using a spectrophotometer

The concentration of nucleic acids in a solution was determined by measuring the absorbance at 260 nm and 280 nm using a spectrophotometer (Geneflow). The genomic DNA sample was diluted 1 µl into 1 ml of sterile water and transferred into

a 1 ml quartz cuvette. The absorbance was measured and the concentration of DNA was calculated using the following formula:

$$\text{Concentration of DNA in sample} = A_{260} \times \text{dilution factor} \times K$$

The dilution factor in this instance would be 1000, as the sample was diluted 1 µl into 1 ml. K is a constant and at an absorbance of 1 unit at A_{260} nm K is equal to 50 µg/ml for double stranded DNA. The purity of DNA was assessed by working out the ratio between the absorbance values at A_{260} and A_{280} nm, a ratio of 1.8 was indicative of pure nucleic acid. On occasions genomic DNA was also quantified using a Nanodrop ND-1000 spectrophotometer (Nanodrop technologies, Inc.). Genomic DNA was also analysed by agarose gel electrophoresis for a visual estimation of DNA concentration.

2.8. Isolating DNA from bacteria

2.8.1. Plasmid DNA preparations from *E. coli*

The QIAprep Miniprep kit (Qiagen, West Sussex) was used for carrying out plasmid DNA preparations of all *E. coli* strains used in this study (Table 2.1). The QIAprep Miniprep method is an adaptation of Birnboim and Doly's original alkaline lysis method. The kit was used in accordance with manufacturer's guidelines. The kit allows you to purify up to 20 µg of high-copy plasmid DNA from 5 ml cultures of *E. coli*, which had been previously grown in LB media overnight with antibiotic selection as appropriate (section 2.2.2). All overnight cultures were initially prepared by inoculating LB media with cells which had originally been derived from a single bacterial colony. Bacterial cells were harvested by centrifugation at 4°C, $3220 \times g$ for 20 minutes. The supernatant was discarded and the pellet was resuspended in 250 µl

of *Buffer P1* (50 mM Tris-HCl, pH 8.0 10 mM EDTA 100 µg/ml RNase A). Cells were then lysed using 250 µl of *Buffer P2* (200 mM NaOH, 1% SDS (w/v)). The cell membrane is composed of a phospholipid bilayer within which protein and other macromolecules are found embedded. The SDS in *Buffer P2* solubilises the cell membrane, whereas the alkaline conditions denature chromosomal and plasmid DNA. Any free cellular RNA is digested by the presence of RNase A. The tube was gently inverted 4-6 times in order to mix. Three hundred and fifty microliters of the neutralization buffer-*Buffer N3* was added to the lysate and once again the tube was mixed gently by inverting the tube.

2.8.2. Large scale genomic preparations from *C. jejuni*

A total of four MHA agar plates with confluent growth of *C. jejuni* were used to carry out large scale chromosomal DNA preparations from wild-type and mutant *C. jejuni* strains (Table 2.1). MHB (3 ml) was used to harvest the cells off the plates after which the cells were centrifuged at 4°C, 3220 × g for 20 minutes. The cell pellet was resuspended in 9.5 ml of Phosphate Buffered Saline (PBS), 2 ml of 10% Sodium Dodecyl Sulphate (SDS), 100 µl of 20 mg/ml Proteinase K (PK) and finally 20 µl of 10 mg/ml RNAase A. The cells were incubated for 1 hour at 37°C after which 1.8 ml of 5 M sodium chloride (NaCl) and 1.5 ml of 10% (w/v) CTAB/0.7 M NaCl were added to the cell suspension before mixing by inverting the tube. The reaction mixture was further incubated at 65°C for 20 minutes. Chloroform:isoamyl alcohol (24:1) was used to remove proteins from the nucleic acid preparation and was subsequently added to the cell suspension. The cells were centrifuged for 20 minutes at 3220 × g at 4°C. The chloroform aided the separation of the nucleic acids; which

were found in the aqueous phase boundary and needed to be removed with care. The DNA was precipitated out of solution by adding 70% (v/v) of pre-chilled isopropanol. A sealed p1000 Gilson pipette tip was used to spool the DNA out of solution and onto the pipette tip. The pipette tip was washed in 70% (v/v) ethanol and left to dry until all of the ethanol had evaporated. The pipette tip was left overnight at 37°C immersed in 2 ml of *Elution Buffer* (EB; 10mM Tris-Cl, pH 8.5) into which the DNA eventually dissolves. The purity of chromosomal DNA was determined by agarose gel electrophoresis (section 2.6.1) and quantified by spectrometry using a Jenway Genova Mk3 Life Science Analyser (Geneflow, UK).

2.8.3. Small scale genomic preparations from *C. jejuni*

The Gentra Systems Puregene DNA purification kit was used when trying to make small scale preparations of genomic DNA from wild-type and mutant *C. jejuni* strains. The protocol used was specifically designed for Gram-negative bacteria. The expected yield from 0.5 ml of bacterial culture is 10-35 µg. An overnight MHA plate with confluent grown *C. jejuni* cells on it was required for the preparation. The cells were harvested off the plate using 0.5 ml of MHB and subjected to centrifugation at $14,100 \times g$ for 5 seconds to pellet the cells. The supernatant was discarded and the pellet was resuspended in 300 µl of Cell Lysis Solution (recipe not given). The samples were incubated at 80°C for 5 minutes. The samples were treated with 1.5 µl of *RNase A* solution and then mixed by inverting the tube 50 times. The samples were then incubated at 37°C for 30 minutes. The sample was briefly cooled to room temperature by placing on ice for 1 minute before 100 µl of Protein Precipitation Solution was added to the cell lysate. The reaction mixture was then

subjected to a cycle of vigorous vortexing for 40 seconds in order to mix the *Protein Precipitation solution* evenly with the cell lysate. The samples were then centrifuged at $14,100 \times g$ for 5 minutes and the supernatant containing the DNA was transferred into a 1.5 ml microfuge tube (Eppendorf, UK), which contained 300 μ l 100% (v/v) isopropanol. The samples were mixed by inverting the tube gently 50 times so that the DNA could precipitate out of solution and was then centrifuged ($14,100 \times g$ for 1 minute). The supernatant was discarded and the DNA was visible as a small white pellet. The DNA was washed with 300 μ l 70% (v/v) ethanol by gently inverting the tube several times. Samples were centrifuged ($14,100 \times g$ for 1 minute) and the ethanol was carefully removed and the pellet was left to air dry for 5-10 minutes. Finally, the DNA was resuspended in 50 μ l of *DNA Hydration Solution* (TE buffer; see section 2.4) and incubated for 1 hour at 65°C and then left to incubate overnight at room temperature in order to aid in rehydration of the DNA. The tube was periodically tapped to help disperse the DNA into solution and was then stored at -20°C for long term storage.

2.9. Purifying DNA

2.9.1. Purifying DNA fragments from PCR or other enzymatic reactions

PCR products and enzymatic reactions were routinely purified according to their size using a QIAquick PCR Purification kit (Qiagen). Fragments ranging from 100 bp to 10 kb were purified using the QIAquick spin columns and smaller fragments ranging from 70 bp to 4 kb were cleaned up using the MinElute PCR Purification kit (Qiagen). This method was carried out according to manufacturer's guidelines. Briefly, five volumes of Buffer PB was added to one volume of PCR/enzymatic

reaction mix and mixed by inverting the tube. A QIAquick Spin column was then placed into a 2 ml collection tube into which the sample was applied. The column was then centrifuged for 30-60 seconds in order to bind the DNA to the spin column. The flow through was discarded and the QIAquick column was placed back into the same collection tube. To wash the DNA, 0.75 ml of Buffer PE was added to the QIAquick column and centrifuged for 30-60 seconds. The flow through was discarded and the tube was placed back into the same collection tube. The tube and column was centrifuged for a further minute. The QIAquick column was then transferred into a clean 1.5 ml microcentrifuge tube. DNA was eluted into 50 µl of Buffer EB or dH₂O and was added directly onto the centre of the QIAquick membrane. The column was allowed to stand for 1 minute before being centrifuged for 1 minute. Plasmid DNA, purified PCR products and DNA that has been modified by restriction digest was all analysed/quantified by agarose gel electrophoresis (section 2.6.1).

2.9.2. Purifying DNA directly from agarose gels

The QIAquick Gel Extraction kit (Qiagen) was used to purify double-stranded DNA of 70 bp to 10 kb from up to 400 mg of low-melt agarose in TAE buffer. All centrifugation steps were carried out at $17,900 \times g$ for one minute in a microcentrifuge. The region of the agarose proposed to contain the target DNA was visualised using UV light and excised from the agarose gel using a sharp scalpel, weighed and then incubated at 55°C in 3 gel volumes (100 mg~100 µl) of *Buffer QG*. The samples were incubated until the gel slice had completely dissolved (up to 10 minutes). To help the agarose dissolve the samples were repeatedly mixed by

vortexing during the incubation. The next step was dependent on the colour of the mixture-if the colour of the mixture was orange or violet, then 10 µl of 3 M sodium acetate (pH 5.0) (section 2.4) were added so that the mixture was at the optimal pH for adsorption of DNA to the QIAquick membrane. One gel volume of isopropanol was added to the samples. The samples were mixed and then transferred to a QIAquick *Spin* column (binds fragments ranging from 70 bp to 10 kb) and centrifuged. To remove all traces of agarose 0.5 ml of Buffer QG was applied to the column and centrifuged. To wash the DNA, 0.75 ml of Buffer PE was added to the QIAquick *Spin* column and centrifuged. Residual wash buffer was removed by centrifuging the sample for an additional minute. DNA was eluted into a clean 1.5 ml microcentrifuge tube by applying 30 µl of either Buffer EB or dH₂O to the centre of the QIAquick membrane, and left to stand for one minute before being centrifuged. The eluted DNA was stored at -20°C.

2.9.3. Ethanol precipitation

Ethanol precipitation was used to purify plasmid DNA. The following was added to the plasmid DNA: 1/10th of the sample volume of 3 M sodium acetate, 2.5 volumes of ice-cold 100% ethanol and 1 µl of glycogen (Roche, Germany). The reaction mixture was incubated for at least 2 hours at 4°C and was then centrifuged at 14,100 × *g* for 30 minutes. The pellet was resuspended in 1 ml of (v/v) 70% ethanol and centrifuged at 11,300 × *g* for 1 minute. Most of the ethanol was aspirated using a pipette, but to ensure that all remaining traces of ethanol were removed the pellet was air dried for 5 minutes in a fume cupboard. The pellet was finally resuspended in 10 µl of dH₂O.

2.10. Enzymatic alteration of DNA

2.10.1. Restriction digests

All enzymes and buffers specific for each enzyme were provided by NEB and were used according to manufacturer's guidelines. Some enzymes required the addition of bovine serum albumin (BSA, NEB). Template DNA varied depending on the desired amount to be digested and was added along with water to give a final reaction volume of 50 µl. The reaction mixture was incubated for 2 hours at 37°C and then further analysed by agarose gel electrophoresis (section 2.6.1).

2.10.2. Dephosphorylation of DNA

Vector DNA which had been restriction digested was dephosphorylated using the enzyme Shrimp Alkaline Phosphatase (SAP, Roche Diagnostics, Germany). SAP treatment of vector DNA helped to prevent self-ligation of vector molecules as it catalyzes the removal of 5' phosphate groups from vector DNA. One µl of SAP was added to a restriction digestion reaction and incubated for 30 minutes at 37°C. The alkaline phosphatase was deactivated by heating to 65°C for 15 minutes.

2.10.3. Ligations

A typical ligation reaction consisted of 1-5 units (for 1 µg DNA) of T4 DNA Ligase (NEB), 10x DNA ligase buffer (final concentration of the buffer was 1x) (NEB), 1 µl of 10 mM adenosine triphosphate (ATP), vector DNA (ng), insert DNA (ng) (molecular ratio of 3:1 of insert to vector) and dH₂O to give a final reaction volume of 20 µl. T4 DNA ligase catalyses the joining of double stranded DNA molecules between the 5'-phosphate and 3'-hydroxyl groups of adjacent nucleotides. The

ligation mixture was incubated overnight at 4°C. The ligation mixture was ethanol precipitated to remove all traces of salt before being used for transformations.

2.11. Introducing DNA into bacteria

2.11.1. Preparation of chemically competent *E. coli*

E. coli cells produced from a single bacterial colony (*E. coli* strains DH5αE and BL21; see Table 2.1) were used to inoculate 5 ml LB liquid cultures which were incubated overnight at 37°C with shaking. Chemically competent *E. coli* cells were made by diluting an overnight culture 1/100 into fresh LB. The cells were incubated at 37°C with shaking until the OD₆₀₀ of the cells had reached 0.6 (which indicated that the cells were mid log-phase). The optical density of the culture was measured at regular pre-determined intervals in 1.6 ml disposable cuvettes (Sarstedt) using a spectrophotometer (Ultrospec 10, Amersham Biosciences). The culture was transferred into two 50 ml centrifuge tubes and centrifuged at $3220 \times g$ at 4°C for 15 minutes. The cells in each tube were then washed in 50 ml of ice-cold 50 mM CaCl₂ and centrifuged as before. The cells were finally resuspended in 10 ml of ice-cold CaCl₂, which contained 20% (v/v) glycerol. The cells were aliquoted (55 µl volumes), snap frozen on dry ice and stored at -80°C.

2.11.2. Preparation of electro-competent *E. coli*

Electro-competent *E. coli* cells were made by inoculating 100 ml of fresh LB with an overnight culture to an OD₆₀₀ of 0.1. The cells were incubated at 37°C with shaking until the OD₆₀₀ of the cells had reached between 0.4 and 0.6. The culture was transferred into two 50 ml centrifuge tubes and centrifuged at $3220 \times g$ at 4°C for 15

minutes. The cells were harvested and washed three times in decreasing volumes of ice-cold dH₂O. The first wash was carried out in 50 ml of ice-cold dH₂O, the second in 25 ml of ice-cold dH₂O and the third and final wash in 10 ml of ice-cold dH₂O, 10% (v/v) glycerol. The cells were finally resuspended in 1 ml of ice-cold dH₂O, 10% (v/v) glycerol. The cells were split into 50 µl aliquots and snap frozen on dry ice and stored at -80°C.

2.11.3. Introducing DNA into *E. coli* by heat shock

A 5 µl ethanol precipitated ligation reaction was routinely used to transform *E. coli*. The ligation reaction was mixed together with 50 µl of chemically competent *E. coli* cells and incubated on ice for 20 minutes. The reaction mixture was heat shocked by placing in a water bath at 42°C between 45-50 seconds and immediately transferred into ice for 2 minutes. After this step 450 µl of room temperature SOC medium (Table 2.4) was added to the reaction mixture and the cells were incubated at 37°C for 90 minutes. The cells were then centrifuged at $17,900 \times g$ for 90 seconds and resuspended in 100 µl of SOC medium. The cells were plated out on LA plates supplemented with selective antibiotics.

2.11.4. Introducing DNA into *E. coli* by electroporation

Plasmid DNA was transformed into electro-competent *E. coli* cells by electroporation. The DNA to be transformed (~50 ng plasmid DNA or half of an ethanol precipitated ligation reaction) was added to 40 µl of electro-competent cells and was transferred into an electroporation cuvette (Geneflow, 2mm gap), that had been previously chilled on ice for 30 minutes prior to the electroporation. The cells

were then electroporated using a Bio-Rad GenePulser (Bio-Rad) and applying one pulse at 2.5 kV, 25 μ F and 200 Ω . The cells were immediately recovered by adding 0.1 ml of SOC and then incubated for 1 hour at 37°C. The cells were plated out onto LA plates which had been supplemented with the appropriate selective antibiotic and incubated overnight at 37°C. The plates were checked for the presence of transformant colonies the following day.

2.11.5. Preparation of electro-competent *C. jejuni*

Four MHA plates with a lawn of *C. jejuni* cells were used to make chemically competent *C. jejuni*. The cells were harvested from plates using 2 ml of CEB per plate (Campylobacter Electroporation Buffer; 0.186 g of sucrose in 2 ml of 15% (v/v) glycerol). The cells were pooled together and centrifuged at $3220 \times g$ for 20 minutes at 4°C. The supernatant was discarded and the pellet was resuspended in 10 ml of CEB (0.931 g of sucrose in 10 ml of 15% (v/v) glycerol). The cells were centrifuged as before and washed a further two times. The pellet was finally resuspended in 0.3 ml of CEB and the cells were split into 50 μ l aliquots and snap frozen on dry ice and stored at -80°C.

2.11.6. Introducing DNA into *C. jejuni* by electroporation

Between 5-10 μ g of plasmid DNA was incubated on ice for 10 minutes with a 50 μ l aliquot of *C. jejuni* electro-competent cells. The cell suspension was then transferred to a pre-chilled electrocuvette with a 2 mm gap (Geneflow). The cells were electroporated using a Bio-Rad GenePulser (Bio-Rad) by applying 1 pulse at 2.5 kV,

25 μ F and 200 Ω . The cells were immediately recovered by adding 0.1 ml of SOC medium. The cells were plated on MHA and incubated overnight at 37°C in the VAIN. The next day the cells were harvested in 1 ml of MHB and centrifuged at 17,900 $\times g$ for 2 minutes. The cells were finally resuspended in 0.2 ml of SOC medium and plated out on MHA plates supplemented with the appropriate selective antibiotics. The plates were checked for the appearance of transformant colonies 3-5 days later.

2.11.7. Introducing DNA into *C. jejuni* by natural transformation

A biphasic method was used to naturally transform *C. jejuni* cells. The *C. jejuni* strain to be naturally transformed was harvested from a MHA plate using 2 ml of MHB. The OD₆₀₀ of the cell suspension was recorded and adjusted using MHB to an OD of 0.5 ($\sim 3 \times 10^9$ cfu/ml). Five hundred micro litres of the diluted cell suspension was added to a 15 ml Falcon tube which contained 1 ml of MHA and was then incubated for 3 hours under microaerobic conditions. The DNA (1-5 μ g) to be naturally transformed was added to the cell suspension and mixed gently and the tubes were incubated for a further 5 hours. The cell suspension was removed and centrifuged and resuspended into a smaller volume so that the cells could be plated onto MHA plates containing the appropriate selective antibiotics. The plates were incubated for 3-5 days and then checked for transformant colonies.

2.12. SDS-polyacrylamide gel electrophoresis

2.12.1. Sample preparation

Protein samples were prepared for SDS-Polyacrylamide Gel Electrophoresis (SDS-PAGE) by mixing the protein samples with an equal volume of SDS-PAGE sample

loading buffer (50 mM Tris-HCl, pH 6.8, 100 mM dithiothreitol (DTT), 2% (w/v) SDS, 0.1% bromophenol blue, 10% (v/v) glycerol). The samples were boiled for 10 minutes, briefly centrifuged at $17,900 \times g$ for 10 seconds and then loaded into the wells in the SDS-polyacrylamide gel; the wells had a capacity of up to 45 μ l. Prestained protein molecular-weight markers were loaded into one well in every polyacrylamide gel and run alongside protein samples so that the size of the protein being expressed could be determined. The protein standards used were Prestained Protomarker (National Diagnostics) and prestained Prosieve color protein marker (Lonza). Ten μ l of the prestained Protomarker or the Prosieve marker was loaded into one well in every gel. The marker sizes in kDa for Protomarker were; 190, 86, 70, 47, 25, 22, 17. The Prosieve color protein marker was pre-warmed to 37°C for 10 minutes before use and the marker sizes in kDa for this marker were; 190, 127, 77, 49, 38, 25, 18, 9.

2.12.2. Electrophoresis of proteins and visualisation

SDS-PAGE (Laemmli, 1970; Sambrook and Russell, 2001) was used to analyse total cellular proteins. SDS-PAGE was performed using the *Mini-PROTEAN II* (Bio-Rad Laboratories) electrophoresis kit. The *Mini-PROTEAN II* apparatus produced mini-gels of dimension 7.2 x 10.2 cm. The gels were electrophoresed at a constant current of 15 mA. The mini-gels were electrophoresed in SDS-PAGE running buffer (0.025 M Tris-HCl, 0.192 M glycine and 0.19% (w/v) SDS, pH 8.3-8.6), until the samples had run off the bottom of the gel. The stacking gels and resolving gels (Table 2.10) were composed of 5% and 10% final acrylamide concentration, respectively, made

using 30% (v/v) acrylamide mixture (National Diagnostics, Protogel, provided as a premixed solution with the ratio of acrylamide to bisacrylamide as 37.5:1).

Following SDS-PAGE gels were stained overnight, on a shaking platform, using Coomassie blue staining solution (0.25% (w/v) Coomassie Brilliant Blue R-250, 40% (v/v) methanol and 10% glacial acetic acid). Excess stain was removed from gels using destaining solution (45% methanol, 10% (v/v) glacial acetic acid and 45% (v/v) dH₂O) until the background colouration had been removed. The gels were then placed in dH₂O for 2 hours before being placed in gel drying solution (20% (v/v) ethanol, 10% (v/v) glycerol and 70% dH₂O) for 1 hour. The gels were briefly re-soaked in gel drying solution, placed in between two pieces of DryEase Mini cellophane sheets (Invitrogen) and clipped inside a DryEase gel drying frame specifically designed for mini-gels (Invitrogen).

Table 2.10. Composition of the resolving and stacking gels used for SDS-PAGE.

Component	5% Stacking Layer	10% Resolving Layer
Gel buffer A (0.75 M Tris-HCl, 0.2% SDS (w/v), pH 8.8)	-	2.70 ml
Gel buffer B (0.25 M Tris-HCl, 0.2% (w/v) SDS, pH 6.8)	1.0 ml	-
30% (v/v) Acrylamide mix	0.330 ml	1.83 ml
10 mg/ml (1% w/v) Ammonium persulphate (APS)	0.050 ml	0.190 ml
<i>N, N, N',N'</i> -Tetramethylethylenediamine (TEMED)	0.008 ml	0.015 ml
dH ₂ O	0.616 ml	0.765 ml

2.13. Immunoblotting proteins

2.13.1. Assembly of apparatus and running a western blot

The presence of GST-tagged proteins in *E. coli* was confirmed by immunoblotting (Towbin *et al.*, 1979 and Sambrook and Russell, 2001). Protein samples needed to be separated first by SDS-PAGE (section 2.11), but rather than staining the SDS-PAGE gel with coomassie blue stain, the proteins on the gel were transferred onto the surface of a polyvinylidene fluoride (PVDF) membrane (Millipore) by applying an electric field. The PVDF membrane was soaked in 100% (v/v) methanol for five minutes, washed in dH₂O and then left to soak in transfer buffer (0.29% (w/v) glycine, 0.58% (w/v) Tris, 0.037% (w/v) SDS and 20% (v/v) methanol) before it could be used for immunoblotting proteins. The equipment required for immunoblotting and the subsequent order of assembly is shown in Table 2.11. The SDS-polyacrylamide gel, PVDF membrane, 6 pieces of 3MM filter paper (Whatman 3MM chromatography paper), four scouring pads were all held together using two cassettes. The immunoblotting apparatus was transferred into a mini-immunoblotting tank (Geneflow), which was filled with pre-chilled transfer buffer. The electro-transfer of proteins from the SDS-polyacrylamide gel to the PVDF membrane was achieved by running the transfer for 1 hour at 100mA.

Table 2.11. The assembly of equipment required for electro-transfer of proteins from an SDS-PAGE gel to a PVDF membrane. The transfer of proteins occurs from the cathode (-) to the anode (+) due to proteins carrying a negative charge.

Layer	Component
Cassette	
6 (Top)	2 scouring pads
5	3 pieces of 3MM paper
4	PVDF membrane
3	SDS-PAGE gel
2	3 pieces of 3MM paper
1 (bottom)	2 scouring pads
Cassette	
Anode (+)	
Cathode (-)	

2.13.2. Antibody incubation and washing

Once the electro-transfer of proteins had been achieved from an SDS-polyacrylamide gel onto the surface of a PVDF membrane, the membrane was placed in a flat box containing blocking solution (5% (w/v) non-fat dried milk powder in 1 x PBS and 0.1% (v/v) Tween-20) for 1 hour at room temperature on a flat bed shaker. The flat box, containing the membrane was then incubated overnight with shaking at 4°C. The next day the membrane was incubated for 1 hour at room temperature. To detect the presence of GST-associated proteins the blocking solution was removed and the membrane was incubated in primary antibody (goat anti-GST antibody), which had been diluted 1:1000 in blocking buffer. The membrane was incubated for 1 hour at

room temperature with shaking, which was followed by two rinses in PBS-Tween (PBS-T; 1 x PBS and 0.1% Tween-20) and 3 further separate washes in PBS-T with 10 minutes incubation between each wash. The membrane was then incubated in secondary antibody that was specific to the sample (goat anti-rabbit IgG, conjugated to horseradish peroxidase; HRP) and had been diluted (1:20,000) in blocking buffer. The membrane was incubated for 1 hour with shaking at room temperature. The membrane was washed twice in PBS-T and then three times for 5 minutes, two times for 15 minutes and finally three times for 5 minutes.

2.13.3. Generation of a signal and subsequent detection

Detection of a signal was achieved using the Enhanced Chemiluminescence (ECL) kit (Amersham Biosciences), specifically designed for use in western blotting. The membrane was placed protein side up on a piece of saran wrap. ECL Advance Solutions A and B were mixed in equal volumes and applied directly onto the membrane surface and allowed to incubate for 2-5 minutes. Excess detection agent was drained off the membrane, after which the membrane was wrapped in fresh saran wrap and placed in a film cassette. The cassette was taken to a dark room where a sheet of autoradiography film (Fuji medical X-ray film) was placed on top of the membrane. The cassette was closed and the film was exposed for a couple of minutes and then developed.

2.14. Protein preparation, expression and purification

2.14.1. GST-tagged Tlp proteins

The C-terminal highly conserved domain (HCD) of Tlp1 and Tlp2 were individually cloned into the pGEX-4T expression vector (Appendix 4; Figure 4.1 (a)). The pGEX-4T vector encodes a GST moiety and the target protein is cloned in the same reading frame as the GST protein. Another unique feature of the pGEX-4T vector is that it includes the recognition sequence for the protease–thrombin. Cleavage by thrombin enables the separation of the desired protein from the GST-tag. The HCD domains of Tlp1 and Tlp2 were amplified by PCR using the appropriate primers (see Table 2.6). The purified PCR products and the pGEX-4T-1 vector were enzymatically modified with the appropriate restriction endonucleases that were compatible with restriction enzyme sites in the pGEX-4T-1 vector and then ligated together (refer to sections 2.10.1 and 2.10.3). The target constructs (see Table 2.3) were transformed into chemically competent *E. coli* BL21 cells by heat shock (2.11.3). The pGEX-4T-1 vector (without an insert) was also transformed into *E. coli* BL21 cells and was used as a negative control.

Five millilitre cultures of *E. coli* BL21 cells containing the appropriate construct vector control (pGEX-4T-1), were prepared in LB supplemented with ampicillin and incubated overnight at 37°C with shaking. The overnight cultures were used to inoculate 500 ml of LB containing ampicillin. The cultures were agitated at 37°C until the OD₆₀₀ of the cells had reached between 0.4-0.6. Protein expression was induced by adding the lactose analogue-IPTG to the cell culture to a final concentration of 1.5 mM. The cells were incubated for a further 3 hours at 37°C with

shaking. Afterwards cells were harvested from liquid cultures by centrifugation at 5400 x g for 20 minutes at 4°C. Cell lysis was achieved by one of two ways: by sonicating the cells or by using a cell lysis solution. For the purpose of sonication, pelleted cells were resuspended in 10 ml of PBS solution and then maintained on ice at all times. A 0.3 cm diameter probe was used to sonicate the cells (Soniprep sonicator, MSE). Cells were sonicated with 5-8 rounds of 20 second bursts, cells were cooled on ice for 1 minute in between each round of sonication. Sonication was carried out on a low output frequency setting with an amplitude of 1.

Chemical lysis was achieved using the cell lysis solution BugBuster HT Protein Extraction Reagent (Novagen). The reagent was stored at 4°C and was pre-warmed to room temperature before use. The BugBuster HT Protein Extraction Reagent was used in accordance with manufacturer's guidelines. In general, 5 ml of the reagent was used per gram of wet cell paste. Thus following centrifugation of the liquid cultures, post IPTG induction, the supernatant was discarded and the cell pellet was weighed and the amount of reagent used to resuspend the cell pellet was adjusted accordingly. In order to improve the efficiency of cell lysis, lysozyme (1 kilo unit) was added to the cell suspension. The cell suspension was incubated on a shaking platform for 20 minutes at room temperature.

Irrespective of the method used to carry out cell lysis, cells were then centrifuged at 16, 000 x g for 20 minutes at 4°C in a Sorvall GSA rotor to remove insoluble cell debris and unlysed cells. The clarified supernatant was then transferred to a 15 ml falcon tube and kept on ice. A 1 ml GSTrap FF column (GE Healthcare) was used to purify the GST-fusion proteins. The columns were used in accordance with manufacturers' specifications. An aliquot (10 µl) of the purified protein extract was visualised on an SDS-PAGE gel (see section 2.12.2). Thrombin Protease (GE

Healthcare; stock was 1 unit/ μ l) was used for cleaving GST-fusion proteins. Post-thrombin cleavage of the protein a HiTrap Benzamidine FF (5 ml) column was used to remove the thrombin protease leaving the cleaved fusion protein. The column was used in accordance with manufacturers' specifications.

2.14.2. His-tagged Tlp proteins

2.14.2.1. His-tagged Tlp1 periplasmic domain

The cloning of the N-terminal-periplasmic signalling domain (PSD) of *cj1506c* was carried out by Dr X. Yang (Protein Expression Laboratory, University of Leicester). The PSD of *cj1506c* was translationally fused to a poly-histidine tag to form the plasmid pRS11 (Table 2.3). The pRS11 plasmid was transformed into chemically competent *E. coli* BL21 cells by heat shock (2.11.3). The pLEICS-05 vector (Table 2.2) was also transformed into *E. coli* BL21 cells and was used as a negative control in experiments.

Five millilitre cultures of *E. coli* BL21 cells containing the appropriate construct (pRS11) or vector control (pLEICS-05), were prepared in LB supplemented with ampicillin and incubated overnight at 37°C with shaking. The overnight cultures were used to inoculate 250 ml of LB containing ampicillin. The cultures were agitated at 37°C until the OD₆₀₀ of the cells had reached between 0.4-0.6. Protein expression was induced by adding the lactose analogue-IPTG to the cell culture to a final concentration of 1.5 mM. The cells were incubated for a further 3 hours at 37°C with shaking. Afterwards cells were harvested from liquid cultures by centrifugation at 5400 x g for 20 minutes at 4°C.

The BugBuster HT Protein Extraction Reagent (Novagen) solution was used for cell lysis. The BugBuster HT Protein Extraction Reagent was used in accordance with manufacturer's guidelines (refer to section 2.14.1 for more information). Lysozyme (1 kilo unit) was added to the cell suspension. The cell lysate was cleared by centrifugation at 16,000 $\times g$ for 20 minutes at 4°C in a microcentrifuge. The supernatant was transferred to a clean tube and the cell pellet was also saved for possible inclusion body purification. A small aliquot of the supernatant was mixed with an equal volume of 2 \times SDS-PAGE sample loading buffer (2.12.1) and visualised by SDS-PAGE. The cell pellet was resuspended in 1 \times SDS-PAGE sample loading buffer and boiled for 10 minutes. The boiled sample was briefly centrifuged at 17,900 $\times g$ for 10 seconds and then a small aliquot of this sample from the pellet cells was visualised on by SDS-PAGE (see section 2.12.2).

2.14.2.2. His-tagged Tlp1 cytoplasmic domain

The cloning of the C-terminal signalling domain of *cj1506c* was carried out by Paul Ainsworth (University of Leicester). The highly conserved signalling domain of *cj1506c* was translationally fused to a poly-histidine tag to create the plasmid pTrc_TLP1 (Table 2.3). The pTrc_TLP1 plasmid was transformed into chemically competent *E. coli* Rosetta cells (Table 2.1) by heat shock. The pTrcHisB vector (Table 2.2) was also transformed into *E. coli* Rosetta cells and was used as a negative control in experiments. Protein expression was induced using the same method used to express the PSD of Tlp1 (2.14.2.1).

Protein purification was achieved using a 5 ml His-Trap FF Crude column (GE Healthcare, UK) and was used in accordance with the manufacturer's instructions. Cell lysis was undertaken as follows. Following harvesting of cells from

liquid cultures (post-IPTG induction), the cell pellet was re-suspended in binding buffer containing a protease inhibitor (Roche; 5 ml buffer for 1 g pellet weight). The cell lysate was sonicated using a Biorupter sonicator (Diagenode, Belgium). Cells were sonicated with ten rounds of 30 second bursts, cells were cooled on ice for 1 minute in between each round of sonication and then centrifuged at 5400 x *g* for 20 minutes at room temperature. The supernatant was filtered using an acrodisc (pore size 0.45 µm; PALL Life Sciences) and applied to the His-Trap column (recommended flow rate of 1 drop/second). The column containing the bound sample was then washed by adding 75 ml binding buffer (see section 2.4; binding buffer) at the recommended flow/rate. The desired protein was eluted using 25 ml elution buffer (see section 2.4; elution buffer). Fractions from each stage of the purification process were retained for analysis by SDS-PAGE. The column was cleaned and stored in 20% ethanol.

2.14.3. Optimisation of protein expression

It is well documented that protein expression is greatly affected by variables such as temperature, the concentration of IPTG used to induce cells with and the incubation period not only post IPTG induction but also before (Sambrook and Russell, 2001; Dr Fred Muskett, personal communication). A protocol from Sambrook and Russell (2001) was used for optimising target protein expression. Overnight cultures were prepared in LB containing ampicillin and then inoculated with *E. coli* BL21 cells containing the recombinant plasmid and the positive control plasmid pGEX-4T-1. The cultures were incubated overnight at 37°C with shaking. The following day, 50 µl of the overnight cultures were used to inoculate several universals containing 5 ml

LB medium supplemented with ampicillin prepared for each sample. The cultures were incubated with shaking at 37°C until the cells had reached mid-log phase of growth ($OD_{600} \sim 0.5-0.7$).

One ml of the uninduced culture was removed before induction and was therein referred to as time point zero. The remaining cultures were induced with varying concentrations of IPTG (0.0625, 0.125, 0.25, 0.5, 1, 1.5, 3, and 5 mM) and then incubated with shaking at different temperatures: 18, 26, 30 and 37°C. One ml of the culture was withdrawn from each universal at different time points during the incubation period (0, 1 and 3 hours). The OD_{600} of the culture was measured using a spectrophotometer. The sample was then centrifuged at maximum speed in a microcentrifuge. The supernatant was removed and discarded. The pellet was resuspended in 100 μ l of 1 x SDS sample loading buffer and boiled for 3 minutes. The samples were briefly centrifuged at maximum speed for 30 seconds and the samples were then stored on ice until all the samples had been processed. The samples were brought to room temperature and 0.15 optical density units at OD_{600} of each sample was loaded onto and SDS-PAGE gel to visualise the induced fusion protein.

2.14.4. Tlp1 C-terminal signalling domain specific labelling of *C. jejuni*

Liquid cultures were incubated with shaking (500 mot 1/min, Vibrax VXR Basic, IKA) for 12-16 hours (overnight). The cells were observed using phase contrast microscopy at the start of each experiment. The OD_{600} of the cells was 0.35 (1×10^9 Cfu/ml) following overnight incubation with shaking. 2 ml of the overnight culture

was harvested by centrifugation for 20 minutes at 5400 x g at room temperature (in an Eppendorf centrifuge 5810 R). The *C. jejuni* cells were resuspended in 0.05 ml of fresh MH broth. 10 µl of the cell suspension was spotted onto a Poly-L-Lysine (0.1% (w/v); Sigma-Aldrich) coated microscope slide (Pre-prepared slides were provided by Adam Berg). The cells were fixed in 4% paraformaldehyde (section 2.4; Sigma Aldrich) solution for 20 minutes. The cells were washed twice in PBS (5 minutes per wash). All wash steps were performed with shaking at room temperature. The cells were permeabilised using Triton X-100 (0.5% (v/v); Sigma-Aldrich) for 10 minutes. In order to determine the optimal method for labelling of cells some cells were treated with Triton X-100 (0.5% (v/v)) prior to fixation. The cells were washed three times (5 minutes per wash) in PBS. The cells were incubated in blocking solution (1% w/v BSA in PBS) for 30 minutes. The cells were incubated in blocking solution (0.1% (w/v) BSA in PBS) for 5 minutes. The cells were treated with primary antibody (Rabbit Tlp1 C-terminal signalling specific antibody (Eurogentec, Belgium) diluted at 1:100 and 1:1000 in blocking solution (0.1% (w/v) BSA in PBS; stock concentration unknown; a sample of the final) for 60 minutes. The cells were washed three times in blocking solution (0.1 % (w/v) BSA in PBS). The cells were then incubated in conjugate specific to the sample secondary antibody (Anti-rabbit-antibody conjugated to FITC; fluorescein isothiocyanate (produced in goat); 3.3 mg/ml diluted 1:160 dilution; purchased from Sigma-Aldrich). The cells were washed in blocking solution (0.1 % (w/v) BSA in PBS) for 10 minutes. The cells were washed finally in PBS buffer three times (5 minutes each). The cells were stained using the nuclear stain DAPI (4',6-diamidino-2-phenylindole; 1 µg/ml); which emits blue fluorescence upon binding to AT regions of DNA. Finally the cells were mounted using mount medium (IMM-ibidi mounting medium, Germany) and a cover slip was overlaid and sealed

with nail varnish. All staining was evaluated using fluorescence microscopy. All slides were viewed using the Olympus FV1000 confocal laser scanning microscope, which was attached to an IX81 Olympus microscope (488 nm argon laser line was used). All microscopy was carried out with the help of Dr Kornelis R Straatman (Department of Biochemistry, University of Leicester).

2.15. Chemotaxis assays

2.15.1. Swarm plate assay

The swarm plate assay is a well accepted assay for assessing chemotaxis (Armstrong *et al.*, 1986; Marchant, PhD thesis; Bridle, MPhil thesis). Bacteria are spotted onto the centre of a nutrient rich agar plate and then incubated. Bacteria begin to grow and metabolise nutrients at the point of inoculation and this subsequently sets up a concentration gradient between the centre of the plate and the nutrient agar towards the edge of the plate. Chemotactic bacteria respond to this gradient and swarm across the agar plate, producing a defined ring formation which is visible under an indirect light source.

A motile variant strain of *C. jejuni* 11168 was used in all swarm assays as the positive control and all *tlp* mutants were naturally transformed onto this background. Motile variant cells had been isolated previously to this work by O. Bridle (MPhil thesis). The motile variant had been generated as follows. Wild-type *C. jejuni* cells were inoculated in the centre of semi-solid Mueller-Hinton agar plates and then incubated under microaerobic conditions. As most of the *C. jejuni* NCTC 11168 cells were non-motile they remained localised in the centre of the plate. However, a few of the non-motile cells which had spontaneously reverted and were motile variants were

identified as blebbing around the edge of the non-expanding colony (data not shown). A few of the cells from this region were picked and subsequently re-plated onto this time solid MHA plates to identify single colonies.

Swarm plates were prepared using MH broth supplemented with 0.4% (w/v) bacteriological agar (8.2 g MH broth powder (Oxoid) and 1.6 g Bioagar (Biogene) per 400 ml). The plates were poured and left to set overnight at room temperature. The following day, 20 µl of *C. jejuni* cell suspension, which had been diluted using MHB to an OD₆₀₀ of 1.0, was spotted on the centre of the swarm plates. The plates were incubated microaerobically for up to 96 hours. The swarm rate was assessed by measuring the diameter of the swarm.

2.15.2. Capillary assay

The capillary assay is a technique that allows you to quantify chemotactic responses of *C. jejuni* towards possible attractants (Adler, 1973; Marchant, PhD thesis; Bridle, MPhil thesis). A method originally developed for determining chemotactic responses in *E. coli*, has been adapted for use with *C. jejuni* (Adler, 1973). *C. jejuni* NCTC 11168 motile variant (NCTC 11168 MV, see Table 2.1) cells were harvested off MHA plates using 1 ml of PBS (cells were in late stationary phase) and centrifuged at room temperature at $6000 \times g$ for 4 minutes. The cells were washed once more as before and the pellet was finally resuspended in 500 µl of PBS. A 1/20 dilution was performed with the neat cell suspension (950 µl PBS plus 50 µl of the neat cell suspension) and the OD₆₀₀ of the culture was measured. The neat cell culture was then diluted using 0.1% PBS-agar (1 x PBS with 0.1% (w/v) Bioagar) to a calculated OD₆₀₀ of 0.5. One millilitre of the diluted cell culture was dispensed into several bijoux. A sample was taken from the starting culture, which would represent the

number of bacteria at the start of the assay. The sample was serially diluted in PBS and 10 µl drops of the following dilutions: 10^{-3} , 10^{-4} and 10^{-5} were plated onto MHA plates to obtain viable counts.

A putative attractant (Hugdahl *et al.*, 1988, see Table 2.12) was drawn up into a 5 µl microcap glass capillary tube (VWR International Ltd, Poole, UK) by capillary action (see Table 2.12; all chemicals were purchased from Sigma-Aldrich). PBS was also drawn up into a capillary tube and served as a negative control. The capillary tubes containing the test chemical or PBS was placed into the bijou containing the *C. jejuni* cell suspension. The lids of the bijou were loosened and the tubes were placed in the VAIN at 37°C and incubated for 30 minutes. The capillary assay is based around the principle that test substrate inside the capillary tube should diffuse out into the bijou containing the bacteria. If the bacteria are chemotactic and the test substrate is a chemoattractant then the bacteria should respond to the increasing gradient. By responding to the gradient and by biasing their movement in favour of the direction in which the attractant resides, the bacteria should eventually reach inside the capillary tube. Contrary to this argument, if the test substrate is a chemorepellent then the bacteria should remain in the bijou.

Following incubation, the tip of the capillary tube that had been immersed in the bacterial suspension was briefly cleaned using sterile cotton. The contents of the capillary tube were expelled, by forcing air through the tube using a sterile 25-gauge needle attached to a 1 ml barrel syringe (Becton Dickinson). The content of the capillary tube was serially diluted in PBS (10^{-1} , 10^{-2} , and 10^{-3}). Five microliter aliquots of the following dilutions: 10^{-2} , 10^{-3} were spotted in triplicates onto one end of an MHA plate. The plate was then tipped so that the each drop spread out over the plate to form a streak (this made it easier to count cells off plates later as the colonies

were separated out). The remaining cell suspension in the bijou was also serially diluted in PBS and 10 µl drops of the following dilutions: 10^{-3} , 10^{-4} and 10^{-5} were plated onto MHA plates (as done previously with the contents from the capillary tube). All plates were incubated in the VAIN for 2 days, at 37°C before the number of colony forming units (CFU)/ml that had accumulated in the capillary tube could be determined. Figure 2.1, provides an overview of the capillary assay.

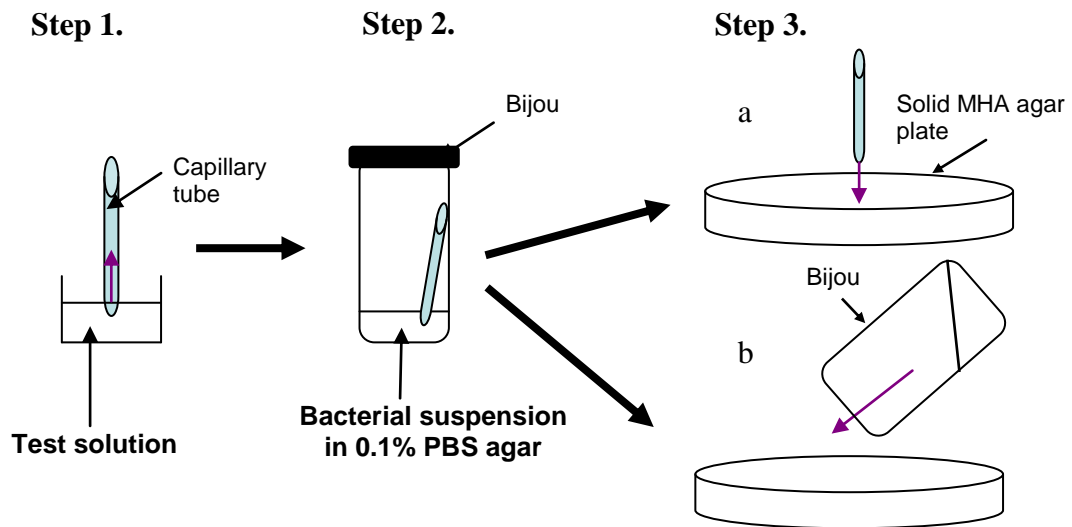


Figure 2.1. An outline of the capillary assay. Briefly, (1) a known chemoattractant is drawn up in the capillary tube by capillary action. (2) The capillary tube is incubated with *C. jejuni* of a known optical density under microaerobic conditions. After which (3a) the contents of both the capillary tube (3a) and the contents of the bijou (3b) were serially diluted and spotted out onto MHA plates. The plates were incubated for 48 hours after which viable counts were performed (this figure was drawn by O. Bridle, personal communication).

2.15.2.1. An alternative to Adler's capillary tube assay

Mazumder *et al.* (1999) developed a more simplified alternative to Adler's capillary tube assay (Adler, 1973). This version of the capillary assay was deemed more suitable for assessing chemotaxis in *C. jejuni* because it had been developed for use with another microaerophilic bacterium, *Pseudomonas*. The capillary assay developed by Mazumder *et al.* (1999) involved minimal preparation and required only a needle, syringe and a disposable 200 µl Gilson pipette tip. *C. jejuni* NCTC 11168 motile variant (NCTC 11168 MV, see Table 2.1) cells were harvested off MHA plates using 1 ml of PBS (cells were in late stationary phase). Thirty microliters of the neat, undiluted cell suspension was resuspended in 1 ml of PBS. One hundred microliters of the diluted cell suspension was drawn into a 200 µl Gilson disposable pipette tip (Fischer Scientific). A 25-gauge needle was used in place of a capillary tube (Adler, 1973) and was firmly attached to a 1 ml tuberculin syringe (Becton and Dickinson). The tuberculin syringe was filled with 100 µl of the test chemical, which in this case was either MHB or MEM. PBS was used as a negative control in all experiments. Sterile cotton was used to wipe off any residual solution that may have over spilled onto the needle.

The tuberculin syringe (containing the test solution) with a 25-gauge needle attached to it was inserted into a 200 µl Gilson disposable pipette tip containing the bacterial cell suspension. The Gilson pipette tip formed a tight seal with the collar of the tuberculin syringe. The 25-gauge needle was immersed approximately 3 mm into the bacterial cell suspension. The needle-syringe-pipette tip assembly was incubated horizontally under microaerobic conditions for 30 minutes. Following incubation, the syringe plus the needle was removed from the pipette tip and the contents of both the syringe and the pipette tip (bacterial suspension) were serially diluted in PBS (10^{-1} ,

10^{-2}). Ten microliter aliquots of the following dilution: 10^{-2} was spotted in triplicates onto one end of an MHA plate (supplemented with trimethoprim and vancomycin). The plates were briefly tipped to one side so that each drop spread to form a streak. All plates were incubated in the VAIN for 2 days, at 37°C before the number of colony forming units (CFU)/ml that had accumulated in the capillary tube could be determined. This time however, rather than looking at the absolute numbers of bacteria, the ratio of the bacteria was determined. The relative ratio of bacteria that had entered the 25-gauge needle containing the test attractant was compared to the control which contained PBS buffer. A relative chemotaxis response (RCR) greater than 2 was considered to be significant (Adler, 1973; Mazumder *et al.*, 1999). All work carried out on the capillary assay (all of section 2.15.2) whether it was based around Adler's (1973) original capillary tube assay or the adapted version by Mazumder *et al.* (1999) was done alongside O. Bridle.

2.15.3. Hard-agar plug (HAP) assay

2.15.3.1. Preparation of HAPs

A modified version of the hard-agar plug (mHAP) assay (Hugdahl *et al.*, 1988; Quinones *et al.*, 2009) was used in this study to determine the chemotactic behaviour of the wild-type *C. jejuni* motile variant and *tlp* mutant strains. The HAP assay helps to identify putative chemoattractants or chemorepellants (Table 2.12). A 2 M stock solution of each test substrate was prepared and diluted in 1 x PBS, this gave a range of concentrations over which responses to each substrate could be tested. Test chemicals were dissolved in 1 x PBS at double the required concentration. All

chemicals were of the highest purity and were obtained from Sigma-Aldrich and were all filter-sterilised using an acrodisc before being tested (PALL Life Sciences, Portsmouth UK). All test chemicals were approximately pH 7, the pH was adjusted using HCl and NaOH. Test chemicals were pre-warmed to 37°C in a heated water bath and maintained at this temperature until required.

Hard agar plugs (HAPs) were prepared by adding 4 ml of the test chemical to an equal volume (4 ml) of 4% PBS-agar (1 x PBS with 4% (w/v) Bioagar). Prior to the preparation of HAPs, the 4% PBS-agar was left in a heated water bath set at 70°C, so that the 4% PBS-agar remained molten. The solutions were mixed briefly by inverting the tube a few times and then poured immediately into Petri dishes (60 x 15 mm, Sterilin). The plates were left to cool and set overnight. The following day the agar was cut using a sterile metal borer, which cut the agar into 8 mm diameter HAPs. A HAP containing each the test chemical along with a HAP containing PBS (negative control) was placed into Petri dishes (90 x 45 mm, Sterilin) using sterile tweezers.

2.15.3.2. Cell preparation

For each strain of *C. jejuni* to be tested in the HAP assay, several MHA plates with confluent growth were required for the HAP assay. Cells were harvested off plates using 2 ml of PBS and pooled together. The cell suspension was transferred into a 15 ml universal tube (Sterilin). A 1/20 dilution of the neat cell suspension was performed using sterile PBS (50 µl neat cell suspension diluted in 950 µl PBS) and the OD₆₀₀ of the cell suspension was measured using a spectrophotometer Ultrospec 10, (Amersham Biosciences). The OD₆₀₀ of the cell suspension was adjusted so that the

final OD₆₀₀ of the cell suspension in the assay was 0.5 ($\sim 3 \times 10^9$ cfu/ml) using 0.8% PBS-agar (1 x PBS with 0.8% (w/v) Bioagar; Biogene Ltd). The cells were warmed to 37°C for 10 minutes using a heated water bath. The cell suspension (7.5 ml) was then added to 7.5 ml of PBS buffer in a 50 ml falcon tube (this halves the concentration of the agar to 0.4%). The PBS-agar plus cell suspension mixture was mixed by inverting the falcon tube twice. Then 7.5 ml of this PBS-agar cell suspension was transferred using a sterile 10 ml disposable plastic pipette into a Petri dish (Sterilin, 90 x 45 mm) that had been previously prepared so that it contained two HAPs; one containing the test chemical, the other containing PBS. The HAP containing PBS was used as a negative control in all subsequent experiments. The HAPs had been specifically positioned either side of the Petri plate and were approximately an equal distance away from each other. The PBS-agar cell suspension had to be carefully overlaid over the HAPs to prevent moving the HAPs. The plates were allowed to stand for approximately 5-10 minutes before being transferred into a microaerobic environment.

2.15.3.3. Quantifying bacterial chemotaxis

The HAP assay plates were examined at various different time points (0, 3, 6, 20, 48 and 96 hours) using an in-direct light source provided by the Syngene Gene Genius Bioimaging System (Syngene, UK) and photographs were taken following overnight incubation (20 hours), using Genesnap software. Positive chemotactic responses were recorded by measuring the diameter of the halo formed around the HAP containing the putative chemoattractant. If a test chemical was a chemorepellant, then there was a clear zone surrounding the HAP, indicating that there was no accumulation of

bacteria around the HAP. Furthermore, if this clear zone was preceded by a band of growth then this would indicate that the putative chemorepellent had driven bacteria away from the HAP

Table 2.12. Putative chemoattractants/chemorepellents screened in the Capillary and HAP assays.

Test Chemical	Concentrations tested *
Amino Acids	
L-Serine	1.0 M, 0.5 M and 0.1 M.
L-Aspartate (potassium)	1.0 M, 0.8 M, 0.6 M, 0.5 M, 0.4 M, 0.2 M and 0.1 M.
L-Glutamate (monosodium)	0.1 M.
Organic Acids	
L-Malate	0.25 M.
Pyruvate	1.0 M and 0.5 M.
α -Ketoglutarate (monosodium)	0.5 M and 0.1 M.
Succinate (disodium)	0.1 M
Carbohydrate	
L-Fucose	0.5 M and 0.1 M.

*Final concentration of the test chemical in the HAPs-all chemicals were made at 2 x the required concentration.

2.16. Bioinformatics

Campylobacter genome sequence data was obtained from <http://xbase.bham.ac.uk/campydb/>. All genome sequences were imported into the Clone Manager Professional Suite for further analysis (Scientific and Educational Software, 2005, version 8).

When analysing the secondary structures of the Tlps, the amino acid sequence of the Tlp under investigation was searched using the Pfam database

(<http://pfam.sanger.ac.uk/>) and TMpred programme (www.cbs.dtu.dk/cgi-bin/nph).

Primers were designed using the clone manager software to amplify by PCR specific regions in the target protein. The TMpred programme predicts the presence of transmembrane regions within your protein of interest and their orientation. A search is made using the amino acid sequence of the protein and the programme searches for the presence of hydrophobic stretches within the target protein. The programme also provides information regarding the orientation of each of the transmembrane helices. The NCBI “conserved domain” search engine was also used when looking at the conserved domains present in the Tlps (<http://www.ncbi.nlm.nih.gov/Structure/cdd>).

2.17. Statistical analyses

Statistical analyses and graphs were performed using either GraphPad Prism, version 5.00 (for Windows; GraphPad Software) or using Microsoft Excel 2007 (version 12.0.6024.5000, Microsoft Corporation). Student’s *t*-test with Welch’s correction were carried out to determine whether the data was statistically significant. A two-tailed test was carried out assuming unequal variances on each set of measurements. A confidence limit of 95% was used and a correlation coefficient value was obtained that ranged between 0 and 1, where 1 was indicative of a perfect correlation.

Chapter 3. Creating isogenic mutants in a specific group of chemoreceptors and genetic complementation of a *cj1506c* mutation

3.1. Introduction

Ten putative Methyl-accepting Chemotaxis Proteins (MCPs; or otherwise known as Tlp for transducer-like protein) receptors and two Aerotaxis protein homologues were identified upon *in silico* analysis of the genome sequence for *Campylobacter jejuni* strain NCTC 11168 (Parkhill *et al.*, 2000; Marchant *et al.*, 2002). A random transposon mutagenesis screen identified amongst a small subset of genes that were unrelated to chemotaxis, Tlp4 (Cj0262c) and Tlp10 (Cj0019) to be determinants of colonisation of the gastrointestinal tract in chickens (Hendrixson *et al.*, 2004). Moreover at the commencement of this project it was also known that CetA and CetB (for *Campylobacter* Energy Taxis; or Tlp9 and Aer2, respectively) are required for energy taxis in *C. jejuni* (Hendrixson *et al.*, 2001; Elliott and DiRita, 2008).

The periplasmic ligand-binding domain (PLD) is distinct in each Tlp and differs from that found in non-Epsilon proteobacteria. Thus, characterising this domain is an imperative in this study, as it is the PLD that is predicted to be involved in responding to signals external to the cell (Parkhill *et al.*, 2000; Marchant *et al.*, 2002). However, it is unknown at this stage what specific ligand/signal(s) are important in initiating chemotactic responses in *C. jejuni*. These objectives need to be addressed using biological assays and cannot be conferred from sequence data alone.

In order to determine the ligand-binding specificities of Tlps1-4, and to establish whether or not any of the Tlps are required for wild-type chemotaxis,

isogenic mutants were created in each of the genes (Figure 3.1; Marchant *et al.*, 2002). The mutagenesis strategy required deleting a significant portion of the open reading frame for each Tlp and then subsequently replacing the deleted region with a selectable marker. One of the objectives of this work was to use different selectable markers in each of the Tlps. This would then allow for double, triple or quadruple mutant strains to be created in a single strain of *C. jejuni*. By inserting different antibiotic markers would enable the identification of each single mutation. The construction of the Tlp1 isogenic mutant is detailed in this chapter, this mutant went on to be used in a study that has gone on to identify Tlp1 to be the aspartate receptor of *C. jejuni* (Hartley-Tassell *et al.*, 2010). A copy of this manuscript can be found in Appendix 1.

The *tlp1* isogenic mutant created in *C. jejuni* NCTC 11168 needed to be complemented i.e. the wild-type phenotype restored, and this was accomplished using an established complementation system (Karlyshev and Wren, 2005). The system is based around the pRR vector and had been used previous to this study, to successfully restore wild-type chemotaxis in a *cheB*, *cheR* and *cheY* chemotaxis mutant (Bridle, MPhil thesis). The complementation strategy undertaken in this work required reintroducing the wild-type copy of the target gene into one of three highly conserved ribosomal RNA (rRNA) clusters present in the *C. jejuni* chromosome. The process of creating the complementing construct for the *tlp1* isogenic mutant is presented in this chapter. The Tlp1 complementing construct produced in this study was also used in the study by Hartley-Tassell *et al.* (2010). The complementing construct helped to validate colonisation data obtained for the *tlp1* isogenic mutant, which showed reduced colonisation ability in chickens. The study by Hartley-Tassell *et al.* (2010; Appendix 1) will be reviewed in the discussion for this chapter.

The arrangement of Tlps1-4 in the *C. jejuni* genome is shown in Figure 3.1.

The genes required for *C. jejuni* chemotaxis are found scattered throughout the genome. Unlike the MCPs in *E. coli* which have been organised into an operon which contains genes involved in motility and chemotaxis, the *C. jejuni* Tlps are instead found adjacent to genes that have no role in chemotaxis or motility. The DNA sequences of the genes lying adjacent to the target Tlps were also incorporated in the mutagenesis strategy used to mutate the Tlps.

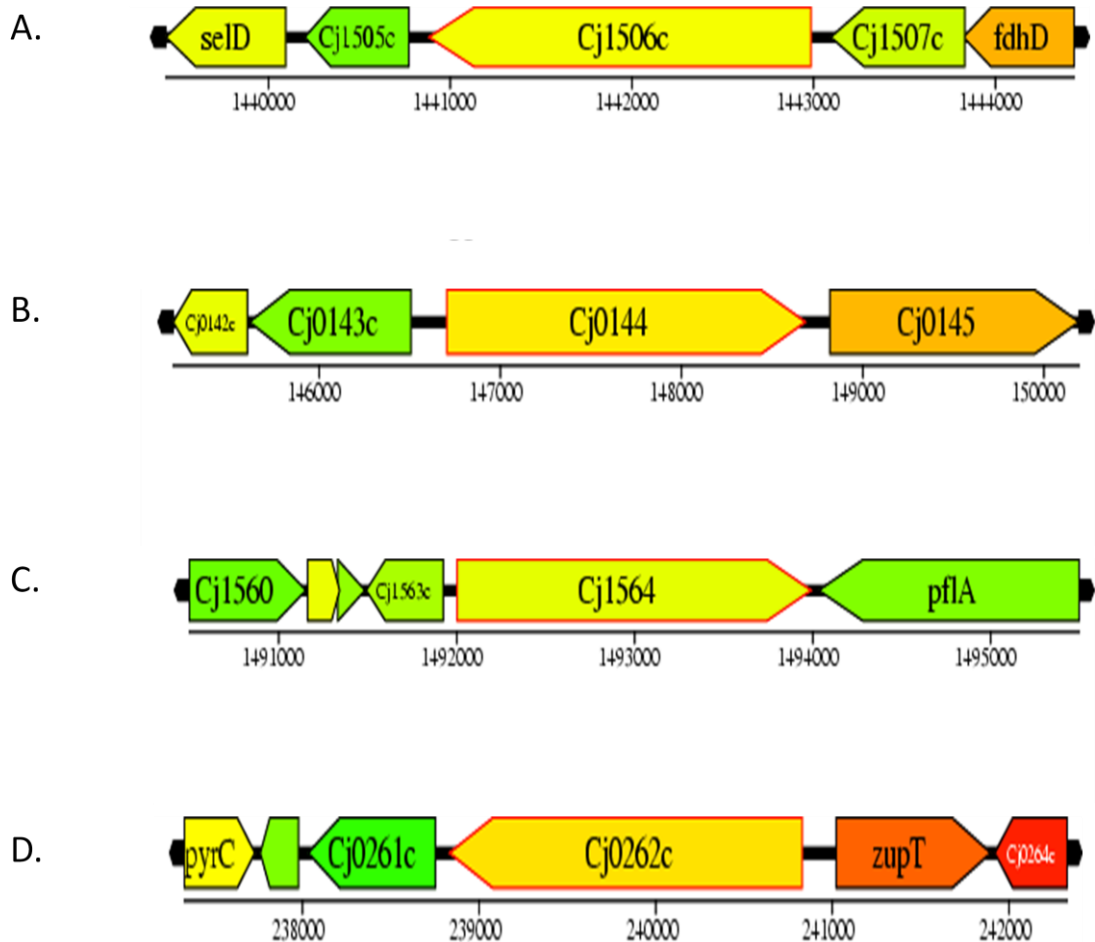


Figure 3.1. Genomic organisation of the Tlps in *C. jejuni* NCTC 11168. The diagram shows that Tlps 1-4 (A-D; Cj1506c-Cj0262c) are located at four distinct regions of the genome. All of the Tlps are found adjacent to genes predicted to have no role in *C. jejuni* chemotaxis. Unlike classical operons which most often contain genes of related function, the Tlps appear to be not part of an operon and instead are found clustered amongst genes of unrelated function. Genes positioned adjacent to the Tlps, have no known role in *C. jejuni* chemotaxis, and have been annotated in the genome sequence as follows: *selD*, putative selenide water dikinase; *fdhD*, formate dehydrogenase accessory protein; *pflA*, paralysed flagellum protein; *pyrC*, dihydroorotase; *zupT*, zinc transporter, and those genes with Cj numbers are of unknown function (Diagram taken from <http://www.xbase.bham.ac.uk/campydb/>).

3.2. Creating isogenic mutants in the Tlps in *C. jejuni* NCTC 11168 using an insertional inactivation strategy

3.2.1. Cloning the Tlps into pUC19

An inverse PCR mutagenesis (InvPCR) strategy was implemented to mutate Tlp1 (Cj1506c), Tlp2 (Cj0144), Tlp3 (Cj1564) and Tlp4 (Cj0262c) in the genome strain *C. jejuni* NCTC 11168. As the same strategy was used to mutate all four Tlps for brevity only the construction of the *cj1506c* mutant strain RS1Tlp1M ($\Delta cj1506c::cat$; Table 2.1) will be described in detail. To begin with, chromosomal DNA was prepared from the wild-type strain *C. jejuni* NCTC 11168 (section 2.8.2). This chromosomal DNA was used as the template in subsequent PCR reactions. The coding sequence for *cj1506c* (*tlp1*) was amplified by PCR (section 2.6) using the primer pair Cj1506F and Cj1506R (Table 2.6 and Table 3.1). A further 400-500 bp of DNA sequence, upstream and downstream of the target gene was also amplified. PCR amplification of *cj1506c* including the flanking regions generated a product of 2875 bp (Figure 3.2.1, lane 2).

Restriction recognition sequences for *KpnI* and *EcoRI* were added to the 5' end of the Cj1506F and Cj1506R primers, respectively. Once the *cj1506c* PCR product had been purified (section 2.9.1), restricted with *KpnI* and *EcoRI* (section 2.10.1) and purified once more, the PCR product was then ready to be directionally cloned into a suitable cloning vector. The cloning vector used was pUC19 (Table 2.2). Prominent features of the pUC19 vector included a multiple cloning site (mcs) that contained restriction recognition sequences for *KpnI* and *EcoRI*, an ampicillin resistance marker encoded by the *beta-lactamase* (*bla*) gene, and finally a *lacZ* gene located in the mcs in pUC19. Insertion of the *cj1506c* PCR fragment into the mcs in

pUC19 disrupted the *lacZ* gene. The pUC19 vector was restricted with *Kpn*I and *Eco*RI, and then dephosphorylated to prevent self ligation of the vector molecules (section 2.10.2). The vector DNA was purified and then ligated (section 2.10.3) with the *Kpn*I and *Eco*RI restricted *cj1506c* PCR product. The ligation reaction was purified by ethanol precipitation (section 2.9.3) and then transformed by either heat shock or electroporation into *Escherichia coli* DH5αE cells (section 2.11.3).

Transformations were plated out onto selective media which had been supplemented with ampicillin, X-gal and IPTG (section 2.2.2). Transformation controls were also set up alongside the ligation reaction. Transforming cells with either pUC19 vector alone or with distilled water served as the positive and negative controls, respectively in all *E. coli* transformations. *E. coli* cells transformed with recombinant plasmids appeared on selective media as white colonies whereas cells transformed with the pUC19 vector alone were identified as blue colonies.

The cloning of Cj0144, Cj1564 and Cj0262c proceeded similarly to *cj1506c*. The predicted fragment size for the *cj0144* gene (including the DNA flanking sequence) was 3234 bp. A fragment of this size could be obtained from the *C. jejuni* chromosome, however non-specific fragments were also being amplified along with the coding sequence for Cj0144. This is evident from the agarose gel shown in Figure 3.2.2. PCR amplification of *cj1564* and *cj0262c* produced fragments of 3009 bp and 1740 bp in size, respectively (data not shown).

The mutagenesis of Cj0262c proceeded differently to Cj1506c, Cj0144 and Cj1564. The size of the insert was significantly smaller at 1740 bp. Instead of incorporating DNA flanking sequences each side of the target gene, which had been done previously with the other Tlps, the Cj0262c primer (Cj0262F) amplified from within the *zupT* (zinc transporter protein) ORF whereas the reverse Cj0262R primer

was positioned mid-way into the Cj0262c ORF. Therefore for Tlp4, DNA flanking sequence was only present on one end of the gene. The process of creating a deletional mutant in *cj0262c* is shown in Figure 3.2.3.

3.2.2. Screening *E. coli* cells for recombinant plasmid constructs containing the *cj1506c* insert

White colonies were re-plated to verify that they were indeed positive transformants and not mixed clones. A colony PCR screen (section 2.6.1) was undertaken on a selection of clones using the pUC19 specific primer pair M13F and M13R (Table 2.6). The binding sites for the M13 forward and reverse primers are found outside of the mcs, and when used together they amplify across the insert. A selection of this colony PCR screen is shown in Figure 3.2.4. The results from this screen showed that only clone 2 (Figure 3.2.4, lane 4) was able to amplify correctly the *cj1506c* insert. The expected size of the cloned insert was 2875 bp. The colony PCR was repeated using the original cloning primers (Table 3.1). The results from this screen verified that clone 2 did indeed contain the required insert. Overnight cultures were prepared, and recombinant plasmids were extracted (section 2.8.1). To determine whether clone 2 contained the correct size construct, each of the recombinant plasmids extracted were digested with *PvuI* (Figure 3.2.5) and *EcoRI* (data not shown). Following digestion with *PvuI* (Figure 3.2.5; Lane 4) and *EcoRI* the recombinant plasmid extracted from clone 2 produced fragments of the expected sizes. The recombinant plasmids were restricted with *EcoRI* which following digestion should generate a single linear product (5553 bp in size, data not shown). Clone 2, produced a fragment of the expected size, whereas the remaining three clones (Figure 3.2.5; lanes 3, 5 and 6) yielded a fragment that was approximately 1 kb bigger than the expected size.

Thus the recombinant plasmid extracted from clone 2 was selected and sequenced (section 2.6.2) using M13F and M13R to screen for possible errors that may have been introduced during PCR reactions. The construct extracted from clone 2, was designated pRS01 (Figure 3.3).

Sequencing data for pRS01 showed a cytosine residue missing at position 2292 in the pRS01 construct (Figure 3.3). More specifically, this was in the DNA flanking sequence before the ATG translational start site for the *cj1506c* gene. The additional flanking sequence before the *cj1506c* gene was part of the coding sequence for *cj1507c*, which is located adjacent to the *cj1506c* gene (refer to Figure 3.1). The deletion of this cytosine residue in *cj1507c* could potentially alter the reading frame of this gene and lead to the premature truncation of the protein. The function of the *cj1507c* gene has not yet been elucidated. However, the pRS01 construct DNA was kept and the cloning of *cj1506c* continued, as it was unlikely that the missing base would be taken up through allelic exchange as the deleted cytosine residue was 364 bp away from the ATG translational start site for the *cj1506c* gene.

The cloning of the *cj0144*, *cj1564* and *cj0262c* genes into the pUC cloning vector proceeded similarly to *cj1506c*. The *cj0144* gene was cloned between *KpnI* and *EcoRI* sites in pUC19 to produce the initial plasmid construct pRS03 (Table 2.3). The *cj1564* and *cj0262c* genes however, were cloned between *EcoRI* and *BamHI* sites in pUC18 and pUC19, respectively, to produce the plasmid constructs pRS05 and pRS07, respectively (Table 2.3; construct maps not shown).

Table 3.1. A list of all *tlp* genes cloned, mutated and complemented in this study.

The primer sets used to amplify the target gene, (from either *C. jejuni* chromosomal DNA or plasmid DNA), the purpose of each set of primers, the expected sizes of PCR products, and finally the size of deletions introduced in target genes using inverse PCR primers is detailed.

Target gene/ region (bp)	Primer set	Purpose of primers	Product size (bp)	Deletion of target gene (bp)	Template Type
<i>cj1506c</i>	Cj1506F and Cj1506R	Cloning	2875	N/A	<i>C. jejuni</i> NCTC chromosomal DNA
<i>cj0144</i>	Cj0144F and Cj0144R	Cloning	3234	N/A	<i>C. jejuni</i> NCTC chromosomal DNA
<i>cj1564</i>	Cj1564F and Cj1564R	Cloning	3009	N/A	<i>C. jejuni</i> NCTC chromosomal DNA
<i>cj0262c</i>	Cj0262F and Cj0262R	Cloning	1740	N/A	<i>C. jejuni</i> NCTC chromosomal DNA
<i>cj1506c</i>	Cj1506invF and Cj1506invR	Inverse PCR	4645	940	pRS01
<i>cj0144</i>	Cj0144invF and Cj0144invR	Inverse PCR	5018	926	pRS03
<i>cj1564</i>	Cj1564invF and Cj1564invR	Inverse PCR	4751	923	pRS05
<i>cj0262c</i>	Cj0262invF and Cj0262invR	Inverse PCR	3736	695	pRS07
<i>cj1506c</i>	Cj1506FC-omp and Cj1506RC-omp	Complementation	2523	N/A	<i>C. jejuni</i> NCTC chromosomal DNA
Poly-linker	pTrcHisBF and pTrcHisBR	Complementation and producing pRRK-poly.	140	N/A	pTrcHisB

Figure 3.2. Summary of the steps undertaken to clone the *cj1506c* gene (including DNA flanking sequence) into pUC19 and PCR amplification of *cj0144*. Results from PCR reactions are presented here, which include the amplification of *cj1506c*. Colony PCR screening of *E. coli cj1506c/pUC19* transformants and the subsequent digestion of putative recombinant plasmids is also illustrated. All results were visualized on a 0.8% TAE agarose gel (see section 2.7.1, for agarose gel electrophoresis method). All relevant marker sizes are indicated to the left of each gel (for DNA markers information, section 2.4).

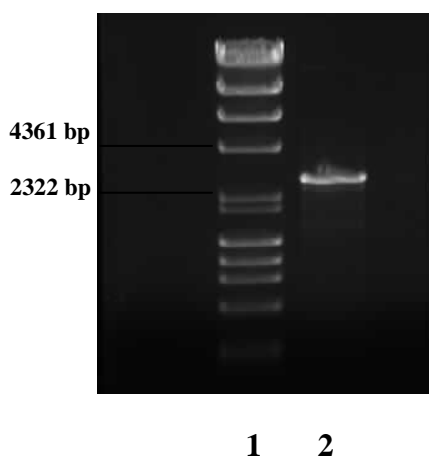


Figure 3.2.1. PCR amplification of *cj1506c*. PCR amplification of *cj1506c* from 25 ng of chromosomal DNA (Lane 2). Amplification of *cj1506c* was achieved using the cloning primers Cj1506F and Cj1506R (table 3.1). The expected size of *cj1506c* was 2875 bp in size. Lane 1, $\lambda\phi$ DNA marker.

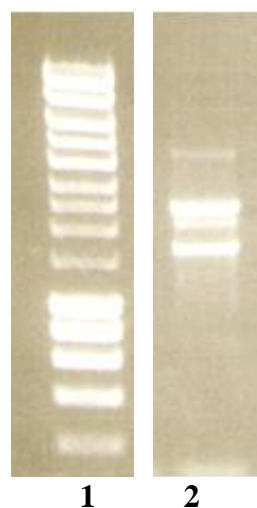


Figure 3.2.2. PCR amplification of *cj0144*. PCR amplification of *cj0144* from 25 ng of chromosomal DNA (Lane 2). The expected size of *cj0144* was 3234 bp in size. Lane 1, 1 kb DNA marker (for primer information refer to table 3.1).

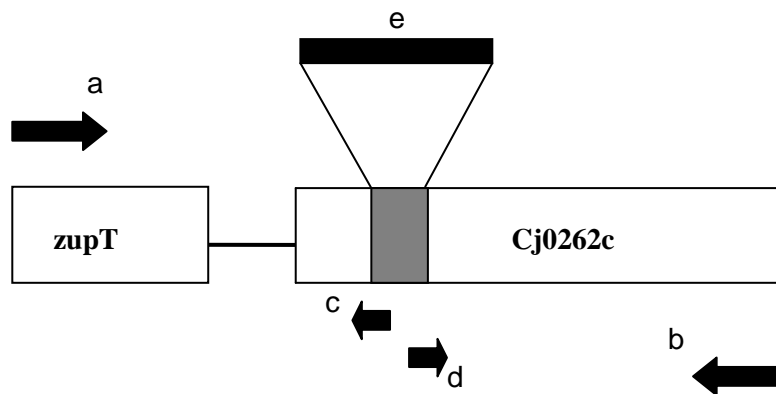


Figure 3.2.3. Planning the mutagenesis of Cj0262c. Primers ‘a’ and ‘b’ are the cloning primers used to amplify the *cj0262c* gene from *C. jejuni* NCTC 11168 chromosomal DNA. These primers amplified a PCR product of 1740 bp. Primer set ‘c’ and ‘d’ indicate the inverse PCR primers used to delete 695bp of the Cj0262c ORF. The deleted region was to be replaced by a selectable marker ‘e’ (e; chloramphenicol acetyl-transferase (*cat*) cassette). Primer ‘a’ was positioned 509 bp from the ATG start site of the *cj0262c* gene and was positioned in the ORF of *zupT* (zinc transporter protein). Refer to Table 3.1 for information regarding the cloning and inverse PCR primers used for the mutagenesis of Cj0262c.

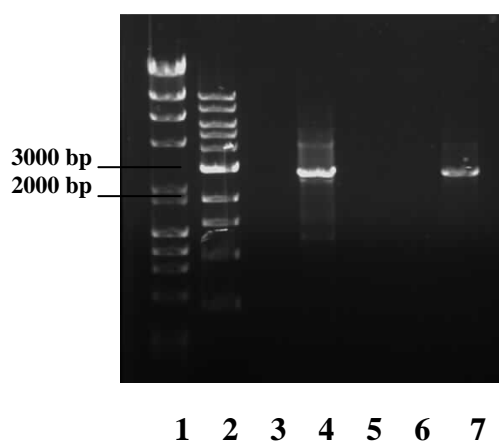


Figure 3.2.4. Colony PCR screen of recombinant plasmid constructs using gene specific primers. Cj1506F and Cj1506R (table 2.6) were used to screen 4 recombinant plasmid constructs (Lanes 3-6). Clone 2 (Lane 4) amplified correctly the *cj1506c* insert (2875 bp); this fragment included the entire coding region for *cj1506c* as well as the DNA flanks each side of *cj1506c*. Lane 1, $\lambda\phi$ DNA marker; Lane 2, 1 kb DNA ladder; Lane 7, 20 ng wild-type *C. jejuni* 11168 (positive control).

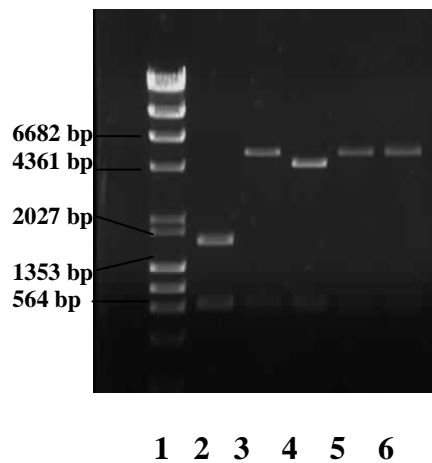


Figure 3.2.5. *PvuI* digest to identify *cj1506c* recombinant plasmid constructs. Lane 1, $\lambda\phi$ DNA marker; Lane 2, pUC19 DNA, following digestion with *PvuI* should give two fragments of 1790 and 896 bp in size (vector only control); Lanes 3-6, contain construct DNA extracted from 4 clones previously screened by colony PCR (Figure 3.2.2). The expected fragment sizes post digestion were 4657 and 896 bp. Only clone 2 (Lane 4) produced fragments of the intended sizes.

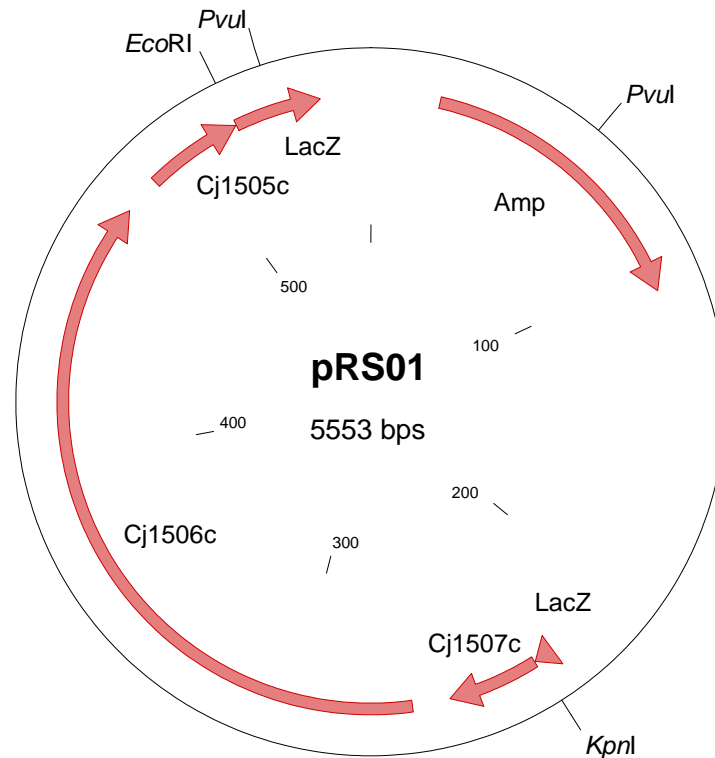


Figure 3.3. Initial construct map of pRS01. The *cj1506c* gene was directionally cloned into the multiple cloning site (mcs) found in the cloning vector pUC19, at the *KpnI* and *EcoRI* restriction sites. Insertion of the *cj1506c* gene into the mcs disrupts the function of the *lacZ* gene. The genes adjacent to *cj1506c* in the *C. jejuni* chromosome have been indicated as have the restriction endonucleases (*PvuI*) used to verify *cj1506c* recombinant plasmid constructs. The size of the plasmid has been indicated (this plasmid is fully detailed in Table 2.3).

3.2.3. Disruption of the Tlp ORFs by inverse PCR mutagenesis

3.2.3.1. Disrupting the Cj1506c ORF

Inverse PCR primers were implemented in this study to disrupt the *cj1506c* gene in *C. jejuni* NCTC 11168. Inverse PCR primers were positioned within the coding region for *cj1506c*, facing outwards. The inverse primers used were Cj1506invF and Cj1506invR (Table 2.6 and 3.1) which created a deletion of 908 bp within the *cj1506c* ORF and produced a linear PCR product of 4645 bp from pRS02 construct DNA (Figure 3.4.1). The amplified fragment contained, (a) part of the coding sequence for *cj1506c*, (b) DNA flanking sequence for the genes located either end of *cj1506c* (*cj1507c* and *cj1505c*; Figure 3.1), and finally (c) pUC19 vector sequence. However, a significant proportion of the coding region for *cj1506c* had been deleted using this mutagenesis strategy.

NotI restriction sites were incorporated onto the 5' end of each inverse PCR primer. The next step involved inserting a chloramphenicol acetyl-transferase (*cat*) cassette into the deleted portion of the *cj1506c* gene. A promoted *cat* cassette was selected and was amplified out of the plasmid pAV35, using *cat* sequence specific primers (pAV35F and pAV35R; Figure 3.4.2). The *cat* cassette specific primers also had *NotI* restriction sites incorporated at the 5' ends. Once the *cj1506c* inverse and *cat* cassette PCR products had been purified, digested with *NotI*, and purified once again, the *cat* cassette, and not the vector on this occasion was dephosphorylated. The *cat* cassette was dephosphorylated to prevent the formation of *cat* cassette concatamers. The *cat* cassette was purified once more before being ligated with the *cj1506c* inverse PCR product. The pRS02 construct was transformed by heat shock into chemically competent *E. coli* DH5 α E cells. Positive pRS02 recombinant

transformants were plated out on recovery media supplemented with chloramphenicol and ampicillin.

3.2.3.2. Disrupting the Cj0144, Cj1564 and Cj0262c ORFs

The majority of the ORF of *cj0144* was deleted by insertion of an erythromycin resistance marker at the point of deletion (encoded by the *ermC'* gene). Following insertion of an erythromycin resistance cassette (*ermC'*) a 926 bp deletion of the *cj0144* ORF was successfully created. The *cj1564* ORF was initially disrupted through insertion of a kanamycin resistance cassette (*aphA-3*), however this was found to be unsuccessful upon transformation into *E. coli* (see section 3.2.4). Therefore, an alternative selectable marker was selected for insertion into the *cj1564* ORF. The *cj1564* gene with 923 bp of the ORF deleted through insertion of an erythromycin resistance cassette (*ermC'*) produced pRS06, which was transformed by heat shock into chemically competent *E. coli* DH5 α E cells (Table 2.3). The Cj0262c inverse primers deleted 691 bp of the *cj0262c* coding region. A *cat* cassette was inserted 64 bp in from the ATG translational start site for *cj0262c*. Following the insertion of the *cat* cassette into the *cj0262c* ORF, 460 bp of *cj0262c* coding sequence still remained. There appeared to be enough flanking sequence to facilitate allelic exchange to occur at the *cj0262c* locus on the *C. jejuni* chromosome. All selectable markers were inserted into a *NotI* site which had been introduced when deleting the ORF of the Tlps.

Figure 3.4. Summary of the steps undertaken to disrupt the *cj1506c* gene in *C. jejuni*. Inverse PCR amplification of *cj1506c* from pRS01 construct DNA and PCR amplification of the *cat* cassette from pAV35 is shown below. The *cj1506c* inverse PCR product was ligated with the *cat* cassette to produce pRS02. Colony PCR screening of pRS02 *E. coli* transformants is presented here. As well as the final transformation of the pRS02 construct into wild-type *C. jejuni* cells. Colony PCR screening of *C. jejuni* $\Delta cj1506c::cat$ transformants is also shown. All results were visualised on a 0.8% TAE agarose gel (see chapter 2, section 2.7.1 for a method on agarose gel electrophoresis). All relevant marker sizes are indicated to the left of each gel.

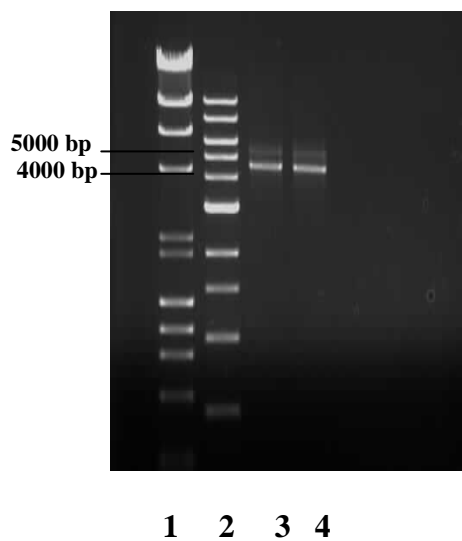


Figure 3.4.1. Inverse PCR amplification of *cj1506c*. 0.25 and 0.5 ng (Lanes 3 and 4 respectively) of pRS01 construct DNA was used as template for PCR. The Cj1506invF and Cj1506invR primer set (table 2.6 and 3.1), amplified around the pRS02 construct, from within the *cj1506c* gene, to produce a fragment of 4645 bp (this included the *cj1506c* DNA flanks, pUC19 vector sequence, but only part of the coding region for *cj1506c*; Lanes 3 and 4). Lane 1, $\lambda\phi$ DNA marker; Lane 2, 1 kb DNA marker.

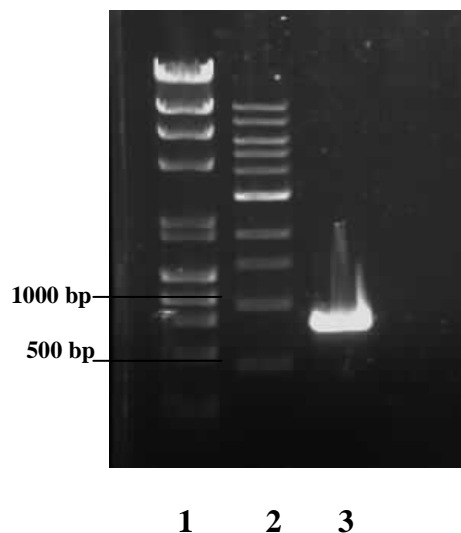


Figure 3.4.2. PCR amplification of the *cat* cassette from pAV35 (lane 3). 0.5 ng of pAV35 DNA was used as template for the reaction. Amplification of the *cat* cassette was achieved using the primer set pAV35F and pAV35R (table 2.6). The expected size of the amplified product was 833 bp. Lane 1, $\lambda\phi$ DNA marker; Lane 2, 1 kb DNA marker.

3.2.4. Screening putative *E. coli* transformants for recombinant plasmids

A colony PCR screen was attempted on ten chloramphenicol resistant, *E. coli* transformants. The colony PCR was carried out using the M13 primers and *cat* cassette specific primers (Table 2.6). The M13 primers were used on their own as well as in combination with the *cat* cassette sequence specific primers. This confirmed the presence of the *cat* cassette in clones, but also the orientation of the *cat* cassette with respect to the orientation of *cj1506c*. A sample of this screen is shown in Figure 3.5.. Clones 3, 5 and 8 to 10 amplified PCR fragments of the expected sizes using the M13F and M13R primers (Gel A; lanes 5, 7, 10 to 12). Only clones 3, 8 and 10 amplified a fragment of the expected size using the M13F in combination with the CatinvR primer (Gel B; lanes 5, 10 and 12). Plasmids were extracted from clones 3, 8 and 10 (Figure 3.5.). These plasmids were sequenced to further verify the presence of the *cat* cassette as well as to check that there were no errors in the remaining cloned insert, particularly in the DNA flanking sequence. Sequencing data for clone 3 came back as error free, and the construct was designated pRS02 (Figure 3.5.2). Furthermore, the sequencing data for pRS02 confirmed previous sequencing data obtained for pRS01, which revealed a missing cytosine residue, located 346 bp from the ATG translational start site for *cj1506c*.

A colony PCR screen was undertaken to identify positive clones of $\Delta cj0144::ermC$, $\Delta cj1564::ermC$ and $\Delta cj0262c::cat$ in *E. coli*. The colony PCR screens and the primers used are indicated in Figure 3.5.2 and in Table 3.1 (Gels A, B and C). The colony PCR screening for positive clones of $\Delta cj0144::ermC$ identified from the 8 clones screened, all but clone 6 (Gel A, lane 9) to have amplified correctly a PCR product of the intended size. *C. jejuni* NCTC 11168 chromosomal DNA was included as a positive PCR control. (Figure 3.5.3; Gel A, lane 2). A fragment of 3354

bp was expected when using the Cj0144F and Cj0144R cloning primers. However, this reaction proved to be unsuccessful. The *cj1564* ORF was initially disrupted through insertion of a kanamycin resistance marker (encoded by the *aphA-3* gene) into the deleted region of the *cj1564* coding sequence. The majority of transformants appeared to contain the kanamycin cassette facing in the reverse (opposite) orientation with respect to the orientation of *cj1564* gene. These constructs were consequently rejected because of the possible polar effects this could have on downstream genes (data not shown). An erythromycin resistance marker was tried as alternative to interrupt the *cj1564* gene. A colony PCR screen was carried out on erythromycin resistant *E. coli* colonies, positive clones are shown in Figure 3.5.3 (Gel B; Lanes 2, 3, 5 and 9). A colony PCR screen on $\Delta cj0262c::cat$ recombinants using M13 primers and *cat* cassette specific primers found seven out of the ten clones screened to contain an insert of the correct size. (Figure 3.5.3; lanes 4-9 and lanes 11 and 13). Positive clones of $\Delta cj0144::ermC$, $\Delta cj1564::ermC$ and $\Delta cj0262c::cat$ were sequenced and those found to be correct were named pRS04, pRS06 and pRS08 respectively (Figure 3.5.4, 3.5.5 and 3.5.6.).

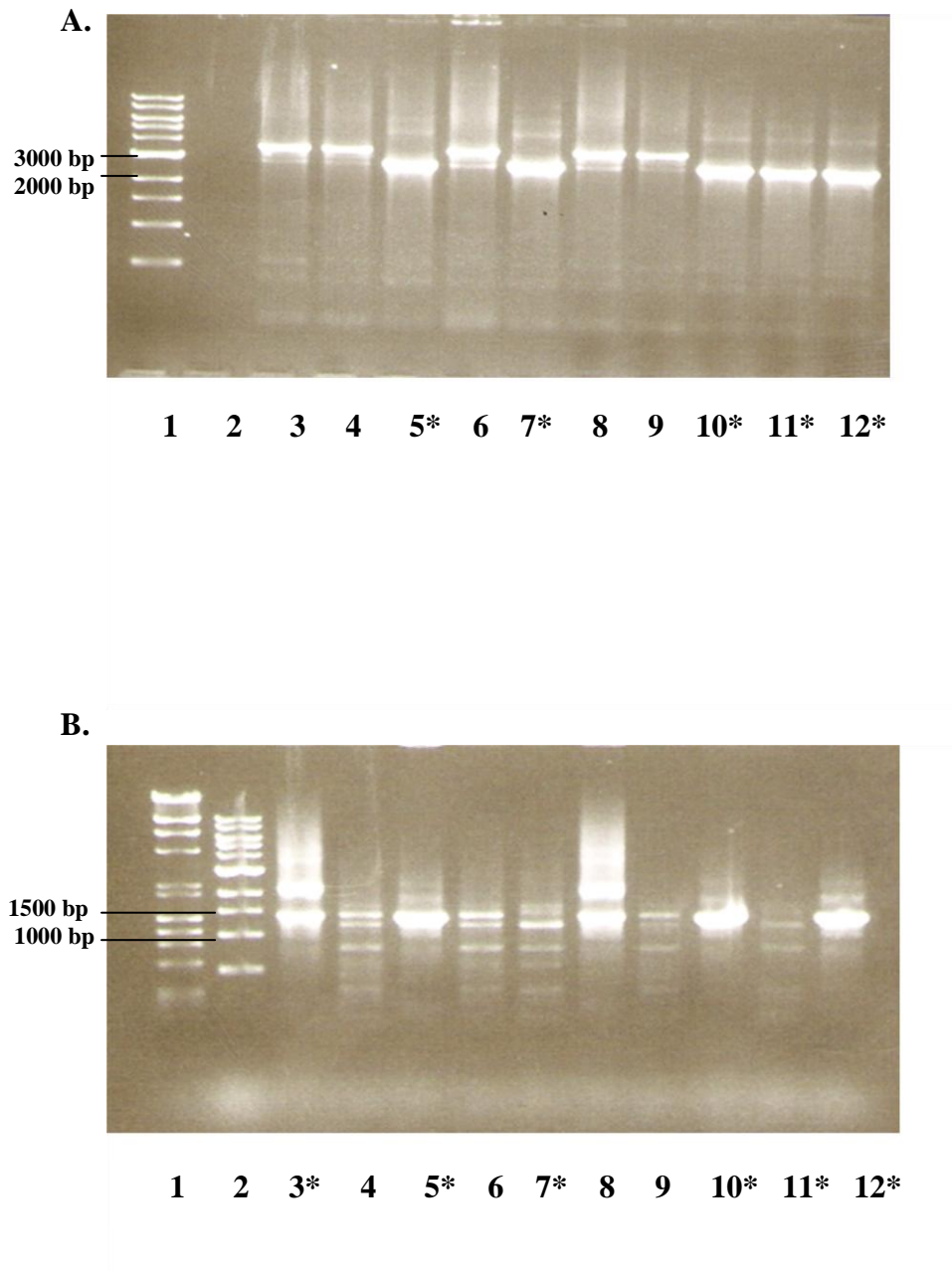


Figure 3.5. Colony PCR screen on putative pRS02 transformants of *E. coli*. A total of ten colonies were screened using the primers M13F and M13R (Gel A) or M13F with CatinvR (Gel B). The expected size of the amplified product using M13F and M13R was 2875 bp, however when using M13F and CatinvR, the predicted fragment size was 1445 bp. The clones which produced fragments of the predicted size have been marked (*) below each gel. Clones 3, 8 and 10 produced fragments of the expected size in both of the colony PCR screening (Gel A and B). Gel A; Lane 1, 1 kb DNA marker; Lane 2, water in place of template DNA (negative control). Gel B; Lane 1, $\lambda\phi$ DNA marker; Lane 2, 1 kb DNA marker.

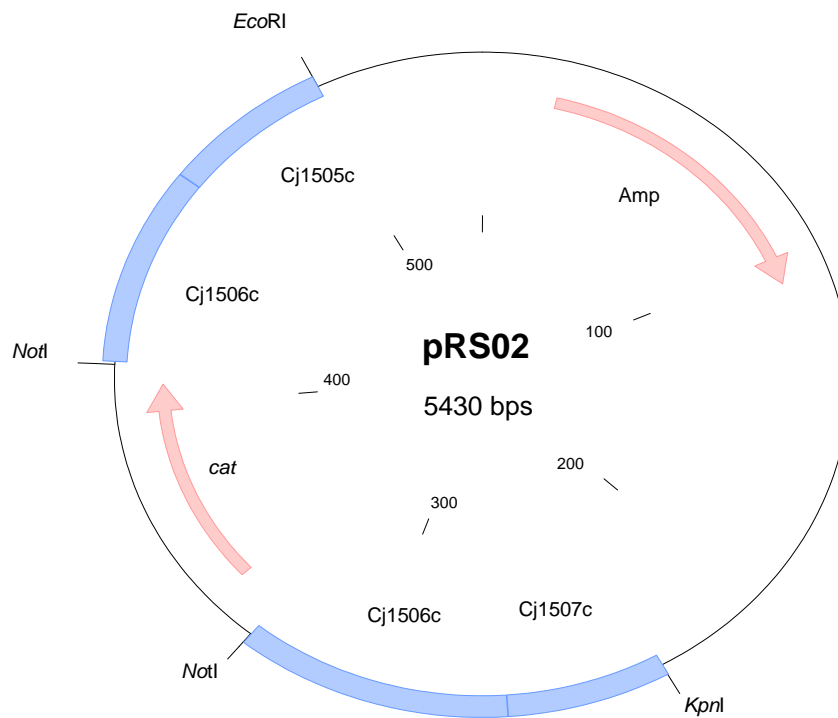


Figure 3.5.1. Final construct map of pRS02. The plasmid map shows the *cj1506c* ORF replaced with a *cat* chloramphenicol acetyl transferase cassette. The *cj1506c* gene was originally cloned into the *lacZ* gene region of pUC19 at the *EcoRI* and *KpnI* restriction sites. A promoted *cat* cassette was ligated together with the *cj1506c* inverse PCR product to produce the construct pRS02. The primers used to amplify the *cat* cassette (shown in pink) and the *cj1506c* inverse PCR product (shown in blue) had *NotI* restriction sites at the 5' end (amp, confers ampicillin resistance (pink); *cat*, confers chloramphenicol resistance). The size of the plasmid has been indicated (this plasmid is fully detailed in Table 2.3).

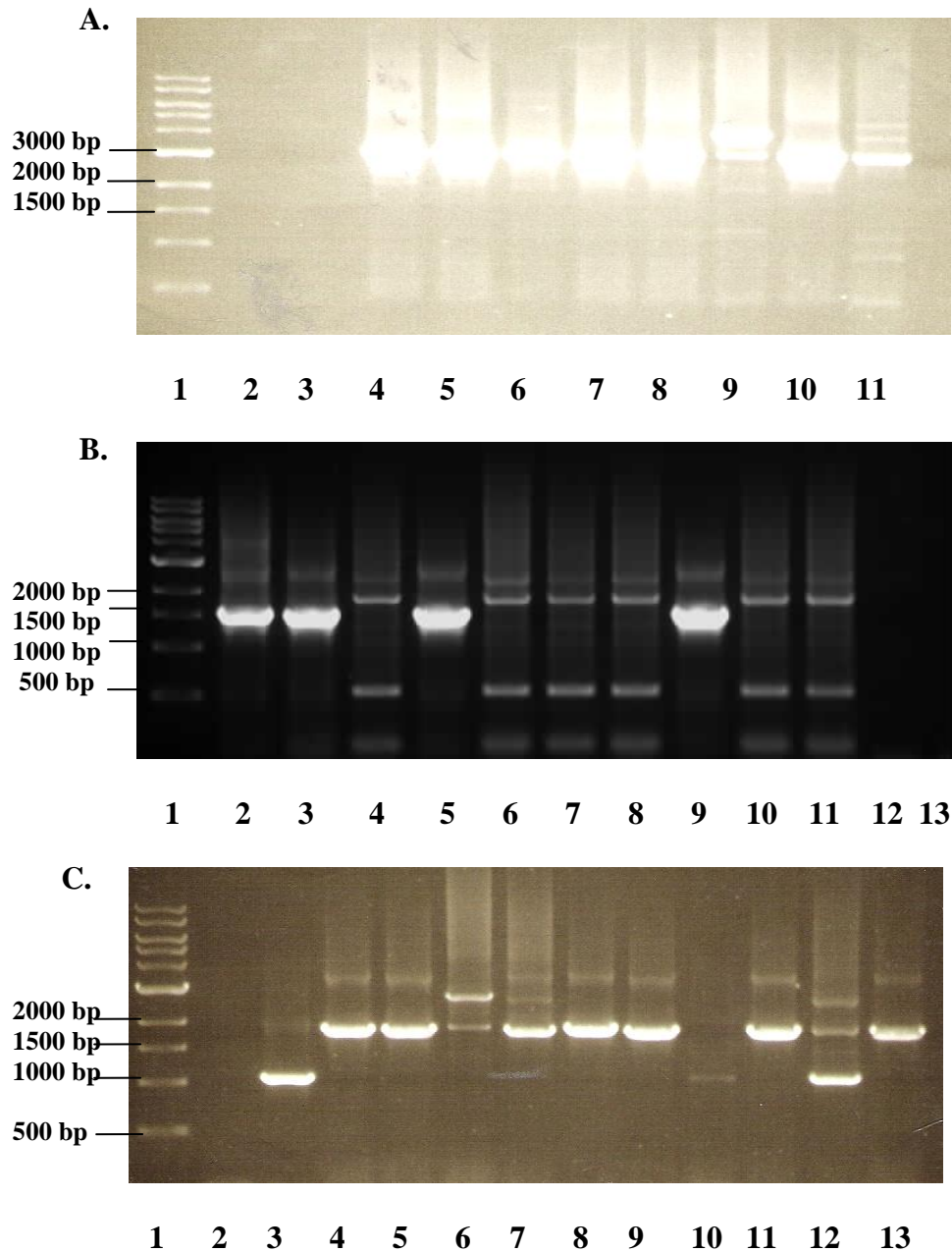


Figure 3.5.2. Colony PCR screen on putative final construct transformants for Cj0144 (Tlp2), Cj1564 (Tlp3) and Cj0262c (Tlp4). Gel A shows *cj0144* erythromycin resistant (Ery^R) *E. coli* colonies screened using Cj0144F and Cj0144R primers. The expected fragment size was 3354 bp. Gel B shows *cj1564* Ery^R *E. coli* colonies, which were screened using Cj1564F and ErmCIR (ErmCIR primer amplifies from within the *ermC'* coding sequence). The predicted fragment size was 1611 bp. Gel C shows *cj0262c* chloramphenicol resistant (cat^R) *E. coli* colonies screened using M13F and M13R primers. The expected fragment size was 1939 bp. Wild-type *C. jejuni* (20 ng chromosomal DNA) was used as a control, and no product was expected from using the Cj1564F and ErmCIR primer set (Gel B; lane 12), although a PCR product of 3354 bp was expected in lane 2 (Gel A). Lane 1, in Gels A, B and C contained the 1 kb DNA marker. In Gels A (lane 3), B (lane 13) and C (lane 2) contained water in place of template DNA (negative control).

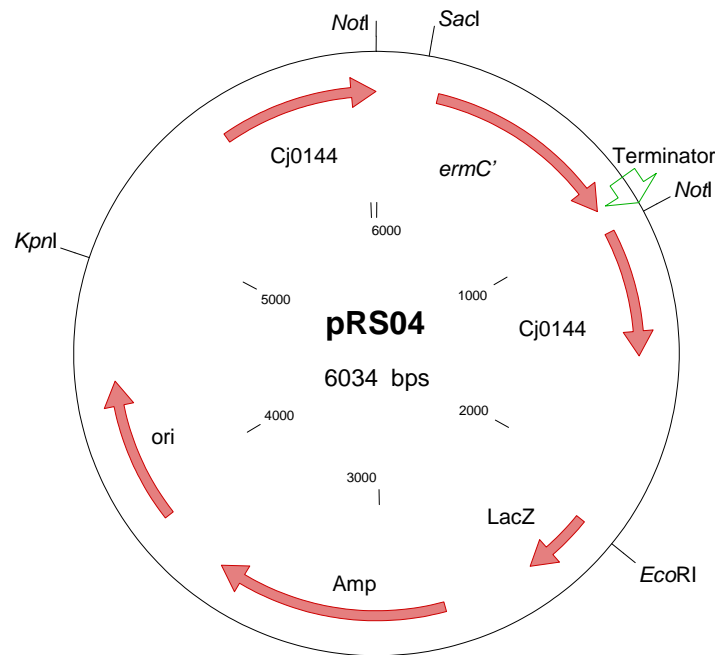


Figure 3.5.3. Final construct map of *cj0144* (pRS04). The plasmid map shows the *cj0144* ORF replaced with the *ermC'* gene (confers erythromycin resistance). The *cj0144* gene was originally cloned into the *lacZ* gene region in pUC19 at the *EcoRI* and *KpnI* restriction sites. The *ermC'* gene has its own promoter and its own transcriptional terminator sequence (shown by the arrow outlined in green) and was ligated together with the *cj0144* inverse PCR product to produce the construct pRS04. The primers used to amplify the *ermC'* gene and the *cj0144* inverse PCR product had *NotI* restriction sites at the 5' end (amp, confers ampicillin resistance). The size of the plasmid has been indicated (this plasmid is fully detailed in table 2.3).

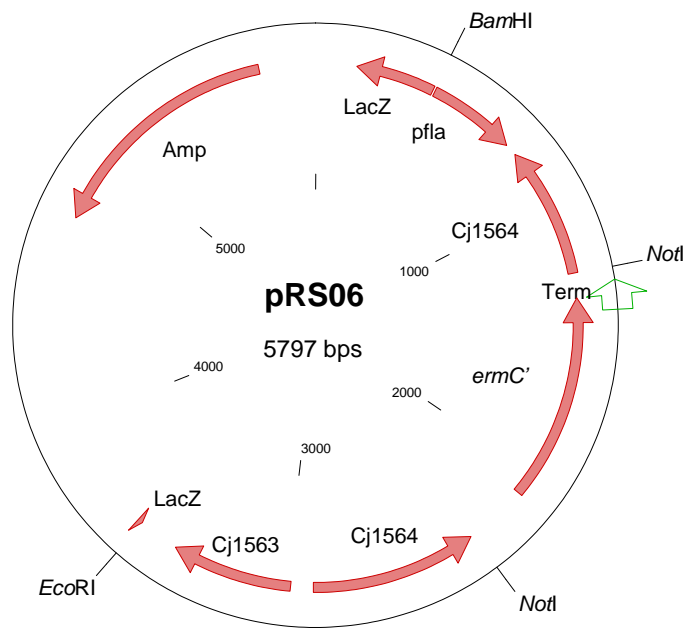


Figure 3.5.4. Final construct map of *cj1564* (pRS06). The plasmid map shows the *cj1564* ORF replaced with the *ermC'* gene (confers erythromycin resistance). The *cj1564* gene was originally cloned into the *lacZ* gene region in pUC18 at the *EcoRI* and *BamHI* restriction sites. The *ermC'* gene has its own promoter and its own transcriptional terminator sequence (shown by the arrow outlined in green), and was ligated with the *cj1564* inverse PCR product to produce the construct pRS06. The primers used to amplify the *ermC'* gene and the *cj1564* inverse PCR product had *NotI* restriction sites at the 5' end (amp, confers ampicillin resistance). The size of the plasmid has been indicated (this plasmid is fully detailed in table 2.3).

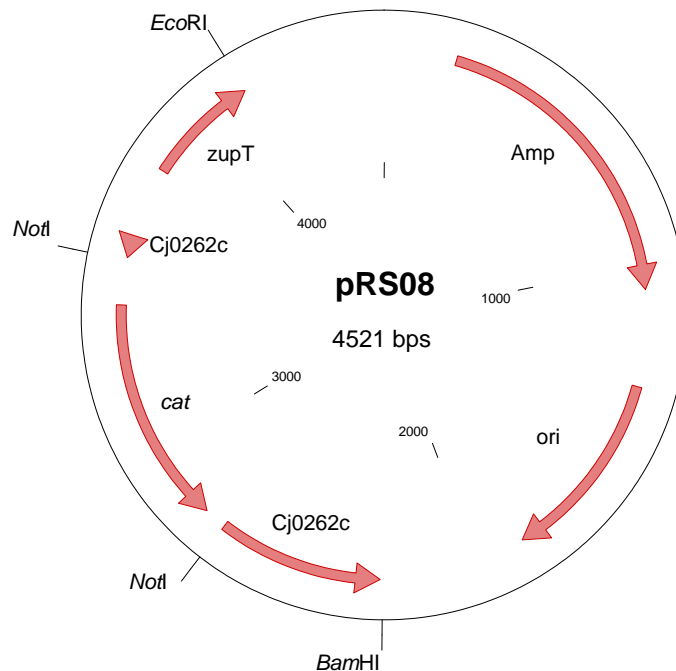


Figure 3.5.5. Final construct map of *cj0262c* (pRS08). The plasmid map shows the *cj0262c* ORF replaced with a *cat* (chloramphenicol acetyl transferase) cassette. The *cj0262c* gene was originally cloned into the *lacZ* gene region of pUC19 at the *EcoRI* and *BamHI* restriction sites. A promoted *cat* cassette was ligated with the *cj0262c* inverse PCR product to produce the construct pRS08. The primers used to amplify the *cat* cassette and the *cj0262c* inverse PCR product had *NotI* restriction sites at the 5' end (amp, confers ampicillin resistance; *cat*, confers chloramphenicol resistance; ZupT, zinc transporter). The size of the plasmid has been indicated (this plasmid is fully detailed in table 2.3).

3.2.5. Allelic replacement of a wild-type *tlp* gene with a mutated copy

Purified pRS02 construct DNA was transformed into chemically competent *C. jejuni* NCTC 11168 cells by electroporation (section 2.11.6). Once inside *C. jejuni* the construct cannot be maintained, and instead behaves as a suicide vector. As the majority of the *cj1506c* coding region had been deleted by inverse PCR, the DNA flanks amplified alongside *cj1506c* were imperative for homologous recombination to occur. In a fraction of the *C. jejuni* cells, a double crossover event takes place at the *cj1506c* locus on the *C. jejuni* chromosome and homologous DNA present in pRS02, resulting in allelic exchange of the wild-type *cj1506c* allele for the mutant allele.

Initially all transformations were recovered on non-selective media but were subsequently transferred onto selective media containing chloramphenicol. *C. jejuni* *cj1506c::cat* transformants that were chloramphenicol resistant were screened by colony PCR. The presence of the *cat* cassette in transformants was verified by colony PCR screening using a *cat* cassette sequence specific primer (Table 2.6) in combination with two newly designed primers, Cj1506FSeq and Cj1506RSeq (Table 2.6). These new primers were outside of the coding regions that had been cloned, and were positioned further out into the *cj1507c* and *cj1505c* coding regions (DNA flanks either side of *cj1506c*). These primers were therefore outside of the region which should have undergone homologous recombination. Performing colony PCR analysis of the target gene and the genes adjacent to *cj1506c* was informative because it confirmed (a) the presence of the *cat* cassette, (b) the orientation of the *cat* cassette with respect to *cj1506c* (same orientation as *cj1506c*) and finally (c) that homologous recombination had taken place at the desired locus on the *C. jejuni* chromosome. A small scale chromosomal DNA extraction (section 2.8.1) was undertaken on *cj1506c::cat* mutant clones 3 and 8. A PCR screen was then attempted using the

chromosomal DNA extracted from these mutants as template, and a primer specific for the *cat* cassette (CatInvR; Table 2.6) and DNA flanking sequence either side of the *cj1506c* gene (Cj1506FSeq and Cj1506RSeq primers; Figure 3.6.1). A PCR product was successfully generated from chromosomal DNA extracted from clone 3, which was then used as template for subsequent sequencing reactions. The sequencing data for the *cj1506c* mutant strain *C. jejuni* RS01Tlp1Mut ($\Delta cj1506c::cat$; Table 2.1), revealed the presence of the missing cytosine residue, which was initially missing in the both the pRS01 and pRS02 constructs. The sequencing data confirmed that allelic exchange had taken place at the expected locus on the *C. jejuni* chromosome and the *cj1506c* gene on the chromosome had been replaced with a *cat* cassette. The sequencing data also revealed that homologous recombination had occurred further in from the *cj1507c* flank, where the missing cytosine residue was originally located.

Gel A in Figure 3.6.2 shows a PCR screen done on chromosomal DNA extracted from a *C. jejuni* *cj0144* erythromycin resistant (Ery^R) mutant. The mutant DNA was screened by PCR using three different combination of primers: Cj0144FMutVer and Cj0144RMutVer primers (Table 2.6; Lanes 2-4), Cj0144F and ErmInvR (Lanes 5-7), Cj0144R and ErmInvF. The predicted sizes of fragments were 2610 (Lane 2), 1246 (Lane 5) and 827 bp (Lane 8), respectively for the $\Delta cj0144::ermC$ mutant. The Cj0144MutVer primers were positioned as follows in the *C. jejuni* genome. The Cj0144FMutVer primer was positioned 325 bp from the Cj0144 ATG start site. The Cj0144RMutVer primer was positioned 185 bp from the TAA stop codon of Cj0144 and was inside the ORF of Cj0145. DNA sequencing was performed from a PCR product to ensure that there were no errors in the DNA

flanking the target gene. Moreover, sequencing across the insert verified that the *cj0144::ermC* mutant was in the correct locus on the *C. jejuni* chromosome.

A colony PCR was undertaken using Cj1564F and Cj1564R (Figure 3.6.3, Gel A; Table 2.6) and Cj1564R and ErmCIF (Figure 3.6.3, Gel B; Table 2.6) on erythromycin resistant *C. jejuni* colonies. When the colonies were screened using the original cloning primers, they produced a fragment of the expected size (3126 bps; Figure 3.6.3, Gel A). However, when screening using the original cloning primer in combination with the erythromycin specific primers (amplified from within the *ermC* gene), contaminating bands were also being amplified along with the desired fragment (desired fragment was 1026 bps; Figure 3.6.3, Gel B). These contaminating bands were also present in the wild-type control, however the desired fragment of 1026 bps was missing in the positive control (Figure 3.6.3; Gel B, Lane 10). A PCR product was generated using the original cloning primers and was sent off for sequence analysis using all of the primers used in the colony PCR screening. No valid sequencing trace could be detected when using the erythromycin primers when sequencing from this PCR product.

Once again chromosomal DNA (20 ng) extracted from a putative $\Delta cj0262c::cat$ *C. jejuni* mutant (clone 1) was used as template for PCR screens performed using three different combinations of primers. Of which included: Cj0262F and Cj0262R (Figure 3.6.4; Lanes 2-4), Cj0262F and CatInvR (Figure 3.6.4; Lanes 5-7), Cj0262R and CatInvF (Figure 3.6.4; Lanes 8-10). The $\Delta cj0262c::cat$ mutant produced PCR fragments of the expected sizes of 1850 (Lane 2), 905 (Lane 5) and 776 bp (Lane 8). Wild-type *C. jejuni* NCTC 11168 DNA was included as a positive PCR control and correctly amplified a PCR fragment of 1740 bp with only the Cj0262cF and Cj0262cR cloning primers (Figure 3.6.3; Lane 3). DNA sequencing

was done across the insert to verify the $\Delta cj0262c::cat$ mutation at the correct loci on the *C. jejuni* chromosome. No sequencing errors were found in the *zupT* DNA flank.

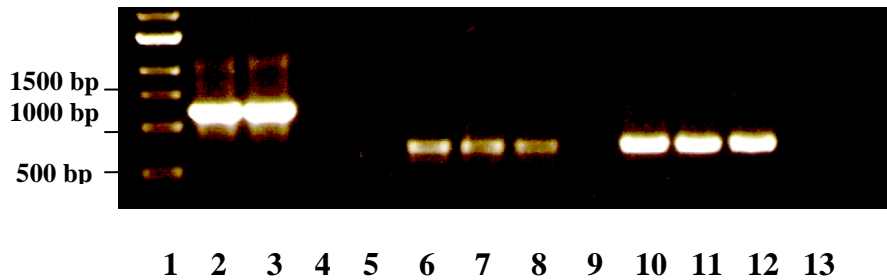


Figure 3.6. PCR screen on two putative *C. jejuni* $\Delta cj1506c::cat$ mutants. Two clones (clones 3 and 8) identified in colony PCR screens were selected for further analysis. Using chromosomal DNA (20 ng) extracted from each clone, PCR screens were attempted using three different combinations of primers. The first set of screens undertaken was done using the primer set Cj1506R and CatinvF. Both clones 3 and 8 (lanes 2 and 3, respectively) amplified a fragment of the size (1226 bp). The second round of colony PCR screens was done using the primers Cj1506F and Cj1506R_Seq (Cj1506R_Seq; Table 2.6) and clones 3 and 8 (lanes 6 and 7, respectively) amplified a product of 732 bp. The third and final round of screening was done using the primer set Cj1506F_Seq (Table 2.6) and Cj1506R. Clones 3 and 8 once again (lanes 10 and 11, respectively) amplified a product of 759 bp. PCR controls were set up alongside putative *C. jejuni* $\Delta cj1506c::cat$ transformants: Lanes 5, 9 and 13 contained water in place of template DNA (negative control); Lanes 4, 8 and 12 contained 20 ng of wild-type *C. jejuni* NCTC 11168 DNA. Lane 1 contained the 1kb DNA marker (see Table 2.6 for more information on the primers used to carry out this colony PCR screen).

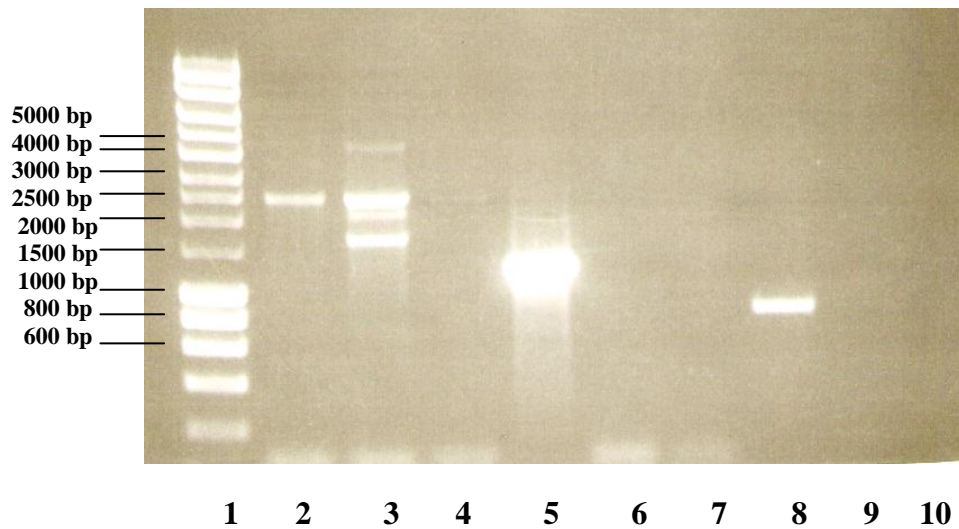


Figure 3.6.1. PCR screen on a putative *C. jejuni* $\Delta cj0144$ mutant containing the *ermC'* gene. Using chromosomal DNA (20 ng) extracted from a putative $\Delta cj0144::ermC'$ *C. jejuni* mutant (clone 1). PCR screens were attempted using three different combinations of primers. These were the Cj0144FMutVer and Cj0144RMutVer (See Table 2.6; Lanes 2-4), Cj0144F and ErmInvR (Lanes 5-7), Cj0144R and ErmInvF, and the predicted sizes of fragments were 2610 (Lane 2), 1246 (Lane 5) and 827 bp (Lane 8), respectively for the $\Delta cj0144::ermC'$ mutant (Table 2.6; Table 3.1). PCR controls were also included in the PCR. Lanes 4, 7 and 10 contained water in place of template DNA (negative control); Lanes 3, 6 and 9 contained 20 ng of wild-type *C. jejuni* NCTC 11168 DNA. A product using wild-type *C. jejuni* DNA was only expected when using the original cloning primers, a fragment of 2490 bp was expected (Lane 3). Lane 1, HyperLadder I. All results were visualised on a 0.8% TAE agarose gel (see section 2.7.1). All relevant marker sizes are indicated to the left of the gel (for DNA marker information, see section 2.4).

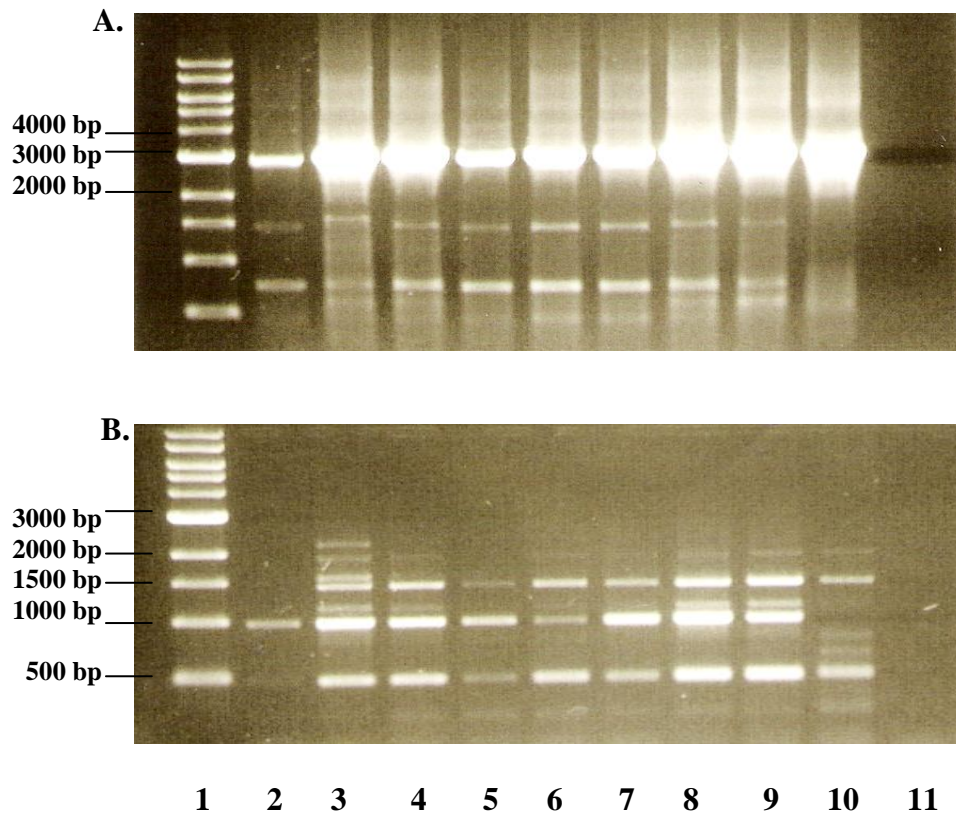


Figure 3.6.2. Colony PCR screen of *C. jejuni* cells transformed with pRS03 containing the $\Delta cj1564::ermC'$ insert. Erythromycin resistant *C. jejuni* colonies were screened using Cj1564F and Cj1564R (Gel A) and Cj1564R and ErmCIF (Gel B). The predicted fragment sizes were 3126 and 1026 bp for Gels A and B, respectively. Wild-type *C. jejuni* (20 ng chromosomal DNA) was used as a positive control in Gels A and B (Lane 10). The predicted fragment size for wild-type *C. jejuni* DNA was 3009 bp (Gel A, Lane 10), but no product was expected in Gel B (Lane 10). Lane 1, in Gels A and B contained the 1 kb DNA marker; Lane 11, contained water in place of template DNA (negative control).

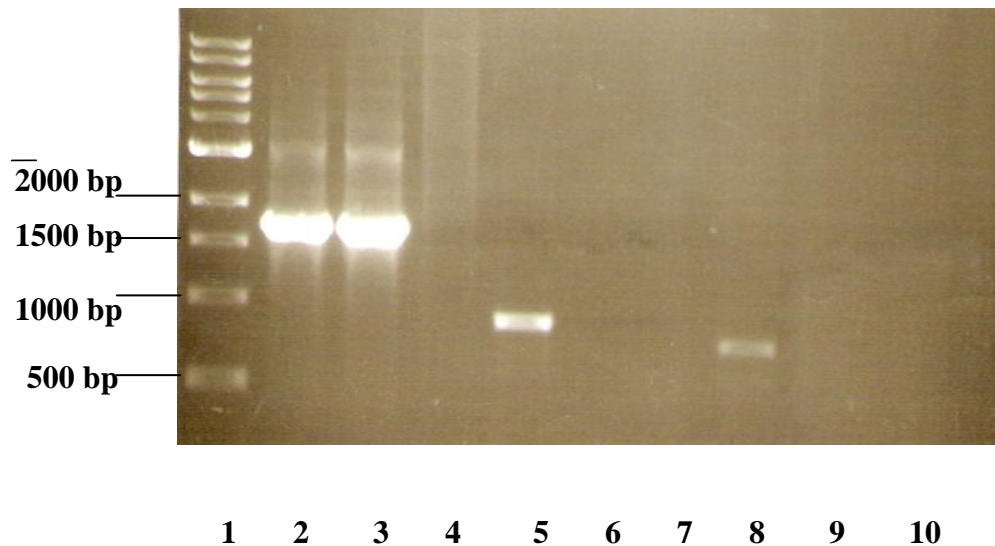


Figure 3.6.3. PCR screen on a putative *C. jejuni* $\Delta cj0262c$ mutant containing a chloramphenicol acetyl transferase (*cat*) cassette. Using chromosomal DNA (20 ng) extracted from a putative $\Delta cj0262c::cat$ *C. jejuni* mutant (clone 1). PCR screens were attempted using three different combinations of primers: Cj0262F and Cj0262R (original cloning primers; Lanes 2-4), Cj0262F and CatInvR (Lanes 5-7), Cj0262R and CatInvF (Lanes 8-10), and the predicted sizes of fragments were 1850 (Lane 2), 905 (Lane 5) and 776 bp (Lane 8), respectively for the $\Delta cj0262c::cat$ mutant (Table 3.1). Lanes 4, 7 and 10 contained water in place of template DNA (negative control); Lanes 3, 6 and 9 contained 20 ng of wild-type *C. jejuni* NCTC 11168 DNA. A fragment of 1740 bp was expected with the cloning primers (Lane 3). Lane 1 contained the 1kb DNA marker. All results were visualised on a 0.8% TAE agarose gel (see section 2.7.1). All relevant marker sizes are indicated to the left of each gel (for DNA marker information, see section 2.4).

3.2.6. Natural transformation of the *C. jejuni* $\Delta cj1506c::cat$ mutation onto a motile variant background

The final stage of the mutagenesis strategy involved naturally transforming (section 2.11.7) purified chromosomal DNA obtained from the successful *C. jejuni* *cj1506c* mutant, onto a motile variant isolate of wild-type *C. jejuni* NCTC 11168 (Table 2.1). This was a necessity if the phenotype of the *tlp* mutants were to be determined. The *tlp* mutants were to be tested in chemotaxis assays, which require the bacteria to be motile, and the laboratory strain *C. jejuni* NCTC 11168 is non-motile.

All positive transformants were once again screened by colony PCR to ensure that the second double homologous recombination had occurred at the desired locus on the *C. jejuni* chromosome and not elsewhere on the chromosome. As before, the positive transformants were verified by selecting for chloramphenicol resistance. The colony PCR screen attempted on *C. jejuni* transformants on a motile variant background is shown in Figure 3.6.4. A summary of all of the stages involved in constructing the *C. jejuni* RS01Tlp1Mut strain ($\Delta cj1506c::cat$) is illustrated diagrammatically in Figure 3.7. Single mutant strains in *C. jejuni* NCTC 11168 created over the course of this project were as follows. RS01Tlp1Mut ($\Delta cj1506c::cat$), RS02Tlp2 ($\Delta cj0144::ermC'$), RS03Tlp3Mut ($\Delta cj1564::ermC'$) and RS04Tlp4 ($\Delta cj0262c::cat$). All bacterial strains are fully detailed in Table 2.1 of this dissertation. As, the *C. jejuni* strains carrying mutant copies of *tlps* *cj1506c*, *cj0144* and *cj0262c* had been constructed successfully and were on a motile variant background they were ready for phenotypic analyses.

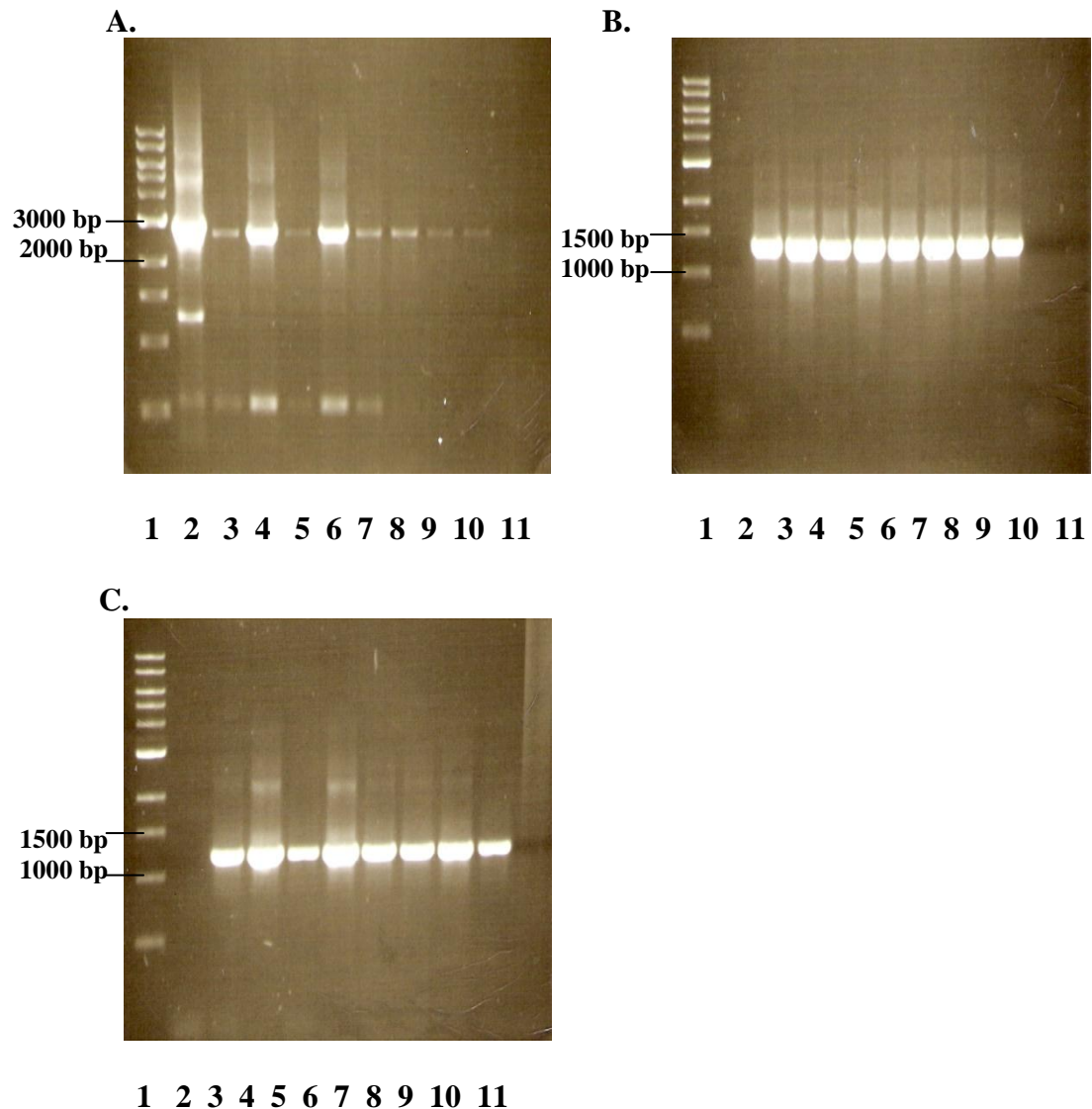


Figure 3.6.4. Colony PCR screen of *C. jejuni* $\Delta cj1506c::cat$ mutants transformed onto a motile variant background (for strain information see Table 2.1). Ten chloramphenicol resistant clones (lanes 3-11 in gels A-C) were screened using the following primer sets (Table 2.6): Cj1506F and Cj1506R (Gel A), Cj1506F and CatinvR (Gel B) or Cj1506R and CatinvF (Gel C). All ten clones amplified correctly the expected fragment sizes produced when using these primer sets (Gel A; 2755 bp; Gel B, 1355 bp; Gel C, 1231 bp). PCR controls were set up alongside, which included wild-type *C. jejuni* NCTC 11168 chromosomal DNA (20 ng; Lane 2 in Gels A-C). A PCR product of 2875 bp was expected when testing the positive control with Cj1506F and Cj1506R (Gel A), but no products were predicted when tested with the remaining primer sets (Gels B and C). A negative control was also included, which contained water in place of template DNA (Lane 11 in Gels A-C).

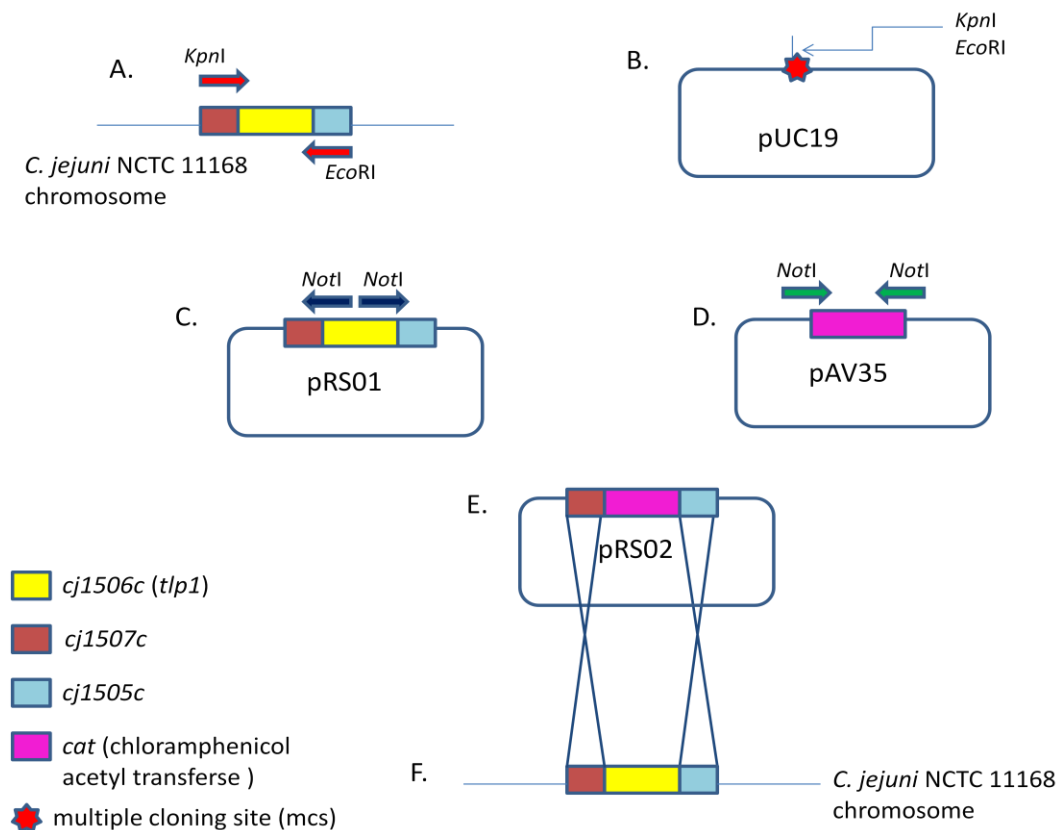


Figure 3.7. Summary of steps undertaken to mutate *cj1506c*. (a) The *cj1506c* gene was amplified from the *C. jejuni* chromosome using gene specific primers (↔). The primers (Cj1506F and Cj1506R) amplified the coding region for *cj1506c* as well as part of the coding region for the genes flanking the target gene (*cj1507c* and *cj1505c*). The primers had 5' restriction enzyme sites incorporated (*KpnI* and *EcoRI*), which enabled directional cloning of the the amplified fragment into the (b) mcs of the cloning vector pUC19. The vector and *cj1506c* PCR fragment were restricted with *KpnI* and *EcoRI* before being ligated to produce (c) pRS01. Once the pRS01 construct sequence had been verified, (c) inverse PCR primers were used to amplify from within the *cj1506c* ORF in pRS01. The primers were facing outwards so that part of the coding region for *cj1506c* could be deleted (the inverse PCR fragment still contained the DNA flanks and vector). A (d) selectable marker was amplified from the plasmid pAV35 (*cat* cassette; confers chloramphenicol resistance). The inverse PCR primers (↔) and the *cat* cassette specific primers (↔) had compatible *NotI* restriction sites at the 5' end. The *NotI* digested, linearized inverse PCR product was ligated with the *NotI* digested *cat* cassette to produce (e) pRS02. So far all cloning steps had been carried out in *E. coli* strain DH5αE cells. However, the final step involved transforming the pRS02 construct into wild-type *C. jejuni* NCTC 11168. As this strain is unable to maintain plasmids, (f) homologous recombination between homologous regions in the construct and the *C. jejuni* chromosome resulted in the replacement of the wild-type *cj1506c* allele on the chromosome with the mutant *cj1506c* allele containing the *cat* cassette.

3.3. Selecting a complementation strategy to restore the wild-type phenotype in a *cj1506c* isogenic mutant

As already stated in the introduction to this chapter, the *cj1506c* isogenic mutant created in this study was used in the study by Hartley *et al.* (2010). Upon testing this mutant *in vivo* in chickens, *cj1506c* was found to be a determinant of intestinal colonisation by *C. jejuni* NCTC 11168. In order to verify these data and establish whether the marked reduction in colonisation ability of the *cj1506c* isogenic mutant was due solely to the loss of this specific *tlp*, this mutant needed to be complemented. Complementation is essentially a procedure that enables restoration of a mutant strain back to its original phenotype, prior to a mutation being introduced in the target gene. At the time of this study there were few efficient complementation systems available for use in *C. jejuni*. Although the use of shuttle vectors had been used to successfully introduce exogenous material back into the *C. jejuni* chromosome, they were still perceived to be relatively inefficient systems. For example, shuttle vectors have been developed, that can be shuttled back and forth between *E. coli* and *C. jejuni* (Labigne-Roussel *et al.*, 1988), however the use of these vectors in this study was not possible, as the strain being used in this study is unable to maintain plasmids. Thus, searching for alternative ways to reintroduce a wild-type copy of *cj1506c* back into a *cj1506c* mutant chromosome was limited. There were essentially two methods available to complement the *C. jejuni* RS01Tlp1Mut strain ($\Delta cj1506c::cat$; Table 2.1) with. The first strategy involved introducing the functional copy of the target gene into a putative insertion sequence element (ISE) transposase pseudogene, *cj0752* (Miller, PhD thesis). The alternative was to insert the functional copy of the target gene into one of three highly conserved ribosomal RNA (rRNA) clusters present in the *Campylobacter* chromosome. Although both strategies required the use of a plasmid

vector, the vector itself would only be required for cloning procedures. Once inside *C. jejuni* NCTC 11168, the plasmid behaves like a suicide vector, and the functional copy of the target gene is integrated into the mutant chromosome through homologous recombination. Although both procedures had been used previous to this study to successfully complement isogenic mutations, in chemotaxis and iron uptake genes in *C. jejuni* NCTC 11168 (Miller, PhD thesis; Bridle, MPhil thesis), the strategy selected to complement the *cj1506c* mutation was based around the pRR vector system (Table 2.2; Karlyshev and Wren, 2005; Bridle, MPhil thesis).

The pRR plasmid was originally constructed by ligating the coding sequences of three of the conserved ribosomal RNA (rRNA) clusters present in the *Campylobacter* genome, into a pGEM-T easy vector (Promega, UK). The pRR plasmid was digested at an *Xba*I restriction site into which a *cat* (for chloramphenicol acetyl transferase) cassette was inserted to produce the pRRC plasmid (Karlyshev *et al.*, 2005). The pRR plasmid system since being created, has been engineered further so that it now contains the *aphA-3* gene (pRRK; Ridley *et al.*, 2006) and the *ermC'* gene (pRRE; Bridle, MPhil thesis), which confer kanamycin and erythromycin resistance respectively. A functional copy of the target gene to be complemented needs to be incorporated into one of the three possible rRNA clusters.

As there are three rRNA clusters present in pRR, there is a strong possibility for more than one homologous recombination event occurring between the complementary rRNA sequences present in pRR and homologous regions on the *C. jejuni* chromosome. The consequences of having more than two functional copies of the *cj1506c* gene would be worth determining and testing in chemotaxis assays to assess for any marked changes in phenotype. Due to the high conservation of the rRNA clusters between different strains of *Campylobacter*, the complementing

construct has the potential to be reused to complement a *cj1506c* mutation in other strains of *Campylobacter*.

3.3.1. Complementation using pRRK

3.3.1.1. Modifying the pRRK vector

In order to introduce a functional copy of the *cj1506c* gene into *C. jejuni*, the target gene needed to be cloned in at the *Xba*I restriction site in pRRK. However this was somewhat problematic since the *cj1506c* gene had an *Xba*I restriction recognition site within its ORF, thus this enzyme could not be used to digest the *cj1506c* PCR product. To try and overcome this problem, the poly-linker from the pTrc-HisB plasmid was cloned into pRRK to produce the newly engineered plasmid, pRRK-poly (Figure 3.8). The Kanamycin resistance cassette, encoded by the *aphA-3* gene in pRRK had its own promoter sequence but was missing a transcriptional terminational signal. The *cj1506c* insert needed to be cloned in the same orientation as the kanamycin cassette in order to achieve continual transcriptional read through from the kanamycin cassette and into the ORF of *cj1506c*. The promoter sequence for *cj1506c* was amplified along with the gene. The poly-linker from the pTrcHisB plasmid (Appendix 4; Figure 4.1 (c)) introduced two unique restriction sites, *Kpn*I and *Bgl*II, as well as a small selection of other restriction enzyme sites (Figure 3.8). A summary of the cloning steps undertaken to produce pRRK-poly are presented in Figure 3.8.

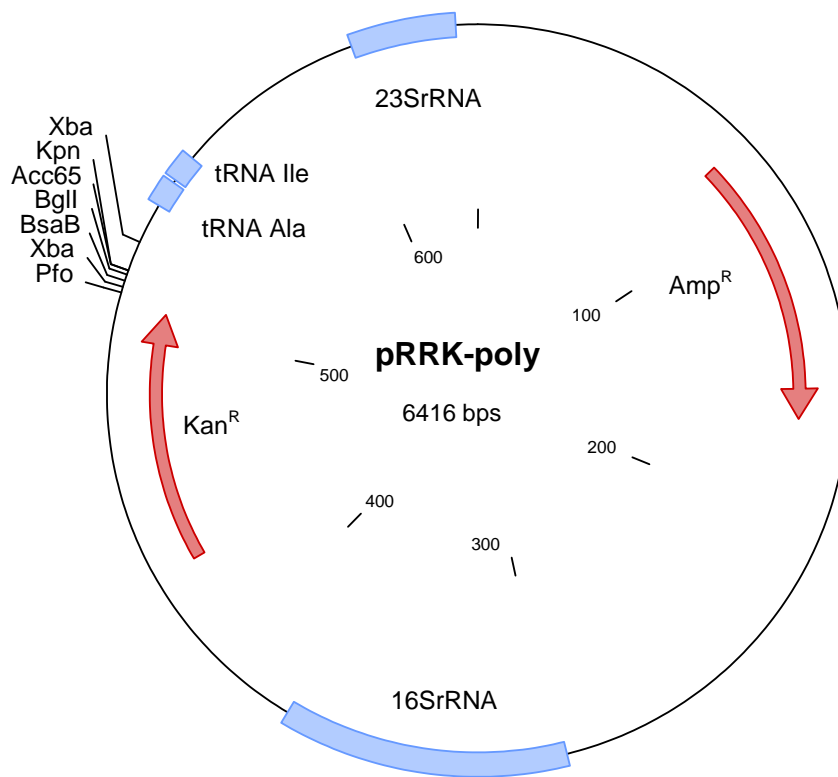


Figure 3.8. Plasmid map of pRRK-poly (pRRK-poly is a derivative of the pRR vector; Karlyshev and Wren, 2005). The pRRK-poly plasmid was used to complement the *cj1506c* mutant strain (*C. jejuni* RS1Tlp1M; Table 2.1). The pRRK plasmid contained partial and complete coding sequences of three of the conserved rRNA clusters present in the *C. jejuni* NCTC 11168 chromosome (note the 23S rRNA gene is truncated in pRRK; only 284 bp of a total 2889 bp of the gene is present). A kanamycin resistance cassette was later inserted (Kan^R) by Ridley *et al.* (2006) in addition to the ampicillin resistance gene (Amp^R). The pRR vector contained an *Xba*I site into which exogenous DNA could be cloned, however *cj1506c* contained an *Xba*I site within the Tlp1 coding region. Thus, it was for this reason a poly-linker containing restriction sequences for *Bgl*II and *Kpn*I (poly-linker taken from the pTrcHisB plasmid) was ligated into pRRK, which was assigned the name pRRK-poly. The *Bgl*II and *Kpn*I restrictions sites were used to directionally clone *cj1506c* into pRRK-poly (this plasmid is fully detailed in Table 2.2).

3.3.1.2. Cloning the poly-linker from the pTrcHisB plasmid into pRRK

The poly-linker from the pTrcHisB plasmid was amplified by PCR using the primer pair pTrcHisBF and pTrcHisBR (Table 3.1). The primers had *Xba*I restriction recognition sequences at the 5' end. The primers amplified a product of 140 bp (Figure 3.9.1). The PCR fragment was purified, digested with *Xba*I and was then ready to be ligated into pRRK. The pRRK plasmid was also digested with *Xba*I, and then dephosphorylated to prevent vector molecules from self-ligating. The ligations were transformed into *E. coli* DH5αE cells by either heat shock or electroporation (section 2.11.3 and 2.11.4). The transformations were plated onto recovery media containing ampicillin and kanamycin. The transformation efficiency was low and there were only a few positive transformants. Therefore, plasmid extractions were performed on all clones. In order to verify the presence of the poly-linker in pRRK, recombinant plasmids were digested with *Bgl*II (data not shown) and *Pst*I. Restriction digests of recombinant plasmids using *Pst*II is shown in Figure 3.9.2. Following digestion with *Pst*I, all recombinant plasmids, except for clone 5 (Figure 3.9.2, Lane 7) produced fragments of the expected sizes. One of the correct sized clones, clone 2 was selected to be analysed further by DNA sequencing. The plasmid construct extracted from clone 2 came back as error free and verified the presence of the poly-linker in pRRK. A summary of the stages involved in cloning a poly-linker into pRRK to produce the pRRK-poly plasmid is presented in Figure 3.9.

Figure 3.9. Summary of the steps undertaken to clone the poly-linker from the pTrcHisB plasmid into pRRK. Recombinant plasmid constructs containing the poly-linker were identified by digestion with *Pst*I. All results were visualized on a 0.8% TAE agarose gel (see chapter 2, section 2.7.1 for a method on agarose gel electrophoresis). All relevant marker sizes are indicated to the left of each gel.

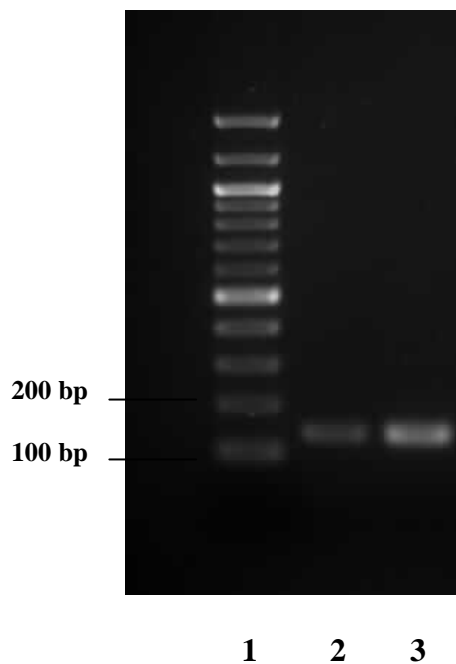


Figure 3.9.1. PCR amplification of the poly-linker from the pTrcHisB plasmid (Lanes 2 and 3). 0.5 ng and 1.0 ng of pTrcHisB DNA was used as template for the reaction (Lanes 2 and 3, respectively). Amplification of the poly-linker was achieved using the primer pair pTrcHisBF and pTrcHisBR (table 2.6). The expected size of the amplified product was 140 bp. Lane 1, 100 bp DNA marker. 1.3% TAE agarose gel.

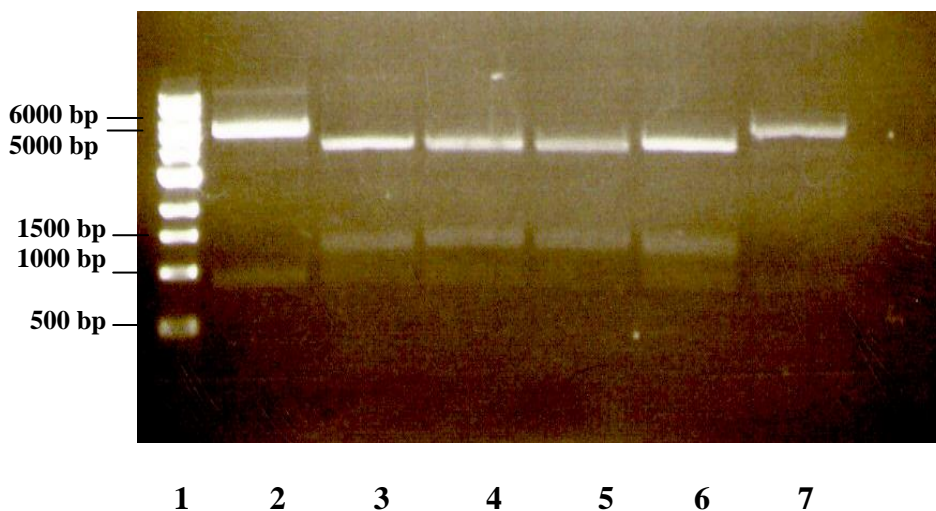


Figure 3.9.2. *Pst*I digest of pRRK-poly recombinant plasmid constructs. Lane 1, 1 kb DNA marker; Lane 2, pRRK-poly plasmid, following digestion with *Pst*I should produce two fragments of the following sizes (bp), one 5411 and the other 873 (vector only control); Lanes 3-7, contain pRRK-poly/*cj1506c* construct DNA. The proposed sizes of fragments produced from the correct pRRK-poly/*cj1506c*, post *Pst*I digestion were 4193, 1350, and 873 bp. All clones, except for clone 5 in lane 7 produced fragments of the intended sizes.

3.3.1.3. Cloning a functional copy of the *cj1506c* gene into pRRK-poly

The *cj1506c* gene was amplified by PCR from *C. jejuni* NCTC 11168 chromosomal DNA using the primer pair Cj1506FComp and Cj1506CRComp (Table 2.6 and 3.1). The primers incorporated *Kpn*I and *Bgl*II restriction sites at the 5' ends. The *cj1506c* PCR fragment was digested with *Kpn*I and *Bgl*II and this is shown in Figure 3.10.1 (Lanes 4 and 5). The plasmid pRRK-poly was also digested with *Kpn*I and *Bgl*II, but the plasmid was also dephosphorylated to prevent self-ligation of the vector molecules. The digested pRRK-poly is shown in Figure 3.10.1 (Lanes 2 and 3). The PCR product and plasmid were then ligated together. By using two unique restriction sites present in pRRK-poly to clone in the *cj1506c* subsequently avoided the need to screen for insert orientation. Furthermore, the *cj1506c* gene was in the same orientation as the kanamycin cassette. The ligation reaction was purified by ethanol precipitation (section 2.9.3) and then transformed by heat shock into *E. coli* DH5 α E. Transformants were recovered on media supplemented with ampicillin and kanamycin. Colonies which were ampicillin and kanamycin resistant were chosen to be screened by colony PCR using the original cloning primers Cj1506CompF and Cj1506CompR. All colonies tested in the colony PCR screen amplified correctly a product of 2523 bp in size. A sample of this screen is shown in Figure 3.10.2. Plasmids were subsequently extracted from two of the colonies which produced positive results in the PCR. The chosen plasmids were sent off to be sequenced to check for possible PCR incorporation errors in the insert. The insert was found to be error free. A summary of the cloning steps involved in cloning a functional copy of *cj1506c* into pRRK-poly to produce pRS12 is shown in Figure 3.10. The final complementing construct was designated pRS12 and is shown in Figure 3.11

Figure 3.10. Summary of the steps involved in cloning a functional copy of *cj1506c* into pRRK-poly. *Bgl*II and *Kpn*I digests of pRRK-poly and *cj1506c* is shown. Following digestion, the *cj1506c* gene was ligated with pRRK-poly to produce the pRS12 construct. pRS12 was transformed into *E. coli* cells and a sample of the colony screen is presented. All results were visualized on a 0.8% TAE agarose gel (see chapter 2, section 2.7.1 for a method on agarose gel electrophoresis). All relevant marker sizes are indicated to the left of each gel.

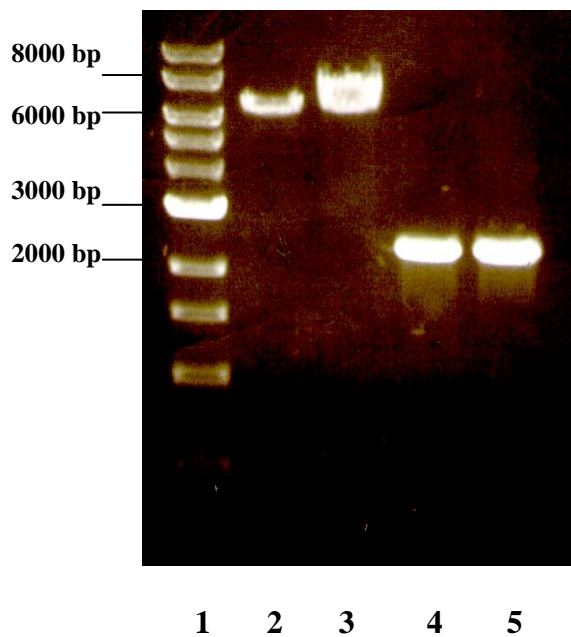


Figure 3.10.1. *Bgl*II and *Kpn*I digests of pRRK-poly and *cj1506c*. Lanes 2 and 3 contain pRRK-poly. Following digestion, pRRK-poly should produce two fragments, one 6400 and the other 16 bp in sizes; Lane 2 contains a 1/10 dilution of neat pRRK-poly plasmid DNA. Lanes 4 and 5 contain *cj1506c* DNA. The expected size of *cj1506c* post digest was 2517 bp. Lane 1, 1 kb DNA marker.

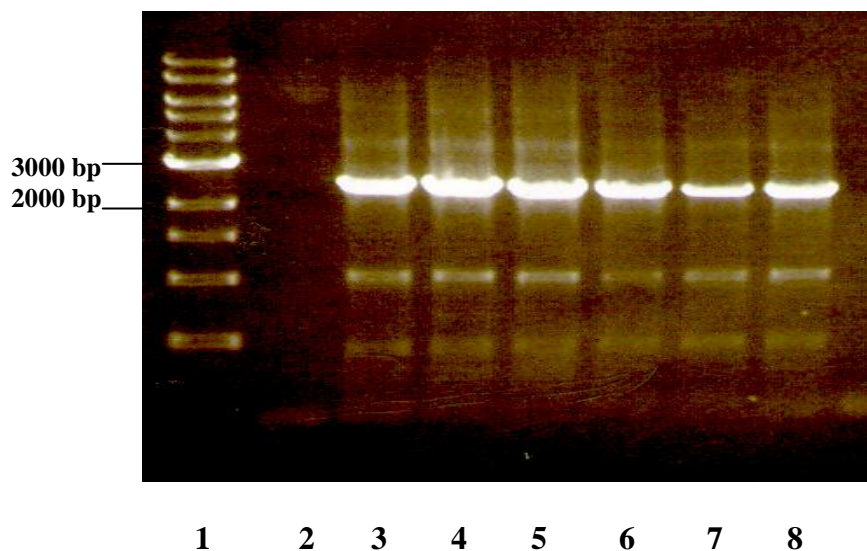


Figure 3.10.2. Colony PCR screen of *E. coli* cells transformed with pRRK-poly containing the *cj1506c* insert. A total of six colonies were screened using the original cloning primers, Cj1506FComp and Cj1506RComp (table 3.1). The expected size of the amplified product was 2523 bp. All *E. coli* clones screened produced fragments of the predicted size (Lanes 3-8). Lane 1, 1 kb DNA marker; Lane 2, water in place of template DNA (negative control).

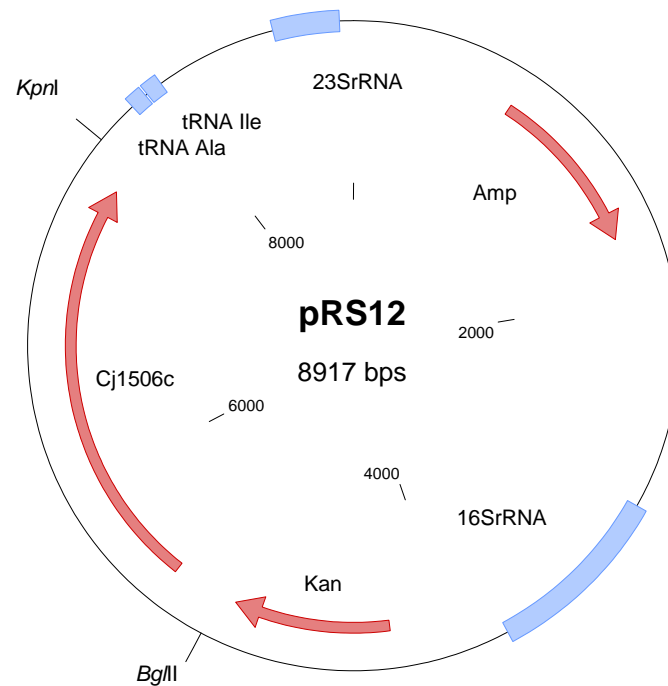


Figure 3.11. Plasmid map showing the construct used to complement the $\Delta cj1506c::cat$ mutation in *C. jejuni* (pRS12). A functional copy of the *cj1506c* gene was PCR amplified using the primer pair Cj1506FComp and Cj1506RComp (Table 2.6). The gene was cloned in its entirety and inserted at the *Kpn*I and *Bgl*II sites in pRRK-poly. There are two antibiotic resistance cassettes present in this pRS12, and these are the Amp and the Kan cassette, which confer ampicillin and kanamycin resistance, respectively. The size of the plasmid has been indicated (this plasmid is fully detailed in Table 2.3).

3.4. Discussion

3.4.1. Introduction

Single Tlp mutant strains in *C. jejuni* NCTC 11168 were successfully created using an insertional inactivation technique in this study. *C. jejuni* Tlp mutant strains constructed were RS01Tlp1Mut ($\Delta cj1506c::cat$), RS02Tlp2 ($\Delta cj0144::ermC'$), RS03Tlp3Mut ($\Delta cj1564::ermC'$) and RS04Tlp4 ($\Delta cj0262c::cat$). Moreover, the *C. jejuni* strains carrying mutant alleles of *cj1506c*, *cj0144* and *cj0262c* in the chromosome were transformed on to a motile variant background so that they could be assessed for changes in chemotaxis. Although *cj1506c*, *cj0144* and *cj0262c* were successfully interrupted using insertional mutagenesis, difficulties were encountered during the cloning of each of these genes. The problems encountered mutating the Tlps, but more importantly how they were overcome will be discussed here in this discussion. Unfortunately, a final mutant in the *cj1564* (*tlp3*) gene in *C. jejuni* NCTC 11168 could not be obtained. Two attempts at inserting different antibiotic markers in to the *cj1564* ORF were made in this work. The selectable markers used were a kanamycin and erythromycin marker, which were encoded by the *aphA-3* gene and *ermC'* genes, respectively. Although the latter (*ermC'* gene) was transformed back in to the *C. jejuni* chromosome homologous recombination did not appear to have occurred at the desired locus on the chromosome. These results will be discussed further in this discussion

In addition to the mutagenesis of a group of *tlp* genes, an attempt was also made in this work to produce a complementing construct which was developed in order to restore the wild-type phenotype in a *tlp1* isogenic mutant. Purified plasmid DNA of the final complementing construct, containing a functional copy of the

cj1506c gene (pRS12, Figure 3.11), was sent off to Australia to be assessed by a group of researchers who we were collaborating with at the time of this study (Group headed by Dr. Victoria Korolik). The pRS12 complementing construct would have been transformed onto the specific background of *C. jejuni* NCTC 11168 that would have been most appropriate for the set of models this construct was to be tested in. The pRS02 and pRS12 constructs have gone on to be analysed *in vivo* caecal colonisation and *in vitro* adherence and invasion cell culture models of *C. jejuni* (Hartley-Tassell *et al.*, 2010; Appendix 1). Most of these data will be reviewed in detail further on in this dissertation (Chapter 5).

3.4.2. Mutagenesis of *cj1506c* and creating a complement

The *cj1506c* gene was successfully mutated in this work by inserting a *chloramphenicol resistance* marker in to the deleted coding region of the target gene. Analysis of the genes surrounding *cj1506c* (Figure 3.1) indicates that *cj1506c* contains its own promoter and termination signal sequence. Furthermore, upstream of *cj1506c* (*cj1507c*) also appears to contain a 105 bp region which appears to resemble a classic promoter region (a -35 box and -10 box; TATTAA; Wosten *et al.*, 1998). The selectable marker (*cat* cassette) used to construct RS01Tlp1Mut strain did have its own promoter but was missing a termination signal. It is however, unlikely that the *cat* cassette should affect the expression of gene downstream of *cj1506c*. The expression of the genes flanking *cj1506c* (*cj1507c* and *cj1505c*) was analysed using real-time PCR (Hartley-Tassell *et al.*, 2010; Appendix 1) and no altered expression of genes found adjacent to *cj1506c* could be detected. This data verified that the *cat*

cassette with its own promoter inserted into the ORF for *cj1506c* is not affecting the expression of downstream genes.

The pRS12 construct was implemented in this study solely to restore the wild-type phenotype in an insertionally inactivated *tlp1* isogenic mutant ($\Delta cj1506c::cat$) in *C. jejuni*. The pRS12 construct was based around the pRRK complementation system (Karlyshev and Wren, 2005), which enabled the efficient delivery and expression of a functional copy of the *cj1506c* gene back into the mutant *C. jejuni* chromosome ($\Delta cj1506c::cat$). The construction of a *tlp1* Δ complementing strain, where the *tlp1* gene was inserted into the rDNA locus adjacent to a kanamycin resistance cassette, was initiated in this study (data not shown) and completed by others (Dr R Haigh, personal communication); this strain is now available to test in the HAP assay. Ideally had there been more time, complements in all of the *tlp* mutants should have been constructed. The complements are necessary in order to verify any possible phenotypes observed due to a mutation in a particular Tlp. Thus, future work would involve making complements for *cj0144*, *cj1564* and *cj0262c*.

3.4.3. Difficulties mutating the Tlps

3.4.3.1. Mutagenesis of *cj0144*

Although the *cj0144* (*tlp2*) gene has been successfully mutated through insertional inactivation, problems were encountered early on when attempting to amplify by PCR the *cj0144* gene from the *C. jejuni* chromosome. The predicted fragment size for the *cj0144* gene (including the DNA flanking sequence) was 3234 bp. A fragment of this size could be obtained from the *C. jejuni* chromosome, however non-specific fragments were also being amplified along with the coding sequence for *tlp2*. This is

evident in the gel image shown in Figure 3.2.2 (Lane 2). Attempts were made to optimize this PCR reaction and involved adjusting the annealing temperatures of the cloning primers (Cj0144F and Cj0144R; Table 2.6) as well as the magnesium ion concentration in the PCR reaction. By altering the annealing temperature of the primers, there was some reduction in the non-specific binding of the primers (data not shown). However, it was not possible to eliminate this completely (Figure 3.2.2; Lane 2). Primers were also re-designed to avoid complementary sequences at the 3' of the primers, which may have been causing the primers to anneal to one another in the PCR reaction and form primer dimers. To try and avoid further problems later on in the mutagenesis of *tlp2*, the desired band proposed to contain the coding sequence of *tlp2* (3242 bp) was excised directly from the agarose gel by gel extraction (section 2.9.2). This excised band, predicted to contain the coding region for *tlp2*, was directionally cloned into the cloning vector pUC19 (pRS03; Table 3.1).

3.4.3.2. Mutagenesis of *cj0262c*

The *cj0262c* (*tlp4*) gene was constructed differently to the other *tlps* (see Figure 3.2.3). Rather than amplify the full coding sequence for the gene as well as the DNA flanking sequence, it was decided that it would be more beneficial if the size of the insert to be cloned could be reduced. All of the *tlp* genes when cloned with the DNA flanking sequences were approximately 3 kb in size, and when cloned into pUC19 the size of the final constructs were exceeding 5 kb. As the cloning of the other *tlps* had proceeded before *cj0262c*, it was apparent by then that a number of initial and final constructs for the other *tlps* which had been transformed into *E. coli* had to be rejected due to point mutations, or larger deletions. Also as the *C. jejuni* genome is

highly AT rich (Parkhill *et al.*, 2000), it is quite possible that these AT rich sequences could be misinterpreted by *E. coli* and resemble a promoter region. A further difficulty was encountered when trying to obtain a final construct containing the insertionally inactivated *cj0262c* gene ($\Delta cj0262c::cat$). Colony PCR screening of *E. coli* transformants went on to show that many *E. coli* clones appeared to contain more than one *cat* cassette. This problem was overcome, by dephosphorylating the *cat* cassette, which was leading to the formation of concatamers. The solution to this problem was discovered whilst cloning *tlp1* (*cj1506c*), which also contained a *cat* cassette.

3.4.3.3. Mutagenesis of *cj1564*

As mentioned at the start of this discussion, it was not possible to achieve a final chromosomal mutation in the *cj1564* gene. Two attempts were made at disrupting the *cj1564* gene through insertional inactivation. Both attempts involved inserting two different selectable markers, namely a kanamycin and an erythromycin resistance marker in the deleted region of the *cj1564* coding sequence (markers encoded by the *aphA-3* gene and *ermC'* genes, respectively). However, due to time constraints, no further attempts were made to obtain a final mutant in *cj1564*. The final constructs containing the disrupted *cj1564* gene, with the two different selectable markers in will be described here.

A kanamycin resistance marker (encoded by the *aphA-3* gene) was inserted into the deleted region of the *cj1564* ORF. When undertaking colony PCR screening of kanamycin resistant *E. coli* transformants with the correct size insert, the majority of transformants appeared to contain the kanamycin cassette facing in the reverse (opposite) orientation to the orientation of *cj1564* gene. These constructs were

rejected because of the possible effects this could have on downstream genes. The kanamycin resistance marker had its own promotor but lacked a transcriptional termination signal. Figure 3.1 shows the arrangement of genes in the region surrounding *cj1564*. It is made apparent from this diagram that although *cj1563c*, which is positioned adjacent to *cj1564*, has no known role in the *C. jejuni* chemotaxis system, this could alter the expression of this gene and could lead to possible polar effects. However, one of the clones which appeared to contain the kanamycin marker in the forward orientation as identified by the colony PCR screens, was analysed further by restriction mapping and DNA sequencing (data not shown). Following restriction digestion with the endonucleases *Bam*HI and *Eco*RI confirmed that the kanamycin marker was indeed in the forward orientation with respect to the *cj1564* coding region (data not shown). However, sequencing data revealed a significant point mutation in what appears to be a divergent promoter region for both *cj1564* and the gene adjacent to *cj1563c*. There are only 79 bps separating the two genes. In this spacer region (79 bps gap) there was an adenine residue missing -32 bps before the ATG translational start site for *cj1564* (48 bps from the ATG translational start site for *cj1563*). This construct was also rejected (Appendix 2; final construct map of *cj1564::aphA-3*). A further colony PCR screen was undertaken to try and identify further *cj1564c* recombinants that contained the kanamycin resistance marker in the forward orientation. Upon restriction mapping of a selection of clones identified by the colony PCR screening, all clones contained the kanamycin resistance marker in the reverse orientation.

A further attempt at remaking the $\Delta cj1564$ mutant was undertaken, this time using an erythromycin resistance marker was used to disrupt the *cj1564* gene. The *ermC'* gene had its own promoter, but this time it contained a transcriptional

termination signal. This meant that if there was a selective pressure for the resistance marker to go in, in the reverse orientation, this should have no detrimental effect on the expression of downstream genes (particularly *cj1563c*). A colony PCR screen was carried out on erythromycin resistant *E. coli* colonies using the primer pair Cj1564F and ErmCIR (ErmCIR primer amplifies from within the *ermC'* coding sequence; Table 2.6). Four out of a possible ten colonies produced a fragment of the correct size of 1611 bp (Figure 3.6.3, Gel A; Lanes 2, 3, 5 and 9). The final construct containing an inactivated copy of the *cj1564* gene (Figure 3.5.6), was transformed by electroporation (section 2.11.6) back into the *C. jejuni* NCTC 11168 chromosome. Colonies which were erythromycin resistant were screened by colony PCR. A colony PCR was undertaken using Cj1564F and Cj1564R (Figure 3.6.3, Gel A) and Cj1564R and ErmCIF (Figure 3.6.3, Gel B). When the *C. jejuni* colonies were screened using the gene specific primers, they produced a fragment of the expected size (3126 bps; Figure 3.6.3, Gel A). However, when the Cj1564 primer was used in combination with the erythromycin specific primer (Erythromycin primers amplifies from within the *ermC'* gene), contaminating bands were present along with the desired fragment (desired fragment was 1026 bps; Figure 3.6.3, Gel B). These contaminating bands were also present in the wild-type control; although the target product of 1026 bps was missing in the positive control (Figure 3.6.3; Gel B, Lane 10). A PCR product was generated using the original cloning primers and was sent off for sequence analysis using all of the primers used in the colony PCR screening. Sequencing data could not be attained from the PCR fragment generated from *cj1564::ermC'* mutant DNA using the gene specific primer. It may be that the erythromycin marker has not recombined in at the desired *cj1564* locus and may have recombined elsewhere on the *C. jejuni* chromosome. As all transformants were erythromycin resistant the presence

of the marker in the chromosome is certain. If time permitted it would have been worthwhile repeating this sequencing data to verify these results.

Chapter 4. Developing chemotaxis assays to determine the chemotactic behaviour of wild-type *C. jejuni* toward different chemical stimuli

4.1. Introduction

The primary objective for this part of the project was to establish a series of methods which could be used to determine chemotaxis phenotypes in *Campylobacter jejuni*. As detailed in the previous chapter, a few of the transducer-like proteins in *C. jejuni* have been successfully disrupted using an insertional-inactivation strategy. Once chemotactic motility had been firmly established in wild-type *C. jejuni* these assays would then be employed to determine the roles of Tlp1 (Cj1506c), Tlp2 (Cj1044) and Tlp4 (Cj0262) in the *C. jejuni* chemotaxis pathway. There have been relatively few studies that have successfully managed to determine chemotactic responses in *Campylobacter* species (Paster and Gibbons, 1986; Marchant, PhD thesis; Hugdahl *et al.*, 1988; Khanna *et al.*, 2006; Hartley *et al.* 2010). At the commencement of this study the methods available for measuring chemotaxis responses were limited and needed optimising taking into account the specific microaerobic growth requirements of the campylobacters. For instance, the capillary assay is a firmly established method for measuring chemotaxis to specific ligands and will be particularly useful in this study for characterising the ligand-binding specificity of the Tlps in *C. jejuni*. However, this method has been developed using the bacterium *Escherichia coli* and will therefore need to be modified to provide the growth conditions necessary for campylobacter survival and growth. It was therefore of vital importance that any procedures that had been developed for investigating chemotactic responses in other

bacteria were first modified for use with campylobacters (Paster and Gibbons, 1986). The chemotaxis assays investigated as possible methods for assessing chemotaxis in *C. jejuni* in this work were the Swarm plate, Hard-Agar Plug (HAP) and Capillary assays. The optimisation of each of these assays using wild-type *C. jejuni* cells is described here.

4.2. Methods available for assessing chemotaxis in wild-type *C. jejuni*

4.2.1. The swarm plate assay

The swarm assay is a frequently used method for assessing chemotaxis in bacteria (Armstrong *et al.*, 1986; Marchant, 1998). The assay is performed as follows. Bacteria are inoculated in the centre of a semi-solid nutrient agar plate and then incubated under the appropriate conditions for a period of time. As the bacteria grow, they metabolise the nutrients at the point of inoculation which consequently generates multiple concentration gradients of individual nutrients. Bacteria which have a functioning chemotaxis system and are motile respond to these nutrient gradients by swimming towards areas of higher nutrient concentration. In the agar of the Petri plate, higher nutrients tend to be around the outer edge of the plate, therefore bacteria collectively spread outwards producing a series of characteristic rings (Wolfe and Berg, 1989).

The outer ring (also the densest) indicates the point to which the majority of bacteria have migrated following incubation. The migration of *C. jejuni* cells on swarm plates is not controlled solely by the chemotaxis system. Swarming on semisolid media is the cumulative effect of several coinciding processes. Other

factors that also need to be taken into consideration in swarming are motility and growth rate. One of the advantages of the swarm plate assay is that it is a simple chemotaxis assay to set up and perform. Moreover, the swarm assay provides a visual demonstration of chemotaxis. It is also particularly useful for determining whether a putative chemotaxis gene is indeed required for chemotaxis in *C. jejuni* (Marchant *et al.*, 1998). This can be verified qualitatively by simple comparative analysis of swarming proficiency between wild-type and mutant cells as determined by distance swarmed, or because of a change in the swarming pattern. Furthermore, chemotactic responses can be quantified by measuring the diameter of the swarm. This is providing of course the cells are evenly distributed in the agar and have produced a swarm phenotype that has a defined and intact edge. Alterations in swarming can sometimes be subtle and affect only the outer edge of the expanding colonies. The swarm assay provides excellent photographic images of chemotaxis. The migration of wild-type campylobacters in the swarm plate assay will be detailed in this chapter, whereas an in-depth analysis of the Tlp mutants in the swarm assay will occur in the following chapter.

4.2.2. The Hard-agar plug (HAP) assay

The swarm assay assesses chemotaxis responses in complex media such as Mueller-Hinton broth. A more specialised chemotaxis assay was needed to ascertain the individual ligand-binding specificity of Tlps 1, 2 and 4 in *C. jejuni* NCTC 11168. Hugdahl *et al.* (1988) developed the HAP assay that enabled for the first, chemotaxis responses to be assessed qualitatively in *C. jejuni*. Moreover, chemicals which induced chemoattraction or chemorepellent properties in *C. jejuni* were discovered. *C. jejuni* showed positive chemotaxis toward amino acids, including L-aspartate, L-

cysteine, L-glutamate and L-serine, the organic acids malic and formate and finally L-fucose, a component of bile and mucin. Chemoattraction toward bile and mucin further illustrates the range of ligands the *C. jejuni* chemotaxis system responds to whilst navigating its way to the intestinal surface. Briefly the HAP assay works as follows. Bacteria are suspended in a low percentage PBS agar medium. Cylindrical plugs made from 1% PBS agar are prepared containing the test chemical. The plugs are placed in with the bacteria and incubated under the appropriate conditions for a period of time. Chemotaxis toward specific chemicals is then measured qualitatively. A positive chemotactic response is recorded when a turbid halo of bacteria is visible around the plug containing a potential chemoattractant (Figure 4.1). In contrast, a negative chemotaxis response is defined by a clear phase around the plug containing a potential chemorepellent (Figure 4.1). To ensure that the test chemical is not toxic to the *C. jejuni* cells and has not induced cell lysis, the zone of clearing around the plug is usually preceded by a turbid zone. This demonstrates that the bacteria are being repelled by the putative chemorepellent and are consequently swimming away from the test solution. More importantly the presence of bacteria in the agar confirms that the bacteria are viable. The HAP assay is the most appropriate method for phenotyping the Tlp mutants. Although, a major drawback of the HAP assay is that chemotaxis in *C. jejuni* is assessed purely qualitatively. Therefore, a chemotaxis assay which could quantitatively measure chemotaxis responses in *C. jejuni* was still necessary. The development of the HAP assay procedure using only wild-type *C. jejuni* cells will be detailed in this chapter.

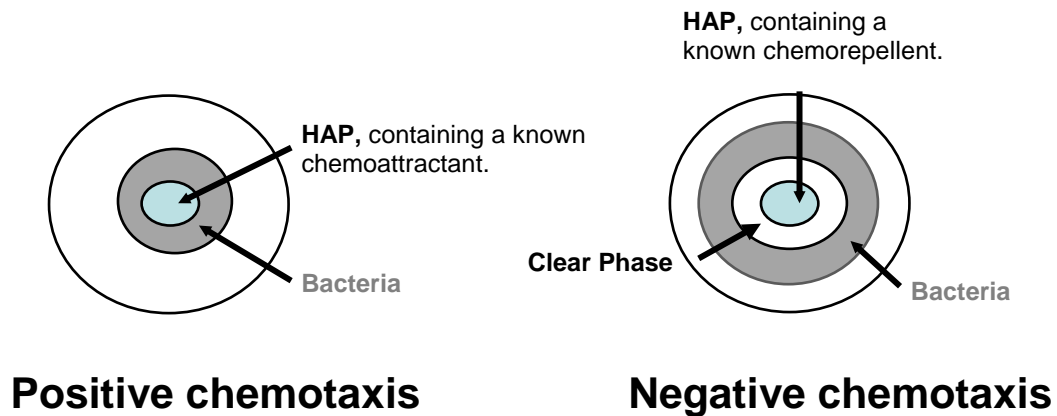


Figure 4.1. Illustration of how positive and negative chemotaxis responses in *C. jejuni* are assessed according to the hard agar plug (HAP) procedure (Hugdahl *et al.*, 1988). If the plug contains a putative chemoattractant then bacteria will produce a turbid zone will be observed around the plug (left). Conversely, if the plug contains a substrate that is having a repellent effect then the bacteria are essentially repelled away from the HAP (right). The latter response is usually observed as a zone of clearance around the plug, preceded by a turbid zone. If the test substrate is toxic then no viable bacteria will be detected around the plug.

4.2.3. Quantifying chemotactic responses in *C. jejuni* using a capillary tube assay

The chemotaxis assays described thus far have been subjective and generously qualitative in their approach (Hugdahl *et al.*, 1988). Therefore, the focus in this project was turned to finding a method that was objective and could quantify chemotactic responses in *C. jejuni*. A capillary assay was investigated in this study to (a) enable quantification of chemotactic responses in *C. jejuni* to individual chemicals and (b) determine the ligand-binding specificity of members of the Group A Tlp receptor family (Marchant *et al.*, 2002). Two different technical approaches were tested for the development of the capillary assay, both of which will be described in detail next in this chapter.

The first of these procedures was based around Adler's capillary tube procedure (Adler, 1973). This particular assay was developed to determine the optimum conditions for chemotaxis in *Escherichia coli* (Tisa and Adler, 1992; Adler, 1973). Adler's capillary assay has since been used to assess chemotaxis in numerous other bacteria including *R. sphaeroides*, *S. meliloti* and *P. aeruginosa* (Sourjik and Schmitt, 1996; Kato *et al.*, 1992). The chemotaxis assay is performed on a microscope slide onto which a U-shaped capillary tube is placed. A cover slip is then positioned on top of the capillary tube to form a chamber which is filled with the bacterial suspension. A capillary tube is filled with a putative attractant and then placed into the chamber filled with bacteria. This method was used to assess the numbers of bacteria that had accumulated into the capillary tube containing the putative attractant. Adler's capillary tube procedure needed to be modified so that it could be used to determine chemotactic responses in *C. jejuni*. Modifications were made to the apparatus used to in Adler's capillary tube assay as the apparatus needed

to be placed into the VAIN cabinet so that the campylobacters could be incubated under microaerobic conditions. Alterations made to Adler's capillary technique and to the apparatus will be detailed in this chapter.

Mazumder *et al.* (1999) developed a simplified capillary assay method which had been designed for use with microaerobic bacteria, specifically, two strains of *Pseudomonas*. This procedure also needed to be optimised so that it could be used to quantify chemotaxis in *C. jejuni*. The equipment required to perform this simplified capillary technique included the following. A hypodermic needle, syringe and a gilson pipette tip. As most of the apparatus were disposable this avoided the need to pre-sterilise the apparatus before the assay. The pipette tip was essentially the "chamber" in which the bacteria were suspended. The needle formed the capillary tube used in Adler's method through which bacteria are required to enter in order to reach the potential attractant (Mazumder *et al.*, 1999). Bacterial chemotactic responses were measured and quantified by determining the number of bacteria accumulated that had accumulated in the capillary tube (Adler, 1973).

The basis of the simplified capillary assay by Mazumder *et al.* (1999) incorporates most, if not all, of the fundamental principles from Adler's method for measuring chemotaxis. However, the method by Mazumder *et al.* (1999) has several advantages over Adler's capillary tube assay (Adler, 1973). Firstly, the Mazumder method was a recently established method for measuring chemotaxis responses and required simple disposable laboratory apparatus which could be purchased pre-sterilised. The method was not only technically simpler than Adler's capillary procedure but, multiple samples could be rapidly processed simultaneously in a single assay, which reduced the risk of contamination. But more significantly, the apparatus could be placed directly into the VAIN cabinet and therefore the bacteria were

incubated under microaerobic conditions. A further advantage of the Mazumder method was that the campylobacters would be exposed for a shorter period of time to atmospheric levels of oxygen during the initial stages of set-up of the assay.

The objective for the work described in this chapter was to develop a series of chemotaxis assays which would allow chemotactic responses in the *tlp* mutants to be determined. The Swarm plate, HAP and Capillary assays were explored as candidate assays and needed to firstly be established and then optimised using wild-type *C. jejuni* 11168 cells, prior to assessing the *tlp* mutants.

4.3. Results: assessing the chemotactic behaviour of wild-type *C. jejuni*

4.3.1. The migration of wild-type *C. jejuni* in semi-solid complex media

The *C. jejuni* strain NCTC 11168 used in this study is a non-motile phase variant. A motile-variant of this strain was needed in order to undertake motility or chemotaxis assays using the *C. jejuni* cells. Motile variants of *C. jejuni* NCTC 11168 had been isolated by O. Bridle (refer to section 2.15.1 for details on how the motile variant was generated; MPhil thesis) previous to the work undertaken in this study. The motile variant was used as a positive control in all chemotaxis assays. The mutated *tlp* alleles had been transformed into this wild-type MV strain background. It was therefore an imperative that the swarm phenotype produced by wild-type MV *C. jejuni* cells was firmly established before assessment of the *tlp* mutants could begin.

The swarm assay assesses chemotactic motility along a nutrient gradient. The swarm phenotype produced by the wild-type motile variant is presented in Figure 4.2 (a). These cells have spread outwards from the original point of inoculation. Furthermore, a bright ring can be seen towards the edge of the swarm. The bright ring or turbid zone demonstrates where the majority of bacteria have accumulated. This is where nutrient concentrations are highest as the bacteria would have utilised those at the centre of the MHA plate. The phenotype produced by wild-type MV cells demonstrates that the bacteria are chemotactic as MHA contains several putative *C. jejuni* chemoattractants (Hugdahl *et al.*, 1988). The swarm phenotype shown in Figure 4.2 (a) for the wild-type MV was observed in all subsequent swarm plate assays. A non-flagellated *flaAB* mutant was used in the swarm plate assay, as a negative control for motility in all swarm plate assays. The *flaAB* mutant was received from M. Wösten and had been generated in *C. jejuni* 81116 (Table 2.1; Wassenaar *et al.*, 1991). The *flaAB* mutant is known to be stable in the *C. jejuni* 81116 (Ketley, personal communication). Figure 4.2 (b) shows the result of the swarming phenotype produced by the *flaAB* mutant after 72 hours. The swarm plate assay incorporates a myriad of factors, of which includes growth, chemotaxis and motility. The *flaAB* mutant was unable to swarm outwards and has remained in the centre of the plate. Although some growth is apparent, this mutant demonstrates the necessity of motility in order for the cells to swarm. The diameter of the swarm produced by *flaAB* mutant cells was recorded and is presented in Figure 4.3 alongside the wild-type motile variant. A *cheY* mutant demonstrated the requirement for chemotaxis in the swarm plate assay. Mutation in the *cheY* gene rendered the cells unable to swarm effectively in the swarm plate assay. The phenotype of the *cheY* mutant assessed in the swarm plate assay is shown in Figure 4.2 (c) (Bridle, MPhil

thesis). Although there was some expansion in the size of the colony in the *cheY* mutant, the phenotype appeared similar to the *flaAB* non-motile mutant (Figure 4.2 (b)). A further example of another chemotaxis mutant assessed in the swarm assay is shown in Figure 4.2 (d). The *cheA* mutant also demonstrated an impairment in chemotaxis and swarmed significantly less than the wild-type motile variant (Bridle, MPhil thesis).

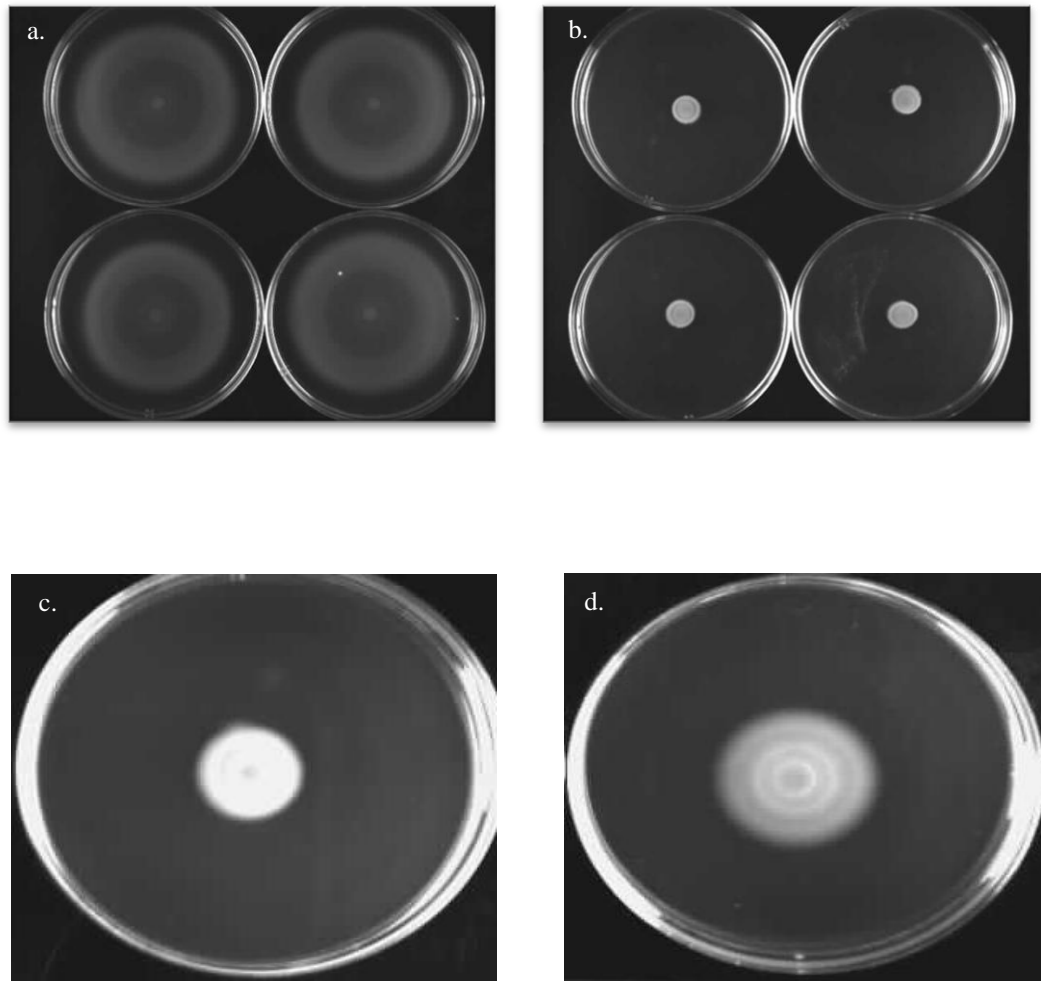


Figure 4.2. The phenotypes of the wild-type motile variant, *flaAB* mutant and chemotaxis mutants in the swarm plate assay. The swarming phenotypes shown are: panel (a), wild-type MV (motile-variant); panel (b), *C. jejuni* (81116) *flaAB* mutant; panel (c), *cheY* mutant and panel (d), *cheA* mutant in *C. jejuni* NCTC 11168 (Bridle, MPhil thesis). Panels (a) and (b) contain replicates of the same cell type. All swarm assay phenotypes are following 72 hours incubation under microaerobic conditions. Swarm plates were produced using Mueller-Hinton agar (MHA; 0.3% agar). The optical density at 600 nm (OD_{600}) was 1.0. The figure shows the assays from an indicative experiment of the three carried out (panels (a) and (b)).

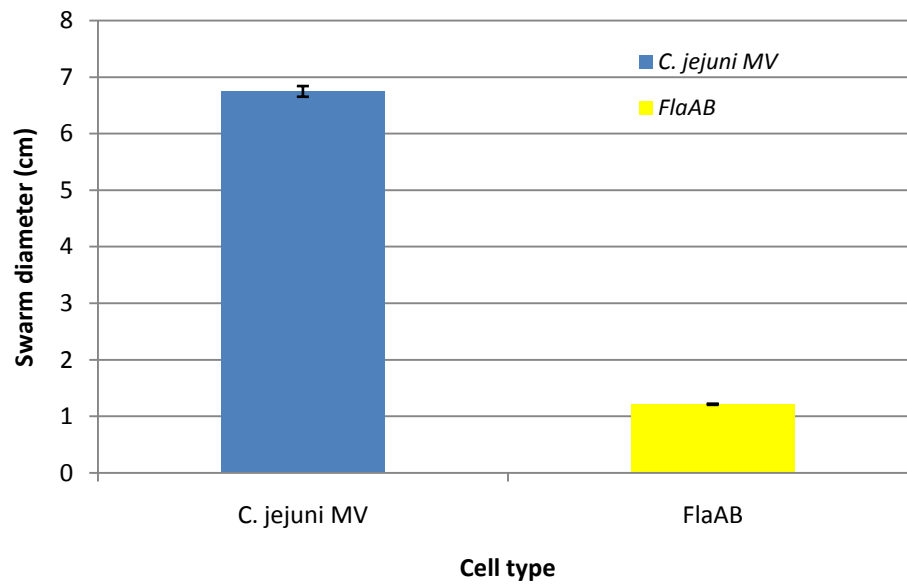


Figure 4.3. Swarm diameters of *C. jejuni* (11168) wild-type motile variant (MV) and *flaAB* mutant (81116) cells. The swarm diameter was measured after 72 hours incubation. The experiment was repeated three times (n=3). Error bars show standard error.

4.3.2. Quantifying chemotaxis responses using Adler's capillary tube assay

Adler's capillary tube assay is a well established method for quantifying chemotactic responses in bacteria. This assay however was not amenable to study chemotaxis in *C. jejuni* in its present form. The original method procedure was tailored for use with *E. coli* and did not take into consideration the specific growth requirements of the campylobacters. Thus, the following changes were made to Adlers' capillary tube assay (see chapter 2.15.2). In place of performing the capillary assay on a microscope slide, as had been done previously in Adler's capillary assay, a bijoux was used to create the chamber in which the bacteria were to be suspended. A 1 µl glass capillary tube containing a putative *C. jejuni* chemoattractant replaced the U-shaped capillary tube in Adler's Capillary assay. A piece of blutak was used to hold the capillary in place so that the tip of the capillary was immersed in the bacterial suspension (see Figure 2.1, chapter 2 where a schematic drawing of the adapted version of the capillary assay can be found). The bacteria were incubated under microaerobic conditions for different time periods (Figure 4.4). The lids of the bijoux were left on loose to encourage gas exchange and to create a microaerobic atmosphere for the campylobacters. Chemotactic responses were tested to putative *C. jejuni* chemoattractants, namely, fucose and malate (Hugdahl *et al.*, 1988; Marchant, PhD thesis).

The data obtained from the adapted version of Adler's capillary assay demonstrated that there was no chemotactic response in *C. jejuni* towards fucose (0.1 M). When the bacteria were incubated for 10 minutes under microaerobic conditions, more bacteria were found entering the capillary tube containing PBS buffer versus the tube containing the putative attractant (Figure 4.4). Similarly, when the assay was

repeated, incubating this time for 30 minutes no chemotaxis was found in response to fucose (Figure 4.4). It is highly unlikely that such a significant proportion of bacteria added at the start of the experiment would accumulate in the capillary tube containing only PBS buffer. Particularly after only 10 and 30 minutes incubation. This 'background' accumulation of bacteria would have been expected to be much lower. The assay was repeated one final time, using this time an extended incubation period of 60 minutes. Although ten-fold more bacteria were present in the capillary tube containing fucose than PBS. The numbers of bacteria had rapidly declined (Figure 4.4).

In addition, no chemotaxis was observed towards the putative *C. jejuni* chemoattractant malate (data not shown). No viable cells were found in the capillary tube containing 0.01 or 0.1 M malate following 15 minute incubation. Viable bacteria were detected in the capillary tube containing PBS after 15 minute incubation. It may have been that the bacteria were eliciting a chemorepellent effect toward malate, however no increase in cell numbers was found for the numbers of bacteria in the cell suspension inside the bijoux. Thus, the results obtained from Adler's capillary assay were highly variable for fucose and malate at different incubation periods and attractant concentrations. The data was inconsistent and often the CFU/ml for the capillary tube containing PBS buffer was higher compared to the capillary containing a putative attractant compound. Adler's capillary tube method was found to be unsuccessful for use with campylobacters.

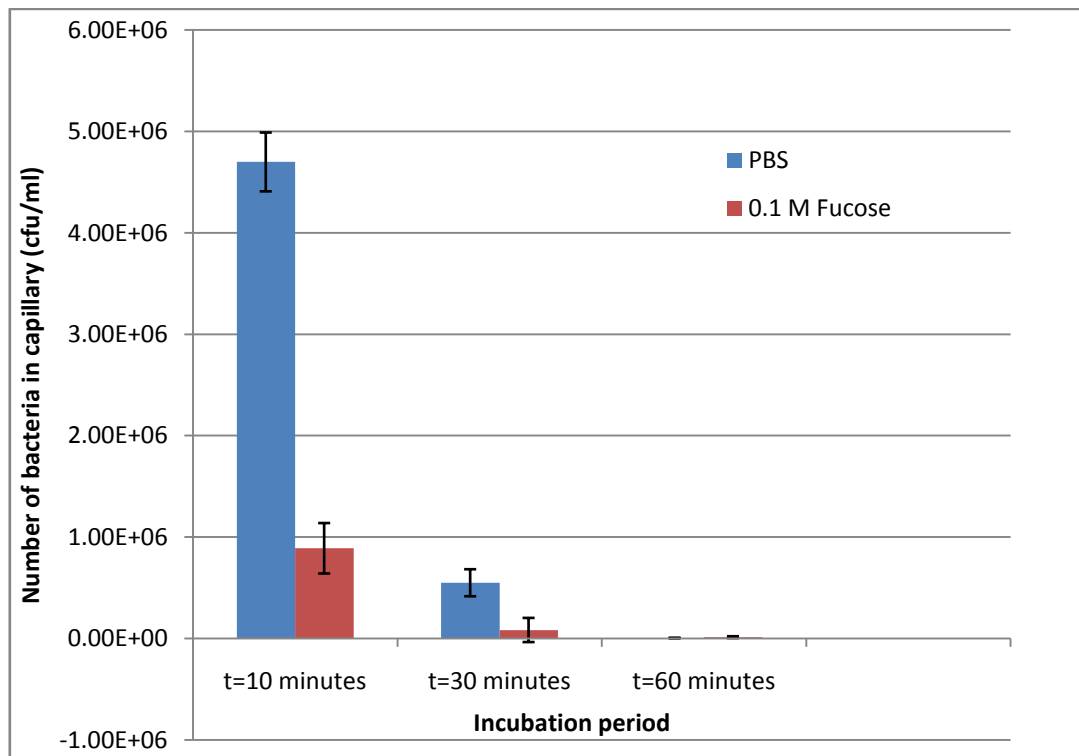


Figure 4.4. Accumulation of wild-type motile variant cells into 1 µl capillary tubes containing either 0.1 M fucose or PBS (buffer only control). The cells were incubated in the VAIN at 37°C under microaerobic conditions for different time periods. Error bars show standard error.

4.3.2.1. A simplified version of the capillary assay designed specifically for use with microaerobic bacteria

Attempts at Adler's capillary tube assay had proved unsuccessful in this work. This may have been because the assay had not been designed for use with microaerobic bacteria and therefore needs of *C. jejuni*. The modifications that had been made to Adler's version of the capillary assay were done so that the apparatus used to perform the assay could be easily placed into the VAIN and thus the bacteria could be incubated under microaerobic conditions. Mazumder *et al.* (1999) developed simplified capillary chemotaxis assay which measured chemotactic responses towards individual ligands (Mazumder *et al.*, 1999, Figure 4.5). The results from this assay were variable. This is illustrated by the large error bars in Figure 4.6. The finalised assay was performed on five separate occasions. In the majority of these experiments there was no detectable difference between the PBS control and the capillary tube containing the attractant (MHB). Moreover, although there appeared to be more bacteria accumulating in the capillary tube containing Mueller-Hinton Broth (MHB), this was not statistically significant (Figure 4.6). The data from these series of experiments were verified by performing a student's *t*-test on the data generated from using the Mazumder *et al.* (1999) method (Figure 4.6). MHB is known to contain a range of putative attractant compounds however, no significant chemotaxis was detected towards MHB using this simplified capillary taxis method.

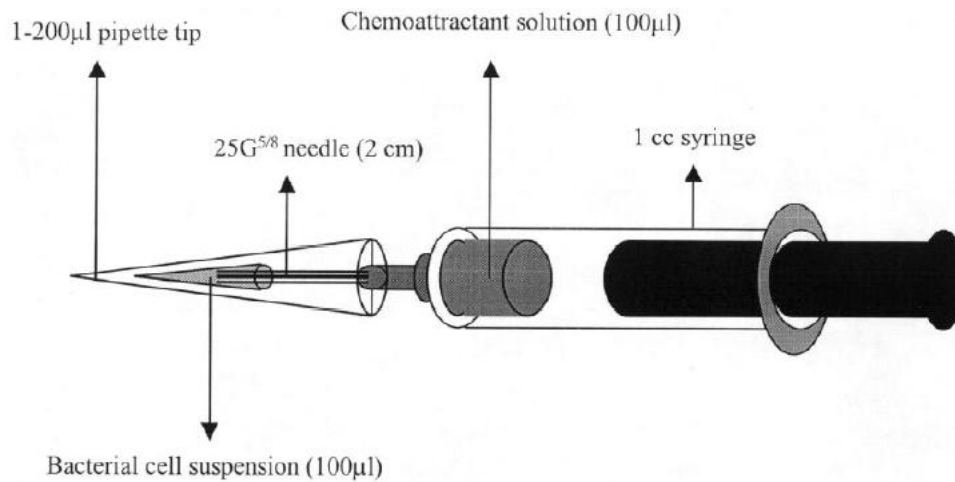


Figure 4.5. An alternative to Adler's capillary tube chemotaxis assay. The assay requires three basic laboratory tools a: needle, syringe and a disposable 200 µl pipette tip. The needle forms the capillary through which bacteria can migrate through into the syringe, where the putative attractant is stored. The pipette tip forms the chamber for the bacterial suspension. The needle, syringe and pipette tip are assembled together and then incubated horizontally, under microaerobic conditions for an appropriate incubation period. Following incubation, the contents of the syringe and the bacterial suspension in the pipette tip are serially diluted in PBS and plated out onto MHA plates for determining CFU/ml that have entered the syringe (Figure taken from Mazumder *et al.*, 1999).

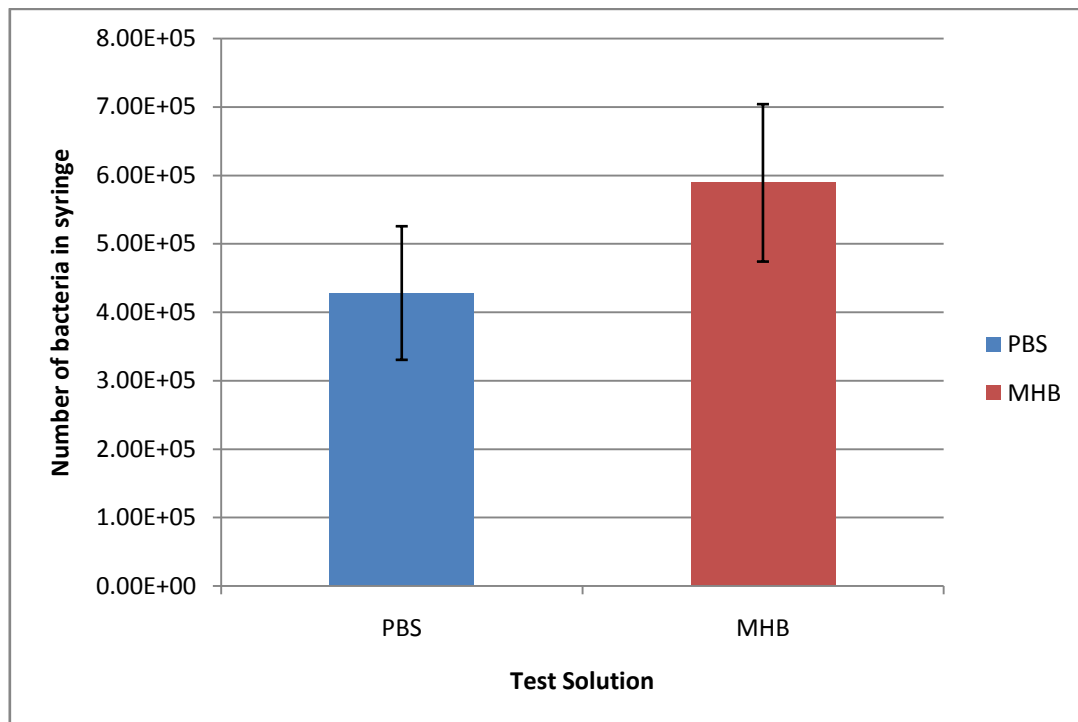


Figure 4.6. Accumulation of wild-type *C. jejuni* into a 1 ml tuberculin syringe containing MHB (Mueller-Hinton Broth) or PBS. The method used here was based on that developed by Mazumder *et al.* (1999). This experiment was repeated five times and the data shown has been collated from all experiments. The results from this experiment showed that that the difference observed here were not statistically significant ($P=0.2963$ and therefore $P<0.05$). This was determined using a student's *t*-test with Welch's correction (section 2.17). Error bars show standard error.

4.3.3. The HAP procedure

4.3.3.1. Modifying the HAP assay

Initial attempts at the HAP assay using the exact methodology detailed in the study by Hugdahl *et al.* (1988) proved unsuccessful (data not shown). Failure to get the HAP procedure to work was believed to be due to unfamiliarity with the techniques involved. For instance, a considerable amount of practice was required to produce the plugs correctly. The test chemicals needed to be dissolved sufficiently in the PBS hard agar in order for the test attractant to diffuse from the plugs and into the surrounding medium (containing the bacteria). Moreover, the numbers of bacteria required to observe chemotactic responses needed to be established. The incubation period necessary to observe the chemotaxis responses needed to be determined. Chemotactic responses were examined over a test period from zero hours up to 96 hours (data not shown). No responses were observed in *C. jejuni* to a range of chemicals all of which were known *C. jejuni* chemoattractants.

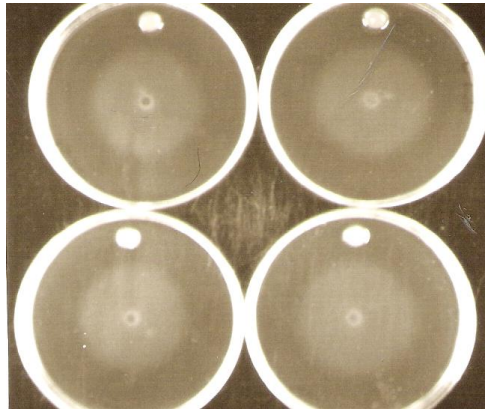
The first modification to be made to the original HAP method (mHAP) was to use an alternative medium to PBS agar (Hugdahl *et al.*, 1988). The medium selected was minimal essential medium-alpha (Full strength, MEM- α plus 0.3% agar). *C. jejuni* cells were inoculated in the centre of MEM- α agar plates and then incubated under microaerobic conditions. The bacteria had visibly swarmed far enough after 48 hours incubation, at which point Hard-agar plugs (HAPs) containing the candidate ligand or PBS (negative control) were added either side of the full strength MEM- α agar plates. The plates were then incubated for a further 48 hours under microaerobic conditions (refer to section 2.15.3.1 for information on the preparation of HAPs). The primary data for the HAP assay using full strength MEM- α media found that chemotaxis responses were apparent in *C. jejuni* towards aspartate (data not shown).

However, these responses were barely visible and consequently could not be photographed. The HAP assay was repeated using this time a lower nutrient concentration threshold to which the campylobacters maybe more responsive towards. The MEM- α media was tested at a half and quarter strength dilutions. Consequently it was found that chemotaxis responses towards putative chemoattractants were more pronounced on half-strength MEM- α media *versus* full-strength (Figure 4.7).

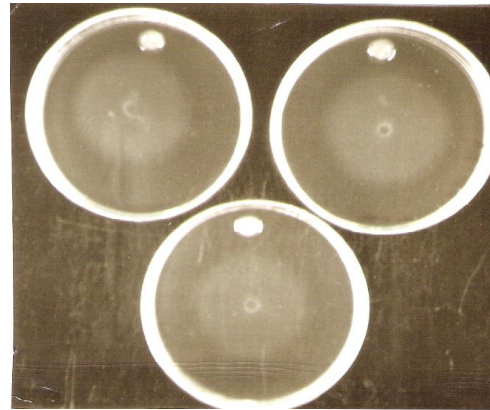
Similar to the swarm plate assay, campylobacters were inoculated in the centre of semi-solid MEM- α media agar plates and then incubated for up to 48 hours. Following incubation, the cells were examined to see whether they had successfully migrated along the nutrient gradient present in the agar medium. This confirmed that the bacteria were (a) motile and (b) chemotactic. Images of the swarms produced following initial incubation are presented in Figures 4.7 (a) and (b)). This was recorded as time zero. Plugs containing the test ligand were added to the Petri plates and incubated further. Positive chemotaxis in response to 0.2 M and 0.4 M aspartate (Figure 4.7 (c)) as well as 0.5 M serine (Figure 4.7 (d)) were observed on half-strength MEM- α medium plus agar. The bacteria were found accumulated around the HAPs containing aspartate and serine. Moreover, more bacteria were found around the HAP containing 0.4 M *versus* 0.2 M aspartate (Figure 4.7 (c)). No bacteria were found accumulated around the control plug containing PBS (Figure 4.7 (d)), negative control). Also no chemotaxis towards aspartate or serine was detected in *C. jejuni* 81116 *flaAB* cells (Figure 4.7 (e) and (f); the *flaAB* mutant was aflagellate and therefore non-motile).

Figure 4.7. Assessing chemotaxis using mem- α medium plus agar (half-strength plus 0.3% agar; see chapter 2, Table 2.4). Wild-type *C. jejuni* motile variant (MV) cells (panels a-d) and *flaAB* mutant cells (panels e & f) were added to the mem- α plates. The OD₆₀₀ of the cells was 0.5.

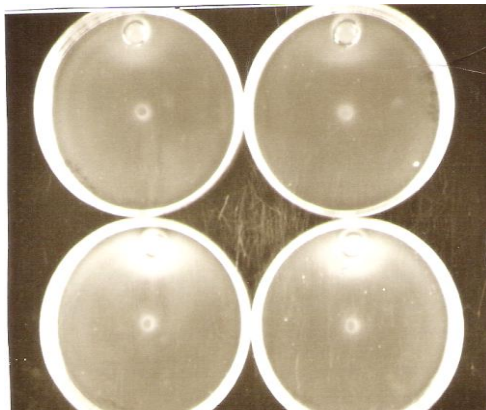
(a) *C. jejuni* MV cells. At 0 hours.
Plus 0.2 (top) & 0.4 M aspartate
(bottom).



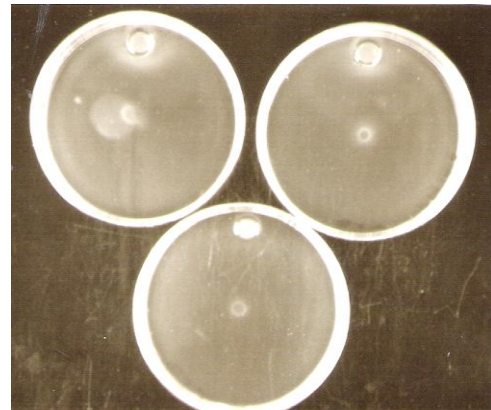
(b) *C. jejuni* MV cells. At 0 hours.
Plus 0.5 M Serine (top) and PBS
(bottom).



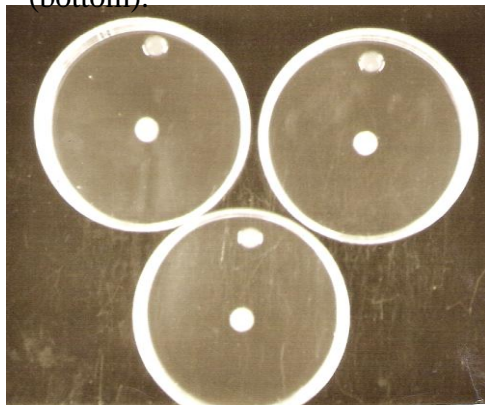
(c) *C. jejuni* MV cells. After 48 hours.
Plus 0.2 (top) & 0.4 M aspartate
(bottom).



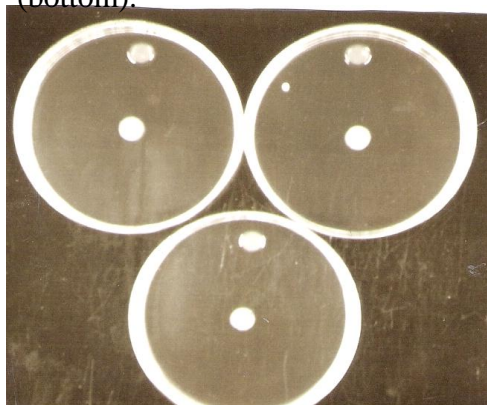
(d) *C. jejuni* MV. After 48 hours.
Plus 0.5 M Serine (top) and PBS
(bottom).



(e) *flaAB* mutant cells. After 48 hours.
Plus 0.2 (top) & 0.4 M aspartate
(bottom).



(f) *flaAB* mutant cells. After 48 hours.
Plus 0.5 M Serine (top) and PBS
(bottom).



4.3.3.2. Reattempting the HAP assay using Hugdahl *et al*'s (1988) original methodology

By modifying the original HAP procedure chemotactic responses were observed in *C. jejuni* in MEM- α media towards serine and aspartate. However, the Mem- α medium is enriched in multiple putative *C. jejuni* chemoattractants. A defined medium such as PBS was the preferred choice as it would enable responses to individual ligands to be determined in *C. jejuni*. The correct preparation of the HAPs was a key element for success of the HAP assay. Other advantages of using the original HAP procedure by Hugdahl *et al.* (1988) *versus* the mHAP version was that responses to putative ligands could be determined in a shorter time span. In the mHAP assay, the bacteria were first inoculated on swarm agar medium and incubated for 48 hours. HAPs would then be added to the plates and incubated further. Thus, it could take up to several days before chemotactic responses to test attractants in *C. jejuni* could be ascertained.

Full details of the exact methodology used to perform the original HAP procedure can be found in chapter 2 (section 2.15.3). Briefly, Hard-Agar Plugs (HAPs; 2 % agar) containing the test compound and a plug containing only PBS medium (negative control) was placed into Petri dishes ready to be assessed in the HAP assay. The bacterial cell suspension ($\sim 3 \times 10^9$ Cfu/ml) in PBS agar medium was poured into the Petri-plate containing the test and control plugs. The plates were then incubated for 20 hours under microaerobic conditions. In the study by Hugdahl *et al.* (1988) chemotactic responses were recorded only qualitatively using a positive and negative scoring system. However, in place of using the same qualitative approach as Hugdahl *et al.* (1988), a semi-quantitative approach was used in the work detailed in this dissertation (Table 4.1). Positive chemotactic responses were determined by measuring the radius of the ring of bacterial accumulation produced around HAPs

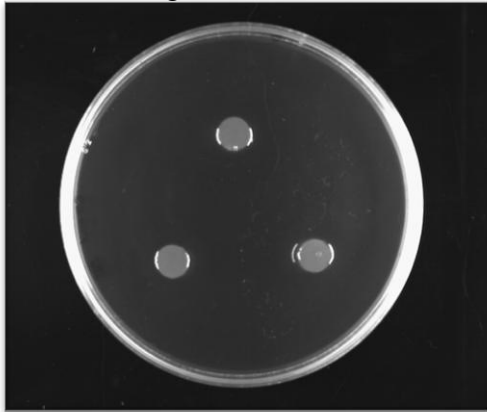
containing the putative chemoattractant (Figure 4.8; Table 4.1). The series of chemicals screened in the HAP procedure included serine, aspartate, glutamate, pyruvate, α -ketoglutarate (Figure 4.8 b-f, respectively; Table 4.1). PBS was used as the control plug (Figure 4.8 (a)). All of these chemicals (excluding mucin and fucose) were tested at 100 mM concentration (Quinones *et al.*, 2009). A turbid zone of bacterial accumulation indicating a positive chemotaxis response was found around all of the chemicals assessed in this study. The area of bacterial accumulation around the plug containing α -ketoglutarate was measured in the same way as had been done previously for the other test chemicals. It is worth noting, that a small area of clearing was observed immediately around the HAP containing α -ketoglutarate. This may have been due to the concentration of α -ketoglutarate being too high. The *flaAB* aflagellate (non-motile) mutant was also assessed alongside the wild-type motile-variant with all of the chemicals screening in this study (Figure 4.8 (g-l)). No responses were observed towards any of the test HAPs in the *flaAB* mutant.

The response to serine was tested at a range of different concentration in the wild-type motile variant (Figure 4.9). In the HAP assay the chemical leaches out into the surrounding agar over time. This makes it difficult to establish the threshold concentration of a particular attractant. The ‘threshold’ concentration of an attractant is the lowest concentration of an attractant that can initiate a chemotactic response. Figure 4.9 demonstrates that upon increasing the concentration of serine from 0.1 to 1.0 M the radius of the zone of bacterial accumulation also increases. If the radius of the zone of accumulation had been recorded over real time it may have been possible to produce a dose-response curve (Adler, 1973; Marchant, PhD thesis). However, responses to serine only became apparent after approximately six hours of incubation. Also, a dose response curve would also only be feasible if this assay was quantitative

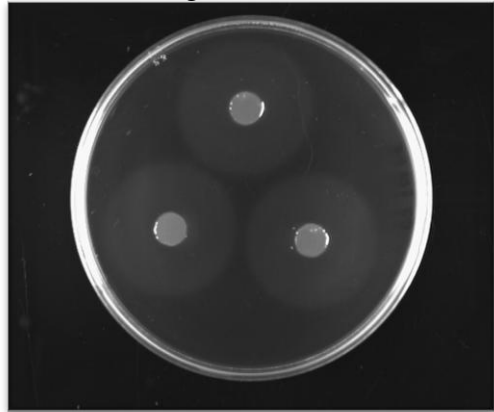
and the rate at which the bacteria accumulated around the plug containing the putative chemoattractant could be determined, similar to Adler's capillary assay (Adler, 1973).

Figure 4.8. Positive chemotaxis towards different chemical stimuli. Wild-type *C. jejuni* motile variant cells (photos a-f) and *flaAB*⁻ mutant cells (photos g-l). All HAPs contained the test chemical at a concentration of 100 mM (excluding the PBS buffer only control). HAP plates were prepared using PBS plus 0.4 % agar. The OD₆₀₀ of the cells in the media was 0.5. All plates were incubated for 20 hours at 37°C under microaerobic conditions.

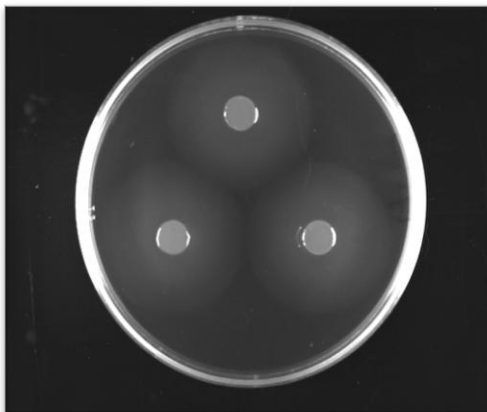
(a) *C. jejuni* MV cells plus 3 x HAPs containing PBS.



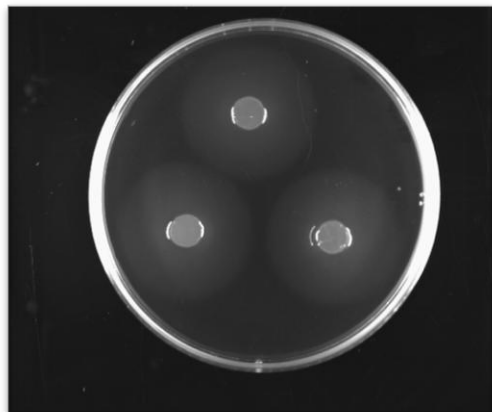
(b) *C. jejuni* MV cells plus 3 x HAPs containing L-Serine.



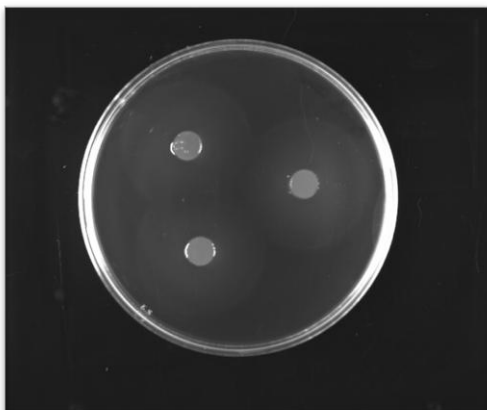
(c) *C. jejuni* MV cells plus 3 x HAPs containing L-aspartate.



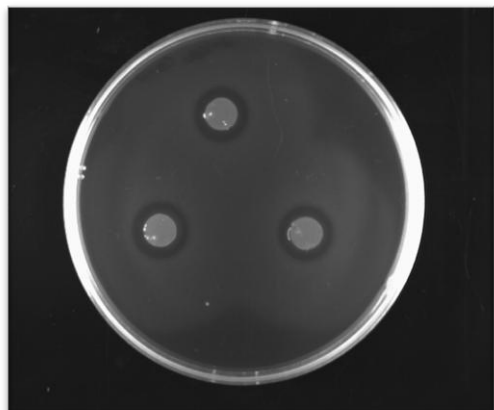
(d) *C. jejuni* MV cells plus 3 x HAPs containing glutamate.

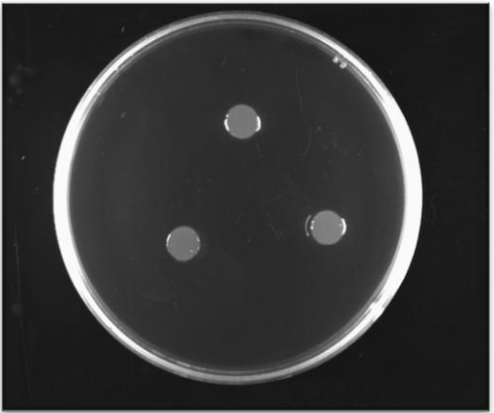
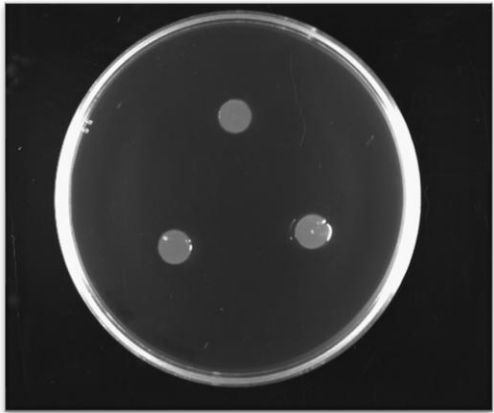
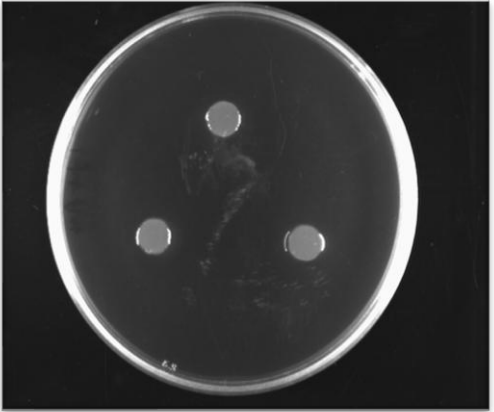
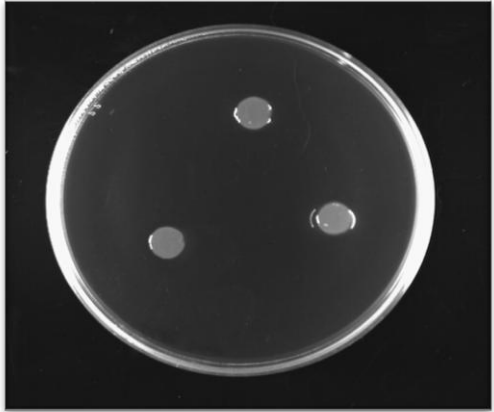
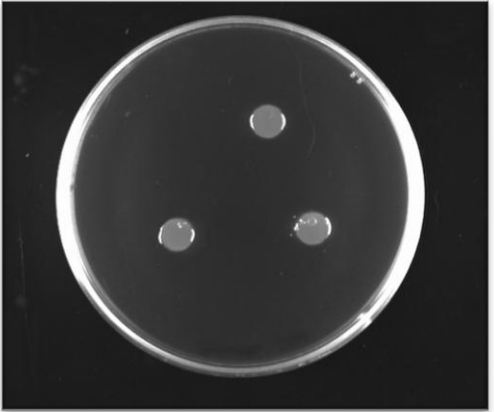
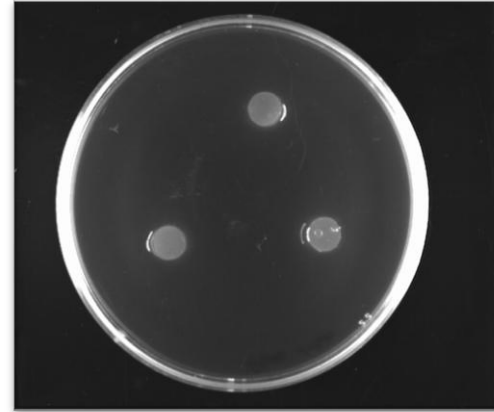


(e) *C. jejuni* MV cells plus 3 x HAPs containing pyruvate.



(f) *C. jejuni* MV cells plus 3 x HAPs containing α -ketoglutarate.



<p>(g) <i>flaAB</i>⁻ (non-motile) cells plus 3 x HAPs containing PBS.</p> 	<p>(h) <i>flaAB</i>⁻ (non-motile) plus 3 x HAPs containing serine.</p> 
<p>(i) <i>flaAB</i>⁻ (non-motile) cells plus 3 x HAPs containing aspartate.</p> 	<p>(j) <i>flaAB</i>⁻ (non-motile) plus 3 x HAPs containing glutamate.</p> 
<p>(k) <i>flaAB</i>⁻ (non-motile) 81116 plus 3 x HAPs containing pyruvate.</p> 	<p>(l) <i>flaAB</i>⁻ (non-motile) plus 3 x HAPs containing α-ketoglutarate.</p> 

Chemoattractant (the final concentration of all chemoattractants in the Haps was 100 mM, unless otherwise stated)	Radius of the zone of the turbid zone surrounding the HAP containing the putative chemoattractant (cm)	Standard deviation (SD)
PBS	Absent	Absent
L-Serine	0.994	0.030
L-Glutamate	1.042	0.022
L-Aspartate	0.967	0.017
Pyruvate	1.112	0.022
α -Ketoglutarate	1.175	0.140
Mucin (0.1, 0.5 & 1.0%)	Absent	Absent
Fucose (0.5 M)	Absent	Absent

Table 4.1. This table shows the responses in wild-type *C. jejuni* motile variant cells to a range of chemicals. The area or zone of bacterial accumulation around the HAP containing the putative chemoattractant is shown (cm). In each experiment there were 3 replicates per test chemoattractant or control. Also three measurements were measured for the radius of the zones produced from bacterial accumulation. The standard deviation from three independent experiments is also presented.

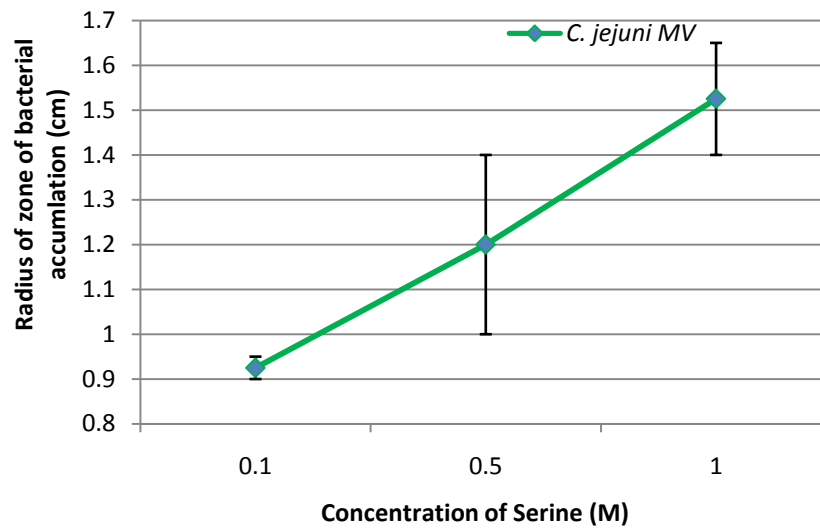


Figure 4.9. Radius of the zone of accumulation around a HAP containing various concentrations of serine. The responses were observed in wild-type motile variant *C. jejuni* cells. Results presented are the means and standard deviations from a single experiment. There were two replicates for each concentration of serine tested. Error bars show standard error.

4.4. Discussion

4.4.1. Motility in wild-type *C. jejuni*

Wild-type, chemotactic campylobacters respond to nutrient spatial gradients by swimming outwardly in the direction of increasing nutrient concentration. The results from the swarm assay were as expected for the wild-type motile variant (Figure 4.2); wild-type *C. jejuni* were evidently motile and chemotactic. Following incubation under microaerobic conditions, these bacteria accumulated within the agar at the position where nutrient concentrations were optimal. As the bacteria collectively swarm through the semisolid nutrient agar multiple concentric bands are produced (Wolfe and Berg, 1989). These concentric bands are produced in response to the multiple spatial nutrient gradients being generated within the agar as the bacteria have used up the nutrients at the point of inoculation (Wolfe and Berg, 1989). The resulting swarm produced by wild-type *C. jejuni* is representative of bacteria that contain a complete network of cytoplasmic chemotaxis proteins (i.e. a CheA, CheY, CheW, CheV, CheR and a CheB) as well homologues of the 12 putative chemoreceptor proteins (two of which are aerotaxis receptors; Marchant *et al.*, 2002).

The swarm plate assay will be an effective tool for assessing the effect of chemoreceptor mutations on the chemotaxis pathway in *C. jejuni*. Simple comparative analysis of the swarming proficiency produced by wild-type cells and the *tlp* mutants will be used to determine the significance of the *tlps* in *C. jejuni* chemotaxis. Quantitative data was extrapolated from the swarm assay by measuring the diameter of the swarms produced by wild-type *C. jejuni* motile-variant cells (Figure 4.3) and this will also be done with the *tlp* mutants. This data will then be

analysed using a student *t*-test and compared with the data generated from the wild-type motile variant.

The swarm assay is however limited in the information it can provide particular with regards to the Tlps. For instance, the swarm plate assay does not allow the assessment of chemotaxis towards individual chemoattractants and therefore the determination of the identity of receptor ligand specificity. Moreover, the *tlp* mutants may not produce perfectly formed swarm phenotype similar to what is typically generated by the wild-type motile variant. This would therefore make it difficult to obtain an accurate measurement of the swarm diameter. The *tlp* mutants may instead produce a swarm that has irregular edges from which an accurate measurement of the swarm diameter would be unobtainable.

A non-motile (aflagellated) *flaAB* mutant (in *C. jejuni* 81116) was used in the swarm plate assay as a negative control for motility. The absence of the flagella in these cells had been confirmed prior to being tested in the assay. Transmission electron microscopy (TEM) verified the absence of the flagella in these cells (Bridle, MPhil thesis). In retrospect, it would have been advantageous had the *flaAB* mutant been in the same strain background as the motile variant and *tlp* mutants i.e. in *C. jejuni* 11168. Thus, future work would be to transform chromosomal DNA from *C. jejuni* strain 81116 (*flaAB*::Kmr) and onto the *C. jejuni* 11168 motile variant background. Moreover, wild type *C. jejuni* 11168 cells should have been tested in the swarm assay and included as an additional positive control.

Previous to this study, the swarm assay has been used to determine the role of the *cheY* gene in *C. jejuni* (Marchant *et al.*, 1998). The *cheY* gene provides a valuable link between the cell signalling pathway and the *C. jejuni* flagellum. This data for the *cheY* mutant has also been reported previously (Marchant *et al.*, 1998). The *cheY*

mutant demonstrated a complete loss of chemotaxis in the swarm plate assay.

Furthermore, when individual *cheY* mutant cells were tracked using a Hobson tracker, they were found to be tumbling less frequently and showed a bias towards smooth swimming (Marchant *et al.*, 1998). Since this study, mutations have been constructed in homologues of the chemotaxis (*che*) genes *cheW*, *cheA*, *cheV*, *cheR* and *cheB* in *C. jejuni* NCTC 11168. When tested in the swarm assay, the *che* mutants demonstrated an altered phenotype in the swarm assay which differed significantly from the wild-type strain (Bridle, MPhil thesis). The swarm assay could be useful for assessing any potential differences in chemotaxis and motility between different *C. jejuni* strains.

4.4.2. Possible explanations for failure of the capillary assay

The results obtained in this study from the two versions of the capillary assay attempted in this work were highly variable and non-reproducible. In some instances more bacteria were migrating into the capillary containing the PBS buffer versus the potential attractant. The numbers of bacteria accumulating into the ‘background’ capillary tube were very high. Perhaps the bacteria were being forced into the capillary through some sort of passive movement of fluid. This could have been caused by a number of errors, some of which will be discussed here. Adler addresses in his study the significance of the lag time and that this varies for different chemicals (Adler, 1973). This is essentially the time before the attractant reaches its threshold concentration for the bacteria to respond. In fact only 11000 bacteria were found in the control capillary tube after 90 minutes in Adler’s capillary assay (Adler, 1973). Furthermore, the concentration of attractant being used in the capillary tube may have been too strong. This could have saturated the chemoreceptors in *C. jejuni*, which would have consequently diminished any chances of a concentration gradient forming between the capillary tube and the bacterial chamber. No cells accumulated into the

capillary tube containing 0.1 M malate. Viable bacteria were present in the capillary tube containing PBS. It is likely that had the un-diluted contents of the capillary tube containing the malate had been plated out eventually viable bacteria would have been detected. It may have been that the bacteria were eliciting a chemorepellent effect towards malate. However, had this been the case then surely there would have been an increase in the number of bacteria present cell suspension in the bijoux.

Nevertheless, malate was identified as a putative chemoattractant in the HAP procedure by Hugdahl *et al.* (1988). Other possible explanations were that malate was causing cell toxicity in the campylobacters. However there was no decline in the number of bacteria present in the bijoux following incubation with malate.

Additionally, there were a greater number of cells in the capillary tube containing 0.1 M fucose than the capillary tube containing 0.5 M fucose. These data demonstrate the importance of testing any potential ligands over a range of different concentrations. The concentration of fucose and malate tested in this study was 0.1 and 0.1 and 1.0 M, respectively. These concentrations were based on those concentrations that had previously been used in the HAP assay (Hugdahl *et al.*, 1988). In the HAP assay the test chemical is added to the plug. The attractant then diffuses into the surrounding medium. This makes it difficult to ascertain the threshold concentration of a putative attractant in the HAP assay.

A rapid decline in cell numbers was observed when cells were incubated for periods longer than 15 minutes. No viable *C. jejuni* cells were detected when plating out the contents of the bijoux (containing the bacterial suspension at 1000-fold dilution) when incubated for 60 minutes in PBS. This rapid decline in cell numbers over time may be due to the cells becoming starved. Interestingly, recent work has demonstrated that the addition of ferrous sulfate, sodium metabisulfite, and sodium

pyruvate (FBP) supplement to the bacterial cell suspension, made in PBS plus agar 0.1 % helps to maintain cell viability when the cells are incubated for longer periods of time (Personal communication, Oliver Bridle). The campylobacters are particularly sensitive to harmful derivatives of oxygen which include: superoxide ions, hydrogen peroxide and a singlet form of oxygen (Jiang and Doyle, 2000). The addition of FBP supplement to the growth media enhanced the growth and aerotolerance of *C. fetus* (George *et al.*, 1978). Therefore, the addition of FBP to the *C. jejuni* bacterial suspension will need to be explored further.

The size of the capillary opening and pH are variables that would need to be taken into consideration in future assays (Adler, 1973). Previous research has shown that *C. jejuni* cells become immobilized when the pH of the growth medium is dropped from pH 8.5 to pH 5.0, where pH 8.5 reflected the pH of the natural host intestine (Szymanski *et al.*, 1995). Carboxymethylcellulose (CMC) can be used as alternative medium to PBS (0.1% agar) as it is known help mimic the natural viscosity of the gut. The viscosity of the bacterial medium does appear to have a significant effect on *C. jejuni* motility, binding and invasion potential of *C. jejuni* cells (Szymanski *et al.*, 1995). The addition of CMC to the bacterial growth media has been linked with longer periods of straight swimming with increased viscosity in bacteria.

One further drawback of Adler's capillary assay was that due to the complexity of the method for the assay often meant the campylobacters were being exposed to prolonged periods of atmospheric levels of oxygen. Therefore, it would be difficult to ascertain whether any possible chemotaxis was genuine or was aerotaxis. This made it difficult to obtain rapid results regarding any potential chemotactic responses in *C. jejuni*. If the capillary assay could be performed under microaerobic

conditions in its entirety perhaps genuine chemotaxis responses could be determined in *C. jejuni*.

No significant difference was found in the relative numbers of *C. jejuni* accumulating in the syringe containing the PBS buffers versus the test attractant using the Capillary method developed by Mazumder *et al.* (1999; Figure 4.7). Once more, the 'background' number of bacteria accumulating onto the control capillary tube containing the PBS buffer was too high. This may have been caused by bacteria being forced up into the needle when the Gilson pipette-tip was being fitted to the needle-syringe apparatus (Mazumder *et al.*, 1999). No alterations needed to be made to the apparatus used to perform the assay. Also, unlike in Adler's capillary assay the samples were being placed this time horizontally *versus* vertically. This may have been a possible drawback of the apparatus design used previously.

There have been studies previous to the work described in this dissertation that have been successful at measuring quantitatively, chemotactic responses in the campylobacters (Paster and Gibbons, 1986; Khanna *et al.*, 2006). In the earliest of these studies, chemotactic behaviour was assessed in *Campylobacter concisus*. Positive chemotaxis in *C. concisus* was only demonstrated towards formate, but no other attractant compounds including sugars, inorganic salts, amino acids or mucin. Although, the experiments were performed aerobically, a specialised buffer was used which contained chemicals that would help shield the campylobacters against oxidative stress. The capillary assay undertaken by Khanna *et al.* (2006) was carried out under microaerobic conditions. However, many responses to putative *C. jejuni* chemoattractants of which include serine and aspartate were absent in their findings. Instead responses to previously unidentified amino acids were discovered. The researchers of this study went onto verify their data by performing a filter-disc based

procedure (Hazeleger *et al.*, 1998). However the positive chemotaxis responses observed using the filter-disc method were not in agreement with those responses seen previously in the capillary assay (Khanna *et al.*, 2006). It is also unclear how chemotaxis and motility were differentiated in this work (Khanna *et al.*, 2006). One of the main finding from this work was that chemotaxis was more pronounced at 37°C versus 42°C in *C. jejuni*. This may have just been an increase in motility in *C. jejuni* versus an increase in chemotaxis.

4.4.3. The HAP procedure

An attempt to semi-quantify chemotactic responses in wild-type *C. jejuni* was done in this work. During the initial optimisation stages, MEM- α medium was used in place of PBS media. This medium is similar to MHB in that it is a complex media that is rich in putative *C. jejuni* chemoattractants. Chemotactic responses using the full-strength MEM- α media were faint and barely visible. This may have been caused by the chemoreceptors in *C. jejuni* becoming saturated by the presence of multiple nutrients. Interestingly, more strong chemotactic responses were observed upon halving the concentration of the MEM- α . This may have essentially established the threshold level for the nutrients in the media to which the campylobacters were responsive towards (Adler, 1973). Furthermore, the quarter strength MEM- α media may have been below this nutrient concentration threshold as chemotactic responses were not as well defined.

The radius of the zones of bacterial accumulation around HAPs containing putative *C. jejuni* chemoattractants was measured (Table 4.1). However, it would have been advantageous if chemotactic responses in *C. jejuni* could have been quantified similarly to the capillary assay. Future work would involve removing a specific section of the agar around the HAP where the bacteria had accumulated and

perform viable counts from this section. For example a 1 ml Gilson pipette tip could have been used to remove a section of the agar. By comparing the viable counts obtained from the area surrounding a HAP containing only PBS (Figure 4.8 (a)) with that containing a potential chemoattractant could have made this a quantitative chemotaxis assay. This would have enabled responses in *C. jejuni* to individual chemicals to be quantified.

Chemotactic responses have been quantified similarly to the capillary assay by adaptation of the original HAP procedure by Hugdahl *et al.* (1988) (Hartley-Tassell *et al.*, 2010). The HAP (supplemented with the test chemical) was removed in its entirety and used to perform viable counts from (Hartley-Tassell *et al.*, 2010). However this particular version of the HAP assay was performed under aerobic conditions. However, previous researchers have not found vast differences in chemotaxis when incubating campylobacters under aerobic *versus* microaerobic conditions (Hazeleger *et al.*, 1998; Marchant, PhD thesis; Khanna *et al.*, 2006).

The HAP procedure has been employed in other studies to examine chemotaxis responses in *C. jejuni* (Hazeleger *et al.*, 1998; Quinones *et al.*, 2009; Hartley-Tassell *et al.*, 2010); it is now a well accepted procedure for measuring chemotaxis responses in bacteria. A study by Quinones *et al.* (2009) undertaken to identify the role of the *luxS* gene in colonisation of the chick gastrointestinal tract in *C. jejuni* 81176 used the HAP procedure to assess chemotaxis response to a series of chemicals. The researchers of this study found positive chemotaxis towards aspartate, glutamate, serine, α -ketoglutarate and pyruvate (Quinones *et al.*, 2009). Although a different strain of *C. jejuni* had been used in the study by Quinones *et al.* (2009), these findings were in support of the chemotactic responses determined in *C. jejuni* 11168 in this work. Moreover, the radiuses of the area of bacterial accumulation

produced in response to these series of chemicals were similar to those readings obtained in this work.

The HAP assay was also modified and used in an earlier study by Hazeleger *et al.*, (1998). In place of using HAPs the chemical to be tested was impregnated onto filter paper. Once the filter discs were soaked through they were placed in the centre of a Petri-plate containing *C. jejuni* cell suspension mixed in with PBS-agar medium. The researchers only tested responses to three chemicals. This included malate, formate and pyruvate with chemotaxis detected towards all three of these chemicals; the weakest of responses was seen with pyruvate. In the HAP assay work described here wild-type *C. jejuni* did respond strongly to pyruvate (Figure 4.8 (e)). The HAP assay using filter discs in place of HAPs was attempted but proved unsuccessful (data not shown).

The HAP procedure will be employed in this study to assess the *tlp* mutants for attractant specific responses to confirmed *C. jejuni* chemoattractants. This will help to determine whether a mutation in a specific Tlp has resulted in loss of chemotaxis to a single *C. jejuni* chemoattractant or has had a more wide-scale effect. The findings obtained in the HAP assay for wild-type *C. jejuni* cells will be used further on in this work to make direct comparisons with *tlp* mutant *C. jejuni* cells.

Chapter 5. Phenotypic studies on Transducer-like protein (Tlp) 1 and the significance of Tlp2 and Tlp4 in *Campylobacter jejuni* chemotaxis

5.1. Introduction

Previous research has proven that chemotactic motility is required for successful colonisation of the intestine in mice (Takata *et al.*, 1992; Yao *et al.*, 1997; Chang and Miller, 2006), pathogenesis of disease in ferrets (Yao *et al.*, 1997) and invasion of the intestinal epithelium (Golden and Acheson, 2002). A ligand-binding domain in only 5 of the 12 Tlps in *C. jejuni* suggests that this group of Tlps bind external ligands and are also therefore required for colonisation. In fact previous research has identified two of these cell surface Tlps to be necessary for successful colonisation of the chick gastrointestinal tract (Hendrixson and DiRita, 2004). Despite their involvement in colonisation of the intestinal tract, the relative function of the Tlp receptors and their respective ligand specificities was not known at the commencement of this study. The *tlp1* isogenic mutant created in the work described in this dissertation was characterised further by our collaborators in Australia. *In vitro* and *in vivo* models were used to determine whether the Tlp1 receptor is required for adherence to or colonisation of the host tissues. These studies have been published and will be reviewed further in the discussion to this chapter.

5.1.1. Tlp receptors in other bacteria

The Tlps in *C. jejuni* appear most similar to the MCPs of *E. coli* and to a family of receptors in *Halobacterium salinarum* (Zhang *et al.*, 1996). *Helicobacter pylori* are

genetically similar to *Campylobacter* and encode four MCP like receptors (Anderman *et al.*, 2002; Terry *et al.*, 2006). Two of these receptors, namely TlpA and TlpC were found to be necessary for disease progression in the stomach of laboratory mice (Anderman *et al.*, 2002). Moreover, TlpB in *H. pylori* was also found to be required for pH taxis and colonisation of the mucosa in the stomach (Croxen *et al.*, 2006). There is some homology in the ligand-binding domain of the *C. jejuni* Group A Tlps with the chemoreceptors TlpA and TlpC in *H. pylori* and TlpA proteins present in *H. hepaticus* and *Wolinella* spp. (Tomb *et al.*, 1997; Baar *et al.*, 2003; Suerbaum *et al.*, 2003). Although there is some similarity in the Tlps in *C. jejuni* and MCPs in other bacteria, the ligand-binding specificity of the Tlps in *C. jejuni* needs to be determined using biological assays and cannot be determined from sequence homology searches alone.

5.1.2. Chemotaxis assays optimised with the *C. jejuni* wild-type motile-variant

Chemotaxis assays were established and optimised in this work to determine the ligand-binding specificity of Tlp1, Tlp2 and Tlp4 (Chapter 4). Chemotaxis assays would enable the phenotypes of the *tlp* mutants to be determined and comparison to the phenotype of the wild-type motile-variant (MV) would subsequently reveal if a mutation in a *tlp* gene affects chemotaxis in *C. jejuni*. Thus, chemotaxis assays were imperative for determining the roles of the Tlps in *C. jejuni* pathogenesis. The swarm assay is a qualitative chemotaxis assay that can establish whether mutation of a Tlp has had a consequence on the chemotactic behaviour of *C. jejuni*. The responses in the swarm assay can be quantified by measuring the diameters of the swarms. However, as the swarm assay is performed in complex nutrient media an alternative assay was essential in which the identity of specific Tlp ligands could be determined.

A capillary assay and a Hard-agar plug assay (Adler, 1973; Hugdahl *et al.*, 1988) were investigated as potential assays to characterise the Tlps. Unfortunately, the two versions of the Capillary assay attempted here in this work were found not to be sufficiently reproducible for effective use with *C. jejuni* NCTC 11168 (Adler, 1973; Mazumder *et al.*, 1999; Chapter 4). Therefore, the focus was switched to the HAP assay. The HAP procedure was of particular importance because it was the only method available at the time of this work to determine the respective ligand-binding specificity of the Tlps. The work described in this dissertation demonstrated for the first time, that *C. jejuni* strain NCTC 11168 is positively chemotactic towards: serine, aspartate, glutamate, pyruvate and α -ketoglutarate (Chapter 4; Figure 4.7 (b-f), Table 4.1); all of which have previously been identified as putative chemoattractants in *C. jejuni* (Hugdahl *et al.*, 1988; Quinones *et al.*, 2009). The optimisation of the HAP procedure using the wild-type MV has been described in this dissertation (Chapter 4, section 4.3.3; Hugdahl *et al.*, 1988). Chemotactic responses determined in the wild-type *C. jejuni* MV cells will be used to make direct comparisons with those responses seen in the *tlp* mutants produced in this work.

5.1.3. Previous research on the Tlps in *C. jejuni* NCTC 11168

At the commencement of this study only Tlp4 (Cj0262c) and Tlp10 (Cj0019c) had been shown to be essential for successful colonisation of the chick gastrointestinal tract (Hendrixson and DiRita, 2004). More recently, Tlp1 has also been found to be required for colonisation (Hartley-Tassell *et al.*, 2010, Appendix 1). There is also evidence to support that *aer2* (*cetB*) and *tlp9* (*cetA*) in *C. jejuni* regulate a similar energy taxis response to *E. coli* (Bibikov *et al.*, 1997; Hendrixson *et al.*, 2001; Vegge *et al.*, 2009). CetA contains an N-terminal transmembrane region which localises the

protein to the inner membrane and a C-terminal domain containing a highly conserved domain (HCD). The latter domain is proposed to function as the docking domain for the interaction with CheA and CheW. Whereas, the CetB protein contains a PAS (an acronym of the genes found to contain the repeat sequences) domain which is predicted to bind to the cofactor flavin adenine dinucleotide (FAD; Bibikov *et al.*, 1997). CetB is proposed to use FAD as a redox sensor to monitor electron transport, then through direct interaction with CetA transduces this signal to the chemotaxis proteins via its HCD to alter flagellar rotation. Such a taxis mechanism would enable the bacterium to move towards environments that can support high electron transport and ATP generation (Hendrixson *et al.*, 2001; Korolik and Ketley, 2008).

The genes encoding Tlps 1, 2 and 4 in *C. jejuni* NCTC 11168 have been successfully inactivated using an insertional inactivation strategy (Chapter 3); the *tlp3* gene could not be inactivated. In the swarm or soft agar method mutation of a major *tlp* may be expected to affect chemotaxis towards a specific chemoattractant ligand, while motility and chemotaxis towards other ligands would remain unaffected. However, the probable formation of receptor clusters at the poles of the cell may therefore result in a specific *tlp* mutant demonstrating a wider-scale affect on chemotaxis which would be observed as a reduction in swarming phenotype. The ligand-binding specificity and the biological roles of the Group A Tlps in *C. jejuni* chemotaxis is unknown and will be determined using the established chemotaxis assays.

5.2. Results

5.2.1. Assessment of the *tlp* mutants in the swarm assay

The swarm assay provides the opportunity to observe the link between the chemotaxis pathway and flagellar based motility in *C. jejuni*. The swarm or soft agar

assay utilises nutrient rich Mueller-Hinton agar media which provides an optimal environment for the bacteria to retain motility. *C. jejuni* cells from the wild-type MV, *flaAB*, *tlp1*, *tlp2* and *tlp4* mutants were spotted near the centre of an MHA plate and then incubated under microaerobic conditions for up to 72 hours (see section 2.15.1; Figure 5.1). Following incubation, the diameter was measured from the swarms produced by the different cell types being assessed in this work (Figure 5.2). There was a minimum of 3 replicates for each cell type and all swarm assays were repeated three times. The results showing images of the different swarm phenotypes produced by wild-type MV, *flaAB*, *tlp1*, *tlp2* and *tlp4* mutants are presented in Figure 5.1 (a-f). Chemotaxis along the concentration gradient developing within the agar due to nutrient metabolism is evident in wild-type MV cells, where the majority of the bacteria can be seen to have accumulated in the outermost ring or band in the agar ($6.7\text{cm} \pm 0.094$ (standard error); Figure 5.1 (a); Figure 5.2; Appendix 3). A *C. jejuni* 81116 *flaAB* mutant was used as a negative control in the swarm assay. These cells were aflagellate and the absence of the flagella had previously been confirmed by Transmission Electron Microscopy (TEM; Bridle, MPhil thesis). The phenotype of the *flaAB* mutant is shown in Figure 5.1 (c). The swarm phenotype produced from these aflagellate cells demonstrate that these cells have been unable to swarm from the point of inoculation. The negative control demonstrates, as expected, that swarming is dependent on flagellum based motility and the observed spread is not due to growth. Furthermore, the requirement of the chemotaxis pathway for swarming was demonstrated by a chemotaxis mutant in the *cheY* gene. The *cheY* mutant was unable to swarm and produced a phenotype similar to the *flaAB* mutant (Figure 4.2(c)).

The *tlp1* mutant swarmed significantly further compared to the wild-type MV (Figure 5.2; Tlp1 Δ : 7.531 cm \pm 0.078, $P < 0.0001$; Appendix 3). This phenotype is shown in both Figure 5.1 (b) and in (c). Figure 5.1 (c) highlights the difference in phenotypes between the *tlp1* mutant (top right), wild-type MV (top left) and *flaAB* mutant (bottom). The *tlp2* mutant showed a peculiar phenotype in the swarm assay, where the cells seem unable to collectively accumulate in the agar at the optimal point for nutrients (Figure 5.1 (e)). The irregularity in swarm diameter rendered this mutant phenotype difficult to quantitate with any accuracy and therefore average swarm diameters are not included in Figure 5.2. The *tlp2* mutant had managed to swarm some distance away from the point of inoculation. However, inactivation of the *tlp2* gene had caused a disruption in the *C. jejuni* chemotaxis system. Although, *tlp4* mutant cells did demonstrate reduced swarming (6.255 cm; \pm 0.083; Figure 5.2 (f)) compared to the wild-type MV (6.848 cm \pm 0.079; Figure 5.2 (a)), the difference in phenotype was not as pronounced as had been seen previously for example with the *tlp2* mutant. Moreover, *tlp4* mutant cells appear to produce a diffuse outer ring which suggests an alteration in the ability of cells to accumulate at the point where nutrient concentrations are highest. The collective accumulation of cells towards the periphery of the swarm plate as seen in the wild-type motile variant is an indication of the collective accumulation of cells at the optimal point in the agar. Although the phenotype produced by *tlp4* mutant cells appears similar to the wild-type, the reduction in swarming does indicate that *tlp4* is required for chemotaxis. The requirement of the Tlp4 receptor in chemotaxis *in vivo* has been previously demonstrated (Hendrixson and DiRita, 2004).

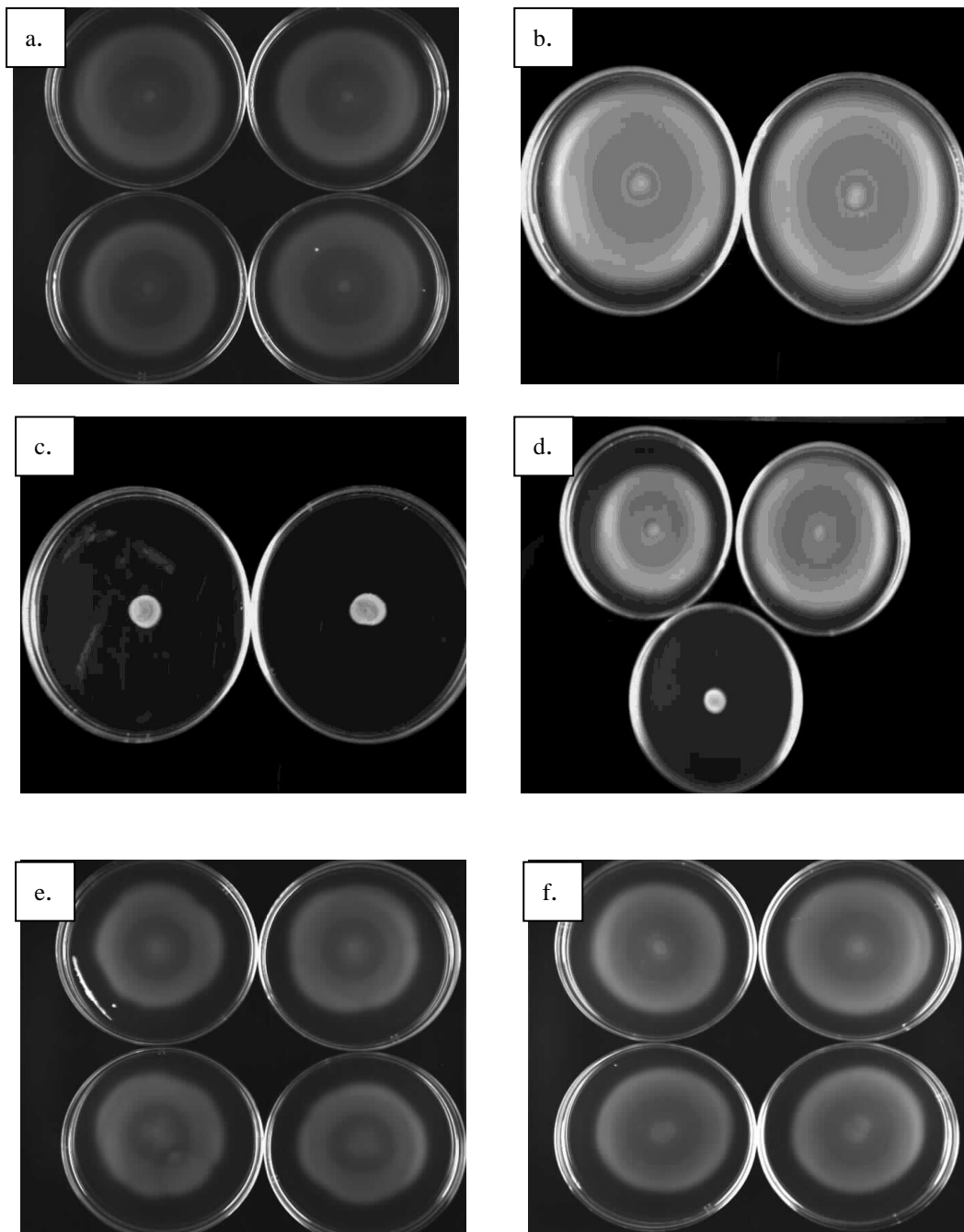


Figure 5.1. Swarming phenotypes of the *tlp* mutants relative to the wild-type *C. jejuni* MV. The swarming phenotypes shown are: panel (a), wild-type MV (motile-variant); panel (b), *tlp1* mutant; panel (c), *flaAB* mutant (*C. jejuni* 81116); panel (d), wild-type MV (top-left), *tlp1* mutant (top-right), *flaAB* mutant (bottom); panel (e), *tlp2* mutant and panel (f) is the *tlp4* mutant. All panels from a-f contain replicates of the same cell type, apart from panel (d). All swarm assay phenotypes are following 72 hours incubation under microaerobic conditions. Swarm plates were produced using Mueller-Hinton agar (MHA; 0.3% agar). The optical density of the bacterial suspensions at 600 nm (OD_{600}) was 1.0. Figure shows the assays from an indicative experiment of the three carried out.

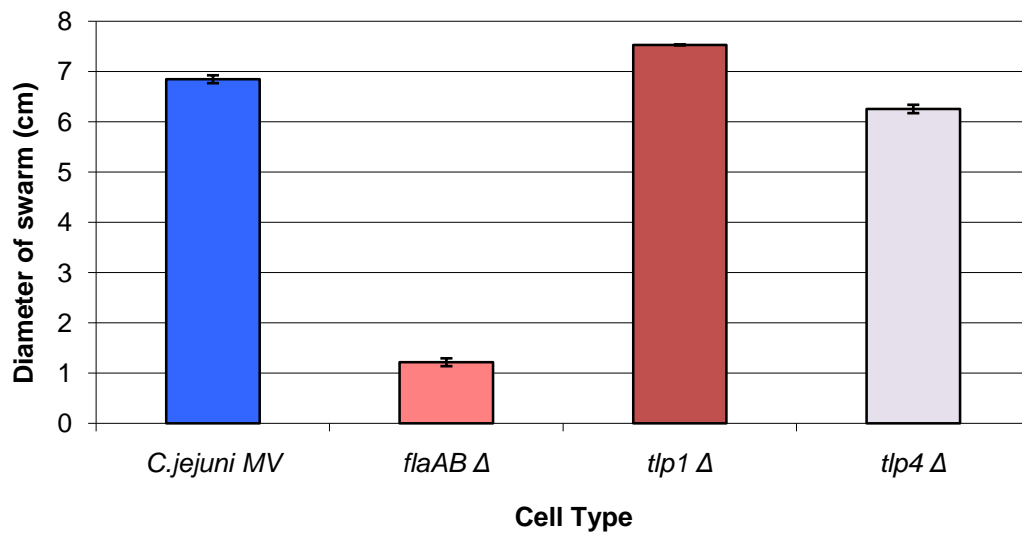


Figure 5.2. Comparing the differences in swarm diameters between the *tlp1* and *tlp4* mutants and the wild-type *C. jejuni* MV (motile variant) and non-motile *flaAB* control. All swarm diameters were measured following 72 hours incubation under microaerobic conditions. Swarm plates were produced using Mueller-Hinton broth (MHB) plus 0.3% agar. The optical density at 600 nm (OD_{600}) was 1.0. Results presented here are the means from three independent experiments and there was a minimum of 3 replicates per experiment (for the *C. jejuni* MV, $n=21$; the *tlp1*Δ, $n=13$; *flaAB*Δ, $n=13$ and the *tlp4*Δ, $n=9$). Error bars show the standard error. See Appendix 3 for the raw data used to produce this data plot and to perform the *t*-test analysis.

5.2.2. Determining the ligand-specificity of the *tlp* mutants in the HAP assay

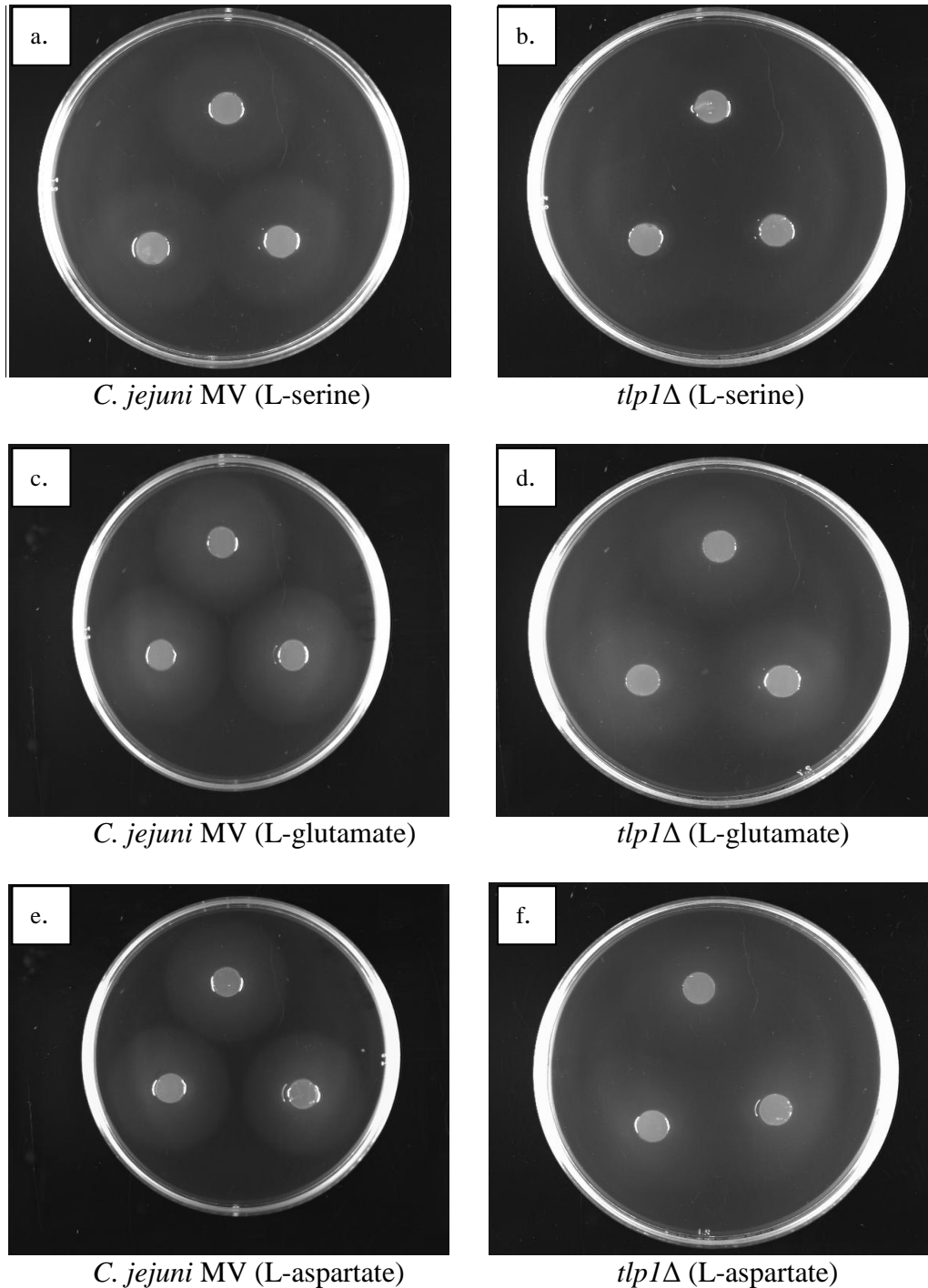
The Hard-agar plug procedure which was originally developed by Hugdahl *et al.* (1988) was modified and used to determine the ligand-binding specificity of the Tlp1, Tlp2 and Tlp4 receptors in *C. jejuni* NCTC 11168 (see section 2.15.3). The established method for the HAP procedure had been optimized for use with wild-type *C. jejuni* NCTC 11168 and these studies are described in chapter 4 (section 4.3.3). A suspension of bacteria (wild-type, *flaAB* or *tlp* Δ ; with an OD₆₀₀ of 0.5, which equates approximately to 5 \times 10⁹ CFU/ml) in PBS-agar (0.4%) media was added to Petri plates that were either 90 by 45 mm (Figure 5.3) or 60 by 15 mm (miniature Petri plates; Figure 5.5). Hard-agar plugs containing either phosphate-buffered saline (negative control) or the test substrate were positioned within the agar. The test substrates were assessed at 100 mM concentration, which had been established in the assay development undertaken in this study and also previously shown to elicit a chemotactic response in *C. jejuni* (strain 81176; Quinones *et al.*, 2009). The Petri plates were then incubated for 20 hours. Similar to the swarm assay, chemotactic motile bacteria respond to the gradient present in the PBS-agar media. The gradient develops as the test chemical diffuses from the plug and into the PBS-agar media. Chemotactic responses were observed by placing the Petri plates under an indirect light source (see Figure 5.3 and 5.6). These responses were quantified by measuring the radius of the zone of bacterial accumulation produced around each of the HAPs containing a putative chemoattractant (Hugdahl *et al.*, 1988). More specifically, the zone of bacterial accumulation was measured (in cm) from the edge of the HAP to the edge of the zone (Figure 5.4). The series of candidate ligands screened in the HAP procedure were serine, aspartate, glutamate, pyruvate and α -ketoglutarate. PBS was

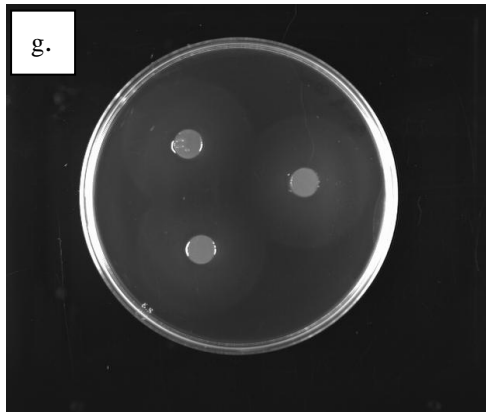
used as the no substrate control plug in all experiments (Figure 5.3, (k)). With the wild-type MV strain a zone of bacterial accumulation was found around all of the HAPs containing a chemoattractant (Figure 5.3). Conversely the 81116 *flaAB* aflagellate (non-motile) mutant showed no bacterial accumulation around any of the plugs containing putative chemoattractants (Chapter 4; Figure 4.8 (g-l)). As observed previously, (Chapter 4; Figure 4.8 (f)) a small area of clearing was noted around the HAP containing α -ketoglutarate. The majority of chemotactic responses observed in the *tlp1* Δ mutant were more diffuse and dispersed in comparison to the responses observed in the wild-type (Figure 5.3). Furthermore, due to the lack of definition in the edge of the turbid zones seen with the *tlp1* Δ mutant (Figure 5.3 (f and j)) it was difficult to make an accurate measurement of the zone of bacterial accumulation around the plug. A small but notably reduced zone of bacterial accumulation was observed in the *tlp1* Δ towards L-serine (Figure 5.3 (b)) and pyruvate (Figure 5.3, (h)). When the radius of these zones of bacterial accumulation were measured the results verified that the zones of bacterial accumulation were smaller around the plugs containing L-Serine ($0.133 \text{ cm} \pm 0.033$) and pyruvate (Figure 5.4; $0.7 \text{ cm} \pm 7.85 \times 10^{-23}$) in comparison to the responses observed in the wild-type MV to L-Serine (Figure 5.4; $1.0 \text{ cm} \pm 0.030$) and pyruvate (Figure 5.4; $1.1 \text{ cm} \pm 0.022$). Furthermore, chemotaxis towards L-aspartate (Figure 5.4; $1.2 \text{ cm} \pm 0.058$) in the *tlp1* Δ also appeared to be affected compared to the wild-type MV (Figure 5.4; $1.0 \text{ cm} \pm 0.017$). Moreover, the possible chemorepellent effect of α -ketoglutarate in the wild-type MV appeared to be absent in the *tlp1* Δ (Figure 5.3 (j)). These data need to be considered with caution as this data was generated from only a single experiment and results need to be repeated before it can be determined whether these initial observations are statistically significant. Similar to the 81116 *flaAB* aflagellate (non-motile) and PBS

control, no zone of bacterial accumulation was observed was observed in the *tlp2* or *tlp4* mutants when tested in the HAP procedure (data not shown). As the *tlp2* and *tlp4* mutants appeared non-responsive in the HAP procedure a small modification was made to the original methodology. The *tlp* mutants appeared to show poor growth on Mueller-Hinton agar plates which often meant that there were not enough cell numbers to perform the HAP procedure. Thus, the small modification was made to the HAP method where by miniature Petri-plates (60 by 15 mm), which required a lower inoculum, were used to perform the HAP assay. These miniature plates had been previously used in the laboratory previous to this study to perform the HAP procedure successfully (Personal communication, Julie Turner). Furthermore, as the turbid zones observed in the *tlp1*Δ using the original HAP procedure lacked definition in the edges it was necessary to adjust the procedure so that accurate quantitative data could be obtained for the *tlp* mutants in future assays. The results showed that upon switching to the smaller Petri plates the clarity and definition of the turbid zones of bacterial accumulation around the HAPs had improved substantially (Figure 5.5). Although the results obtained had not been verified due to time constraints, initial data for the *tlp1*Δ is presented in Figure 5.5. The results in Figure 5.5 (a-f), showed that this time positive chemotactic responses were detected towards all of the *C. jejuni* putative chemoattractants including serine (Figure 5.5 (d)) and pyruvate (Figure 5.5 (e)), which had previously shown an altered response in the HAP assay relative to the wild-type MV (Figure 5.3 (b and h)). Upon measuring the radius of the zone of bacterial accumulation around the plug containing L-serine, there was still a small reduction in this zone in the *tlp1*Δ (mean diameter= 0.7 cm; Figure 5.5 (d)) compared to the wild-type MV (mean diameter =0.80 cm; data not shown). Although no notable response could be observed in the *tlp2*Δ using the smaller Petri plates

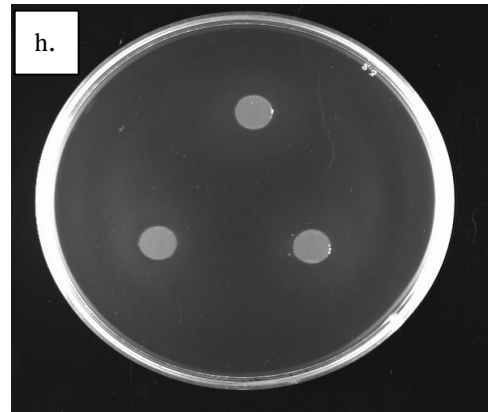
(Figure 5.6) a possible chemorepellent effect towards α -ketoglutarate was observed in the *tlp4* Δ (Figure 5.7) which had not been observed previously using the original HAP procedure.

Figure 5.3. Chemotactic responses in the *tlp1* mutant towards a range of putative chemoattractants. A suspension of wild-type *C. jejuni* motile variant (MV) and *tlp1Δ* cells (5×10^9 CFU/ml; panels a-k) in PBS agar (0.4%) were added to several petri plates (90 by 45 mm) containing triplicate Hard-Agar Plugs. Each substrate was tested at 100 mM concentration (excluding the PBS control, panel k). All plates were incubated for 20 hours at 37°C under microaerobic conditions. Figure shows an indicative from one assay (assay only performed once).

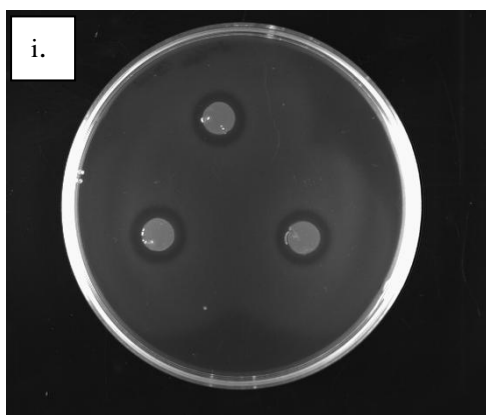




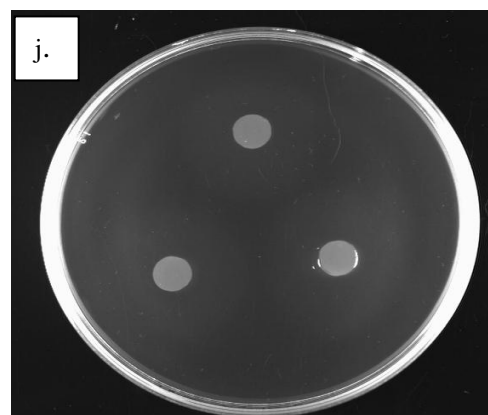
C. jejuni MV (pyruvate)



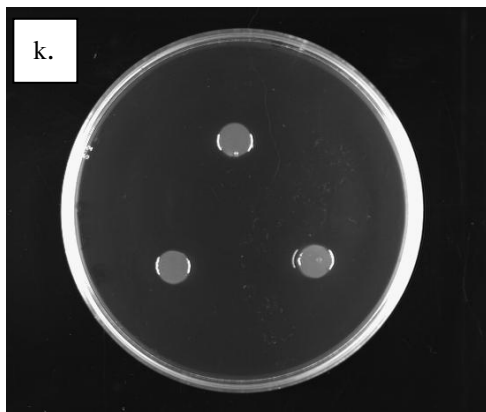
tlp1Δ (pyruvate)



C. jejuni MV (α -ketoglutarate)



tlp1Δ (α -ketoglutarate)



C. jejuni MV (PBS)

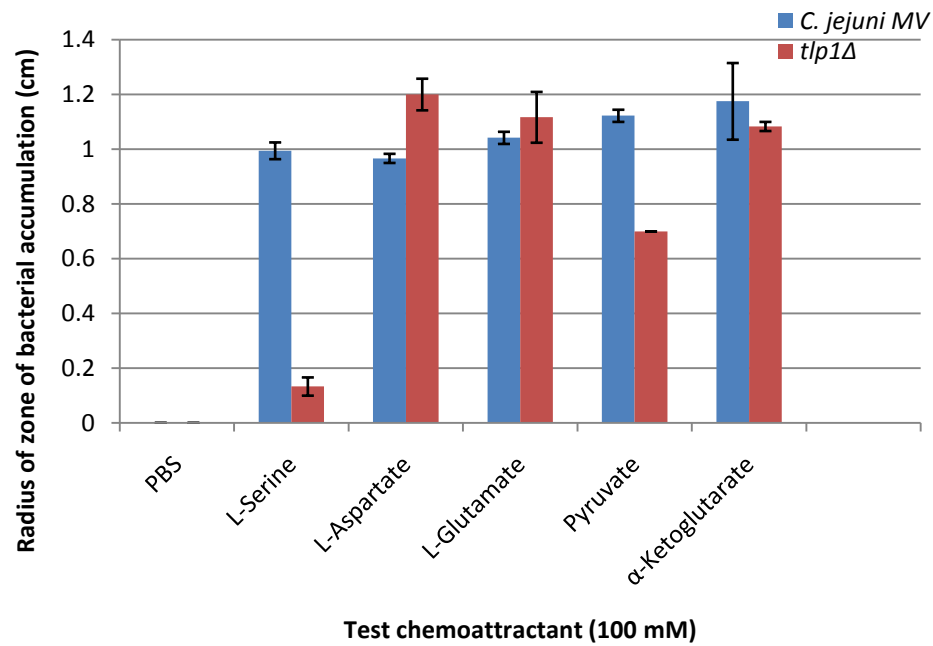
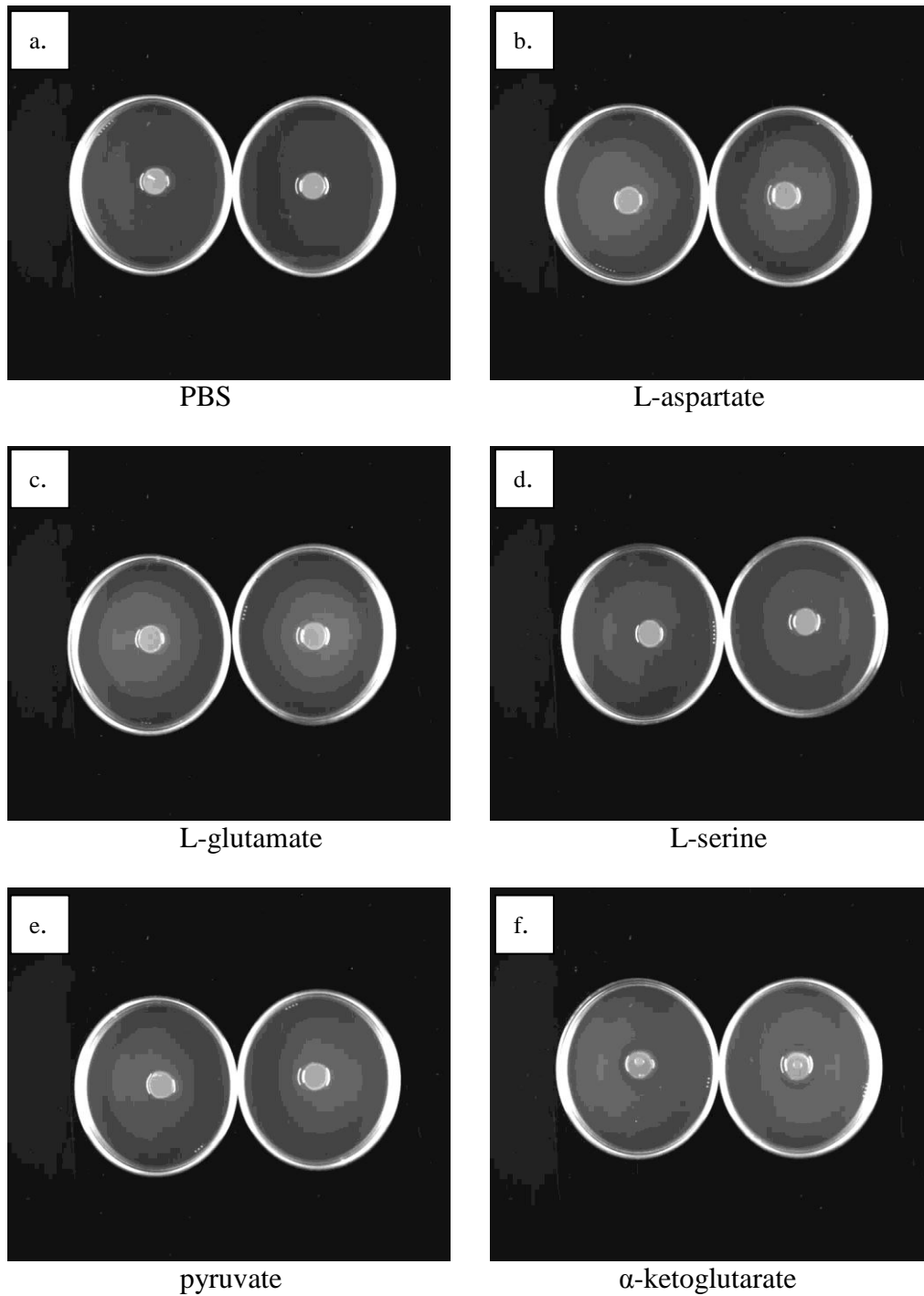


Figure 5.4. Determining chemotactic responses in the wild-type MV strain and the *tlp1* mutant using the Hard-agar plug (HAP) assay. Responses in the *C. jejuni* *tlp1*Δ were compared with those seen in the wild-type motile variant (MV). The radius of the zone of accumulation (cm) around HAPs containing the different *C. jejuni* putative chemoattractants is shown. All putative chemoattractants were tested at 100 mM concentration (excluding the phosphate-buffered saline (PBS) solution). Results presented here are the means from a single experiment and all plugs were tested in triplicate (n=3). Error bars show standard error.

Figure 5.5. Chemotactic responses in the *tlp1* mutant towards a range of putative *C. jejuni* chemoattractants. A suspension of *tlp1* Δ cells (panels a-f) in PBS agar (0.4%) were added to several miniature Petri plates (60 by 15 mm) containing Hard-agar plugs (n=2), containing the test substrate (100 mM; excluding the PBS control, photo a). This experiment was performed only once. All plates were incubated for 20 hours at 37°C under microaerobic conditions.



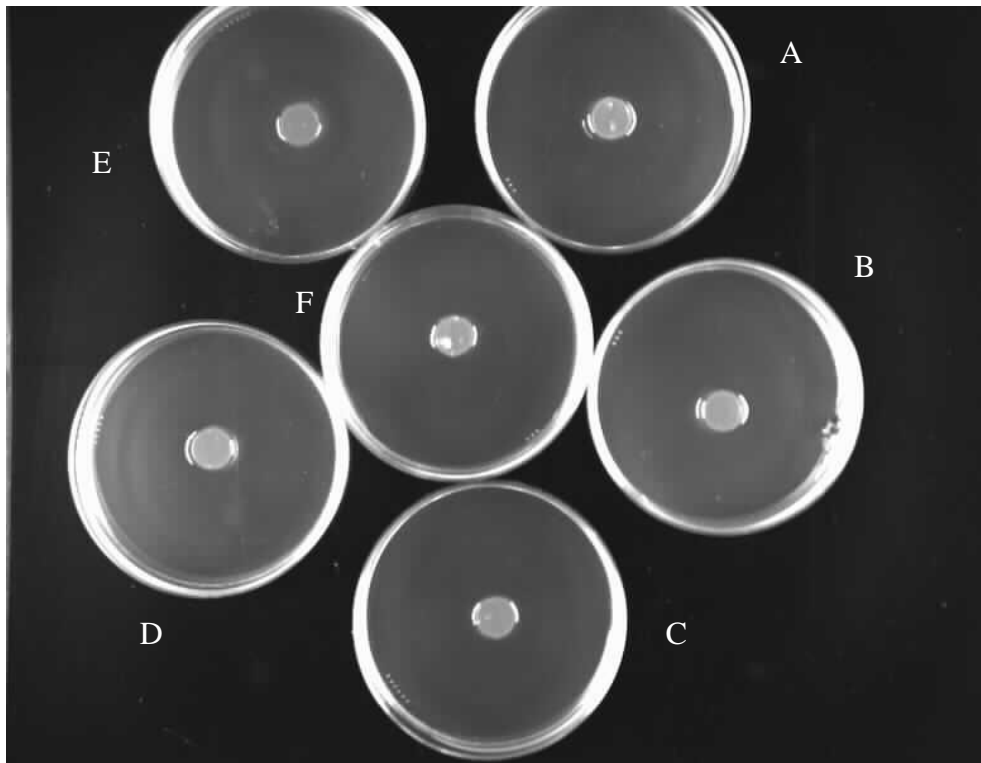


Figure 5.6. Chemotactic responses in the *tlp2* mutant towards a range of putative *C. jejuni* chemoattractants. A suspension of *tlp2Δ* cells (5×10^9 CFU/ml) in PBS plus 0.4 % agar was added to several miniature Petri plates (60 by 15 mm) containing a single Hard-agar plug (HAP; n=1) containing the test substrate. Test HAPs contained the following: (A) L-glutamate; (B) L-serine; (C) L-aspartate; (D) pyruvate; (E) α -ketoglutarate and (F) phosphate-buffered saline. Each test chemical was tested at a concentration of 100 mM (excluding the PBS control). This experiment was performed only once. All plates were incubated for 20 hours at 37°C under microaerobic conditions.

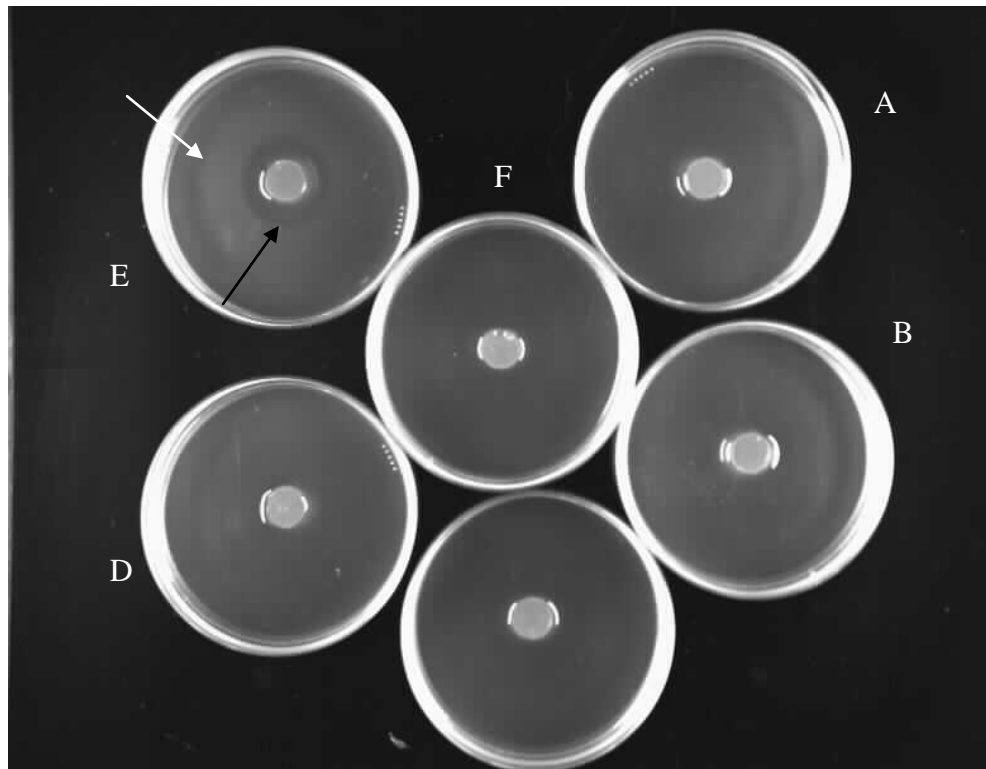


Figure 5.7. Determining chemotactic responses in the *tlp4* mutant towards a range of putative *C. jejuni* chemoattractants. A suspension of *tlp4Δ* cells (5×10^9 CFU/ml) in PBS plus 0.4 % agar was added to several miniature Petri plates (60 by 15 mm) containing a single Hard-agar plug (HAP; $n=1$) containing the test substrate. Starting from the top going clockwise round each test HAP contained the following: (A) L-glutamate; (B) L-serine; (C) L-aspartate; (D) pyruvate; (E) α -ketoglutarate and (F) phosphate-buffered saline (central Petri plate). Each test chemical was tested at a concentration of 100 mM (excluding the PBS control). All plates were incubated for 20 hours at 37°C under microaerobic conditions. This experiment was performed only once ($n=1$). The black arrow shows an area of clearing around the HAP containing α -ketoglutarate and the white arrow indicates the edge of the zone of bacterial accumulation.

5.3. Discussion

5.3.1. The requirement of the Tlps in colonisation of the host

The *tlp1* (*cj1506c*), *tlp2* (*cj0144*) and *tlp4* (*cj0262c*) mutants all showed an altered phenotype when assessed in the swarm assay. This data indicates that mutation in a Tlp is having a wider-scale effect on chemotaxis than initially predicted. The data for *tlp1Δ* in the HAP assay described in this dissertation has demonstrated that the *tlp1Δ* mutant shows an altered chemotactic response toward L-serine, pyruvate and L-aspartate. In fact upon reexamination of the *tlp1Δ* in a modified version of the HAP assay, chemotaxis to only L-serine was found to be affected. The importance of the Tlps in the colonisation of the intestine had already been demonstrated prior to the Tlp studies detailed in this dissertation. Tlp1 (Cj1506c), Tlp4 (Cj0262c) and Tlp10 (Cj0019c) were all shown to be essential for successful colonisation of the chick gastrointestinal tract (Hendrixson and DiRita, 2004; Hartley-Tassell *et al.*, 2010). Since colonisation of the intestine is a necessary prerequisite for both commensalism and pathogenesis the Tlps must be an important sensory mechanism in intestinal colonisation by *C. jejuni*. The *tlp1* isogenic mutant and complement, both of which were constructed in the work detailed in this dissertation, went onto be analysed by our collaborators both *in vivo* and *in vitro* studies (Hartley-Tassell *et al.*, 2010). The aim of these studies was to characterise the role and ligand-binding specificity of the Tlp1 chemoreceptor in colonisation of the host. Chemotaxis assays similar to those described in this dissertation were also employed in the study reported by Hartley *et al.* (2010). The phenotype of the *tlp1* isogenic mutant in these chemotaxis assays will be analysed and compared with those seen from testing the *tlp1* mutant in the assays developed in this work and will be the focus of this discussion.

5.3.2. Phenotypes of the *tlp* mutants in the swarm plate assay

The swarm assay is a qualitative chemotaxis assay that can quickly establish whether mutation in a *tlp* has had a consequence on the chemotactic behaviour of *C. jejuni*. The *tlp* mutants, namely *tlp1*, *tlp2* and *tlp4* all showed an altered phenotype in the swarm assay. Interestingly the *tlp1* mutant swarmed significantly further than the wild-type (Figure 5.1 (b)). Such a phenotype has been observed previous to this study, namely in a *cheR* mutant constructed in *C. jejuni* NCTC 11168 (Bridle, MPhil thesis). The *tlp2* mutant showed a peculiar phenotype in the swarm assay (Figure 5.1 (e)), which showed the edge of the swarm being irregular in shape. The *tlp2* mutation appears to affect the way the cell population moves in the direction of increasing nutrients. A phenotype such as this had been also been observed previously in a *cheB* mutant (Bridle, MPhil thesis). Due to time constraints, it was not possible to make a detailed examination of the growth rates of the *tlp2* or *tlp4* mutants in order to establish if the phenotypes are due to a growth defect alone. The *tlp4* mutant which is shown in Figure 5.1 (f) swarmed significantly less than the wild-type (Figure 5.2). This phenotype possibly indicates a bias towards a tumbling motion which is determined by CW rotation of the flagella. Subsequently this would not enable the bacteria to successfully swarm through the porous holes in the agar by smooth swimming but instead the cells would tumble at a higher frequency than would be normally expected in wild-type *C. jejuni* cells. In the absence of a chemotactic stimulus, the swimming phenotype observed in the wild-type MV is random with frequent switching between random tumbling and smooth swimming (Stock and Re, 1999).

The *C. jejuni tlp1* mutant strain created in this work (RS01Tlp1Mut; Chapter 3) was sent to our collaborators in Australia who also tested the mutant in the swarm

assay. Their assessment of the *tlp1* mutant on semi-solid Brucella agar was that it demonstrated significantly increased swarming ($22.2 \text{ mm} \pm 2.8$; $P < 0.05$) compared to the wild-type MV ($19.2 \text{ mm} \pm 2.2$). The swarm plate assay was performed using a similar method to the one described in this dissertation and similarly in this work the *tlp1* mutant (Figure 5.2; $7.531 \text{ cm} \pm 0.078$, $P < 0.0001$) also swarmed significantly further than the wild-type (Figure 5.2; $6.7 \text{ cm} \pm 0.094$). Due to time constraints it was not feasible for us to test the *tlp1* mutant for any alterations in growth relative to the wild-type strain. However, our collaborators were able to and found that the *tlp1Δ* did not show any significant difference in growth rate (examined over 48 hour period; Hartley-Tassell *et al.*, 2010). Moreover, no gross differences in growth were observed with *tlp2* and *tlp4* when generating inoculum for experiments (data not shown). One of the drawbacks of the swarm assay is the limitation in the information it can provide regarding the effect of mutation in a *tlp* gene on flagella rotation. Thus using techniques such as video tracking to monitor the movement of individual cells it may be possible to determine the effect of mutation in individual *tlp* genes on flagella rotation. It would also be worth using video tracking of cells to determine if there is a bias in flagella rotation in the presence of putative chemoattractant and chemorepellents. The alteration in the swarming phenotype in the *tlp* mutants suggests that the Tlps are required for wild-type chemotaxis.

5.3.3. Determining the specificity of the Tlp receptors

The Hard-Agar Plug (HAP) assay was employed in this work to determine the ligand specificities of the Group A Tlp receptors. Prior to using the HAP assay to assess the phenotypes of the *tlp* mutants, the assay had been optimised using the wild-type MV strain (chapter 4, section 4.3.3; Hugdahl *et al.*, 1988). The chemicals screened in the

HAP procedure were putative chemoattractants that had been used successfully previous to this work to determine chemotactic responses in *C. jejuni* (Hugdahl *et al.*, 1988; Quinones *et al.*, 2009). Zones of bacterial accumulation were found around the plugs supplemented with L-serine, L-aspartate, L-glutamate and pyruvate for the wild-type MV (Figure 5.3). However, it was unclear whether α -ketoglutarate was inducing a chemorepellent effect with *C. jejuni* MV as an area of clearing was observed around the HAP (Figure 5.3 (i)). According to the Hugdahl *et al.* (1988) methodology, when a zone of clearing is found around a HAP, which is then subsequently proceeded by a dense zone of bacterial accumulation, this indicates a chemorepellent effect. Thus, it may be that α -ketoglutarate is a chemorepellent in *C. jejuni*. Alternatively, this area of clearing around the HAP could reflect the concentration of α -ketoglutarate being toxic, although a less defined border would have been expected. This could be confirmed by screening α -ketoglutarate over a range of lower concentrations than the concentration used in the HAP assay (100 mM). If the same response is observed in the wild-type MV at a lower concentration of this substrate then this would verify that α -ketoglutarate is indeed a chemorepellent for *C. jejuni* NCTC 11168.

The zone of bacterial accumulation around plugs containing L-serine, L-aspartate, pyruvate and α -ketoglutarate in the *tlp1* Δ mutant appeared notably different from the wild-type MV (Figure 5.3). The zone of accumulation around plugs containing putative *C. jejuni* chemoattractants for the *tlp1* Δ appeared diffuse, with responses extending over a centimeter (except for L-serine and pyruvate; Figures 5.4 and 5.5). This made it difficult to obtain accurate measurements of chemotaxis responses for the *tlp1* Δ . In addition, chemotactic responses in the *tlp2* and *tlp4* mutants were absent. Thus, the original HAP procedure was modified and

subsequently a more dense and narrow area of bacterial accumulation was observed in the *tlp1* Δ mutant (Figure 5.5.). The edge of the zone of bacterial accumulation surrounding the plug was clearly defined enabling accurate measurements of the radius of the zone to be measured. An area of clearing was observed around the plug containing the α -ketoglutarate (Figure 5.5 (f)) in the *tlp1* Δ mutant, which had not been seen in the previous version of the HAP assay (Figure 5.3 (j)). More significantly, a response towards α -ketoglutarate was detected in *tlp4* Δ which had not been observed previously (Figure 5.7). All of the chemotactic responses in *tlp1* Δ towards L-aspartate, L-glutamate, pyruvate and α -ketoglutarate appeared similar to the responses seen in the wild-type MV (data not shown for the wild-type MV). However, there was a slight, but notable, reduction in the zone of bacterial accumulation around the L-serine plug in the *tlp1* Δ mutant (0.7 cm, mean diameter; Figure 5.5 (d)) versus wild-type MV (0.8 cm, mean diameter; data not shown). The HAP procedure developed in this study will need to be optimised using the *tlp* mutants similarly to how the assay was optimized using the wild-type MV (chapter 4, section 4.3.3) before the ligand-binding specificity of individual Tlps can be determined as the assay needs to be able to generate reproducible data regarding chemotactic responses in *tlp* mutants. Once a clear and reproducible chemotactic response phenotype has been established in the Tlp mutants, complementation can be assessed using the assay to confirm the genetic locus responsible for the mutant phenotype. If chemotactic responses in individual *tlp* mutants, as determined in a reproducible HAP assay, towards several chemoattractants were found to be disrupted when compared to the wild-type MV (Figure 5.3), then this could suggest that there may be redundancy in Tlp responses. The Group A Tlps contain different periplasmic ligand-binding domains which indicates that, similar to the MCPs in *E. coli*, the Tlps

in *C. jejuni* are also likely to respond to different signals (Marchant *et al.*, 2002) and are therefore unlikely to show redundancy in ligand binding.

The HAP procedure was used in a modified form by Hartley-Tassell *et al.* (2010), but the researchers of this study found that for the *tlp1*Δ mutant significantly fewer bacteria were found around the plug containing aspartate compared with the wild-type MV. The presence of the bacteria around the plug was verified by performing viable counts as well as fluorescent based microscopic detection (Hartley-Tassell *et al.*, 2010). In contrast, the data for *tlp1*Δ in the HAP assay described in this dissertation showed that the *tlp1*Δ mutant showed an altered chemotactic response to L-serine, pyruvate and L-aspartate (Figure 5.3). Moreover, upon reanalysis of the *tlp1*Δ in a modified version of the HAP assay, the chemotactic response to only L-serine was found to be affected (Figure 5.5). Attempts were made to optimise the HAP assay using the *tlp1* mutant where chemotactic responses were tested to only individual plugs. The data showed that only the response to L-serine to be affected (data not shown). The difference in results obtained for *tlp1*Δ may be due to the alterations made to the original HAP procedure (Hugdahl *et al.*, 1988). However, you would not expect to see such a significant difference in result from testing the same mutant in a slightly modified chemotaxis assay. Moreover, the difference in specificity of the Tlp1 receptor between the studies reported in this dissertation and those by Hartley *et al.* (2010) could also be a direct result of difference in the strain background of NCTC 11168 strain used in this work and by our collaborators.

Upon discussion as part of our collaboration in the study reported by Hartley-Tassell *et al.* (2010) it is apparent that they made the following modifications to the HAP procedure. Firstly, the bacteria were suspended in 0.1% bacteriological agar whereas 0.4% PBS media was used here in the work described in this dissertation.

While it is difficult to comprehend how the assay could be carried out technically with such a low agar concentration, it is possible that the difference in viscosity may affect chemotactic motility (Szymanski *et al.*, 1995). Furthermore, the Petri plates containing the HAPs were incubated for up to 12 hours at 37°C. As the HAP assay was not performed under microaerobic conditions it makes it difficult to determine whether the results being observed are being differentially affected by aerotaxis due to the presence of different oxygen gradients (Hartley-Tassell *et al.*, 2010). In the original HAP assay the chemotactic behaviour of two faecal isolates of *C. jejuni* (74C and 108C) was determined in the presence of a range of compounds which included a variety of organic acids, mucin and bile and the components thereof. It is important to establish chemotactic responses in *C. jejuni* towards a range of substrates before the ligand-binding specificity of the Tlps can be determined with complete certainty.

5.3.4. Testing the *tlp1* isogenic mutant ($\Delta cj1506c::cat$) and complementing mutant *in vitro* and *in vivo* models of colonisation

The *tlp1* mutant showed an 11-fold reduction (statistically significant) in colonisation ability compared to the wild-type strain in an avian model. Moreover the *tlp1* complemented mutant demonstrated a further reduction in colonisation potential compared to the wild-type strain (24-fold reduction) and the *tlp1* isogenic mutant (2.2-fold reduction). *In vitro* studies revealed adherence of the *tlp1* mutant to intestinal Caco-2 human intestinal cells was significantly higher compared to the wild-type (Hartley-Tassell *et al.*, 2010). The numbers of adherent bacteria for the *tlp1* mutant were 5×10^6 compared to 5×10^5 for the 11168 wild-type. Furthermore, the *tlp1* isogenic mutant also showed increased invasion compared to *C. jejuni* NCTC 11168 wild-type cells (where 2.5% of the adhered *tlp1* mutant cells were able to

invade the Caco-2 cells versus only 1.5% of the adhered wild-type *C. jejuni* cells).

The *tlp1* complement demonstrated no significant difference in adherence or invasion compared with the wild-type.

Real-time PCR showed elevated levels of expression of the *tlp1* gene was detected in the complemented mutant compared with the wild-type and *tlp1* mutant (Hartley-Tassell *et al.*, 2010). There are three highly conserved ribosomal RNA (rRNA) clusters present on the *C. jejuni* chromosome. It is therefore feasible for more than one homologous recombination to take place between the three rRNA sequences present on the complementing construct and the *C. jejuni* chromosome. It would have been advantageous to identify clones which contained a functional copy of the *cj1506c* gene in each of the three rRNA clusters. The expression of *tlp1* could then be analysed by real time PCR to determine whether the levels of expression of the *tlp1* gene are comparable to the wild-type, or are in fact increased or vice versa. The expression of the *cj1506c* gene was significantly elevated in the *tlp1* complementing mutant. This may have been due to the *tlp1* promoter element being cloned along with the gene. Future work would require cloning the coding sequence for the *cj1506c* gene without its promoter so that the expression of this gene could be regulated solely by the kanamycin gene promoter. More importantly, this may help to match the normal expression levels of the wild-type copy of the *cj1506c* gene. The study by Hartley-Tassell *et al.* (2010) found no significant difference in growth rates between the *tlp1* mutant ($\Delta cj1506c::cat$), complemented mutant (wild-type copy of *cj1506c* cloned into pRRK-poly; pRS12) and wild-type *C. jejuni* cells. This data is particularly important when interpreting the results produced from testing the *tlp1* mutant/complemented mutant in chemotaxis assays. Being able to differentiate between chemotactic phenotypes and growth response is a necessity. Unfortunately,

due to time constraints it was not feasible to test deletional mutants created in *tlps* 2-4 in a growth assay, which would have assessed for any possible alterations in growth rates.

5.3.5. Alternative chemotaxis assays

An attempt was made in this work to develop a chemotaxis assay on a microscope slide (data not shown). Viable campylobacters were stained using the compound 3', 6'-diacetyl fluorescein (FDA) that is rapidly hydrolysed by the bacteria to fluorescein which is then stored intracellularly (Brunius, 1980). Similar to the capillary tube assay developed by Adler (1973), campylobacters were spotted in the centre of a microscope slide onto which a cover slip was placed. Five µl of L-aspartate was added to one end of the cover slip and then the bacteria were examined under the microscope to see if their movement was biased towards the side of the cover slip where the putative chemoattractant had been added. Phosphate-buffered saline was used as a negative control for comparison. Although the campylobacters had excellent motility at the start of the experiment (checked microscopically), unfortunately they lost motility within 15 minutes. Due to the rapid loss of motility, attempts at further developing this technique were halted.

Chapter 6. Cloning, expressing and purifying different domain structures from the Tlps

6.1. Introduction

6.1.1. Protein domains of interest in the Group A transducer-like proteins (Tlps)

Marchant *et al.* (2002) classified the Tlp (for transducer-like proteins) in *Campylobacter jejuni* NCTC 11168 into groups according to shared domain structures. The focus of much of this study has primarily been on one family of chemoreceptors in *C. jejuni*, which is comprised of Tlp1, Tlp2, Tlp3, Tlp4, Tlp7 and Tlp10; collectively referred to as Group A. Similar to the methyl-accepting chemotaxis proteins (MCPs) of *Escherichia coli*, the core components of the Group A Tlps of *C. jejuni* consist of a periplasmic, transmembrane and cytoplasmic region (Wadhams and Armitage, 2004; Falke *et al.*, 1997). It is the presence of a periplasmic and transmembrane region in the Group A receptors that suggests that these receptors are important in how *C. jejuni* monitors and responds to the environment. An attempt was made here to clone, express and purify domains in the Tlp1 receptor of NCTC 11168. There were domains within the Tlp1 receptor that were of particular interest in this work. These were the N-terminal periplasmic ligand-binding domain (PLD) and highly conserved signalling domain (HCD). Bioinformatic analysis of the amino acid sequence encoding the PLD in Tlp1 of *C. jejuni* revealed that this region is highly variable and is not homologous to PLDs present in other bacteria. Furthermore, the PLD is unique in each Tlp in *C. jejuni* indicating that the Tlps have different ligand-binding potential. This is indicated in Figure 6.1. There is some homology in the

ligand-binding domains of the Group A Tlps in *C. jejuni* and TlpA and TlpC in *Helicobacter pylori* (Tomb *et al.*, 1997). The Tar receptor in *E. coli* is the best characterised chemoreceptor to date (Moual and Koshland, 1996; Levit *et al.*, 1998; Lux and Shi, 2004). There is a wealth of information available regarding the structure and function on the enteric MCPs. X-ray crystallography has revealed that the extracellular ligand-binding domain in MCPs of the enteric bacteria forms an anti-parallel four-helix bundle (Milburn *et al.*, 1991; Yeh *et al.*, 1993). However, there has been no structural or functional work performed on the Tlps in *C. jejuni*, although, the N-terminal PLD of Tlp1 has been purified and expressed previous to this work (Hartley-Tassell *et al.*, 2010; Appendix 1). The purified protein was used to determine the ligand-binding specificity of the Tlp1 (Cj1506c) receptor in NCTC 11168. The results from this study will be analysed in the discussion to this chapter.

6.2. Do the Tlps localise to the poles of the cell in *C. jejuni* similar to other bacteria and archaea?

Monomers of MCPs in *E. coli* form stable homodimers (dimer-dimer interactions) in the cytoplasmic membrane. It is reported that these homodimers are further organised and packed into groups of three (i.e. trimer of dimers) to produce what appears to resemble a polar lattice at the poles of the cell (Kim *et al.*, 1999; Lamanna *et al.*, 2005). This phenomenon was first observed in *Caulobacter crescentus* (Alley *et al.*, 1992) and was then discovered in *E. coli* (Maddock and Shapiro, 1993). The clustering of MCPs at the cell poles has since been demonstrated for not only *Bacillus subtilis* and *Rhodobacter sphaeroides* but in all bacteria and archaea tested to date (Kirby *et al.*, 2000; Harrison *et al.*, 1999 Gestwicki *et al.*, 2000). It was therefore an imperative in this study to establish whether the same phenomenon occurred in *C.*

jejuni. The carboxyl-terminal HCD, as opposed to the PLD, is highly conserved amongst bacteria. The HCD in Tlps1-4 of *C. jejuni* demonstrate extensive sequence homology with the signalling domain of the *E. coli* Tar receptor (Moual and Koshland, 1996). In fact the C-terminal signalling domain is one of the best conserved domains present in bacteria. It is important to note that although the NCTC 11168 genome contains very few repeats in the sequence (only a total of four; Parkhill *et al.*, 2000) the C-terminal signalling domain in Tlp2, Tlp3 and Tlp4 is identical (amino acid sequence). This region in Tlp2, Tlp3 and Tlp4 encoding the HCD was also purified along with the HCD and PLD of Tlp1. Thus, once the HCD of Tlp1 and Tlp2 to 4 had been cloned, expressed and purified, the protein would be used to generate a polyclonal antibody. A polyclonal antibody raised to the C-terminal signalling domain in Tlp1 and Tlp2 to 4 would determine for the first time, whether the Tlps cluster at the poles of the *C. jejuni* cell. Antibodies raised to the cytoplasmic signalling region of the MCPs in other bacteria including *B. subtilis*, have been used successfully previous to this work (Kirby *et al.*, 2000). The reason for producing two separate antibodies to the HCD in the Tlps was to prevent cross-reactivity occurring between the HCDs in each of the Tlps domain structures. Producing antibodies to individual receptors will also enable comparisons to be made between the results obtained for each antibody.

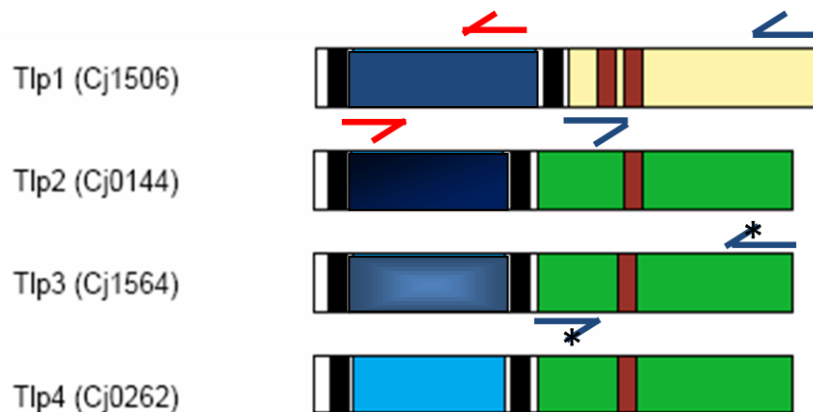


Figure 6.1. Figure showing the arrangement of domains in Tlp1-4. The coloured boxes are as follows: the shaded navy boxes, show the different periplasmic ligand-binding domain in Tlps 1 to 4; the black box, indicates the transmembrane regions; the yellow box, is the signalling domain; the green box, is the signalling domain with identical sequence (amino acid) and the brown boxes, are the proposed methylation sites. The arrow heads \rightarrow/\rightarrow indicates the domains in the Tlps to be cloned, expressed and purified. The * indicates the signalling domain with identical amino acid sequence (Figure adapted from Marchant *et al.*, 2002).

6.3. Protein purification strategies

Affinity tags enable the efficient purification of a desired protein and can help obtain a large yield of recombinant protein. The gene encoding the target protein is translationally fused with a protein or peptide based tag. The tag then aids the subsequent isolation of the target protein from an otherwise mixed batch of heterogeneous proteins. There are advantages and disadvantages for using any of the commercially available affinity tags, a few of which have been highlighted in Table 6.1 (Waugh, 2005). The majority of tags are available in two forms, either as a short peptide sequence or a polypeptide. Examples of some commonly used affinity tags

are: GST (glutathione S-transferase), MBP (maltose-binding protein) and Hexahistidine (His) tag.

Glutathione S-transferase (GST) is a 26 kDa protein that is often used to create GST tagged protein fusions. The tagged proteins can then be purified directly from bacterial cell lysates by affinity chromatography using immobilized glutathione. A GSTrap column was used to perform the purification of GST tagged proteins (GE healthcare; section 2.14.1). The GST coding sequence is present in the pGEX series of vectors (Table 2.2, materials and methods). The vector map of the pGEX-4T-1 vector is shown in Appendix 4; Figure 4.1 (a). The gene encoding the target protein must be in the same reading frame as the gene encoding the GST moiety. The tag can then be cleaved off once the fusion protein had been purified. The GST tag can be removed by cleaving at one of three specific protease recognition sites which are found located immediately upstream of the multiple cloning site (mcs).

Hexahistidine (His; six histidine repeats) is also a frequently used peptide tag for protein purification. The His-tag binds to immobilised transition metals such as nickel ions (Ni^{2+}) with a high affinity. Applying bacterial lysates containing the His-tagged protein onto a HisTrap column (GE healthcare) pre-packed with nickel sepharose enables high-throughput purification of a desired protein. The pLEIC-05 plasmid obtained from the Protein Expression Laboratory (University of Leicester) was used to create an in-frame fusion with the region of the *tlp1* gene encoding the PLD and the His peptide sequence (Appendix 4; Figure 4.1 (b)). The PLD of Tlp1 was cloned into pLEIC-05 plasmid (Appendix 4; Figure 4.1 (b)). The affinity tags selected for purification of the periplasmic and cytoplasmic domains in the *C. jejuni* Tlps were His and GST, respectively. The GST affinity tag was used in this work to create GST tagged protein fusions with the HCD of Tlp1 and Tlp2 to 4.

Fusion partner/Affinity Tag	Advantages	Disadvantages
GST	Good translation initiation. Inexpensive resin. Mild elution conditions.	High metabolic burden on cells. Poor solubility. Formation of inclusion bodies.
His	Low metabolic burden on cells. Inexpensive resin.	Not as specific as some of the other fusion tags.
MBP	Good translation initiation. Inexpensive resin. Mild elution conditions. Good solubility.	High metabolic burden on cells.
STREP	Low metabolic burden on cells. Excellent specificity.	Expensive resin.

Table 6.1. The advantages and disadvantages for using different protein or peptide based fusion tags. All the tags detailed in the table above are commonly used to aid in the purification of a desired protein. GST, glutathione S-transferase; MBP, maltose-binding protein; His, hexahistidine; STREP, streptavidin-binding peptide (Waugh, 2005).

6.4. Results

6.4.1. The proposed structure and function of the Group A Tlps

It is proposed that there are two transmembrane segments in each Tlp belonging to the Group A chemoreceptor family (Marchant *et al.*, 2002). The first TM domain is positioned just before the start of the periplasmic ligand-binding domain (PLD) whereas the second (TM2) is found immediately after. The presence of a HAMP (histidine kinase, adenyl cyclase, methyl-accepting chemotaxis and phosphatase) relays the signal of attractant binding to the C-terminal highly conserved signalling domain (HCD). The HCD is multi-functional. This domain contains conserved glutamate and glutamine residues which are susceptible to methylation and demethylation by the chemotaxis proteins CheR and CheB, (methyltransferase and methylesterase, respectively). CheR and CheB are part of the adaptation pathway in *C. jejuni*. Furthermore, the HCD provides a docking domain for CheA and CheW to bind. Collectively, the HCD, CheW and CheA form a ternary complex in the cytoplasm (Kim *et al.*, 1999).

It is important to highlight that not all strains of *C. jejuni* contain a complete set of the Group A Tlps (Korolik and Ketley, 2008). In fact only the Tlp1 receptor is universally present in all 16 strains of *C. jejuni* examined to date (Korolik and Ketley, 2008). The Tlp1 receptor also appears to be best conserved along with Tlp10, showing 98-100% amino acid sequence identity (Korolik and Ketley, 2008). The remaining Group A Tlps (excluding Tlp7, which is proposed to be a pseudogene at least in NCTC 11168), are less well conserved (92% amino acid homology in a few strains of *C. jejuni*). The Tlp1 receptor does however show less sequence homology along its length when compared with different strains of *Campylobacter*. For example, homologues of the Tlp1 receptors in *Campylobacter fetus* only showed a

56% match and *C. upsaliensis* shared 64% coverage. Moreover, a blast search performed using the amino acid sequences for Tlp1, Tlp2, Tlp3 and Tlp4 showed that most of the hits were to the C-terminal portion, which corresponds to the HCD.

6.4.2. Bioinformatic analysis of the secondary structures of the Tlps

Campylobacter genome sequence data was obtained from <http://xbase.bham.ac.uk/campydb/>. All genome sequences were imported into the Clone Manager Professional Suite for further analysis (Scientific and Educational Software, 2005, version 8).

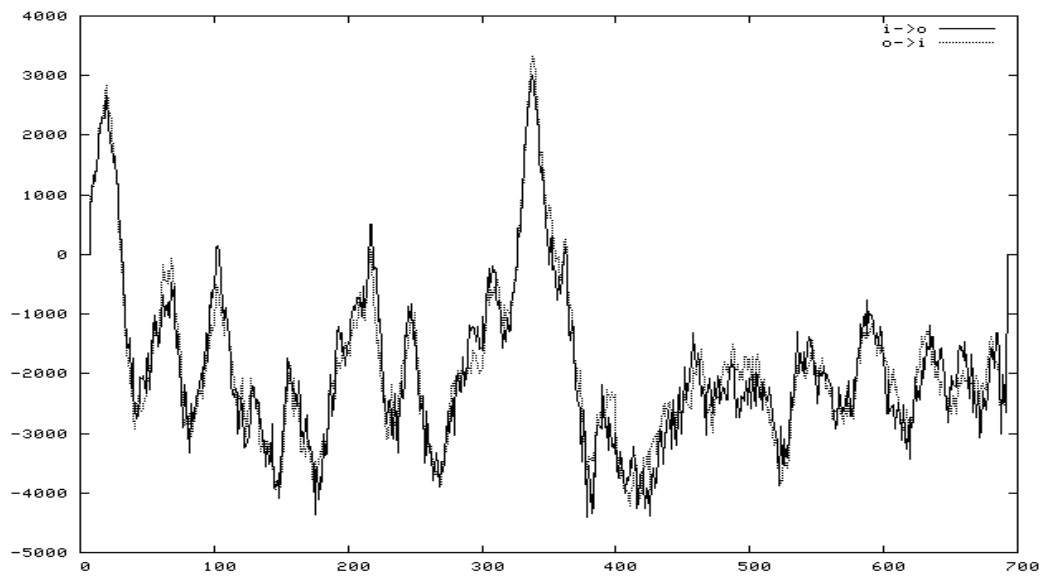
When trying to predict the function of the Tlps, the amino sequence of the Tlp under investigation was searched using the Pfam database (<http://pfam.sanger.ac.uk/>). The Pfam database provided predictions for the secondary structures present in the Tlp and information on their position within each Tlp. This database also indicated the location of the two transmembrane domains present in each of the Tlps. Marchant *et al.* (2002) had already provided some information regarding the overall domain organisation in the Tlps and also the likelihood of there being two transmembrane domains present in each of the Tlps. Primers were designed using the clone manager software specifically to amplify by PCR the HCD present in Tlp1 and Tlp2 to 4. It was important that the second transmembrane domain in each of the Tlps was not amplified along with the HCD (TMpred programme; www.cbs.dtu.dk/cgi-bin/nph).

The TMpred programme predicts the presence of transmembrane regions within your protein of interest and their orientation. The algorithm is based on the statistical analysis of TMbase; which is a database compiled of naturally occurring transmembrane proteins (Hofmann and Stoffel, 1993). The predictions are made using a combination of weight matrices and scoring. A search was made using the amino acid sequence of the Tlps from which domains were to be purified (Tlp1, Tlp2, Tlp3 and Tlp4). The TMpred programme searches for the presence of hydrophobic

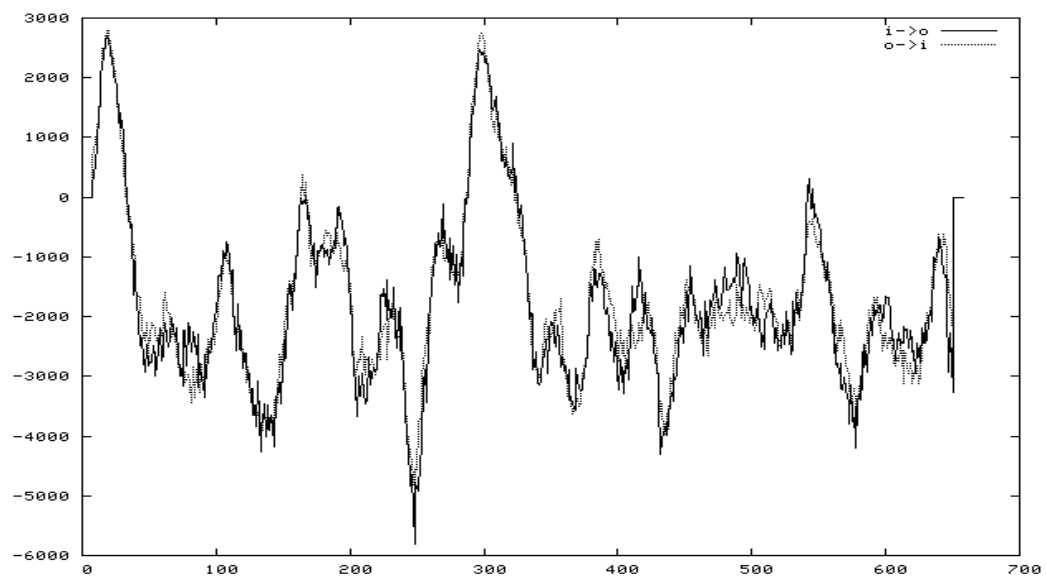
residues within the search protein and then calculates the location of possible transmembrane helices. The results from the search were received in the form of a histogram (as shown in Figure 6.2) along with a table that has assigned a score for each predicted transmembrane region (scores of >500 are only considered significant). The programme also provides a score for the probability of the orientation of each of the transmembrane helices. For example a score is assigned for the likelihood that the helix is being directed “in to out” (cytoplasm to the periplasm) and “out to in” (periplasm back into the cytoplasm). The orientation which has the highest score is an indication of the direction of the transmembrane domain. More specifically, the orientation of the transmembrane domains is deduced either from annotation of the orientation itself or from taking into consideration features such as glycosylation or phosphorylation sites. Only those entries with consistent annotations have an orientation assigned to them.

The Tmpred database was also used when designing primers to amplify the periplasmic region of Tlp1. The NCBI “conserved domain” search engine was used to find the conserved domains present in the Tlps (<http://www.ncbi.nlm.nih.gov/Structure/cdd>). The approximate location for the transmembrane regions in the coding region for each Group A Tlp is shown in Table 6.2. The data collated from the Pfam and Tmpred databases meant that there was a better understanding of the secondary domain structures in the Tlps and enabled the correct regions from the Tlps to be amplified by PCR (Figure 6.1). This information then meant that primers could be designed to amplify the target regions in the Tlps, without including the transmembrane region. The presence of the transmembrane regions may have presented potential difficulties when trying to solubilise the proteins out of *E. coli*.

TMpred output for Tlp1 (Cj1506c)



TMpred output for Tlp2 (Cj0144)



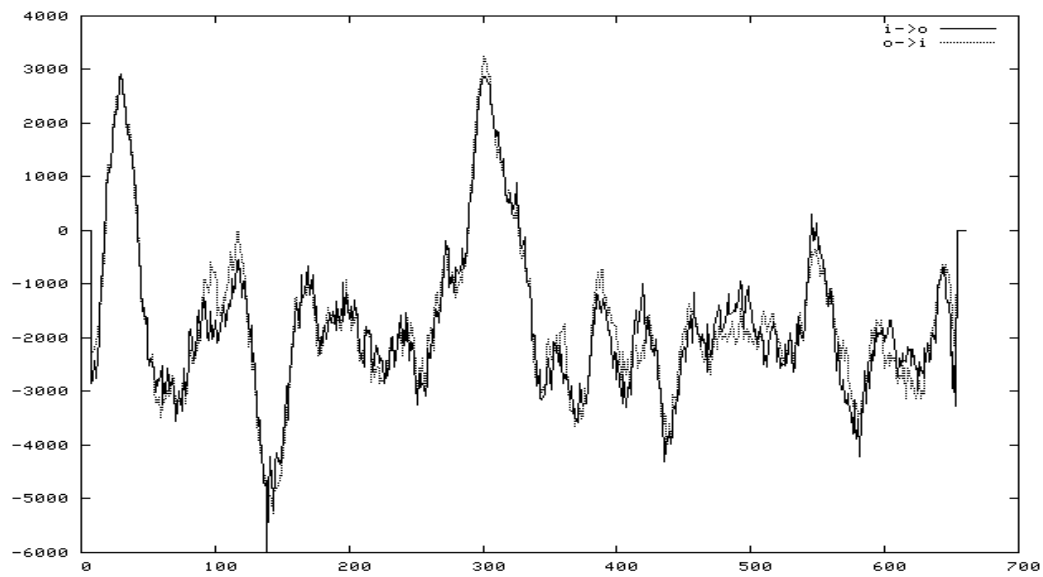
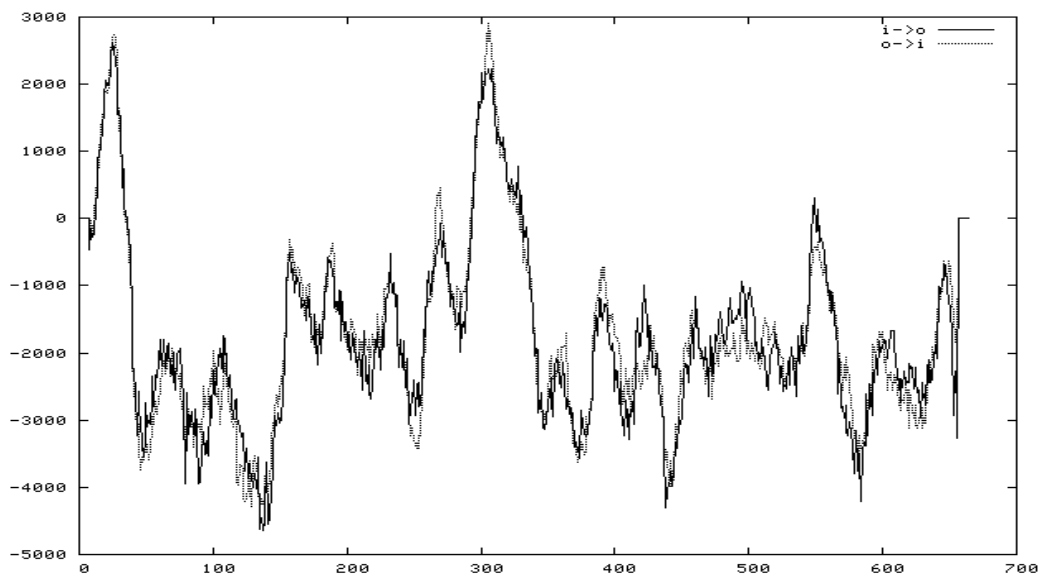
TMpred output for Tlp3 (Cj1564)TMpred output for Tlp4 (Cj0262c)

Figure 6.2. Histograms showing the putative transmembrane helices in Tlps 1 to 4. The amino acid sequence for each Tlp was analysed for putative transmembrane regions within the secondary domain structure of each Tlp. The amino acid sequence for each Tlp is shown along the x-axis. The y-axis shows the relative score given for the likelihood of a transmembrane domain (only scores >500 are considered to be significant; i=inside (cytoplasm) and o=outside (periplasm)). The TMpred programme was used to generate the data plots. The TMpred programme searches for the presence of hydrophobic residues within the search protein.

Tlp	Size of Tlp (amino acids)	Prediction of the location of the transmembrane domains in Tlps (aa)	Orientation of the transmembrane helices
Tlp1	700	First domain: from 11 to 30	cytoplasm to periplasm
		Second domain: from 327-349	periplasm to cytoplasm
Tlp2	659	First domain: from 8 to 31	cytoplasm to periplasm
		Second domain: from 287-310	periplasm to cytoplasm
Tlp3	662	First domain: from 21 to 41	cytoplasm to periplasm
		Second domain: from 290-313	periplasm to cytoplasm
Tlp4	665	First domain: from 16 to 34	cytoplasm to periplasm
		Second domain: from 297-316	periplasm to cytoplasm
Tlp7	526	First domain: from 12 to 28	cytoplasm to periplasm
		Second domain: from 176 to 192	periplasm to cytoplasm
Tlp10	592	First domain: from 12 to 32	cytoplasm to periplasm
		Second domain: from 239-259	periplasm to cytoplasm

Table 6.2. A summary of the proposed location of the transmembrane domains within the secondary domain structures of the Group A Tlps. The sizes of the Tlps (amino acids) are indicated as well as the proposed location of the transmembrane regions in each of the Tlps. The orientation of the transmembrane domains is shown; this tells you whether the transmembrane domain is predicted to be orientated from the cytoplasm to the periplasm or from the periplasm to the cytoplasm.

6.4.3. The cloning of the domains of Tlp1 and Tlp2 to 4 into a suitable expression vector containing a peptide or protein tag

6.4.3.1. Cloning the carboxyl-terminal signalling domain of Tlp1 and Tlp2 to 4 into pGEX-4T-1

The glutathione-S-transferase protein tag was used in this work to create a fusion with the cytoplasmic HCD of Tlp1 and Tlp2 to 4. As these gene fusions were produced by the same process, only the production of the Tlp1HCD/pGEX-4T-1 construct (pRS09; Figure 6.4(a)) will be presented here. To begin with, chromosomal DNA was prepared from the wild-type strain *C. jejuni* NCTC 11168 (section 2.8.2). This chromosomal DNA was used as the template in subsequent PCR reactions. The coding sequence for the carboxyl-terminal HCD in *tlp1* (*cj1506c*) was amplified by PCR (section 2.6) using the primer pair Tlp1CtermF and Tlp1CtermR. These primers amplified a product of the expected size of 996 bp (Figure 6.3 (a); Table 6.3). The amplification of the Tlp2 to 4 HCD by PCR is also shown in Figure 6.3 (a) and amplified correctly a product of 1067 (bp) (Table 6.3). Specifically, the Tlp1Cterm PCR primers amplified the amino acid region: 358-689 of the Tlp1 protein sequence. Restriction recognition sequences for *Bam*HI and *Eco*RI were added to the 5' end of the Tlp1CtermF and Tlp1CtermR primers, respectively. Once the PCR product encoding the Tlp1 HCD had been purified (section 2.9.1), restricted with *Bam*HI and *Eco*RI (section 2.10.1) and purified once more, the PCR product was then ready to be cloned directionally into a suitable cloning vector. The cloning vector used was pGEX-4T-1 (Appendix 4; Figure 4.1 (a); Chapter 2, Table 2.2). Unique features of the pGEX-4T-1 vector included a multiple cloning site (mcs) that contained six unique restriction recognition sequences including those for *Bam*HI and *Eco*RI, an ampicillin resistance marker encoded by the *betalactamase* (*bla*) gene, and finally the

coding region for the glutathione moiety (Figure 6.3 (a)). The pGEX-4T-1 vector was restricted with *Bam*HI and *Eco*RI, and then dephosphorylated to prevent self ligation of the vector molecules (section 2.10.2). The vector DNA was purified and then ligated (section 2.10.3) with the *Bam*HI and *Eco*RI restricted Tlp1 HCD PCR product. The ligation reaction was purified by ethanol precipitation (section 2.9.3) and then transformed into *Escherichia coli* DH5 α E cells (section 2.11.3). Transformations were plated out onto selective media and checked for ampicillin resistance (section 2.2.2). Transformation controls were also set up alongside the ligation reaction. Transforming cells with either pGEX-4T-1 vector alone or with distilled water served as the positive and negative controls, respectively in all *E. coli* transformations.

6.4.3.2. Screening *E. coli* cells for potential plasmid constructs containing the correct *tlp1* HCD insert

A colony PCR screen (section 2.6.1) was performed on a selection of clones using the primer pair Tlp1CtermF and Tlp1CtermR (Table 6.3). A selection of this colony PCR screen is shown in Figure 6.3 (b). The results from this screen showed that from the 10 transformants screened, 8 amplified correctly the Tlp1 HCD insert (Figure 6.3 (b), lanes 3-13 excluding lanes 4 and 6). The expected size of the cloned insert was 996 bp. Overnight cultures were prepared, and recombinant plasmid DNA was extracted (section 2.8.1). Plasmid DNA from one of the positive transformants was sequenced to ensure that the insert was error free (clone 1; Figure 6.3 (b), lane 3). This construct came back with no errors (pRS09; Figure 6.4 (a)) and was subsequently transformed into *E. coli* BL21. This construct, pRS09 (Figure 6.4 (a)) was once again checked for ampicillin resistance by plating on selective media plates. A further colony PCR was performed as before, on several positive transformants using the original cloning

primers (Table 6.3). The results from this screen are shown in Figure 6.3 (c). All seven of the transformants screened amplified correctly the Tlp1 HCD insert (996 bp). Plasmid maps of pRS09 and pRS10 (pRS10 contained the Tlp2 to 4 HCD) are shown in Figure 6.4 (a) and (b), respectively.

Target Domain in Tlp	Position within ORF to be amplified (amino acids)	Size of PCR product(s) (bp)
Tlp1 C-terminal HCD.	358-689	996
Tlp1 C-terminal HCD.	373-700	986
Tlp2 to 4 C-terminal HCD.	311-659	Tlp2; 1067 Tlp3; 1045 Tlp4; 1038
Tlp1 N-terminal Periplasmic ligand-binding	30-326	891

Table 6.3. Table showing the PCR reactions performed to amplify target domains in the Tlps.

Figure 6.3. A summary of the steps involved in cloning the carboxyl-terminal HCD of Tlp1 into the expression vector pGEX-4T-1.

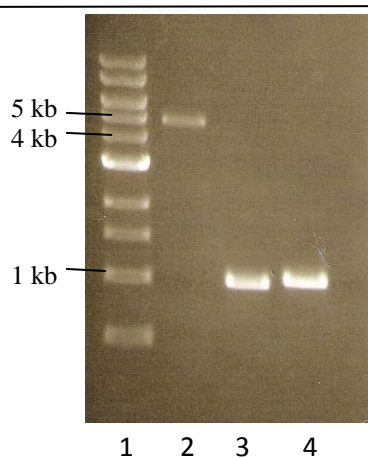


Figure 6.3 (a). PCR amplification of the cytoplasmic domains of Tlp1 and Tlp2. Lane 1 contains the 1 kb marker. Lane 2 shows linearized pGEX-4T-1 vector. Lanes 3 and 4 show PCR amplification of the cytoplasmic domains of Tlp1 and 2, respectively. Primer set Tlp1CtermF and Tlp1CtermR were used to produce an amplicon of 996 bp. Primer set Tlp2CtermF and Tlp2CtermR were used to produce an amplicon of 1067 bp.

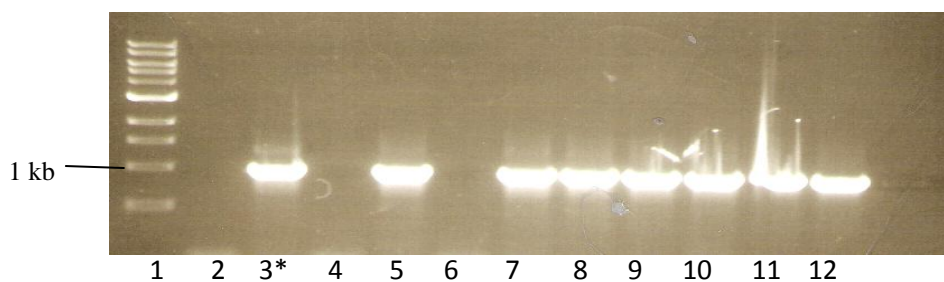


Figure 6.3 (b). Colony PCR screen of putative pRS09 constructs in *E. coli* DH5α. Lane 1 contains 1 kb marker. Lane 2 contains no template DNA. Lanes 3-12 contain transformants with pGEX-4T-1 containing the HCD of Tlp1. Clone 1 (*; lane 3) was selected for sequencing.

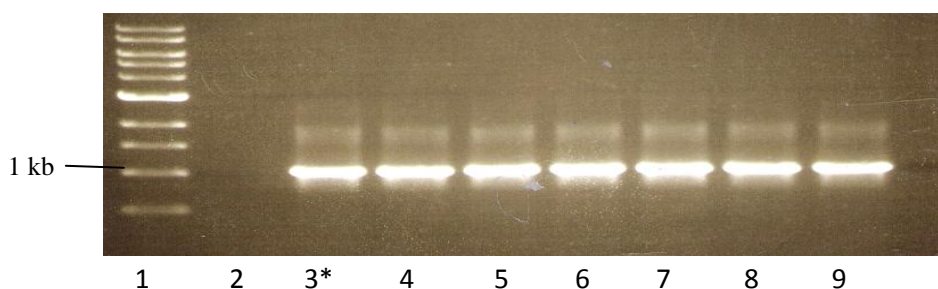


Figure 6.3 (c). Colony PCR screen of putative pRS09 constructs in *E. coli* BL21. Lane 1 contains 1 kb marker. Lane 2 contains no template DNA. Lanes 3-9 contain transformants with pGEX-4T-1 containing the HCD of Tlp1. Clone 1 (*; lane 3) was used in all subsequent protein expression studies.

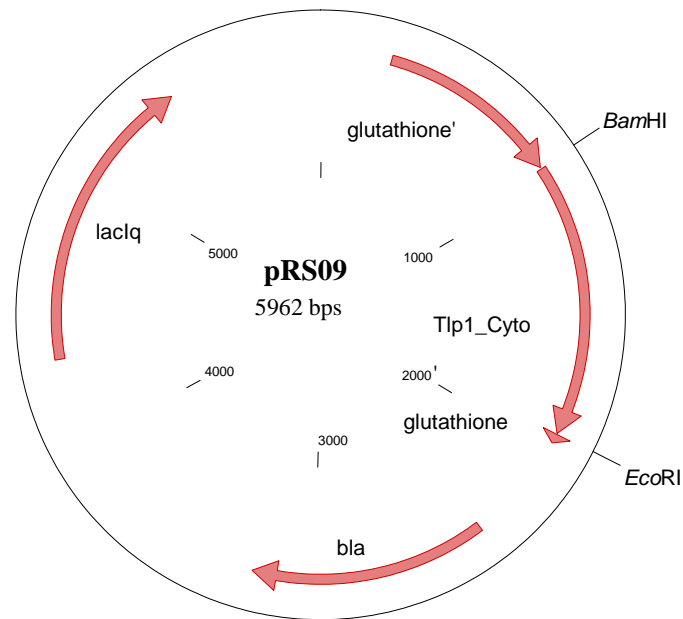


Figure 6.4 (a). Figure showing the gene encoding the HCD of Tlp1 cloned into pRS09. The cytoplasmic signalling domain of Tlp1 was translationally fused to the gene encoding the glutathione-S-transferase moiety. The *bla* gene encodes beta-lactamase which confers ampicillin resistance. The *Eco*RI and *Bam*HI restriction recognition sites used for cloning and restriction digests are indicated.

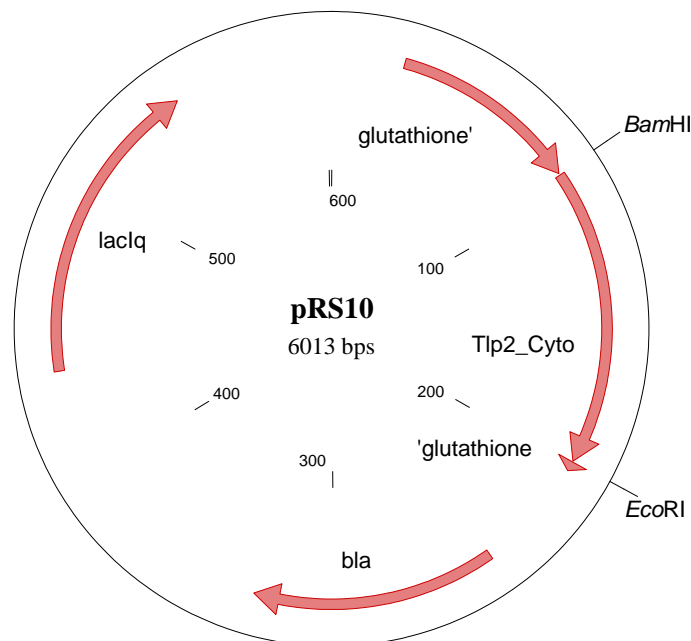


Figure 6.4 (b). Figure showing the gene encoding the HCD of Tlp2 to 4 cloned pRS10. The cytoplasmic signalling domain of Tlp2 to 4 was translationally fused to the gene encoding the glutathione-S-transferase moiety. The *bla* gene encodes beta-lactamase which confers ampicillin resistance. The *Eco*RI and *Bam*HI restriction recognition sequences used for cloning and restriction digests are indicated.

6.4.4. Cloning the periplasmic domain of Tlp1 into the pLEIC-05 plasmid containing a His-tag

The region of the *tlp1* (*cj1506c*) gene encoding the N-terminal PLD (Tlp1_Peri) was amplified by PCR (section 2.6) using the primer pair Tlp1PeriF and Tlp1PeriR (Table 6.3). The primers amplified correctly from chromosomal DNA of NCTC 11168 to produce a fragment of the expected size, which was 891 bp (Figure 6.5 (a); Table 6.3). The PCR product was purified and then given to Dr X. Yang (Protein Expression Laboratory, University of Leicester), who was responsible for ligating the region of the *tlp1* gene encoding the periplasmic domain with a C-terminal poly-histidine tag (pLEIC-05 contained the His-tag; Appendix 4; Figure 4.1 (b)). Purified plasmid DNA of pRS11 (Figure 6.5 (b)) was transformed into *E. coli* BL21 cells and positive transformants were screened as had been done previously with the Tlp1/pGEX-4T-1 construct (section 6.4.3.2), by colony PCR and checked for ampicillin resistance. One of the positive transformants was then used in subsequent protein expression studies.

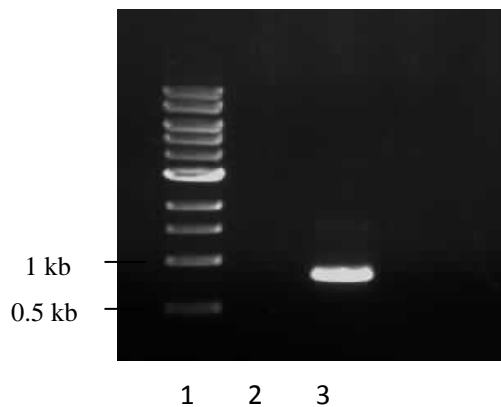


Figure 6.5 (a). PCR amplification of the N-terminal periplasmic ligand-binding domain (PLD) of Tlp1. Lane 1 contains the 1 kb marker. Lane 2 contains water in place of template DNA (negative control). Lane 3 shows PCR amplification of the Tlp1 N-terminal periplasmic domain (Tlp1_Per; amino acids: 30-326). Primer set Tlp1PeriF and Tlp1PeriR were used to produce an amplicon of 891 bp. 0.8% TAE gel.

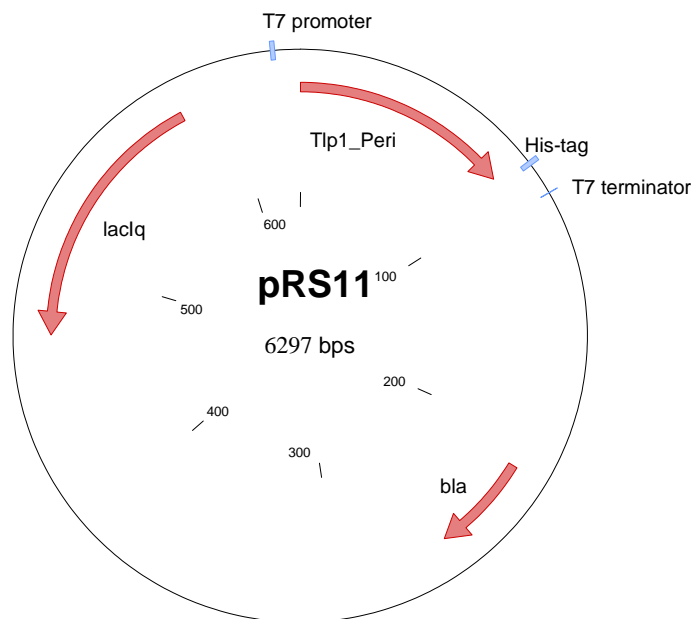


Figure 6.5 (b). Figure showing the gene encoding the PLD of Tlp1 cloned into the expression vector pLEIC-05 to produce pRS11. The PLD for Tlp1 was cloned into the pLEIC05 vector which contains a hexahistidine (His) peptide tag which will enable purification of the PLD. The *bla* gene encodes beta-lactamase which confers ampicillin resistance. The T7 promoter and terminator are also shown (pRS11 was created by Dr X. Yang, see section 6.4.4; Table 2.2).

6.4.5. Purifying the N-terminal ligand-binding domain in Tlp1

6.4.5.1. Optimising the extraction protocol for the His-tagged Tlp1 periplasmic (Tlp1 Peri) protein.

The PLD in Tlp1 is highly variable and is not homologous to PLDs present in other bacteria. Moreover, the PLD is unique in individual Tlps in *C. jejuni* indicating that the Tlps have different ligand-binding potential. The Tlp1_Peri protein will be used to determine the ligand-binding specificity of the Tlp1 receptor using an amino acid array similarly to Hartley *et al.* (2010). Once purified the PLD of the Tlp1 receptor will be used to identify specific interactions with any of the 20 amino acids present on the array. Any interaction found between the Tlp1 sensory domain and any amino acid these results will be verified by saturation transfer difference nuclear magnetic resonance spectroscopy.

The pRS11 construct (Figure 6.5 (b)) was transformed into chemically competent *E. coli* BL21 cells by heat shock (2.11.3). The pLEICS-05 vector (Appendix 4; Figure 4.1 (b); Table 2.2) was also transformed into *E. coli* BL21 cells and was used as a negative control in experiments. An optimisation experiment was performed to determine the optimal levels of IPTG to use and length of incubation (once induced) in order to obtain the best possible yield of the His-tagged fusion protein (containing the Tlp1_Peri domain; Figure 6.5 (b)). The amounts of IPTG tested were 0.5, 1.0, 1.5, 3 and 5 mM. The cells were incubated post-induction for varying time periods (1, 3 and 5 hours). BL21 cells were centrifuged and the cell pellets were lysed open and an equal amount of cells from each sample was loaded onto an SDS-PAGE gel (0.15 optical density units loaded; see section 2.12.1). The results from this initial experiment found that optimal yields of the His-tagged Tlp1_Peri protein could be obtained when inducing cells with 1.5 mM of IPTG and

incubating the cells for a period of 3 hours (data not shown). This optimisation experiment showed that when incubating the cells for too short a period or vice versa this resulted in reduced yield of the target protein. Furthermore, this initial optimisation study also showed the importance of establishing the optimal culture conditions for each fusion protein as the conditions may vary.

Chemical cell-lysis was tried as an alternative to sonication to recover the His-tagged Tlp1_Per1 protein. BL21 cells were induced with IPTG at the optimal conditions that had been determined specifically for the His-tagged Tlp1_Per1 protein. The target protein was recovered from the cells by chemical lysis, specifically using a protein extraction reagent (section 2.14.2). A small scale extraction was performed using the protein extraction reagent, which had been supplemented with Lysozyme (1 Kilo-unit was used; section 2.14.2). The cell lysate was cleared by centrifugation and the supernatants and the pellets from the BL21 cells containing the His-tagged Tlp1_Per1 protein and the vector only control (pLEIC-05) were visualised on a coomassie stained SDS-PAGE gel. The results from the extraction revealed that the His-tagged Tlp1_Per1 protein was absent in the soluble extraction but was instead found in the cell pellet, possibly being packaged into inclusion bodies (data not shown). Attempts were made to optimise the extraction protocol for the His-tagged Tlp1_Per1 protein in order to try and solubilise the desired protein. An alternative approach was used which involved lowering the growth temperature as well as altering the levels of IPTG which may help to solubilise the target protein (personal communication from Dr F. W. Muskett). Figure 6.6 (a-d) shows the *E. coli* cell lysates obtained from the soluble fraction (supernatants) versus the cell pellets post-IPTG induction at the different temperatures. BL21 cells were induced with varying concentrations of IPTG (1.0, 0.5, 0.25, 0.125 and 0.0625 mM) and were then

incubated for 3 hours at three different temperatures (18, 26 and 30°C). The results from the optimisation of the His-tagged Tlp1_Per1 showed that protein expression at the different temperatures using altered levels of IPTG failed, still resulting in the target protein being in the cell pellet (Figure 6.6 (a-d)). The approximate size of the Tlp1_Per1 protein is 33 kDa (see Table 6.4). This protein is visible on the SDS-PAGE gel in Figure 6.6 ((a) lanes 9 & 10; (b) lanes 2-4; (c) lanes 3-7; (d) lanes 6-10). The Tlp1_Per1 protein appears relatively pure with very few contaminating proteins further suggesting that the Tlp1_Per1 protein is being packaged into inclusion bodies.

Construct name	Vector	Affinity tag	Target region in Tlp1	An estimate of the size of fusion protein (kDa*)
pRS09	pGEX-4T-1	GST	C-terminal signalling domain.	63
pTrc_Tlp1	pTrcHis	His	C-terminal signalling domain.	39.9
pRS10	pGEX-4T-1	GST	C-terminal signalling domain.	65
pRS11	pLEIC-05	His	Periplasmic (Peri)	33

Table 6.4. Different domains in the Tlps expressed and purified. In-frame fusions were created between the Tlp proteins and either a hexahistidine (His) or glutathione-S-transferase (GST) tag. *The estimated size of each fusion protein includes the size of the respective tag.

Figure 6.6. Optimising the extraction protocol for the His-tagged Tlp1 periplasmic (Tlp1_Peri) protein. Figures a-d shows the *E. coli* lysates obtained from the soluble fraction (supernatants) versus the cell pellets post-induction. The cells were induced using varying concentrations of IPTG (1.0, 0.5, 0.25, 0.125 and 0.0625 mM) and were then incubated for 3 hours at three different temperatures (18, 26 and 30°C). The approximate size of the Tlp1_Peri protein is 33 kDa (see Table 6.4).

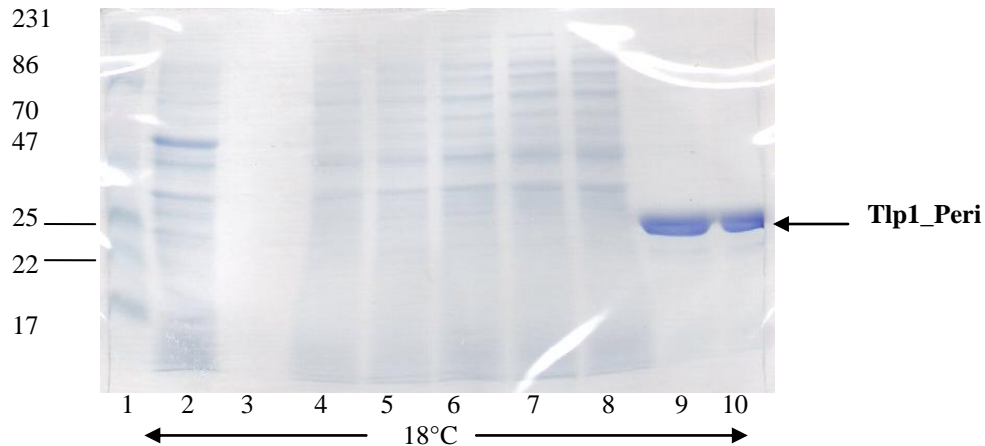


Figure 6.6 (a). The effects of using varying concentrations of IPTG and then incubating cells at 18°C on the solubility of the His-tagged Tlp1 periplasmic protein (Tlp1_Peri).

Lane 1 contains Bio-Rad Low Range protein standards (sizes are marked to the left of the gel in kDa). Lanes 4-8 contain: 1.0, 0.5, 0.25, 0.125 and 0.0625 mM IPTG, respectively. Lanes 4-8 contain the soluble fractions obtained post cell lysis whereas lanes 9 and 10 contain the solubilised cell pellet. Lanes 9 and 10 contain 1.0 and 0.5mM IPTG, respectively. Lane 2 contains the pLEIC-05 vector only control (without the Tlp1_Peri domain). Lane 3 contains *E. coli* BL21 cells alone.

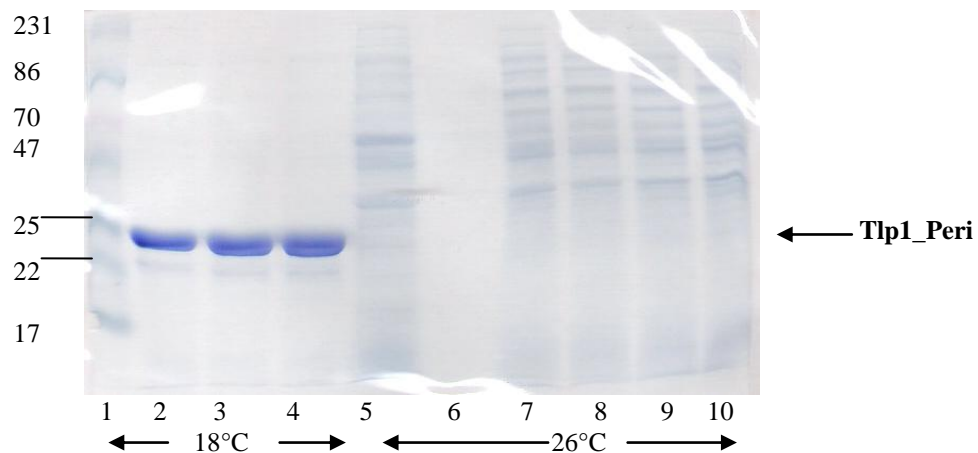


Figure 6.6 (b). The effects of using varying concentrations of IPTG and then incubating cells at 18°C & 26°C on the solubility of the His-tagged Tlp1 periplasmic protein (Tlp1_Peri). Lane 1 contains Bio-Rad Low Range protein standards (sizes are marked to the left of the gel in kDa). Lanes 2-4 contain: 0.25, 0.125 and 0.0625 mM IPTG and contain the solubilised cell pellet whereas lanes 7-10 contain the soluble fractions obtained post cell lysis. Lanes 7-10 contain 1.0, 0.5, 0.25 and 0.125 mM IPTG, respectively. Lane 5 contains the pLEIC-05 vector only control (without the Tlp1_Peri domain). Lane 6 contains *E. coli* BL21 cells alone.

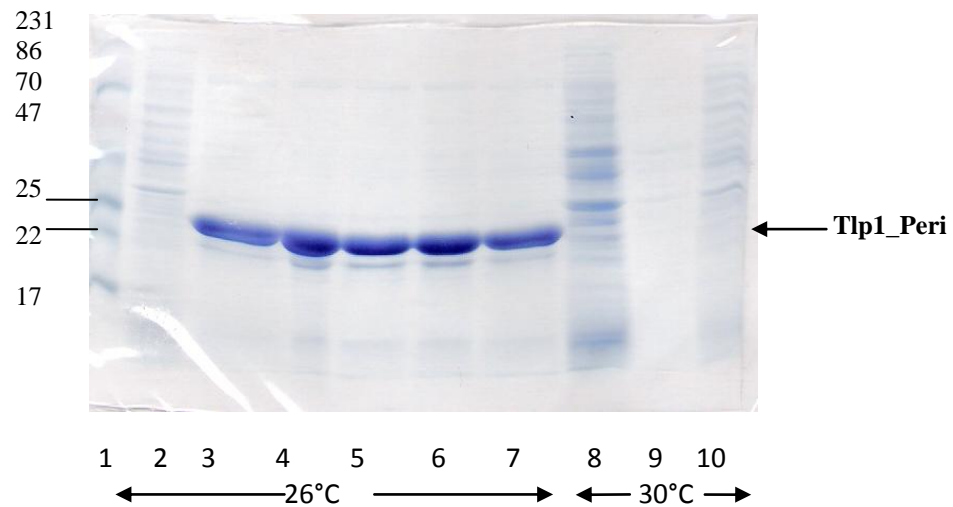


Figure 6.6 (c). The effects of using varying concentrations of IPTG and then incubating cells at 26°C & 30°C on the solubility of the His-tagged Tlp1 periplasmic protein (Tlp1_Peri). Lane 1 contains Bio-Rad Low Range protein standards (sizes are marked to the left of the gel in kDa). Lanes 3-7 contain: 1.0, 0.5, 0.25, 0.125 and 0.062 mM IPTG, respectively and are the solubilised cell pellet samples. Lane 10 contains the soluble fraction obtained post cell lysis and contains 1.0 mM IPTG, respectively. Lanes 2 & 8 contains the pLEIC-05 vector only control (without the Tlp1_Peri domain). Lane 9 contains *E. coli* BL21 cells alone.

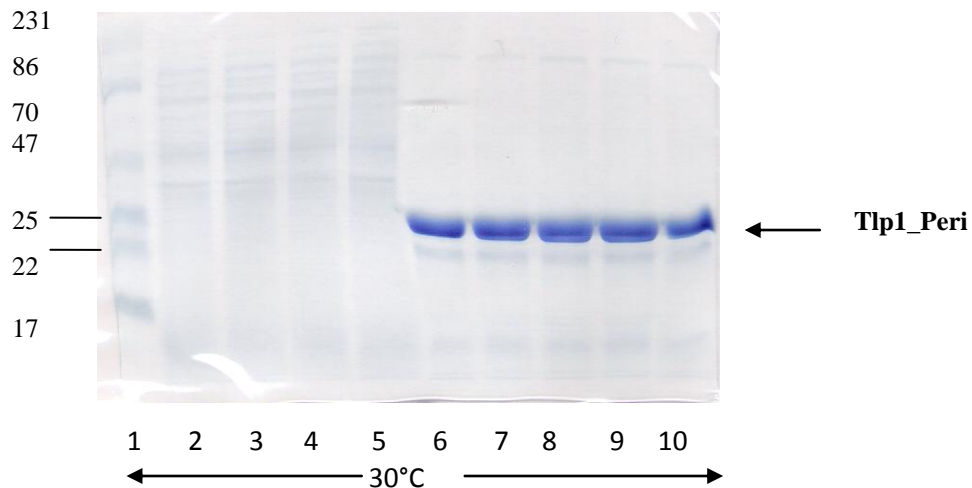


Figure 6.6 (d). The effects of using varying concentrations of IPTG and then incubating cells at 30°C on the solubility of the His-tagged Tlp1 periplasmic protein (Tlp1_Peri). Lane 1 contains Bio-Rad Low Range protein standards (sizes are marked to the left of the gel in kDa). Lanes 2-5 contains: 0.5, 0.25, 0.125 and 0.0625 mM IPTG, respectively. Lanes 2-5 contain the soluble fractions obtained post cell lysis whereas lanes 6 to 10 contain the solubilised cell pellet. Lanes 6 to 10 contain 1.0, 0.5, 0.25, 0.125 and 0.062 mM IPTG, respectively.

6.4.6. Purifying the C-terminal signalling domain in Tlp1

6.4.6.1. Expression and purification of the C-terminal signalling domain in Tlp1 and Tlp2 to 4 using a GST-tag

The pRS09 and pRS10 (Figure 6.4 (a) and (b)) constructs were transformed into chemically competent *E. coli* BL21 cells by heat shock (2.11.3). The pGEX-4T-1 vector (without an insert) was also transformed into *E. coli* BL21 cells and was used as a negative control. Protein expression was induced by adding the lactose analogue-IPTG (1.5mM) to induce expression in BL21 cells of the GST-fused target proteins (Tlp1 and Tlp2 to 4_HCD; data not shown). Cells incubated at 30°C for a period of 3 hours had been found to induce optimal levels of protein expression in cells (data not shown). BL21 cells were centrifuged and the cell pellets were lysed and an equal amount of cells of each sample was loaded onto an SDS-PAGE gel (0.15 optical density units loaded; see section 2.12.1). The coomassie stained gel presented in Figure 6.7 (a) shows the selected GST-tagged proteins following induction with IPTG under the established optimal conditions for expression. The GST-tag in the vector only control (Figure 6.7 (a), lane 1) shows that there is a strong band near the 25 kDa marker; the GST protein is 26 kDa so this is as expected. The predicted sizes of the GST-tagged Tlp1 and Tlp2 to 4 cytoplasmic domain proteins are 63 and 65 kDa, respectively (Table 6.4). There are bands corresponding to the proposed size of these proteins in lanes 2 and 3 (Figure 6.7 (a)).

An attempt was made in this work to purify the GST-tagged Tlp1_HCD protein (Figure 6.7 (b)). BL21 cells were induced with IPTG at the optimal conditions determined for the GST-tagged Tlp1_HCD protein and the target protein was then recovered from the cells through cell lysis. BL21 cells containing the target protein were lysed open using sonication (section 2.14.1). Some of the unwanted cell debris

was removed by centrifugation and filtration, although there was still a large quantity of cell debris and unwanted proteins in the cell lysate along with the target fusion protein. The clarified supernatant was applied to a GSTrap FF column (section 2.14.1). Figure 6.7 (b) shows that when the GST-tagged Tlp1_HCD fusion protein was added to the GSTrap column the majority of the sample came through in the flow through (lanes 1 and 2). This suggested poor binding of the GST-tag to the immobilised glutathione sepharose. Furthermore, when the GSTrap column was washed with binding buffer the majority of the sample still failed to bind with a high affinity to the column (lanes 3 and 4). Once the elution buffer was added to the column containing the glutathione sepharose the majority of the contaminating proteins appeared to disappear (lanes 4-8). The strongest of the bands (indicated by a black arrow (lanes 7 and 8) appeared to be a little bigger than the proposed size of the Tlp1_HCD fusion protein (63 kDa). There appeared to be a further protein underneath the desired protein (this faint band underneath the densest band has been marked by a red arrow). Further fractions were collected (data not shown) but the target protein was absent on this gel (data not shown). Performing a western blot on Tlp1 and Tlp2 to 4 protein preparations would be useful as it would not only confirm the presence of the GST-tag in the fusion proteins but would also verify the sizes of the target proteins.

Figure 6.7. The expression and purification of GST-tagged fusion proteins. The expression of the Tlp1 and Tlp2 to 4 C-terminal highly conserved signalling domain (HCD) proteins in BL21 cells is shown below (a). The purification of the Tlp1 HCD using a GSTrap column (see section 2.14.1) is also presented (b).

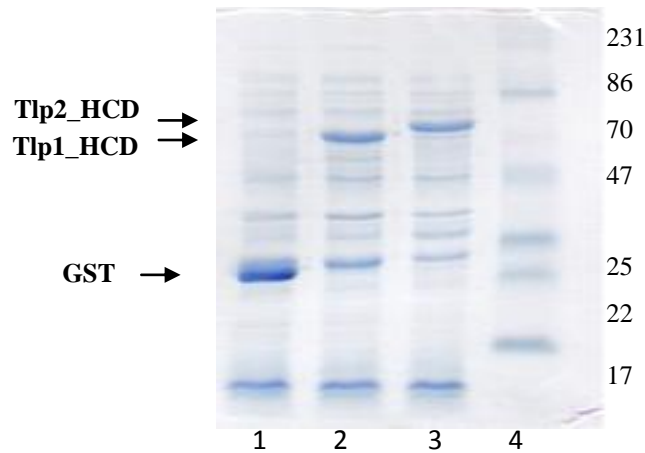


Figure 6.7 (a). Coomassie stained SDS-PAGE gel showing the expression of GST-tagged Tlp1 and Tlp2 to 4 HCD. Lane 1 shows *E. coli* BL21 cells plus pGEX-4T-1 vector alone. Lanes 2 & 3 shows the expression of the GST-tagged Tlp1 and Tlp2 HCD, respectively. The GST-tag is 26 kDa (lane 1). Expression was up-regulated in cells using IPTG (1.5 mM). The Tlp1 and Tlp2 to 4 HCD are estimated to be 63 and 65 kDa, respectively. Bio-Rad Low Range protein standards (lane 4, sizes (kDa) of the marker are shown to the right of the gel).

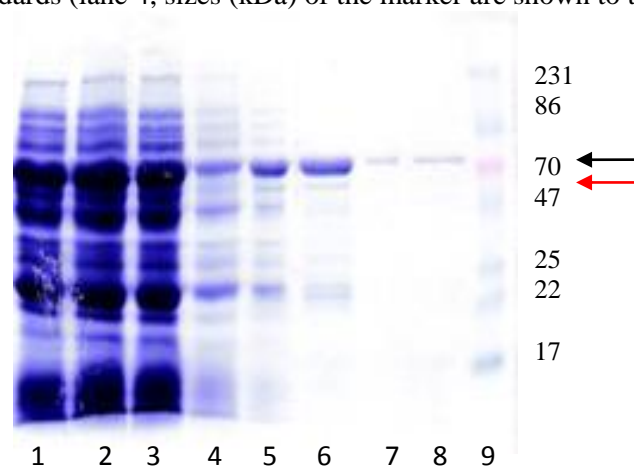


Figure 6.7 (b). Coomassie blue stained SDS-PAGE gel showing the purification of the GST-tagged Tlp1 HCD protein. A GSTrap column (see methods section 2.14.1) containing immobilised reduced glutathione was used to purify the Tlp1_HCD GST fusion protein. Lanes 1 (10µl) & 2 (20µl) shows when the GST-Tlp1_HCD fusion protein was first added to the GSTrap column. Lanes 3 (10µl) & 4 (20µl) shows when the samples were washed with binding buffer. Lanes 5 (10µl) & 6 (20µl) shows the first fraction collected using elution buffer (plus 10mM glutathione). Lanes 7 (10µl) & 8 (20µl) shows the second fraction collected (eluate). The approximate size of the Tlp1_HCD protein is 63 kDa; although the position of the Tlp1_HCD on the SDS-PAGE gel appears to be slightly bigger than the size proposed (marked with a black arrow). The red arrow indicates a possible *E. coli* host protein. Lane 9 contains Bio-Rad Low Range protein standards (sizes are marked to the right of the gel in kDa).

6.4.6.2. Detecting the GST-tag in the purified cytoplasmic proteins of Tlp1 and Tlp2 to 4 using an anti-GST antibody

The presence of GST-tagged fusion proteins in BL21 cells was verified by immunoblotting (section 2.13.1). Protein samples were first separated by SDS-PAGE (Sodium Dodecyl Sulphate-Polyacrylamide Gel Electrophoresis; section 2.11), but rather than staining the SDS-PAGE gel with coomassie blue stain, the proteins on the gel were transferred onto the surface of a polyvinylidene fluoride (PVDF) membrane by applying an electric field (section 2.13.1). Once the electro-transfer of proteins had occurred, the membrane was probed with an anti-GST antibody (see Figure 6.8; section 2.13.2). Figure 6.8 shows that the GST-tag was detected successfully using the anti-GST antibody (26 kDa; lanes 2 and 4). More importantly the anti-GST antibody detected the Tlp1 and Tlp2 to 4 HCD (lanes 5-8). The approximate sizes of the Tlp1 and Tlp2 to 4 HCD are 63 and 65 kDa, respectively and these appear to be the sizes of the proteins shown on the blot (Figure 6.8). The most intriguing aspect of the western blot is that the cells show a high basal level of expression of the GST (lane 3), Tlp1_HCD (lane 5) and Tlp2 to 4_HCD (lane 7) proteins in the absence of an inducer (minus IPTG). The basal level of expression can be controlled by catabolite repression, using glucose. The *lac* promoter in the pGEX-4T-1 vector (Appendix 4; Figure 4.1 (a)) may be contributing to the increased level of expression. In addition to this, upon induction of protein expression using IPTG multiple bands can be seen below the target GST-tagged fusion protein (lanes 6 and 8). This may be due to partial breakdown of the fusion proteins by proteases or once more could be due to over sonication resulting in the degradation of the protein. The addition of protease inhibitors such as PMSF to the cell lysis solution could prevent this problem from occurring in future work.

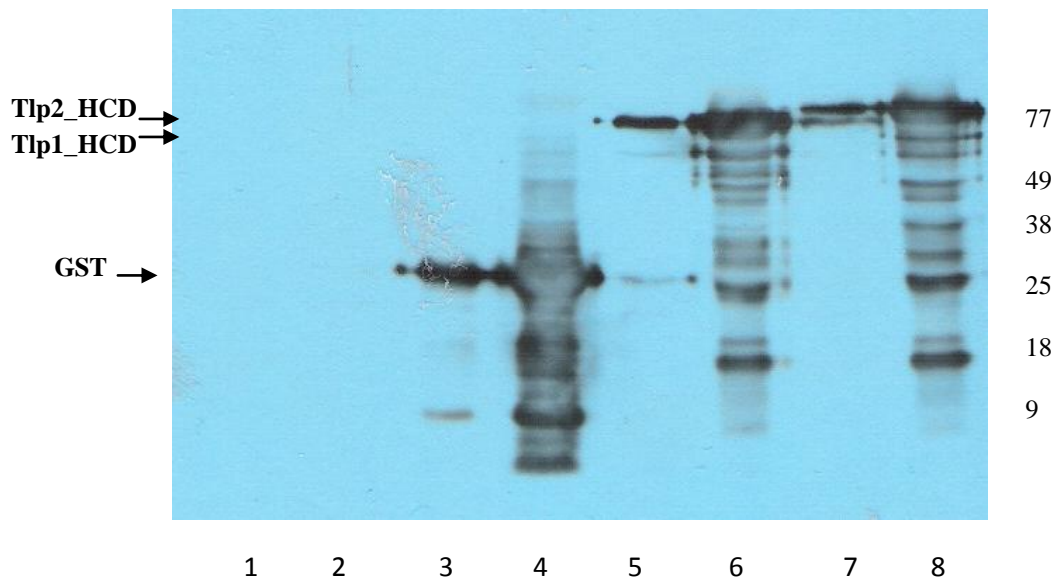


Figure 6.8. Western blot analysis of solubilised Tlp1 and Tlp2 to 4 HCD proteins (prepared from *E. coli* BL21 cells) using an anti-GST antibody. Lanes 1 & 2 contains *E. coli* BL21 cells alone. Lanes 3 & 4 contains BL21 cells plus pGEX-4T-1 vector only. Lanes 5 & 6 contains pGEX-4T-1 plus the Tlp1 HCDHCD. Lanes 7 & 8 contains pGEX-4T-1 plus the protein encoding the Tlp2 to 4 HCD. Lanes 2, 4, 6 & 8 shows cells plus IPTG (1.5 mM) post-induction. Lanes 1, 3, 5 & 7 show cells minus IPTG, although there is a basal level of gene expression present in these cells. The GST-tag is 26 kDa; the tag has been indicated on the blot (lane 3). The approximate sizes of the Tlp1 and Tlp2 to 4 HCD proteins are 63 and 65 kDa, respectively (these proteins have been indicated to the left of the blot). The loading of protein in the SDS page wells was equalised by pellet weight to reduce experimental error and blots were repeated twice. Protein marker sizes are indicated in kDa on the right.

6.4.6.3. Optimising the yield of Tlp1 HCD recombinant protein

The GST-tagged Tlp1 HCD protein has since the commencement of the writing of this dissertation, been purified successfully (Laura Perrett, personal communication; Figure 6.9). The work undertaken in this study found that the GST-tagged Tlp1_HCD fusion protein when added to the GSTrap column failed to bind to the immobilised glutathione sepharose with a strong affinity (section 6.4.6.1). Therefore to improve the extraction protocol for the Tlp1 HCD fusion protein the target protein was solubilised prior to purification on the GSTrap column. Denaturants such as 4-6 M guanidine hydrochloride, 4-8 M urea, using an alkaline pH >7, Triton X-100 or other detergents can be used to solubilise the fusion protein (Sambrook and Russell, 2001). The Tlp1_HCD protein was un-folded using 6M guanidine hydrochloride. The use of a denaturant was to help expose the GST tag and subsequently increase the binding affinity of the target protein binding to the GST sepharose. The denaturant was removed by slow dialysis. The latter is necessary to permit the correct refolding of the protein and the formation of the necessary intramolecular interactions. The protein was refolded and returned into its correct native state by buffer exchange with PBS and was then applied to a GSTrap column and purified. A western blot was performed by probing the fractions collected from the GSTrap purification with an anti-GST antibody. The results from the western blot are shown in Figure 6.9. The results from the western blot show that post-treatment of the GST-tagged Tlp1_HCD protein with 6M guanidine hydrochloride (HCl) and subsequent refolding of the protein has reinstated column binding. The latter enabled the successful purification of the Tlp1_HCD protein. The eluates collected following washing with elution buffer containing glutathione show purified Tlp1_HCD protein (Figure 6.9; lanes 5-11). Now that purified Tlp1_HCD protein had been obtained, the next step was to

cleave the GST-tag off from the Tlp1_HCD protein. Purified Tlp1_HCD protein without the GST-tag was required for antibody development

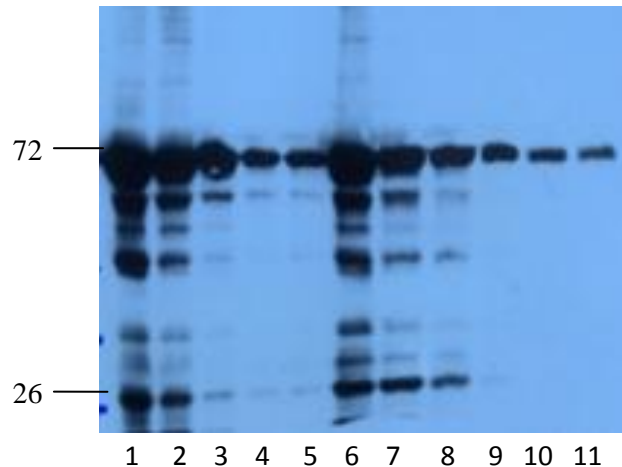


Figure 6.9. Western blot analysis of the purified Tlp1_HCD protein post-treatment with 6M guanidine hydrochloride (HCl). An anti-GST antibody was used to probe the fractions collected from a GSTrap column (section 2.14.1). Tlp1_HCD protein was treated with the denaturant 6M guanidine HCl. Following buffer exchange, the treated sample was applied to a GSTrap column. Lane 1 shows crude cell lysate following buffer exchange (into PBS buffer). Lane 2 shows the sample flow through. Lanes 3 & 4 contains the first two wash steps, when the sample in the GSTrap column is washed with binding buffer (PBS). Lanes 5-11 contain the eluates collected following washing with an elution buffer (plus 40 mM glutathione). The eluates collected in lanes 5-11 represented the 1st, 3rd, 5th, 7th, 10th, 15th and 20th of the eluted fractions. The approximate size of the Tlp1_HCD protein is 63 kDa. Loading in lanes was equalised by pellet weight to reduce experimental error and the blot was repeated at least twice. Protein marker sizes are indicated in kDa on the left (Data from Laura Perrett).

6.4.6.4. Cleavage of the GST-tag

Since the commencement of the write-up of this dissertation the GST-tag has been cleaved off the Tlp1_HCD protein (Laura Perrett, personal communication). The GST-tag was cleaved using the protease thrombin. The pGEX-4T-1 vector contains a thrombin recognition cleavage upstream of the GST-tag (Appendix 4; Figure 4.1 (a)). Thrombin cleavage can be done in one of two ways: (a) whilst the fusion protein is still bound to the GSTrap column (“on-column cleavage”) or (b) on a sample of the eluted protein in solution (“off column cleavage”). It is reported that “off column” cleavage is more efficient (Personal communication, Laura Perrett) at least with the Tlp1_HCD protein. Other advantages of performing “off column cleavage” of the GST-tag is that the proteins can be maintained in elution buffer which helps to keep the proteins stable and minimises the risk of degradation of the fusion protein. Once digestion was completed, the glutathione was removed by passing the sample to an equilibrated GSTrap column for the removal of GST. The final step was to remove the protease from the eluted Tlp1_HCD protein. This was achieved using a HiTrap Benzamidine column. The results were as predicted, following incubation with thrombin the eluates collected showed the intensity of the GST-tagged Tlp1_HCD protein to decrease whilst the intensity of the GST tag (26 kDa) increased (Laura Perrett, data not shown). A faint band could be seen just above the 34 kDa marker indicating the presence of the Tlp1_HCD protein (estimated to be 36.5 kDa; excluding the GST-tag). However, this was a very faint band and appeared to disappear instead of increasing in its intensity which would have been the expected outcome. To conclude, the Benzamidine sepharose appeared to be binding out the Tlp1_HCD protein as well as the thrombin protease, leaving very little Tlp1_HCD protein (Personal communication, Laura Perrett).

6.4.6.5. Further attempts to clone the Tlp1 HCD

A further attempt was made during the write-up of this dissertation to clone the C-terminal HCD (Paul Ainsworth, Personal communication; see section 2.14.2.2 for details of methodology). However, the protein of interest was His-tagged in place of fused to a GST-tag. The peptide tag was significantly smaller in size compared to the GST-tag (approximate 23 kDa difference in size). Moreover, the GST-tag may have been interfering with the binding affinity of the target protein with the column. The coding sequence for the carboxyl-terminal HCD in *tlp1* (*cj1506c*) was amplified by PCR (section 2.6) using the primer pair Tlp1_F and Tlp1_R (see Table 2.6 for primer sequences). These primers amplified a product of the expected size of 1005 bp (Paul Ainsworth, data not shown). The PCR primers specifically amplified the amino acid sequence beginning from 373 to 700 of the ORF of Tlp1 (328 aa). Restriction recognition sequences for *Bgl*III and *Kpn*I were added to the 5' end of the Tlp1F and Tlp1R primers, respectively. Once the PCR product encoding the Tlp1 HCD had been purified (section 2.9.1), restricted with *Bgl*III and *Eco*RI (section 2.10.1) and purified once further, the PCR product was then directionally cloned into the pTrcHisB vector (Appendix 4; Figure 4.1 (c)). The PCR fragment was cloned in-frame with the His-tag. The vector was transformed into the *E. coli* strain Rosetta (see Table 2.1 for information on the strain used). A colony PCR screen (section 2.6.1) was performed on a selection of clones using primers specific to the target protein. Plasmid DNA from one of the positive transformants was sequenced to ensure that the insert was error free. The plasmid map of the pTrc_Tlp1 construct is shown in Figure 6.10. Optimal protein expression was found to be successful when incubating *E. coli* Rosetta cells for 3 hours with 1.5 mM of IPTG (Personal communication, Paul Ainsworth). The clarified cell lysate was applied to a HisTrap column (section

2.14.2.2). The desired protein was successfully purified using the competing chelator imidazole. Specifically 20mM imidazole was found to eliminate the binding of non-specific contaminating proteins. The purified Tlp1 protein encoding the C-terminal signalling domain was sent off to Eurogentec (Belgium) for polyclonal antibody development.

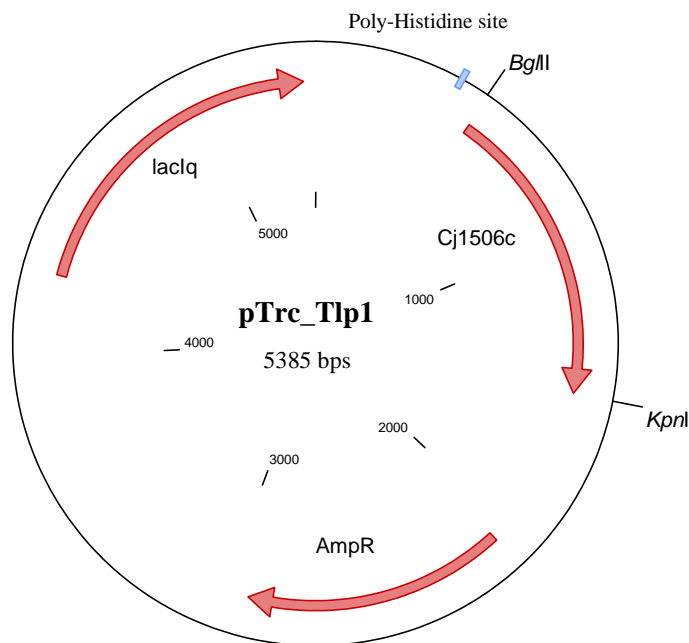


Figure 6.10. Figure showing the gene encoding the HCD of Tlp1 cloned into the pTrcHisB plasmid. The HCD of Tlp1 (specifically, amino acids 373 to 700 of the Tlp1 ORF) was cloned into the vector pTrcHisB and in-frame with the coding sequence for the hexahistidine (His) peptide tag. The *bla* gene encodes beta-lactamase which confers ampicillin resistance (pTrc_Tlp1 was created by Paul Ainsworth; Table 2.2).

6.4.6.6. Testing the Tlp1_HCD polyclonal antibody

C. jejuni 11168 cells which had been grown overnight in Mueller-Hinton broth (MHB) with gentle agitation under microaerobic conditions, were harvested by centrifugation and resuspended in fresh MHB. The cells were observed using phase contrast microscopy at the start of each experiment. The campylobacters were highly motile following overnight incubation in liquid MHB and had a typical “cork-screw” swimming pattern. The campylobacters were seen to be swimming at fast speeds with frequent, random changes in direction. A sample of these cells (2×10^7 Cfu/ml) were spotted (10µl) onto a Poly-L-Lysine coated microscope slide. The cells were then fixed using the cross-linking reagent (4%) paraformaldehyde (section 2.4). To ensure free access of the Tlp1_HCD antibody the cells were permeabilised using Triton X-100 (0.5%). In order to determine the optimal method for labelling of cells some cells were treated with Triton X-100 (0.5%) prior to fixation. Following multiple wash steps with PBS buffer, the cells were treated with the primary Tlp1_HCD antibody at 1/100 and 1/1000 dilution of the stock solution. The cells were washed repeatedly in PBS buffer containing BSA (0.1 %) and were then incubated with an anti-rabbit-FITC (fluorescein isothiocyanate) secondary antibody, which had been produced in goats. The secondary antibody was tested at 1/160 dilution (stock at 3.3 mg/ml). Following further wash steps the cells were stained using the nuclear stain DAPI (4',6-diamidino-2-phenylindole; 1µg/ml); which emits blue fluorescence upon binding to AT regions of DNA. Finally the cells were mounted using mount medium and a cover slip was overlaid and sealed. For full details of the method used refer to section 2.14.4 (Chapter 2). All staining was evaluated using fluorescence microscopy. *C. jejuni* cells stained with DAPI are presented in Figure 6.11 (a). *C. jejuni* cells were

stained using only the secondary FITC (fluorescein isothiocyanate) labelled secondary antibody and was included to establish fluorescence (Figure 6.11 (b)).

The Tlp1 polyclonal antibody generated against the HCD has shown for the first time in *C. jejuni* NCTC 11168 that Tlp1 localises in clusters at the poles of the cell (Figure 6.12; clusters shown by marked arrows). The results presented here are for those cells stained using 1/100 dilution of the primary polyclonal Tlp1_HCD antibody (Figure 6.12). The labelling of cells visualised using 1/1000 dilution of the primary antibody appeared too diffuse and for this reason have not been presented. Furthermore, the negative control, whereby *C. jejuni* wild-type cells had been only stained with the secondary antibody, verified that the level of background fluorescence was low (Figure 6.11 (c)) and that the clustering of Tlp1 was not due to non-specific staining of the secondary antibody and there is no visible localisation of the antibody to any particular focal point in the *C. jejuni* cell. Moreover no difference was found in the immunolabelling of those cells that had been treated with Triton X-100 (0.5%) prior to fixation or vice-versa (Figure 6.12 panels (a) and (b)). As the primary and secondary antibodies used in this work appear to have free access to its target antigen.

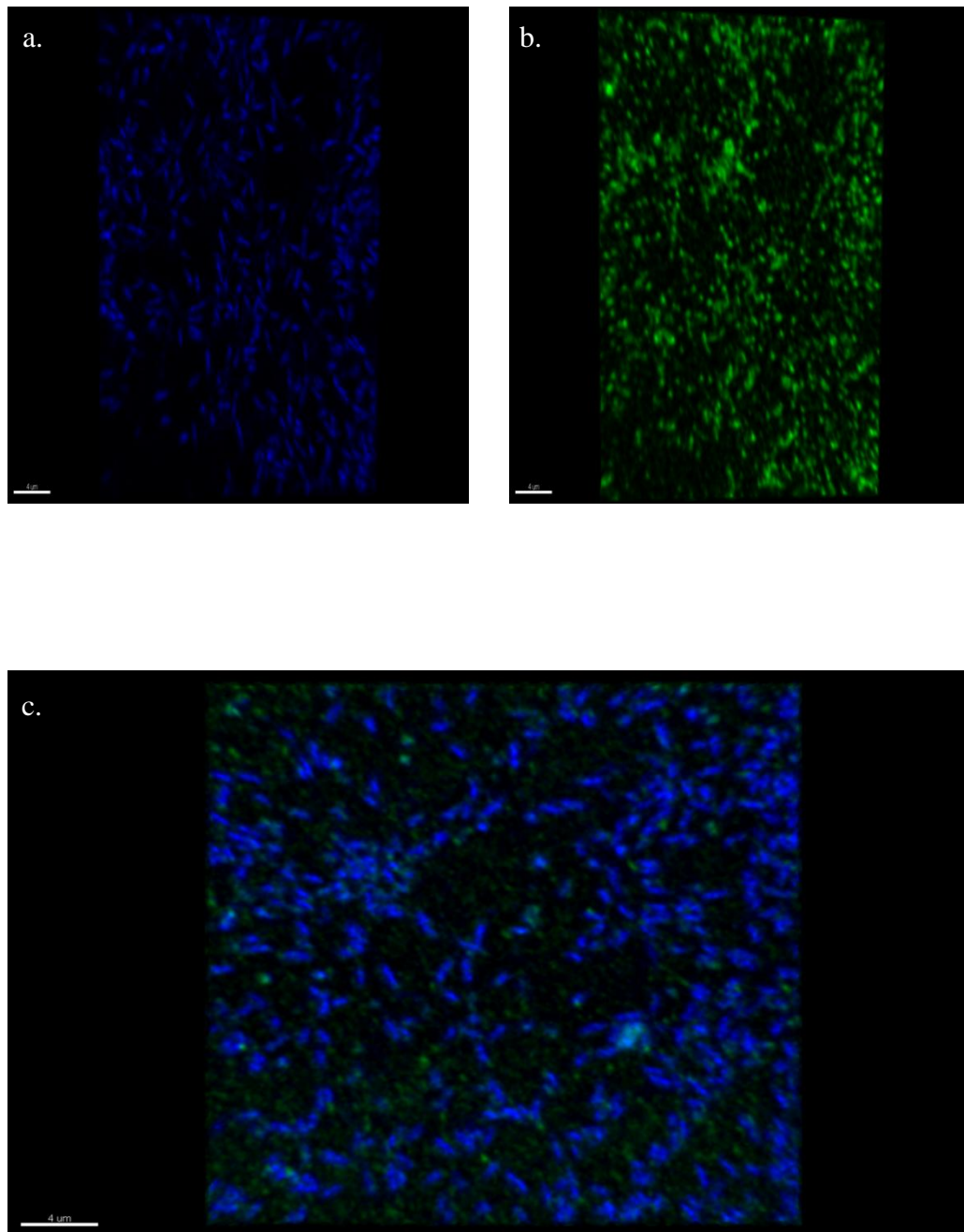


Figure 6.11. Controls used for the staining of *Campylobacter jejuni* cells for the Tlp1 localisation immunofluorescence light microscopy studies. Panel (a). *C. jejuni* DNA stained and visualised through the incorporation of DAPI (4',6-diamidino-2-phenylindole; 1 µg/ml). Panel (b) shows *C. jejuni* stained only with the fluorescein-labelled secondary antibody. Panel C shows *C. jejuni* stained with DAPI nuclear stain and secondary antibody only (negative control; see section 2.14.4 for details on method).

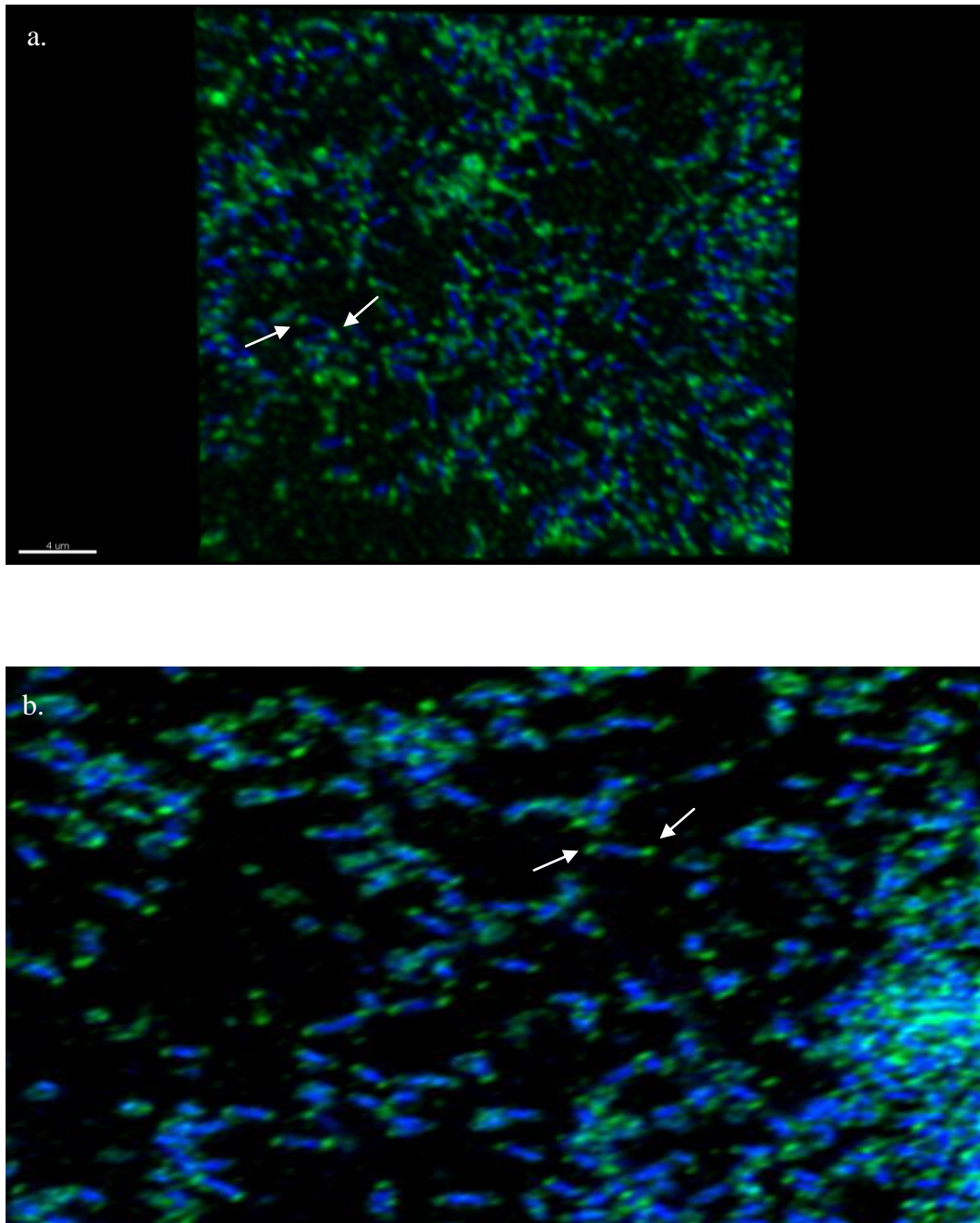


Figure 6.12. Determining the Intracellular positioning of the Tlp1 chemoreceptors in *Campylobacter jejuni* (NCTC 11168) by indirect immunofluorescence light microscopy. The localisation of Tlp clusters at the poles of the cell, as confirmed by examination with immunofluorescence microscopy. The primary antibody was produced in rabbit and was raised against the C-terminal HCD region in Tlp1 (Tlp1_HCD). Tlp1_HCD reactive epitopes were visualised using a fluorochrome labelled secondary antibody; anti-rabbit IgG conjugated to FITC (fluorescein isothiocyanate; produced in goats). The arrows indicate clusters of Tlp1 receptors at the poles of the bacterial cell. Panel (a) shows *C. jejuni* cells that have been permeabilised first using Triton X-100 prior to being fixed with paraformaldehyde. Whereas Panel (b) shows *C. jejuni* cells fixed first and then permeabilised. No difference was observed between the two methods; both methods were found to be effective for staining.

6.5. Discussion

6.5.1. Summary of key findings

The highly conserved signalling domains (HCDs) in Tlp1 and Tlp2 to 4 were purified successfully using a glutathione S-transferase affinity tag. However, initial attempts at purifying the Tlp1_HCD protein proved unsuccessful as the GST-tag was found to be hidden or blocked presumably by the HCD domain rendering it unable to bind to the specific affinity column. By denaturing the protein and subsequent refolding restored column binding. However, upon cleavage of the GST-tag using the protease thrombin; the Tlp1_HCD protein could not be isolated when applying the Tlp1_HCD protein to the Benzamidine column; the Benzamidine sepharose appeared to be binding out the target protein as well as the thrombin. Thus, the GST-tagged Tlp1_HCD could not be used to develop a polyclonal antibody until it could be successfully isolated and the thrombin protease removed from the desired protein. Size-exclusion chromatography would be an alternative approach to try, however the similarity in weight between the Tlp1_HCD protein (36.5 kDa) and the molecular weight of thrombin (36 kDa) would make this somewhat problematic. Since this work however, the Tlp1 and Tlp2 to 4 HCD have been cloned into the pTrcHisB vector, expressed and purified successfully using a histidine-tag (Paul Ainsworth). These purified proteins were sent off for polyclonal antibody production (Eurogentec, Belgium). Initial screening using the Tlp1 primary polyclonal antibody generated against the HCD of Tlp1 with wild-type *C. jejuni* cells, has shown for the first time using immunofluorescence labelling that Tlp1 is found clustered at the cell poles (Figure 6.12).

6.5.2. Problems purifying GST-tagged Tlp proteins

An attempt was made in this work to clone, express and purify the C-terminal highly conserved signalling domain (HCD) in Tlp1 and Tlp2 to 4 (the C-terminal HCD in Tlp2 to 4 is identical in Tlp3 and Tlp4). The HCD in Tlp1 and Tlp2 to 4 was fused to an GST-tag to aid the successful purification of the target protein (domains) from a bacterial cell lysate containing other unwanted proteins. The Tlp1 and Tlp2 to 4 HCD were successfully cloned into an expression vector and protein expression proceeded as expected. However, difficulties were encountered when attempting to purify the Tlp1 HCD fused protein using a GSTrap column (Figure 6.7 (b)). When the crude cell lysate sample was first applied to the GSTrap column the majority of the target GST-tagged protein passed through the glutathione sepharose without binding to the immobilised glutathione ions and came out in the flow through (Figure 6.7 (b); lanes 1 and 2). The fusion protein continued to demonstrate poor binding when the wash buffer was applied to the GSTrap column (Figure 6.7 (b); lanes 3 and 4). Over sonication of the fusion protein could have denatured the GST-tag and therefore reduced the affinity of the fusion protein binding to the GSTrap column. This could explain the co-purification of other host proteins (Figure 6.7 (b)). Once the elution buffer was applied to the GSTrap column the majority of the contaminating proteins were no longer present (Figure 6.7 (b); lanes 4-8) although there was a band at the proposed position for the Tlp_1 HCD protein (63 kDa; Figure 6.7 (b); indicated with a black arrow). The target protein appeared to be masked by further band directly below the target protein which was approximately (Figure 6.7 (b); indicated with a red arrow). This may be a host protein in *E. coli* that has been purified along with the Tlp1_HCD protein. The chaperone protein DnaK is 70 kDa and this may have quite possibly been purified along with the fusion protein. The presence of the GST-tag and

the sizes of the Tlp1 and Tlp2 to 4 HCD fusion proteins were verified by western blot analysis (Figure 6.8) as well as by Mass Spectrometry (Data not shown; Personal communication, Laura Perrett). Due to time constraints the GST-tagged Tlp2 to 4 HCD has not been purified yet using the GSTrap column.

6.5.3. Future work using the polyclonal antibodies generated to the Tlps HCD

The primary data presented here has shown for the very first time that similarly to other bacteria the Tlps in *C. jejuni* are likely to localise at the poles of the *C. jejuni* cell (Figure 6.12). The work presented in this dissertation has only shown that this is the case for the Tlp1 chemoreceptor. A negative control was included in the experiments to establish background fluorescence and was used to confirm that the polar localisation of the Tlp1 chemoreceptors in *C. jejuni* was not due to non-specific staining of the secondary antibody (Figure 6.11 (c)). It would have been advantageous had further controls been set up in the immunofluorescence imaging studies. For example *C. jejuni* cells should have been treated with only the primary polyclonal antibody (no secondary antibody). This would have added further support to the data presented in this dissertation. No staining besides DAPI emitted blue fluorescence would have been expected upon staining cell using only the primary antibody. Analysis of the literature shows the carboxyl-terminal HCD to be highly conserved amongst all bacteria (Moual and Koshland, 1996). The clustering of the MCPs at the cell poles was originally discovered in *Caulobacter crescentus* followed by the enterics (Alley *et al.*, 1992; Maddock and Shapiro, 1993). In *C. crescentus* it is proposed that the N-terminal PLD of the MCP (which contains the transmembrane region) localises the MCP to the membrane whereas a region in the C-terminal

signalling domain is responsible for polar clustering (Alley *et al.*, 2007). The clustering of the MCPs at the cell poles has been observed in all bacteria and archaea to date (Gestwicki *et al.*, 2000). Antibodies raised to the cytoplasmic signalling region of the MCPs in other bacteria including *B. subtilis*, have been used successfully previous to this work (Kirby *et al.*, 2000). A secondary antibody tagged with a fluorescent marker could be used effectively, to visualise the MCPs within the cell by fluorescent microscopy (Maddock and Shapiro, 1993; Lamanna *et al.*, 2005). Further, the antibodies generated from the proteins purified in this work could be used to localise the Tlps in other strains of *C. jejuni*.

6.5.4. Expressing the Tlp1 Periplasmic domain of Tlp1

The N-terminal periplasmic ligand-binding domain of Tlp1 has been expressed since the commencement of this project using an N-terminal poly-histidine affinity tag (Hartley-Tassell *et al.*, 2010; Appendix 1). The Tlp1_Peri protein was used to determine the ligand-binding specificity of Tlp1 through an amino acid based array, which was further verified by saturation transfer difference-nuclear magnetic resonance spectroscopy (STD-NMR; Hartley-Tassell *et al.*, 2010). In the amino acid arrays, the His-tagged Tlp1_Peri fusion protein demonstrated a strong binding affinity to only L-aspartic acid. No binding was observed with other amino acids which have been reported to be chemoattractants in *C. jejuni* (Hugdahl *et al.*, 1988). These results were further verified by STD NMR analysis. The STD NMR spectrum showed that the Tlp1_Peri protein only contained peaks upon binding to the aspartate ligand.

As the His-tagged Tlp1_Peri fusion protein expressed in this study failed to solubilise (Figure 6.6), future work would be focused on performing inclusion body preparations on the Tlp1_Peri protein. Inclusion bodies can also be solubilised using

detergents such as 6 M guanidine hydrochloride. The use of this detergent (6 M guanidine hydrochloride) has already proven to be successful for purifying the GST-tagged Tlp1 protein. Thus, once purified Tlp1_Peri protein, the purified protein would be used to verify the biological data obtained for the receptor ligand specificity of the Tlp1 receptor. Potential applications for the Tlp1_Peri protein could be to use this protein to perform structural data on this domain and discover whether this domain produces an anti-parallel four-helix bundle similar to the Tar receptor of *E. coli* (Yeh *et al.*, 1993). Further work using the Tlp1_Peri protein will be discussed further in the final discussion chapter of this thesis.

Chapter 7. General discussion

7.1. Summary of main findings and conclusions

In the present work the genes encoding Transducer-like proteins (Tlp) 1, 2 and 4 in *Campylobacter jejuni* NCTC 11168 have been successfully inactivated using an insertional inactivation strategy (Chapter 3). The mutagenesis strategy undertaken involved deleting a significant portion of the open reading frame for each Tlp and then subsequently replacing the deleted region with a selectable marker.

Unfortunately, a final mutant in the *cj1564* (*tlp3*) gene in *C. jejuni* NCTC 11168 could not be obtained. A *tlp1* complement was constructed in this study to restore the wild-type phenotype in the *tlp1* isogenic mutant ($\Delta cj1506c::cat$) in *C. jejuni*. The *tlp1* complement was produced using the pRRK complementation system (Karlyshev and Wren, 2005). The use of this system enabled the efficient delivery and expression of a functional copy of the *cj1506c* gene back into the mutant *C. jejuni* chromosome ($\Delta cj1506c::cat$). Purified plasmid DNA of the final *tlp1* complementing construct (pRS12), containing a functional copy of the *cj1506c* gene (Chapter 3), was provided for our collaborator (Dr Victoria Korolik) along with chromosomal DNA from the *tlp1* mutant. Since the commencement of the writing of this dissertation the *tlp1* complement and *tlp1* isogenic mutant in *C. jejuni* have been analysed in *in vivo* caecal colonisation and *in vitro* adherence and invasion cell culture models using intestinal Caco-2 human intestinal cells (Hartley-Tassell *et al.*, 2010; Appendix 1). The adherence and invasion of the *tlp1* mutant to Caco-2 cells was found to be significantly higher compared to the wild-type (Hartley-Tassell *et al.*, 2010; Appendix 1). In order to verify the role of Tlp1 in colonisation of the host intestine,

both the *tlp1* isogenic mutant and the complemented mutant were tested *in vivo* for their ability to colonise the caecal tract in an avian model. The data demonstrated that there was an 11-fold reduction in colonisation ability of the *tlp1* mutant strain versus the wild-type strain and therefore providing evidence that the Tlp1 is required for colonisation of the host intestine by *C. jejuni* (Hartley-Tassell *et al.*, 2010; Appendix 1) and supports the importance of chemoreceptor based chemotaxis in colonization (Hendrixson and DiRita, 2004; Takata *et al.*, 1992; Yao *et al.*, 1997; Chang and Miller, 2006).

The *tlp1*, *tlp2* and *tlp4* mutants all showed an altered phenotype in the swarm assay (Chapter 5). The *tlp1* mutant swarmed significantly further than the wild-type motile-variant, whereas the *tlp4* mutant showed a reduction in spreading on plates. The *tlp2* mutant demonstrated a peculiar phenotype in the swarm assay where the edge of the swarm was irregular in shape, which rendered this mutant phenotype difficult to quantitate. The data from the swarm assay demonstrates that mutation in a Tlp is having a wider-scale effect on chemotaxis than originally predicted. Mutation in a Tlp perhaps is affecting the probable formation of receptor clusters at the poles of the cell (Kim *et al.*, 1999).

The Capillary assay (Adler, 1973) and a Hard-Agar Plug (Hugdahl *et al.*, 1988) assay were investigated and developed as methods to ascertain the ligand specificities of the Group A Tlp receptors. Unfortunately, the two versions of the Capillary assay attempted here in this work proved to be insufficiently reproducible for effective use with *C. jejuni* NCTC 11168 (Chapter 4; Adler, 1973; Mazumder *et al.*, 1999). Using a modified version of the HAP procedure, the work described in this dissertation has shown for the first time that *C. jejuni* NCTC 11168 is positively chemotactic towards serine, aspartate, glutamate and pyruvate (Chapter 4).

Furthermore, α -ketoglutarate may be a possible chemorepellent in *C. jejuni* as a zone of clearing was observed around a plug containing this substrate. The chemotactic responses determined in the wild-type *C. jejuni* motile-variant were used as the framework for comparing chemotactic responses in the *tlp* mutants.

The work undertaken to clone, express and purify domains in the Tlp1 and Tlp2 receptors of *C. jejuni* has been described in this dissertation in Chapter 6. The highly conserved signalling domains (HCDs) in Tlp1 and Tlp2 to 4 were purified successfully using a glutathione S-transferase affinity tag (Chapter 6). Interestingly, the GST tag was found to be hidden or blocked presumably by the HCD domain rendering it unable to bind to the specific affinity column; denaturation and subsequent refolding reinstated column binding. However, upon cleavage of the GST-tag using the protease thrombin; the Tlp1_HCD protein could not be isolated when applying the Tlp1_HCD protein to the Benzamidine column; the Benzamidine sepharose appeared to be binding the target protein as well as the thrombin. Since this work, the Tlp1 and Tlp2 to 4 HCD have been cloned into the pTrcHisB vector (Appendix 4.3 (c)), expressed and purified successfully using a histidine-tag (Paul Ainsworth; Chapter 6). These purified proteins were sent off for polyclonal antibody production (Eurogentec, Belgium). Initial screening using the Tlp1 primary antibody generated against the HCD of Tlp1 with wild-type *C. jejuni* cells, has shown for the first time using immunofluorescence labelling that the Tlps cluster at the cell poles.

At the commencement of this project the ligand-binding specificity of the Tlp1 receptor was unknown. Therefore, an attempt was made here in this project to purify the periplasmic ligand-binding domain (PLD) of Tlp1 from *C. jejuni* using a polyhistidine tag (Chapter 6). The PLD could not be purified successfully in the time available as the protein was found to be in-soluble and packaged into inclusion bodies

(Chapter 6). However, the PLD of Tlp1 has been successfully purified by other researchers and was used in an amino acid array (20 amino acids were screened in the array), whereby the Tlp1 PLD purified protein demonstrated a strong binding affinity for L-aspartic acid. These data were further verified by saturation transfer difference-nuclear magnetic resonance spectroscopy (STD NMR), which showed that the Tlp1_peri protein only contained peaks upon binding to the ligand aspartate (Hartley-Tassell *et al.*, 2010).

7.2. Chemoreceptors in other bacteria

The MCPs of *E. coli* are able to bind to ligands directly, for example to serine and aspartate, or to an attractant through a periplasmic binding protein (PBP) such as the maltose and glucose binding proteins (Grebe and Stock, 1998). No such PBP orthologue or sequence homologue has been identified to date in *C. jejuni*. The adaptation mechanism present in *C. jejuni* differs significantly from bacteria that are phylogenetically related. For instance, neither *Helicobacter pylori* nor *Wolinella succinogenes* have homologues of *cheR* and *cheB*. The HCD in Tlps1-4 as well as Tlp9 (CetA, Group B receptor) contains conserved glutamate and glutamine residues that are susceptible to methylation and demethylation by the chemotaxis proteins CheR and CheB, (methyltransferase and methylesterase, respectively; Figure 7.1). Nevertheless, both *H. pylori* and *W. succinogenes* possess multiple *cheV* genes and therefore it is quite possible that the CheV proteins may regulate an alternative adaptation pathway in these species. It is noteworthy that whilst *W. succinogenes* is also regarded as a close relative of *C. jejuni*, the presence of 26 putative MCPs in *W. succinogenes* suggests that *C. jejuni* is not as well adapted to different environments as *W. succinogenes* (Barr *et al.*, 2003).

7.3. A proposed model for chemoreceptor based chemotaxis signal transduction and pathogenesis in *C. jejuni*

The Group A Tlps share strong structural homology with the well characterised MCPs of *E. coli*. Monomers of MCPs in *E. coli* form stable homodimers (dimer-dimer interactions) in the cytoplasmic membrane. It is reported that these homodimers are further organised and packed into groups of three (i.e. trimers of dimers) to produce what appears to resemble a lattice at the poles of the cell (Kim *et al.*, 1999; Lamanna *et al.*, 2005). Furthermore, the packaging of the receptors to the poles of the cell is proposed to further enhance the sensitivity of the bacterial receptors to chemoeffectors (Lux and Shi, 2004; Sourjik, 2004). The Group B receptor in *C. jejuni* is CetA (Tlp9/Cj1190), for *Campylobacter* energy taxis (Figure 7.1). The CetA protein works together with CetB (Aer2/Cj1189) to co-ordinate responses involved in energy taxis in *C. jejuni* (Figure 7.1; Hendrixson *et al.*, 2001). It is proposed that while CetB monitors redox potentials this information is fed into the *C. jejuni* chemotaxis signal transduction pathway through the HCD in CetA to subsequently affect flagella rotation (Figure 7.1). A mechanism such as this would be beneficial in the microaerophilic campylobacters as they are extremely sensitive to levels of high oxygen (Hendrixson *et al.*, 2001; Bibikov *et al.*, 1997).

The Tlps 5, 6 and 8 form group C. These receptors are different to the other MCPs in *C. jejuni* in that they only contain the HCD domain. Interestingly, these are very similar to the group C receptors found in *H. salinarum* (Zhang *et al.*, 1996). The group C receptors are proposed to regulate chemotaxis in response to intracellular signals, which may require other cytoplasmic based ligand-binding proteins.

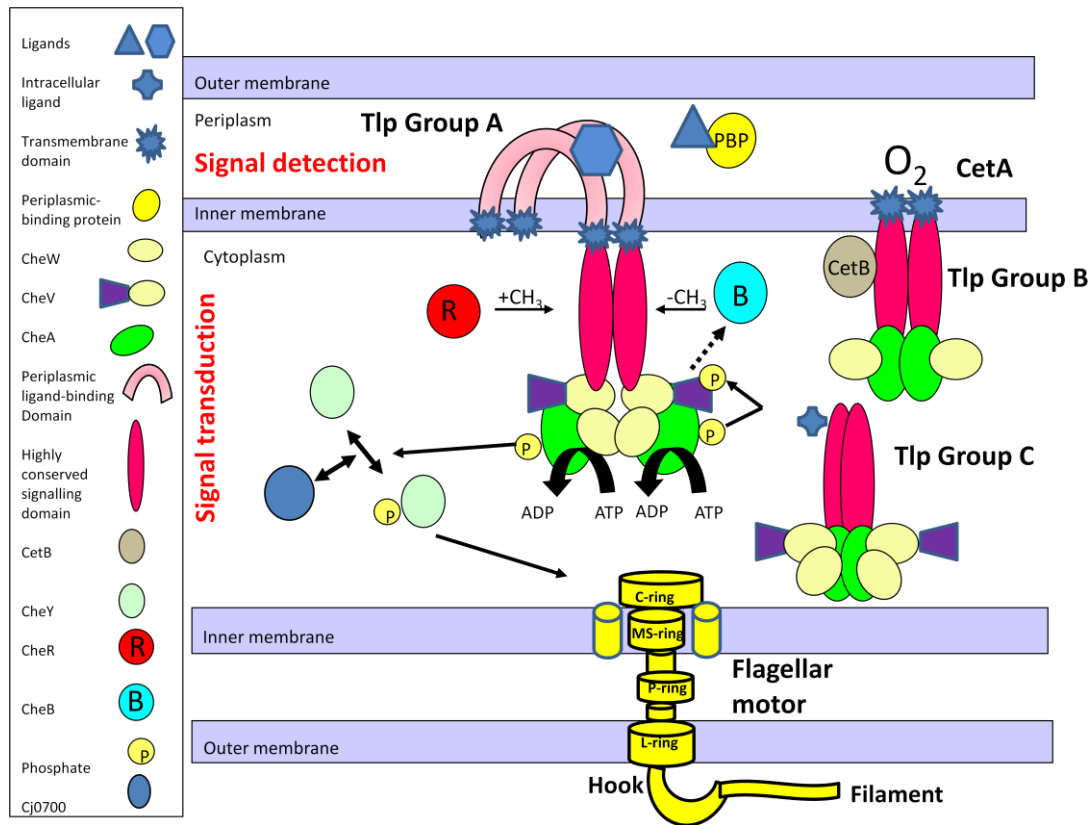


Figure 7.1. Proposed model for chemoreceptor based chemotaxis signal transduction in *Campylobacter jejuni*. There are three key pathways proposed to be in operation in *C. jejuni* in response to chemotactic signals. The group A chemoreceptors are located in the inner membrane of the cell and respond to external cues by either binding to ligand directly or through a PBP. *C. jejuni* is positively chemotactic towards the ligands L-serine, L-glutamate, L-aspartate and pyruvate. With α -ketoglutarate being a possible chemorepellent in *C. jejuni*. The Group A receptors are proposed to form a large cluster at the cell poles helping to accumulate mixed receptors with different ligand specificities at one position. For the Group B receptors, CetB responds to changes in redox potential and conveys this signal to the CetA protein as part of the aerotaxis chemotactic response. The group C receptors may regulate chemotactic responses to intracellular signals, these responses may be aided by other cytoplasmic based ligand-binding proteins. A potential PBP is shown in the diagram, but no PBP orthologue has been described in *C. jejuni*. Notable differences in the signal transduction pathway compared to the *E. coli* paradigm are: the presence of CheV and its proposed control of CheB due to the lack of response regulator domain in CheB; the presence of a response regulator domain on CheA (not shown) that likely indicates the existence of additional regulatory pathways; proposed role of Cj0700 in dephosphorylation of CheY despite poor homology with *E. coli* CheZ.

7.4. Future work and implications of research

The potential applications for the polyclonal antibodies raised to the HCD in Tlp1 and Tlp2 to 4 will be discussed here. The clustering of MCPs at the cell poles has been observed in all bacteria and archaea tested to date (Kirby *et al.*, 2000; Harrison *et al.*, 1999 Gestwicki *et al.*, 2000) and primary data from the work presented in this dissertation has indicated that it is likely to be the case for *C. jejuni* also. It may be advantageous if monoclonals specific to individual Group A receptor types are produced to determine relative receptor raft content and the effect of receptor mutation on cluster structure. CheR and CheB are part of the adaptation pathway in *C. jejuni*. The antibody developed in the present study could also be used to block the interaction of the putative methylation domains in Tlps 1-4 with CheB and CheR. In conjunction with the use of methylation assays and CheR/B mutants, such antibodies could be used to investigate the role of methylation in chemotaxis to different ligands. Furthermore, the HCD provides a docking domain for CheA, CheV and CheW to bind to, the antibody could be used to see if the binding of these proteins to the HCD has also been affected. Together, the HCD, CheW, and CheA form a ternary complex in the cytoplasm (Kim *et al.*, 1999) and the relative roles of CheW and CheV to binding to individual receptor HCDs could be investigated.

The swarm assay has been quite limited in the information it can provide regarding the *tlp* mutants. For example, the swarm assay cannot reveal whether a mutation in a Tlp has had any consequence on the rate of flagellar switching. A further drawback of the swarm assay is that the *tlp2* mutant constructed in the present study produced a deformed swarm phenotype from which an accurate measurement of the swarm diameter could not be obtained. Although a modified HAP assay was developed in this project, the reproducibility and quantitation of the assay was found

to be less than ideal. In the work described in this dissertation mutation of several Tlp receptors was not able to be conclusively used to establish receptor specificity. It is likely that this is due to the limitations of the HAP assay, but alternatively may reflect redundancy in receptor binding or, more likely, a pleiotropic effect due to receptor cluster disruption. Further modification and optimisation of the HAP assay is clearly necessary and the work of our collaborators (Hartley-Tassell *et al.*, 2010) has indicated some approaches to pursue; preliminary work along these lines has not been successful (data not shown). Given the problems encountered with the swarm and HAP assay, future work should focus more on establishing alternative chemotaxis assays such as video tracking or a tethered cell assay. A video tracking device has been employed previous to this study to assess a *cheY* mutant in *C. jejuni* which demonstrated a complete loss of chemotaxis in the swarm plate assay (Marchant *et al.*, 1998). Furthermore, by tracking individual *cheY* mutant cells they were found to be tumbling less frequently and showed a bias towards smooth swimming (Marchant *et al.*, 1998). Briefly, the tethered assay works as follows. In some methods such as the one described by Kirby *et al.* (2001) for *B. subtilis* the majority of the flagella is removed in the first instance, after which the cells are tethered to a glass coverslip using an anti-flagellin antibody. The coverslip is then inverted so that it forms the ceiling of a laminar flow chamber. Putative chemoattractants are then added to the flow chamber. The effects of individual attractants on the tethered cells is monitored using a combination of specialised equipment including a phase contrast microscope, a video recorder and a Hobson tracking program (Kirby *et al.*, 2001). The latter is used to track the motility of individual bacterial cells (Marchant, PhD thesis). An anti-flagellin antibody specific for *C. jejuni* is currently being developed (Abdullah Jama, personal communication). Assays based on video tracking or tethered cells

present different technical difficulties such as the delivery of ligand in slide based tracking set-ups (Dr Marchant found responses to ligands were very difficult to determine due to the rapid time scale of the response (Ketley, personal communication)) and maintenance of motility with tethered cells due to the need for microaerobic conditions.

It is proposed here that as the HCD in chemoreceptors is so well conserved amongst all bacteria and this domain is present within all of the secondary structures of ten out of the 12 Tlps in *C. jejuni* this would make an excellent candidate for targeting to disrupt colonisation. The importance of the Tlps in colonisation has already been demonstrated for *C. jejuni* (Takata *et al.*, 1992; Hendrixson and DiRita, 2004; Hartley-Tassell *et al.*, 2010) and chemotaxis is an important virulence mechanism in the *C. jejuni* infectious process (Takata *et al.*, 1992; Yao *et al.*, 1997; Golden *et al.*, 2002). The research undertaken in the present work will hopefully provide an insight into the chemoreceptor based signal transduction pathway in *C. jejuni* with the underlying aim of addressing the pressing issue of reducing the intestinal colonisation of this organism in poultry and subsequently in the human food chain.

Bibliography

Adak, G. K., Long, S. M. & O'Brien, S. J. 2002. Trends in indigenous food borne disease and deaths, England and Wales: 1992 to 2000. *Gut*. 51:832-841.

Adler, J. 1973. A method for measuring chemotaxis and use of the method to determine optimum conditions for chemotaxis by *Escherichia coli*. *Journal of General Microbiology*. 74:77-91.

Adler, J., Hazelbauer, G. L. & Dahl, M. M. 1973. Chemotaxis toward sugars in *Escherichia coli*. *Journal of Bacteriology*. 115:824-847.

Alam, M. & Hazelbauer, G.L. 1991. Structural features of methyl-accepting taxis proteins conserved between *Archaeobacteria* and *Eubacteria* revealed by antigenic cross-reaction. *Journal of Bacteriology*. 173:5837-5842.

Alexandre, G. & Zhulin, I. B. 2001. More than one way to sense chemicals. *Journal of Bacteriology*. 183:4681-4686.

Alley, M. R., Maddock, J. R. & Shapiro, L. 1992. Polar localization of a bacterial chemoreceptor. *Genes Dev*. 6:825-836.

Allos, B. M. 2001. *Campylobacter jejuni* Infections: update on emerging issues and trends. *Clinical Infectious Diseases*. 32:1201-1206.

Andermann, T. M., Chen, Y. & Ottemann, K. M. 2002. Two Predicted Chemoreceptors of *Helicobacter pylori* Promote Stomach Infection. *Infection and Immunity*. 70:5877-5881.

Armitage, J. P. 1999. Bacterial tactic responses. *Advances in Microbial Physiology*. 41:229-289.

Armitage, J. P. & Schmitt, R. 1997. Bacterial chemotaxis: *Rhodobacter sphaeroides* and *Sinorhizobium meliloti*--variations on a theme? *Microbiology*. 143:3671-3682.

Baar, C., Eppinger, M., Raddatz, G., Simon, J., Lanz, C., Klimmek, O., Nandakumar, R., Gross, R., Rosinus, A., Keller, H., Jagtap, P., Linke, B., Meyer, F., Lederer, H. & Schuster, S. C. 2003. Complete genome sequence and analysis of *Wolinella succinogenes*. *Proceedings of the National Academy of Sciences of the United States of America*. 100:11690-11695.

Bacon, D. J., Alm, R. A., Burr, D. H., Hu, L., Kopecko, D. J., Ewing, C. P., Trust, T. J. & Guerry, P. 2000. Involvement of a Plasmid in Virulence of *Campylobacter jejuni* 81-176. *Infection and Immunity*. 68:4384-4390.

Bardy, S. L. & Maddock, J. R. 2005. Polar Localization of a Soluble Methyl-Accepting Protein of *Pseudomonas aeruginosa*. *Journal of Bacteriology*. 187:7840-7844.

- Beery, J. T., Hugdahl, M. B. & Doyle, M. P.** 1988. Colonization of gastrointestinal tracts of chicks by *Campylobacter jejuni*. *Applied and Environmental Microbiology*. 54:2365-2370.
- Berg, H. C.** 2003. The rotary motor of bacterial flagella. *Annual Review of Biochemistry*. 72:19-54.
- Berry, R. M. & Armitage, J. P.** 1999. The bacterial flagella motor. *Advances in Microbial Physiology*. 41:291-337.
- Bereswill, S. & Kist, M.** 2003. Recent developments in *Campylobacter* pathogenesis. *Current Opinion in Infectious Diseases*. 16:487-491.
- Berg, H.C.** 2000. The rotary motor of bacterial flagella. *Annual Review of Biochemistry*. 72:19-54.
- Bibikov, S. I., Biran, R., Rudd, K. E. & Parkinson, J. S.** 1997. A signal transducer for aerotaxis in *Escherichia coli*. *Journal of Bacteriology*. 179:4075-4079.
- Black, R. E., Levine, M. M., Clements, M. L., Hughes, T. P. & Blaser, M. J.** 1988. Experimental *Campylobacter jejuni* infection in humans. *Journal of Infectious Diseases*. 157:472-479.
- Blaser, M. J., Hardesty, H. L., Powers, B. & Wang, W. L. L.** 1980. Survival of *Campylobacter fetus* subsp. *jejuni* in biological milieus. *Journal of clinical microbiology*. 11:309-313.
- Boin, M. A., Austin, M. J. & Häse, C. C.** 2004. Chemotaxis in *Vibrio cholerae*. *FEMS Microbiology Letters*. 239:1-8.
- Bren, A. & Eisenbach, M.** 2000. How Signals Are Heard during Bacterial Chemotaxis: Protein-Protein Interactions in Sensory Signal Propagation. *Journal of Bacteriology*. 182:6865-6873.
- Bridle, O.** 2007. An investigation into Chemotaxis in *Campylobacter jejuni*. *Department of genetics*. MPhil; University of Leicester.
- Bridle, O., Sandhu, R. & Ketley, J.M.** 2007. Identifying Protein-protein interactions in the chemotaxis system of *Campylobacter jejuni*. *Zoonoses Public Health*. 54:54.
- Brunius, G.** 1980. Technical Aspects of the use of 3', 6' – Diacetyl Fluorescein for Vital Fluorescent Staining of Bacteria. *Current Microbiology*. 4:321-323.
- Butzler, J. P., Dekeyser, P., Detrain, M. & Dehaen, F.** 1973. Related vibrio in stools. *The Journal of Pediatrics*. 82:493-495.
- Caldwell, M. B., Guerry, P., Lee, E. C., Burans, J. P. & Walker, R. I.** 1985. Reversible expression of flagella in *Campylobacter jejuni*. *Infection and Immunity*. 50:941-943.

- Calva, J. J., Ruiz-Palacios, G. M., Lopez-Vidal, A. B., Ramos, A. & Bojalil, R.** 1988. Cohort study of intestinal infection with *Campylobacter* in Mexican children. *Lancet*. I:503-506.
- Chang, C. & Miller, J.** 2006. *Campylobacter jejuni* colonization of mice with limited enteric flora. *Infection and Immunity*. 74:5261–5271.
- Chi, Y.I., Yokota, H. & Kim, S.H.** 1997. Apo structure of the ligand-binding domain of aspartate receptor from *Escherichia coli* and its comparison with ligand-bound or pseudoligand-bound structures. *FEBS Lett*. 414:327–332.
- Correa, N.E., Lauriano, C.M., McGee, R. & Klose, K.E.** 2000. Phosphorylation of the flagellar regulatory protein FlrC is necessary for *Vibrio cholerae* motility and enhanced colonization. *Molecular Microbiology*. 35:743–755.
- Croxen, M. A., Sisson, G., Melano, R. & Hoffman, P.S.** 2006. The *Helicobacter pylori* chemotaxis receptor TlpB (HP0103) is required for pH taxis and for colonization of the gastric mucosa. *Journal of Bacteriology*. 188:2656-2665.
- Dekeyser, P., Gossuin-Detrain, M., Butzler, J. P. & Sternon, J.** 1972. Acute enteritis due to related vibrio: first positive stool cultures. *Journal of Infectious Diseases*. 125:390-392.
- de Melo, M.A. & Pechere, J.C.** 1988. Effect of mucin on *Campylobacter jejuni* association and invasion on HEp-2 cells. *Microbial Pathogenesis*. 5:71-76.
- Dorrell, N., Gyselman, V. G., Foynes, S., Li, S. R. & Wren, B. W.** 1996. Improved efficiency of inverse PCR mutagenesis (IPCRM). *Biotechniques*. 21:604-608.
- Eaton, K. A., Suerbaum, S., Josenhans, C. & Krakowka, S.** 1996. Colonization of gnotobiotic piglets by *Helicobacter pylori* deficient in two flagellin genes. *Infection and Immunity*. 64:2445-2448.
- Elliott, K. T. & DiRita, V. J.** 2008. Characterization of CetA and CetB, a bipartite energy taxis system in *Campylobacter jejuni*. *Molecular Microbiology*. 69:1091-1103.
- Escherich, T.** 1886. Beiträge zur Kenntniss der Darmbakterien. III. Über das Vorkommen van Vibrionen im Darmcanal und den Stuhlgängen der Säuglinge. *Münchener Medizinische Wochenschrift* 33:815-817, 833-835.
- Everest, P., Goossens, H., Butzler, J. P., Lloyd, D., Knutton, S., Ketley, J. M. and Williams, P. H.** 1992. Differentiated Caco-2 cells as a model for enteric invasion by *Campylobacter jejuni* and *C. coli*. *Journal of Medical Microbiology*. 37:319-325.
- Falke, J. J. & Hazelbauer, G. L.** 2001. Transmembrane signaling in bacterial chemoreceptors. *Trends in Biochemical Sciences*. 26:257-265.
- Falke, J. J., Bass, R. B., Butler, S. L., Chervitz, S. A. & Danielson, M. A.** 1997. The two-component signaling pathway of bacterial chemotaxis: a molecular view of

signal transduction by receptors, kinases, and adaptation enzymes. *Annual Review of Cell and Developmental Biology*. 13:457-512.

Fauchère, J. L., Rosenau, A., Véron, M., Moyen, E.N., Richard, S. & Pfister, A. 1986. Association with HeLa cells of *Campylobacter jejuni* and *Campylobacter coli* isolated from human faeces. *Infection and Immunity*. 54:283-287.

Fisher, M. 1956. An unusual variant of acute idiopathic polyneuritis (syndrome of ophthalmoplegia ataxia and areflexia). *New England Journal of Medicine*. 255:57-65.

Fouts, D. E., Mongodin, E. F., Mandrell, R. E., Miller, W. G., Rasko, D. A., Ravel, J., Brinkac, L. M., DeBoy, R. T., Parker, C. T., Daugherty, S. C., Dodson, R. J., Durkin, A. S., Madupu, R., Sullivan, S. A., Shetty, J. U., Ayodeji, M. A., Shvartsbeyn, A., Schatz, M. C., Badger, J. H., Fraser, C. M. & Nelson, K. E. 2005. Major structural differences and novel potential virulence mechanisms from the genomes of multiple *Campylobacter* species. *PLoS Biology*. 3:0072-0085

Galibert, F., Finan, T. M., Long, S. R., Puhler, A., Abola, P., Ampe, F., Barloy-Hubler, F., Barnett, M. J., Becker, A., Boistard, P., Bothe, G., Boutry, M., Bowser, L., Buhrmester, J., Cadieu, E., Capela, D., Chain, P., Cowie, A., Davis, R. W., Dreano, S., Federspiel, N. A., Fisher, R. F., Gloux, S., Godrie, T., Goffeau, A., Golding, B., Gouzy, J., Gurjal, M., Hernandez-Lucas, I., Hong, A., Huizar, L., Hyman, R. W., Jones, T., Kahn, D., Kahn, M. L., Kalman, S., Keating, D. H., Kiss, E., Komp, C., Lelaure, V., Masuy, D., Palm, C., Peck, M. C., Pohl, T. M., Portetelle, D., Purnelle, B., Ramsperger, U., Surzycki, R., Thebault, P., Vandenbol, M., Vorholter, F. J., Weidner, S., Wells, D. H., Wong, K., Yeh, K. C. & Batut, J. 2001. The composite genome of the legume symbiont *Sinorhizobium meliloti*. *Science*. 293:668-672.

Gaynor, E.C., Cawthraw, S., Manning, G., MacKichan, J.K., Falkow, S., and Newell, D.G. 2004. The genome-sequenced variant of *Campylobacter jejuni* NCTC 11168 and the original clonal clinical isolate differ markedly in colonization, gene expression, and virulence-associated phenotypes. *Journal of Bacteriology*. 186:503–517.

George, H. A., Hoffman, P. S., Smibert, R. M. & Krieg, N. R. 1978. Improved media for growth and aerotolerance of *Campylobacter fetus*. *Journal of Clinical Microbiology*. 8:36-41.

Gestwicki, J. E., Lamanna, A.C., Harshey, R.M., McCarter, L.L., Kiessling, L.L. & Adler, J. 2000. Evolutionary conservation of methyl-accepting chemotaxis protein location in bacteria and archaea. *Journal of Bacteriology*. 182:6499-6502.

Golden, N. J. & Acheson, D. W. K. 2002. Identification of motility and autoagglutination *Campylobacter jejuni* mutants by random transposon mutagenesis. *Infection and Immunity*. 70:1761-1771.

Golden, N. J., Camilli, A. & Acheson, D. W. K. 2000. Random Transposon Mutagenesis of *Campylobacter jejuni*. *Infection and Immunity*. 68:5450-5453.

- Grant, C. C., Konkel, M. E., Cieplak, W. J. & Tompkins, L. S.** 1993. Role of flagella in adherence, internalization, and translocation of *Campylobacter jejuni* in nonpolarized and polarized epithelial cell cultures. *Infection and Immunity*. 61:1764-1771.
- Grebe, T. W. & Stock, J.** 1998. Bacterial chemotaxis: The five sensors of a bacterium. *Current Biology*. 8:R154-R157.
- Güvener, Z. T., Tifrea, D. F. & Harwood, C. S.** 2006. Two different *Pseudomonas aeruginosa* chemosensory signal transduction complexes localize to cell poles and form and remould in stationary phase. *Molecular Microbiology*. 61:106-118.
- Hanlon, D. W. & Ordal, G. W.** 1994. Cloning and characterization of genes encoding methyl-accepting chemotaxis proteins in *Bacillus subtilis*. *Journal of Biological Chemistry*. 269:14038-14046.
- Harris, L. A., Logan, S. M., Guerry, P. and Trust, T. J.** 1987. Antigenic variation of *Campylobacter* flagella. *Journal of Bacteriology*. 169:5066-5071.
- Harrison, D. M., Skidmore, J., Armitage, J. P. & Maddock, J. R.** 1999. Localization and environmental regulation of MCP-like proteins in *Rhodobacter sphaeroides*. *Molecular Microbiology*. 31:885-892.
- Hartley-Tassell, L.E., Shewell, L.K., Day, C.J., Wilson, J.C., Sandhu, R., Ketley, J.M. & Korolik, V.** 2010. Identification and characterization of the aspartate chemosensory receptor of *Campylobacter jejuni*. *Molecular Microbiology*. 75:710-730.
- Hazeleger, W.C., Wouters, J.A., Rombouts, F.M. & Abee, T.** 1998. Physiological activity of *Campylobacter jejuni* far below the minimal growth temperature. *Applied and Environmental Microbiology*. 64:3917-3922.
- Hendrixson, D. R., Akerley, B. J. & DiRita, V. J.** 2001. Transposon mutagenesis of *Campylobacter jejuni* identifies a bipartite energy taxis system required for motility. *Molecular Microbiology*. 40:214-224.
- Hendrixson, D. R. & DiRita, V. J.** 2004. Identification of *Campylobacter jejuni* genes involved in commensal colonization of the chick gastrointestinal tract. *Molecular Microbiology*. 52:471-484.
- Hofmann, K. & Stoffel, W.** 1993. TMbase- A database of membrane spanning protein segments. *Biological Chemistry. Hoppe-Seyler*. 347:166
- Hofreuter, D., Tsai, J., Watson, R. O., Novik, V., Altman, B., Benitez, M., Clark, C., Perbost, C., Jarvie, T., Du, L. & Galán, J. E.** 2006. Unique features of a highly pathogenic *Campylobacter jejuni* strain. *Infection and Immunity*. 74:4694-4707.
- Hou, S., Larsen, R.W., Boudko, D., Riley, C.W., Karatan, E., Zimmer, M., Ordal, G.W. & Alam, M.** 2000. Myoglobin-like aerotaxis transducers in Archaea and Bacteria. *Nature*. 403:540-544.

- Hu, L. & Kopecko, D.J. (Edited by Ketley J. M. & Konkel. M. E.).** 2005. *Invasion*; in *Campylobacter: Molecular and Cellular Biology*, Horizon Bioscience. pp. 369-385.
- Hugdahl, M. B., Beery, J. T. & Doyle, M. P.** 1988. Chemotactic behavior of *Campylobacter jejuni*. *Infection and Immunity*. 56:1560-1566.
- Jagannathan, A., Constantinidou, C. & Penn, C. W.** 2001. Roles of *rpoN*, *fliA*, and *flgR* in expression of flagella in *Campylobacter jejuni*. *Journal of Bacteriology*. 183:2937-2942.
- Jagannathan, A. & Penn, C. (Edited by Ketley J. M. & Konkel. M. E.).** 2005. *Motility*; in *Campylobacter: Molecular and Cellular Biology*, Horizon Bioscience. pp. 331-348.
- Jin, S., Joe, A., Lynett, J., Hani, E. K., Sherman, P. & Chan, V. L.** 2001. JlpA, a novel surface-exposed lipoprotein specific to *Campylobacter jejuni*, mediates adherence to host epithelial cells. *Molecular Microbiology*. 39:1225-1236.
- Josenhans, C. & Suerbaum, S.** 2002. The role of motility as a virulence factor in bacteria. *International Journal of Medical Microbiology*. 291:605-614.
- Karatan, E., Saulmon, M. M., Bunn, M. W. & Ordal, G. W.** 2001. Phosphorylation of the response regulator CheV Is required for adaptation to attractants during *Bacillus subtilis* chemotaxis. *Journal of Biological Chemistry*. 276:43618-43626.
- Karlyshev, A. V. & Wren, B. W.** 2005. Development and application of an insertional system for gene delivery and expression in *Campylobacter jejuni*. *Applied and Environmental Microbiology*. 71:4004-4013.
- Karlyshev, A. V., Ketley, J. M. & Wren, B. W.** 2005. The *Campylobacter jejuni* glycome. *FEMS Microbiology Reviews*. 29:377-390.
- Karlyshev, A. V., Linton, D., Gregson, N. A. & Wren, B. W.** 2002. A novel paralogous gene family involved in phase-variable flagella-mediated motility in *Campylobacter jejuni*. *Microbiology*. 148:473-480.
- Ketley, J. M.** 1997. Pathogenesis of enteric infection by *Campylobacter*. *Microbiology*. 143:5-21.
- Khanna, M.R., Bhavsar, S.P. & Kapadnis, B.P.** 2006. Effect of temperature on growth and chemotactic behaviour of *Campylobacter jejuni*. *Letters in Applied Microbiology*. 43:84-90.
- Kim, K. K., Yokota, H. & Kim, S. H.** 1999. Four-helical bundle structure of the cytoplasmic domain of a serine chemotaxis receptor. *Nature*. 400:787-792.
- Kim, C., Jackson, M., Lux, R. & Khan, S.** 2001. Determinants of chemotactic signal amplification in *Escherichia coli*. *Journal of Molecular Biology*. 307:119-135.

Kinsella, N., Guerry, P., Cooney, J. & Trust, T. J. 1997. The *flgE* gene of *Campylobacter coli* is under the control of the alternative sigma factor σ^{54} . *Journal of Bacteriology*. 179:4647-4653.

Kirby, J. R. , Kristich, C. J., Saulmon, M. M., Zimmer, M. A., Garrity, L. F., Zhulin, I. B. & Ordal, G. W. 2001. CheC is related to the family of flagellar switch proteins and acts independently from CheD to control chemotaxis in *Bacillus subtilis*. *Molecular Microbiology*. 42:573-585.

Kirby, J. R., TB Niewold, T. B., Maloy, S. & Ordal, G. W. 2000. CheB is required for behavioural responses to negative stimuli during chemotaxis in *Bacillus subtilis*. *Molecular Microbiology*. 35:44-57.

Kirby, J. R., Saulmon, M. M., Kristich, C. J. & Ordal, G. W. 1999. CheY-dependent methylation of the asparagine receptor, McpB, during chemotaxis in *Bacillus subtilis*. *Journal of Biological Chemistry*. 274:11092-11100.

Konkel, M. E., Garvis, S. G., Tipton, S. L., Anderson, D. E. & Cieplak, W. 1997. Identification and molecular cloning of a gene encoding a fibronectin-binding protein (CadF) from *Campylobacter jejuni*. *Molecular Microbiology*. 24:953-963.

Konkel, M. E., Grey, S. A., Kim, B. J., Garvis, S. G. & Yoon, J. 1999. Identification of the enteropathogens *Campylobacter jejuni* and *Campylobacter coli* based on the *cadF* virulence gene and its product. *Journal of Clinical Microbiology*. 37:510-517.

Korolik, V. & Ketley, J.M. (Edited by Nachamkin, I., Szymanski, C.M., and Blaser, M.J.). 2008. *Campylobacter chemosensory pathway*; in *Campylobacter*, 3rd edn, American Society for Microbiology, pp. 351–366.

Kristich, C. J. & Ordal, G. W. 2002. *Bacillus subtilis* CheD Is a chemoreceptor modification enzyme required for chemotaxis. *Journal of Biological Chemistry*. 277: 25356-25362.

Kunst, F., Ogasawara, N., Moszer, I., Albertini, A.M., Alloni, G., Azevedo, V., , Bertero, M.G, Bessieres, P., Bolotin, A., Borchert, S., , Borriss, R., Boursier, L., Brans, A., Braun, M., Brignell, S.C., Bron, S., Brouillet, S., Bruschi, C.V., Caldwell, B., Capuano, V., Carter, N.M., Choi, S.K., Codani, J.J., Connerton, I.F. *et al.* 1997. The complete genome sequence of the gram-positive bacterium *Bacillus subtilis*. *Nature*. 390:249–256.

Labigne-Roussel, A., Courcoux, P. & Tompkins, L. 1988. Gene disruption and replacement as a feasible approach for mutagenesis of *Campylobacter jejuni*. *Journal of Bacteriology*. 170:1704-1708.

Lamanna, A.C., Ordal, G.W. & Kiessling, L.L. 2005. Large increases in attractant concentration disrupt the polar localization of bacterial chemoreceptors. *Molecular Microbiology*. 57:774-785.

Lastovica, A. J. & Skirrow, M. B. 2008. Clinical significance of *Campylobacter* and related species other than *Campylobacter jejuni* and *C. coli*; in *Campylobacter*, 3rd edn, *American Society for Microbiology*. pp. 89-120.

Lee, A., O'Rourke, J. L., Barrington, P. J. & Trust, T. J. 1986. Mucus colonization as a determinant of pathogenicity in intestinal infection by *Campylobacter jejuni*: a mouse cecal model. *Infection and Immunity*. 51:536-546.

Lee, L. H., Burg III, E., Baqar, S., Bourgeois, A. L., Burr, D. H., Ewing, C. P., Trust, T. J. & Guerry, P. 1999. Evaluation of a Truncated Recombinant Flagellin Subunit Vaccine against *Campylobacter jejuni*. *Infection and Immunity*. 67:5799-5805.

Levit, M. N., Liu, Y. & Stock, J. B. 1998. Stimulus response coupling in bacterial chemotaxis: receptor dimers in signalling arrays. *Molecular Microbiology*. 30:459-466.

Linton, D., Karlyshev, A. V. & Wren, B. W. 2001. Deciphering *Campylobacter jejuni* cell surface interactions from the genome sequence. *Current Opinion in Microbiology*. 4:35-40.

Linton, D., Gilbert, M., Hitchen, P. G., Dell, A., Morris, H. R., Wararchuk, W. W., Gregson, N. A. & Wren, B. W. 2000. Phase variation of a β -1,3 galactosyltransferase involved in generation of the ganglioside GM1-like lipo-oligosaccharide of *Campylobacter jejuni*. *Molecular Microbiology*. 37:501-514.

Lux, R. & Shi, W. 2004. Chemotaxis-guided movements in bacteria. *Critical Reviews in Oral Biology Medicine*. 15:207-220.

Macnab, R. M. 2003. How bacteria assemble flagella. *Annual Review of Microbiology*. 57:77-100.

Maddock, J. R. & Shapiro, L. 1993. Polar location of the chemoreceptor complex in the *Escherichia coli* cell. *Science*. 259:1717-1723.

Madigan, M. T., Martinko, J. M. & Parker, J. 2003. *Brock Biology of Microorganisms*, 10th edn, Pearson Education. pp. 82-85.

Manson, M. D., Armitage, J. P., Hoch, J. A. & Macnab, R. M. 1998. Bacterial locomotion and signal transduction. *Journal of Bacteriology*. 180:1009-1022.

Marchant, J.E. 1999. Studies into the chemotaxis of *Campylobacter jejuni*. *Department of Genetics*. PhD; University of Leicester.

Marchant, J., Wren, B. & Ketley, J. 2002. Exploiting genome sequence: predictions for mechanisms of *Campylobacter* chemotaxis. *Trends in Microbiology*. 10:155-159.

Marchant, J.E., Henderson, J., Wren, B. & Ketley, J.M (Edited by Lastovica, A.J., Newell, D. & Lastovica, E. E.). 1998. Role of the *cheY* gene in the chemotaxis

of *Campylobacter jejuni*; in *Campylobacter, Helicobacter and Related Organisms. Institute of Child Health*. pp. 306-311.

Martin, A. C., Wadhams, G. H. & Armitage, J. P. 2001. The roles of the multiple CheW and CheA homologues in chemotaxis and in chemoreceptor localization in *Rhodobacter sphaeroides*. *Molecular Microbiology*. 40:1261-1272.

Mattick, J. S. 2002. Type IV pili and twitching motility. *Annual Review of Microbiology*. 56:289-314.

Mazumder, R., Phelps, T. J., Krieg, N. R. & Benoit, R. E. 1999. Determining chemotactic responses by two subsurface microaerophiles using a simplified capillary assay method. *Journal of Microbiological Methods*. 37:255-263.

McBride M.J. 2001. Bacterial gliding motility: multiple mechanisms for cell movement over surfaces. *Annual Review of Microbiology*. 55:49-75.

McFadyean, F. & Stockman, S. 1913. *Report of the departmental committee appointed by the board of agriculture and fisheries to enquire into epizootic abortion, III*. London: HMSO.

McSweegan, E. & Walker, R. I. 1986. Identification and characterization of two *Campylobacter jejuni* adhesins for cellular and mucous substrates. *Infection and Immunity*. 53:141-148.

Meier, V., Muschler, P. & Scharf, B. 2007. Functional Analysis of Nine Putative Chemoreceptor Proteins in *Sinorhizobium meliloti*. *Journal of Bacteriology*. 189:1816-1826.

Merrell, D.S., Butler, S.M., Qadri, F., Dolganov, N.A., Alam, A., Cohen, M.B., Calderwood, S.B., Schoolnik, G.K. & Camilli, A. 2002. Host-induced epidemic spread of the cholera bacterium. *Nature*. 417:642-645.

Miller, W. G. & Mandrell, R. E. (Edited by Ketley J. M. & Konkel. M. E.). 2005. *Prevalence of Campylobacter in the food and water supply: Incidence, outbreaks, isolation and detection*; in *Campylobacter: Molecular and Cellular Biology*, Horizon Bioscience. pp. 101-163.

Miller, C. E., Rock, J. D., Ridley, K. A., Williams, P. H. & Ketley, J. M. 2008. Utilization of Lactoferrin-Bound and Transferrin-Bound Iron by *Campylobacter jejuni*. *Journal of Bacteriology*. 190:1900-1911.

Milligan, D. L. & Koshland, D. E., Jr. 1988. Site-directed crosslinking. Establishing the dimeric structure of the aspartate receptor of bacterial chemotaxis. *Journal of Biological chemistry*. 263:6268-6275.

Morooka, T., Umeka, A. & Amako, K. 1985. Motility as an intestinal colonization factor for *Campylobacter jejuni*. *Journal of General Microbiology*. 131:1973- 1980.

- Motaleb, M. A., Miller, M. R., Li, C., Bakker, R. G., Goldstein, S. F., Silversmith, R. E., Bourret, R. B. & Charon, N. W.** 2005. CheX Is a Phosphorylated CheY Phosphatase Essential for *Borrelia burgdorferi* Chemotaxis. *Journal of Bacteriology*. 187:7963-7969.
- Moual, H. L. & Koshland D. E.** 1996. Molecular evolution of the C-terminal cytoplasmic domain of a superfamily of bacterial receptors involved in taxis. *J. Mol. Biol.* 261:568–585.
- Müller, J., Schiel, S., Ordal, G.W. & Saxild, H.H.** 1997. Functional and genetic characterization of mcpC, which encodes a third methyl-accepting chemotaxis protein in *Bacillus subtilis*. *Microbiology*. 143:3231–3240.
- Nachamkin, I., Allos, B. M. & Ho, T.** 1998. *Campylobacter* species and Guillain-Barré syndrome. *Clinical Microbiology Reviews*. 11:555-567.
- Nachamkin, I., Yang, X. H. & Stern, N. J.** 1993. Role of *Campylobacter jejuni* flagella as colonization factors for three-day-old chicks: analysis with flagellar mutants. *Applied and Environmental Microbiology*. 59:1269-1273.
- Nuijten, P. J., van Asten, F. J., Gaastra, W. & van der Zeijst, B. A.** 1990a. Structural and functional analysis of two *Campylobacter jejuni* flagellin genes. *Journal of Biological Chemistry*. 265:17798-17804.
- Nuijten, P. J., Bartels, C., Bleumink-Pluym, N. M., Gaastra, W. & van der Zeijst, B. A. M.** 1990b. Size and physical map of the *Campylobacter jejuni* chromosome. *Nucleic Acids Research*. 18:6211-6214.
- Nuijten, P. J. M., van den Berg, A. J. G., Formentini, I., van der Zeijst, B. A. M. & Jacobs, A. A. C.** 2000. DNA rearrangements in the flagellin locus of a *flaA* mutant of *Campylobacter jejuni* during colonization of chicken ceca. *Infection and Immunity*. 68:7137-7140.
- On, S. L. W. (Edited by Ketley J. M. & Konkel. M. E.).** 2005. *Taxonomy, phylogeny, and methods for the identification of Campylobacter species; in Campylobacter: Molecular and Cellular Biology*, Horizon Bioscience. pp. 13-42.
- Ottemann, K. M. & Miller, J. F.** 1997. Roles for motility in bacterial host-interactions. *Molecular Microbiology*. 24:1109-1117.
- Palyada, K., Threadgill, D. & Stintzi, A.** 2004. Iron acquisition and regulation in *Campylobacter jejuni*. *Journal of Bacteriology*. 186:4714-4729.
- Park, S. F.** 2002. The physiology of *Campylobacter* species and its relevance to their role as foodborne pathogens. *International Journal of Food Microbiology*. 74:177-188.
- Park, S. Y., Chao, X., Gonzalez-Bonet, G., Beel, B. D., Bilwes, A. M. & Crane. B. R.** 2004. Structure and function of an unusual family of protein phosphatases: The bacterial chemotaxis proteins CheC and CheX. *Molecular Cell Biology*. 16:563-574.

Parkhill, J., Wren, B. W., Mungall, K., Ketley, J. M., Churcher, C., Basham, D., Chillingworth, T., Davies, R. M., Feltwell, T., Holroyd, S., Jagels, K., Karlyshev, A. V., Moule, S., Pallen, M. J., Penn, C. W., Quail, M. A., Rajandream, M.-A., Rutherford, K. M., van Vliet, A. H. M., Whitehead, S. & Barrell, B. G. 2000. The genome sequence of the food-borne pathogen *Campylobacter jejuni* reveals hypervariable sequences. *Nature*. 403:665-668.

Parrish, J.R., Yu, J., Liu, G., Hines, J.A., Chan, J.E., Mangiola, B.A., Zhang, H., Pacifico, S., Fotouhi, Dirita, F.V.J., Ideker, T., Andrews, P. & Finley, R.L. Jr. 2007. A proteome-wide protein interaction map for *Campylobacter jejuni*. *Genome Biology*. 8:R130.1-R130.19

Paster, B. J. & Gibbons, R. J. 1986. Chemotactic response to formate by *Campylobacter concisus* and its potential role in gingival colonization. *Infection and Immunity*. 52:378-383.

Pearson, B. M., Gaskin, D. J. H., Segers, R. P. A. M., Wells, J. M., Nuijten, P. J. M. & van Vliet, A. H. M. 2007. The complete genome sequence of *Campylobacter jejuni* strain 81116 (NCTC11828). *Journal of Bacteriology*. 189:8402-8403.

Pei, Z., Burucoa, C., Grignon, B., Baqar, S., Huang, X. Z., Kopecko, D. J., Bourgeois, A. L., Fauchère, J. L. & Blaser, M. J. 1998. Mutation in *peb1A* of *Campylobacter jejuni* reduces interactions with epithelial cells and intestinal colonization of mice. *Infection and Immunity*. 66:938-943.

Pham, H., K. J. Dery, D. J. Sherratt & M. E. Tolmasky. 2002. Osmoregulation of dimer resolution at the plasmid pJHCMW1 *mwr* locus by *Escherichia coli* XerCD recombination. *Journal of Bacteriology*. 184:1607-1616.

Pickett, C. L. & Lee, R.B. (Edited by Ketley J. M. & Konkel. M. E.). 2005. *Cytolethal distending toxin*; in *Campylobacter: Molecular and Cellular Biology*, Horizon Bioscience. pp. 385-396.

Pittman, M. S., Goodwin, M. & Kelly, D. J. 2001. Chemotaxis in the human gastric pathogen *Helicobacter pylori*: different roles for CheW and the three CheV paralogues, and evidence for CheV2 phosphorylation. *Microbiology*. 147:2493-2504.

Porter, S.L. & J.P. Armitage. 2002. Phosphotransfer in *Rhodobacter sphaeroides* chemotaxis. *Journal of Molecular Biology*. 324:35-45.

Porter, S.L., Warren, A.V., Martin, A.C. & Armitage J.P. 2002. The third chemotaxis locus of *Rhodobacter sphaeroides* is essential for chemotaxis. *Molecular Microbiology*. 46:1081–1094.

Purdy, D., Buswell, C.M., Hodgeson, A.E., McAlpine, K., Henderson, I. & Leach, S.A. 2000. Characterisation of cytolethal distending toxin (CDT) mutants of *Campylobacter jejuni*. *Journal of Medical Microbiology*. 49:473-479.

- Quinones, B., Miller, W. G., Bates, A. H. & Mandrell, R. E.** 2009. Autoinducer-2 Production in *Campylobacter jejuni* Contributes to Chicken Colonization. *Applied and Environmental Microbiology*. 75:281-285.
- Ridley, K. A., Li, Y., Rock, J. D. & Ketley, J. M.** 2006. Heme utilization in *Campylobacter jejuni*. *Journal of Bacteriology*. 188:7862-7875.
- Rollins, D. M. & Colwell, R. R.** 1986. Viable but nonculturable stage of *Campylobacter jejuni* and its role in survival in the natural aquatic environment. *Applied and Environmental Microbiology*. 52:531-538.
- Rosario, M. M., Fredrick, K. L., Ordal, G. W. & Helmann, J. D.** 1994. Chemotaxis in *Bacillus subtilis* requires either of two functionally redundant CheW homologs. *Journal of Bacteriology*. 176:2736-2739.
- Sambrook, J. & Russell, D.** 2001. *Molecular cloning: a laboratory manual*, 3rd edn, Cold Spring Harbor Laboratory Press.
- Saulmon, M. M., Karatan, E. & Ordal, G. W.** 2004. Effect of loss of CheC and other adaptational proteins on chemotactic behaviour in *Bacillus subtilis*. *Microbiology*. 150:581-589.
- Schmitt, R.** 2002. Sinorhizobial chemotaxis: a departure from the enterobacterial paradigm. *Microbiology*. 148:627-631.
- Schubert, S., Fischer, D. & Heesemann, J.** 1999. Ferric Enterochelin Transport in *Yersinia enterocolitica*: Molecular and Evolutionary Aspects. *Journal of Bacteriology*. 181:6387-6395.
- Sébal, M. & Véron, M.** 1963. Teneur en bases de l'ADN et classification des vibrions. *Ann Inst Pasteur*. 105:897-910.
- Shanker, S., Lee, A. & Sorrell, T.C.** 1990. Horizontal transmission of *Campylobacter jejuni* amongst broiler chicks: experimental studies. *Epidemiology and Infection*. 104:101-110.
- Shreeve, J. E., Toszeghy, M., Pattison, M. & Newell, D. G.** 2000. Sequential spread of *Campylobacter* infection in a multipen broiler house. *Avian Diseases*. 44:983-988.
- Skirrow, M. B.** 1994. Diseases due to *Campylobacter*, *Helicobacter* and related bacteria. *Journal of Comparative Pathology*. 111:113-149.
- Skirrow, M. B. & Blaser, M. J. (Edited by Nachamkin, I., Blaser, M. J. & Tompkins L. S.)** 1992. *Clinical and epidemiological considerations; in Campylobacter jejuni: current status and future trends*, American society for microbiology. pp 3-8.
- Skirrow, M. B.** 1977. *Campylobacter* enteritis: a 'new' disease. *British Medical Journal (Clinical Research Ed)*. 2:9-11.

- Smith, M. A. & Bidochka, M. J.** 1998. Bacterial fitness and plasmid loss: the importance of culture conditions and plasmid size. *Canadian Journal of Microbiology*. 44:351-355.
- Sourjik, V.** 2004. Receptor clustering and signal processing in *E. coli* chemotaxis. *Trends in Microbiology*. 12:569-576.
- Sourjik, V. & Schmitt, R.** 1998. Phosphotransfer between CheA, CheY1, and CheY2 in the chemotaxis signal transduction chain of *Rhizobium meliloti*. *Biochemistry*. 37:2327-2335.
- Sourjik, V. & Schmitt, R.** 1996. Different roles of CheY1 and CheY2 in the chemotaxis of *Rhizobium meliloti*. *Molecular Microbiology*. 22:427-436.
- Stock, J. & Re, S. D.** 1999. A receptor scaffold mediates stimulus-response coupling in bacterial chemotaxis. *Cell Calcium*. 26:157-164.
- Suerbaum S, Josenhans C, Sterzenbach T, Drescher B, Brandt P, Bell M, Droge M, Fartmann B, Fischer HP, Ge Z, Horster A, Holland R, Klein K, Konig J, Macko L, Mendz GL, Nyakatura G, Schauer DB, Shen Z, Weber J, Frosch M, Fox JG.** 2003. The complete genome sequence of the carcinogenic bacterium *Helicobacter hepaticus*. *Proceedings of the National Academy of Sciences of the United States of America*. 100:7901-7906.
- Szurmant, H., Bunn, M. W., Cannistraro, V. J. & Ordal, G. W.** 2003. *Bacillus subtilis* hydrolyzes CheY-P at the location of its action, the flagellar switch. *Journal of Biological Chemistry*. 278:48611-48616.
- Szurmant, H. & Ordal, G. W.** 2004. Diversity in Chemotaxis Mechanisms among the Bacteria and Archaea. *Microbiol. Mol. Biol. Rev.* 68:301-319.
- Szymanski, C. M., King, M., Haardt, M. & Armstrong, G. D.** 1995. *Campylobacter jejuni* motility and invasion of Caco-2 cells. *Infection and Immunity*. 63:4295-4300.
- Szymanski, C. M., Logan, S. M., Linton, D. & Wren, B. W.** 2003. *Campylobacter* - a tale of two protein glycosylation systems. *Trends in Microbiology*. 11:233-238.
- Taylor, D. N., Echeverria, P., Pitarangsi, C., Seriwatana, J., Bodhidatta, L. & Blaser, M. J.** 1988. Influence of strain characteristics and immunity on the epidemiology of *Campylobacter* infections in Thailand. *Journal of Clinical Microbiology*. 26:863-868.
- Takata, T., Fujimoto, S. & Amako, K.** 1992. Isolation of nonchemotactic mutants of *Campylobacter jejuni* and their colonization of the mouse intestinal tract. *Infection and Immunity*. 60:3596-3600.
- Terry, K., Go, A. C. & Ottemann, K. M.** 2006. Proteomic mapping of a suppressor of non-chemotactic cheW mutants reveals that *Helicobacter pylori* contains a new chemotaxis protein. *Molecular Microbiology*. 61:871-882.

Tisa L.S. & Adler J. 1992. Calcium ions are involved in *Escherichia coli* chemotaxis. *Proceedings of the National Academy of Sciences of the United States of America*. 89:11804–11808.

Tomb, J.F., White, O., Kerlavage, A.R., Clayton, R.A., Sutton, G.G., Fleischmann, R.D., Ketchum, K.A., Klenk, H.P., Gill, S., Dougherty, B.A., Nelson, K., Quackenbush, J., Zhou, L., Kirkness, E.F., Peterson, S., Loftus, B., Richardson, D., Dodson, R., Khalak, H.G., Glodek, A., McKenney, K., Fitzegerald, L.M., Lee, N., Adams, M.D., Hickey, E.K., Berg, D.E., Gocayne, J.D., Utterback, T.R., Peterson, J.D., Kelley, J.M., Cotton, M.D., Weidman, J.M., Fujii, C., Bowman, C., Watthey, L., Wallin, E., Hayes, W.S., Borodovsky, M., Karp, P.D., Smith, H.O., Fraser, C.M. & Venter, J.C. 1997. The complete genome sequence of the gastric pathogen *Helicobacter pylori*. *Nature*. 388:539-547.

van Vliet, A. H. M. & Ketley, J. M. 2001. Pathogenesis of enteric *Campylobacter* infection. *Journal of Applied Microbiology*. 90:45S-56S.

Wadhams, G. H. & Armitage, J. P. 2004. Making sense of it all: bacterial chemotaxis. *Nature Reviews*. 5:1024-1037.

Ward, M. J., Harrison, D.M., Ebner, D. M., Packer, H. L. & Armitage, J. P. 1995. Identification of a methyl-accepting chemotaxis protein in *Rhodobacter sphaeroides*. *Molecular Microbiology*. 18:115-121.

Wassenaar, T. M. 1997. Toxin production by *Campylobacter* spp. *Clinical Microbiology Reviews*. 10:466-476.

Wassenaar, T. M., Bleumink-Pluym, N. M., Newell, D. G., Nuijten, P. J. & van der Zeijst, B. A. 1994. Differential flagellin expression in a *flaA flaB*⁺ mutant of *Campylobacter jejuni*. *Infection and Immunity*. 62:3901-3906.

Wassenaar, T. M., Bleumink-Pluym, N. M. & van der Zeijst, B. A. M. 1991. Inactivation of *Campylobacter jejuni* flagellin genes by homologous recombination demonstrates that *flaA* but not *flaB* is required for invasion. *EMBO Journal*. 10:2055-2061.

Welch, M., Oosawa, K., Aizawa, S. & Eisenbach, M. 1993. Phosphorylation-dependent binding of a signal molecule to the flagellar switch of bacteria. *Proceedings of the National Academy of Sciences of the United States of America*. 90:8787-8791.

Whitehouse, C.A., Balbo, P.B., Pesci, E. C., Cottle, D. L., Mirabito, P. M. & Pickett, C. L. 1998. *Campylobacter jejuni* cytolethal distending toxin causes a G2-phase cell cycle block. *Infection and Immunity*. 66:1934-1940.

Wolfe, A.J. & H.C. Berg. 1989. Migration of bacteria in semisolid agar. *Proceedings of the National Academy of Sciences of the United States of America*. 86: 6973-6977.

- Wooldridge, K. G. & Ketley, J. M.** 1997. *Campylobacter*-host cell interactions. *Trends in Microbiology*. 5:96-102.
- Wooldridge, K. G. & van Vliet, A. H. M. (Edited by Ketley J. M. & Konkel. M. E.).** 2005. *Iron transport and regulation*; in *Campylobacter: Molecular and Cellular Biology*, Horizon Bioscience. pp. 293-310.
- Wosten, M. M. S. M., Boeve, M., Koot, M. G. A., van Nuenen, A. C. & van der Zeijst, B. A. M.** 1998. Identification of *Campylobacter jejuni* Promoter Sequences. *Journal of Bacteriology*. 180:594-599.
- Wren, B. W., Henderson, J. & Ketley, J. M.** 1994. A PCR-based strategy for the rapid construction of defined bacterial deletion mutants. *Biotechniques*. 16:994-996.
- Yao, R., Burr, D. H., Doig, P., Trust, T. J., Niu, H. & Guerry, P.** 1994. Isolation of motile and non-motile insertional mutants of *Campylobacter jejuni*: The role of motility in adherence and invasion of eukaryotic cells. *Molecular Microbiology*. 14:883-893.
- Yao, R., Burr, D. H. & Guerry, P.** 1997. CheY-mediated modulation of *Campylobacter jejuni* virulence. *Molecular Microbiology*. 23:1021-1031.
- Yeh, J.I., Biemann, H.P., Pandit, J., Koshland, D.E. Jr. & Kim, S.H.** 1996. High-resolution Structures of the Ligand Binding Domain of the Wild-type Bacterial Aspartate Receptor. *Journal of Molecular Biology*. 262:186-201.
- Yeh, J.I., Biemann, H.P., Pandit, J., Koshland, D.E. Jr. & Kim, S.H.** 1993. The three-dimensional structure of the ligand-binding domain of a wild-type bacterial chemotaxis receptor. *Journal of Biological Chemistry*. 268:9787-9792.
- Young, V. B. & Mansfield, L.S. (Edited by Ketley J.M. & Konkel. M. E.).** 2005. *Campylobacter infection – Clinical context*; in *Campylobacter: Molecular and Cellular Biology*, Horizon Bioscience. pp. 1-12.
- Zhang, W., Brooun, A., Mccandless, J., Banda, P. & Alam, M.** 1996. Signal transduction in the archaeon *Halobacterium salinarum* is processed through three subfamilies of 13 soluble and membrane-bound transducer proteins. *Proceedings of the National Academy of Sciences of the United States of America*. 93:4649-4654.
- Zimmer, M. A. Szurmant, H., Saulmon, M. M., Collins, M. A., Bant, J. S. & Ordal, G.W.** 2002. The role of heterologous receptors in McpB-mediated signalling in *Bacillus subtilis* chemotaxis. *Molecular Microbiology*. 45:555-568.
- Zimmer, M.A., Tiu, J., Collins, M.A., Ordal, G.W.** (2000) Selective methylation changes on the *Bacillus subtilis* chemotaxis receptor McpB promote adaptation. *J Biol Chem* 275: 24264–24272.

Ziprin, R. L., Young, C. R., Stanker, L. H., Hume, M. E. & Konkel, M. E. 1999. The absence of cecal colonization of chicks by a mutant of *Campylobacter jejuni* not expression bacterial fibronectin-binding protein. *Avian Diseases*. 43:586-589.